

THE ROLE OF OSTEOMACS IN REGULATING STEM CELL FUNCTION AND THE
HEMATOPOIETIC NICHE

Safa F. Mohamad

Submitted to the faculty of the University Graduate School
in partial fulfillment of the requirements
for the degree
Doctor of Philosophy
in the Department of Microbiology and Immunology,
Indiana University

February 2020

Accepted by the Graduate Faculty of Indiana University, in partial fulfillment of the requirements for the degree of Doctor of Philosophy.

Doctoral Committee

Edward F. Srour, Ph.D., Chair

Angela Bruzzaniti, Ph.D.

November 7, 2019

Laura S. Haneline, MD

Louis M. Pelus, Ph.D.

Melissa A. Kacena, Ph.D.

© 2020

Safa F. Mohamad

ACKNOWLEDGEMENT

I would first like to thank my mentor Dr. Edward F. Srouer for giving me the opportunity to work in his laboratory. His passion for hematology and immense knowledge of the field is the reason I have reached this point in my career. He is an excellent mentor who urged me to push myself towards excellence and never give up. He helped me learn multiple cutting edge technologies and provided me with several opportunities to attend conferences and hone my communication skills. His constant mentorship has made me a skilled and successful scientist.

I would also like to thank my committee Dr. Angela Bruzzaniti, Dr. Laura S. Haneline, Dr. Louis M. Pelus and Dr. Melissa A. Kacena. All five of my committee members chaired by Dr. Edward F. Srouer have helped shaped my project and given me insightful feedback at every point in the past five years. Each committee member's unique expertise helped me understand different facets of my project and overall made me a better student.

Several people have contributed towards making my thesis project successful. I am extremely grateful to past and present Srouer laboratory members including Dr. Linlin Xu who started this project and Dr. Joydeep Ghosh who has helped me not only with his technical expertise but also with his intellect. I would also like to thank Andrea M. Gunawan who runs the CyTOF and is a very big part of the laboratory.

I have had the opportunity to collaborate with several laboratories during my Ph.D. My biggest collaboration has been with Dr. Melissa A. Kacena and her laboratory. I would like to thank Rachel Blosser, Irushi Abeysekara, Evan R. Himes, Dr. Paul Childress, Dr. Marta

Alvarez, Dr. Kevin A. Maupin and Dr. Deepa Sheik for their constant help and support. I would also like to thank my collaborator Dr. Angela Bruzzaniti and her lab members including Dr. Alexandra Aguilar-Perez and Dr. Jungmin Hong.

A special thanks to Dr. Malgorzata M. Kamocka for her help with the confocal microscope; and Dr. Justin Layer for helping me with my lentiviral knockdowns. Also, my project would have been incomplete without the constant help of Indiana University's Flow Cytometry Core facility.

I would also like to thank the entire Microbiology and Immunology department for their support. Dr. Margaret Bauer for being an awesome academic advisor and organizing the student seminars; and Cindy Booth for always making the department feel like home.

I am also grateful to Dr. Joyce Lloyd who was my mentor during my master's project and is the reason why I entered the field of hematology.

Finally, the people who were my support system away from work. Being an international student, my friends back from India, as well as the friends I made in Indianapolis played an important role in helping me adjust to life in Indianapolis. Lastly, I would like to thank my parents without whom I would never have reached this point in my career. Their sacrifice, love, support and encouragement has been key to my growth as a human being and as a student.

Safa F. Mohamad

THE ROLE OF OSTEOMACS IN REGULATING STEM CELL FUNCTION AND THE
HEMATOPOIETIC NICHE

Maintenance of hematopoietic stem cell (HSC) function is an orchestrated event requiring the participation of multiple cell types within the hematopoietic niche. Among the key cellular components of the niche are a group of specialized bone-resident macrophages known as osteomacs (OM). Reported here is a detailed characterization of OM and description of discriminating phenotypic and functional properties that clearly distinguish OM from bone marrow-derived macrophages (BM M ϕ). Furthermore, it was established that OM support hematopoiesis enhancing activity of osteoblasts and that this activity was augmented by megakaryocytes. Serial transplantation demonstrated that HSC repopulating potential was best maintained by in vitro cultures containing OM, osteoblasts and megakaryocytes. Interestingly, BM M ϕ were unable to mediate the same hematopoiesis enhancing activity regardless of whether megakaryocytes were present in co-culture or not. Subsequently, to understand the importance of networking between the residents of the niche, 3D tissue cytometry was performed on fixed and stained unperturbed bone marrow sections. This approach identified the spatial relationships between OM, osteoblasts, megakaryocytes and HSC within the niche and defined parameters, under which these cell types coexist in undamaged bone marrow. In addition, single cell mRNAseq and CyTOF was performed to assess genetic and proteomic expression changes in OM following their interaction with megakaryocytes. These studies revealed the upregulation of CD166 and embigin on OM via osteoblast and megakaryocyte interactions. Clonogenic assays were conducted to examine the impact of these molecules in hematopoietic function. When these assays were initiated with CD166

KO OM or shRNA-mediated embigin knockdown OM, it was established that loss of these surface molecules on OM caused a decline in the normal OM-mediated hematopoietic enhancing activity. Conversely, recombinant CD166 and embigin partially substituted for OM activity thus identifying potential mediators through which OM maintain hematopoietic function. This data, for the first time, reveal intimate spatial interactions between OM, osteoblasts, megakaryocytes and HSC in the hematopoietic niche. They also illustrate the importance of crosstalk between OM, osteoblasts and megakaryocytes and reveal novel mediators such as CD166 and embigin that cooperate with other elements of the niche to support HSC function.

Edward F. Srour, Ph.D., Chair

TABLE OF CONTENTS

List of Tables.....	xiii
List of Figures.....	xiv
List of Abbreviations	xvi
Chapter One: Introduction	19
1.1 Ontogeny of murine hematopoiesis.....	21
1.2 Endosteal bone marrow niche vs Vascular bone marrow niche	22
1.3 Cellular components participating in the hematopoietic niche	25
1.3.1 Osteoblasts	25
1.3.2 Megakaryocytes.....	28
1.3.3 Macrophages	29
1.3.3.1 Erythroblastic island macrophages (EIM).....	30
1.3.3.2 Osteomacs (OM)	31
1.3.3.3 Bone marrow derived macrophages (BM M ϕ)	33
1.3.4 Other cellular components	35
1.4 CD166 as a regulator of the hematopoietic niche.....	37
1.5 Embigin as a regulator of the hematopoietic niche.....	39
1.6 Significance of the hematopoietic niche	40
Chapter Two: Methods	43
2.1 Mice.....	43
2.2 Cells	43
2.2.1 Preparation of fresh neonatal calvarial cells	43
2.2.2 Preparation of fresh neonatal bone marrow	44
2.2.3 Preparation of fetal liver-derived megakaryocytes.....	45

2.2.4 Preparation of 8-12 wk bone marrow.....	45
2.2.5 Preparation of 8-12 wk digested bone	47
2.3 Cell staining, flow cytometry and cell sorting	48
2.4 Phagocytosis assay	50
2.5 Single cell qRT-PCR.....	50
2.5.1 Data collection	50
2.5.2 Data analysis of single cell qRT-PCR.....	52
2.6 Single cell mRNA sequencing.....	52
2.6.1 Data collection	52
2.6.2 scRNA-seq data analysis	53
2.7 Mass cytometry (CyTOF).....	54
2.7.1 Custom conjugation of CyTOF antibodies	54
2.7.2 Staining protocol for cell surface and intracellular antibodies	55
2.7.3 ViSNE analysis of normalized CyTOF events.....	56
2.8 Quantitative global proteomic comparison of protein levels in OM obtained from fresh NCC and NCC cultured in the absence and presence of megakaryocytes	58
2.8.1 Cell lysis, protein assay and proteolytic digestion.....	59
2.8.2 “De-salting” of peptides from other low molecular weight organic matter and salts	59
2.8.3 Tandem Mass Tags (TMT) based peptide labelling, reaction quenching and mixing	60
2.8.4 “De-salting” of labelled peptide mixtures	60
2.8.5 Nano-LC-MS/MS analysis.....	61
2.8.6 Data analysis	62
2.9 3D Tissue cytometry	63

2.10 qRT-PCR	64
2.11 shRNA knockdown.....	67
2.12 Colony forming assays.....	68
2.13 Competitive repopulating assays	69
2.14 Recombinant, block and other proteins.....	70
2.15 Statistical analysis	71
Chapter Three: Characterization of osteomacs and their phenotypic and functional differences from bone marrow derived macrophages	
3.1 Introduction.....	72
3.2 Characterization of osteomac origin and phenotypic expression of surface markers	73
3.3 CD166 and CSF1R co-expression distinguish between OM and BM M ϕ from neonatal and adult donors	77
3.4 Single cell genomics identifies transcriptional changes between neonatal OM and BM M ϕ	79
3.5 Single cell CyTOF analysis reveals a novel set of markers expressed on neonatal OM.....	82
3.6 OM are a subset of macrophages that phagocytose and differentiate into osteoclasts	89
3.7 OM, osteoblast and megakaryocyte interactions are essential for maintaining murine hematopoietic stem cell function	92
3.8 Discussion	95
Chapter Four: Megakaryocytes interact with osteomacs and osteoblasts to regulate murine hematopoiesis	
4.1 Introduction.....	101
4.2 Crosstalk between OM, osteoblasts and megakaryocytes is essential to	

maintain murine hematopoiesis	103
4.3 Early stage megakaryocytes are functionally important for OM proliferation	109
4.4 Direct interactions between OM, osteoblasts and megakaryocytes are essential for maintaining hematopoiesis	111
4.5 3D tissue cytometry helps define the spatial localization of OM, osteoblasts and megakaryocytes relative to HSC in the hematopoietic niche	115
4.6 Discussion	120
Chapter Five: CD166 and embigin are molecular mediators through which OM maintain hematopoietic function	125
5.1 Introduction.....	125
5.2 Single cell mRNA sequencing identified several targets through which OM potentially maintain hematopoietic function.....	127
5.3 Quantitative comparison of protein levels using TMT based peptide labeling and LC-MS/MS	131
5.4 Single cell CyTOF analysis identified CD166 and embigin as potential mediators through which OM maintain hematopoietic function	135
5.5 Characterization of OM as potential osteolineage cells proximal to HSC	140
5.6 Recombinant CD166 and embigin partially substitute OM mediated hematopoietic function	143
5.7 CD166 as a molecular mediator through which OM maintain hematopoietic function of osteoblasts	146
5.8 Embigin as a molecular mediator through which OM maintain hematopoietic function of osteoblasts	152
5.9 Discussion	158

Chapter Six: Future Directions.....	163
6.1 The requirement of a phenotypic marker distinguishing adult OM from BM M ϕ	163
6.2 To identify the localization of OM, osteoblasts and megakaryocytes with respect to HSPCs in stressed and aged mice	165
6.3 To determine the molecular mediators through which OM maintain hematopoietic activity <i>in vivo</i>	168
References.....	170
Curriculum Vitae	

LIST OF TABLES

Table 2.1 List of fluorophore conjugated antibodies used in this study	49
Table 2.2 List of metal conjugated CyTOF antibodies used in this study	57
Table 2.3 List of qRT-PCR primers for genes investigated in this study.....	66
Table 3.1 Summary of similarities and differences between OM and BM M ϕ	100
Table 5.1 List of proteins upregulated in NCC+MK in comparison to NCC.....	132
Table 5.2 List of proteins downregulated in NCC+MK in comparison to NCC	133

LIST OF FIGURES

Figure 3.1 Phenotypic characterization of fresh and cultured osteomacs.....	74
Figure 3.2 OM are radioresistant and are derived from HSC	76
Figure 3.3 Phenotypic analysis of OM and BM M ϕ derived from neonatal and adult donors	78
Figure 3.4 CD110/MPL differentiates OM from BM M ϕ in neonates	80
Figure 3.5 Differential expression patterns of surface and intracellular antigens on OM and BM M ϕ from neonates	85
Figure 3.6 Multidimensional CyTOF analysis of OM and BM M ϕ from neonates	86
Figure 3.7 Developmental loss of CD206 expression on OM.....	87
Figure 3.8 OM perform phagocytosis comparable to BM M ϕ	90
Figure 3.9 OM can differentiate into functional osteoclasts	91
Figure 3.10 OM are bone-resident macrophages that are functionally different from BM-derived M ϕ	94
Figure 4.1 Effect of megakaryocytes on OM and osteoblast function.....	105
Figure 4.2 <i>In vivo</i> assays of cells maintained <i>in vitro</i> with NCC or sorted fractions of NCC	108
Figure 4.3 Early stage megakaryocytes promote OM proliferation <i>in vitro</i>	110
Figure 4.4 Direct interaction is required for megakaryocytes to enhance OM numbers	112
Figure 4.5 Direct interactions between OM, osteoblasts and megakaryocytes are important to maintain hematopoietic enhancing activity	114
Figure 4.6 Use of 3D cytometry to determine localization of hematopoietic niche residents.....	117

Figure 4.7 Model depicting functional interaction between OM, osteoblasts and megakaryocytes	124
Figure 5.1 Single cell mRNA sequencing of OM sorted from NCC and NCC+MK.....	128
Figure 5.2 Quantitative analysis of OM protein levels using LC-MS/MS.....	134
Figure 5.3 Multidimensional CyTOF analysis of OM contained within NCC cultured in the absence and presence of megakaryocytes	137
Figure 5.4 Characterization of OM in relation to proximal osteolineage cells	141
Figure 5.5 CD166 and embigin are potential mediators through which OM maintain hematopoietic function.....	144
Figure 5.6 The CD166+ fraction of OM mediates hematopoietic enhancing activity of osteoblasts	147
Figure 5.7 CD166 is one of the molecular mediators through which OM maintain hematopoietic function of osteoblasts.....	149
Figure 5.8 Blocking embigin expression on NCC causes a decline in hematopoietic activity	154
Figure 5.9 Embigin is one of the molecular mediators through which OM maintain hematopoietic function of osteoblasts.....	155
Figure 5.10 Summary of previous and current studies.....	162
Figure 6.1 Phenotypic characterization of young and old osteomacs.....	167

LIST OF ABBREVIATIONS

ADIPOQ:	Adiponectin
AGM:	Aorta gonad mesonephros
ALCAM:	Activated leukocyte cell adhesion molecule
BFU-E:	Burst forming unit-erythroid
BM M ϕ :	Bone marrow derived macrophages
BM:	Bone marrow
BMPR1:	Bone morphogenetic protein receptor 1
CAR cells:	CXCL12 abundant reticular cells
CCL-4:	C-C motif chemokine ligand-4
CFU:	Colony forming unit
COX-2:	Cyclooxygenase-2
CSF1R:	Colony stimulating factor 1 receptor
CSF3:	Colony stimulating factor 3
CXCL12:	C-X-C Motif Chemokine Ligand 12
CXCR4:	C-X-C Motif Chemokine Receptor 4
DAPI:	4',6-diamidino-2-phenylindole
DMEM:	Dulbecco's minimal essential medium
EIM:	Erythroblastic island macrophages
EPO:	Erythropoietin
FGF-2:	Fibroblast growth factor-2
FGF-4:	Fibroblast growth factor-4
G-CSF:	Granulocyte-colony stimulating factor
GEMM:	Granulocyte erythroid macrophage megakaryocyte

GFP:	Green fluorescent protein
GM:	Granulocyte macrophage
HSC:	Hematopoietic stem cell
HSPC:	Hematopoietic stem and progenitor cell
IFC:	Integrated fluidic circuit
IFN γ :	Interferon γ
IGF-1:	Insulin growth factor-1
IL-18:	Interleukin:18
IMDM:	Iscove's modified Dulbecco's Medium
LC-MS:	Liquid chromatography-mass spectrometry
LECT-2:	Leukocyte cell derived chemotaxin-2
LEPTR:	Leptin receptor
LT-HSC:	Long term-hematopoietic stem cell
MCSF:	Macrophage colony stimulating factor
MDS:	Multidimensional scaling plots
MK:	Megakaryocyte
MMP-9:	Matrix metalloproteinase-9
MPL:	Myeloproliferative leukemia/ thrombopoietin receptor
MPP:	Multipotent progenitors
MSC:	Mesenchymal stromal cell
NBM:	Neonatal bone marrow
NCC:	Neonatal calvarial cells
OB:	Osteoblast
OM:	Osteomac
PBS:	Phosphate buffer saline
PCA:	Principle component analysis

PDGF- β :	Platelet derived growth factor- β
PF4:	Platelet factor 4
PRM:	Parallel reaction monitoring
PTH:	Parathyroid hormone
PTH1R:	Parathyroid hormone receptor-1
qRT-PCR:	Reverse transcriptase-polymerase chain reaction
ROS:	Reactive oxygen species
SCF:	Stem cell factor
SDF-1:	Stromal derived factor-1
SLAM:	Signaling lymphocyte activation molecule
ST-HSC:	Short term-hematopoietic stem cell
TCEP:	tris(2-carboxyethyl)phosphine hydrochloride (TCEP)
TGF- β :	Transforming growth factor- β
TMT:	Tandem mass tag
TNF- α :	Tumor necrosis factor- α
TPO:	Thrombopoietin
TRAP:	Tartrate resistant acid phosphatase
VCAM-1:	Vascular cell adhesion molecule-1
α -MEM:	Minimum Essential Medium Eagle - Alpha Modification
α -SMA:	α -Smooth muscle actin

CHAPTER ONE: Introduction

Every day, the human body produces $>10^{11}$ blood cells through a process called hematopoiesis (Catlin, Busque et al. 2011), derived from the Greek word *Haima* or *haimatos* meaning blood and *poiesis* meaning to make. The main protagonist in this process is the hematopoietic stem cell (HSC) which has the capability to self-renew, as well as differentiate into myeloid, erythroid and lymphoid lineages (Till and Mc 1961). Hematopoiesis occurs in the bone marrow which is encapsulated within the bone and interconnected with a complex vasculature. This leads to the formation of a highly enriched bone marrow microenvironment called the niche. The concept of a niche where HSC reside was first introduced by Schofield in 1978. He stated, “the cellular environment which retains the stem cell is called a stem cell ‘niche’”. He also proposed that, “the stem cell is seen in association with other cells that determine its behavior”. His findings concluded that the location of a stem cell is important for it to retain its stemness. Within the niche, HSC maintain their quiescent behavior. However, they leave the niche as mature differentiated cells at the cost of their immortality (Schofield 1978).

Schofield’s revelation caused the expansion of the field of hematopoiesis and led to the identification of several niche components. However, even before Schofield introduced the concept of a niche, in 1977, Dexter et al. described the importance of stromal cells in maintaining the proliferation of HSC and granulopoiesis. He demonstrated that “feeding” HSC cultures at regular intervals with stromal cells is essential to increase HSC numbers (Dexter, Allen et al. 1977). Next, in 1994, human osteoblasts were identified as supporters of hematopoiesis through the production of granulocyte-colony stimulating factor (G-CSF) (Taichman and Emerson 1994, Taichman, Reilly et al. 1996). G-CSF also known as colony

stimulating factor-3 (CSF3) is a cytokine that controls the production, differentiation and function of granulocytes. Following this discovery, the role of murine osteoblasts in the hematopoietic niche was further validated in the early 2000's by two independent groups who demonstrated the importance of parathyroid hormone (PTH) and bone morphogenetic protein (BMP) signaling in HSC maintenance (Calvi, Adams et al. 2003, Zhang, Niu et al. 2003). Next, in 2009, Dominici et al. introduced megakaryocytes as an imperative niche resident. They demonstrated the importance of megakaryocytes in the restoration of the HSC niche post radioablation (Dominici, Rasini et al. 2009). In 2010, Winkler et al. introduced a subset of macrophages called osteomacs (OM) as important players of the niche. They established that depletion of these osteomacs caused hematopoietic stem and progenitor cell (HSPC) mobilization to the peripheral blood (Winkler, Sims et al. 2010).

Besides the residents mentioned above, several other cellular and soluble elements which participate in the niche have been identified. These participants include hematopoietic cells such as neutrophils and osteoclasts, neuronal and glial cells, mesenchymal stem cells, endothelial and perivascular cells and adipocytes. It is believed that HSC maintenance (quiescence, self-renewal, engraftment, mobilization and differentiation) in the hematopoietic niche is mediated by intimate interactions between cellular and soluble elements of the niche and stem cells. Discussed below are some of these cellular components and their role in the maintenance of hematopoiesis. Also detailed, is the importance of the anatomical location of these cell types in relation to HSC within the niche.

1.1 Ontogeny of murine hematopoiesis

Studies of adult hematopoiesis postulate that all myeloid, erythroid and lymphoid cells emerge from HSC. However, where do HSC originate from? This question can be answered by characterizing the ontogeny of murine hematopoiesis which, in the mammalian system occurs over two waves. The first wave involves primitive hematopoiesis which is responsible for generating primitive erythrocytes and certain myeloid cells such as macrophages and megakaryocyte progenitors; and definitive hematopoiesis which involves the origin of myeloid, lymphoid and erythroid cells from the definitive HSC (Dieterlen-Lievre 1975, Orkin and Zon 2008, Medvinsky, Rybtsov et al. 2011). Primitive hematopoiesis which occurs in the yolk sac (extra-embryonic mesoderm ingresses into the posterior primitive streak) paradoxically in the absence of definitive HSC marks the onset of hematopoiesis. Maturing erythroid cells can be seen in the yolk sac as early as embryonic day 7.5 (E7.5) and macrophage and megakaryocyte progenitors by E9.0 (Silver and Palis 1997). Interestingly, these fetal-derived macrophage progenitors are responsible for maintaining and replenishing several tissue resident macrophages in adult hematopoiesis (Schulz, Perdiguero et al. 2012, Yona, Kim et al. 2013).

Definitive hematopoiesis begins in the aorta gonad mesonephros (AGM) where functional HSC with engrafting activity are observed by E10.5 (Müller, Medvinsky et al. 1994, Medvinsky and Dzierzak 1996). It was proposed that hemangioblasts are formed in the yolk sac during primitive hematopoiesis. These hemangioblasts are tripotent cells that can differentiate into hematopoietic and endothelial cells; and are capable of forming murine smooth muscle cells *in vitro* (Choi, Kennedy et al. 1998, Ema and Rossant 2003). In the AGM, hemangioblasts act as precursors for hemogenic endothelial cells which form on the ventral wall of the aorta and bud off HSC (North, De Bruijn et al. 2002, Lancrin, Sroczynska et al. 2009, Boisset and Robin 2010). This leads to the hypothesis that

hemangioblasts from the yolk sac are precursors for the hemogenic endothelial cells formed in the AGM. However, fate-mapping studies indicate that the yolk sac and AGM derive independently at different times of development (Turpen, Kelley et al. 1997). Since HSC are first observed on E8.5 in the AGM, before the onset of circulation; there is a low possibility of cells being circulated from the yolk sac into the AGM before this time. Also, even though HSC are observed in the AGM at E8.5, HSC-like activity is observed in the yolk sac by E9.0 and functional activity of AGM HSC occur by E11. It is possible that cells from the yolk sac colonize the AGM through circulation between E8.5 and E11 to activate HSC function (Palis, Chan et al. 2001). From this point on, HSC migrate to the fetal liver by E12.5, which becomes the major source of hematopoiesis prior to birth. After birth, HSC home primarily to the bone marrow which is the main location of the hematopoietic niche (Medvinsky and Dzierzak 1996, Orkin and Zon 2008, Medvinsky, Rybtsov et al. 2011).

1.2 Endosteal bone marrow niche vs Vascular bone marrow niche

The anatomic localization of HSC is dynamic making it very difficult to pinpoint their exact location via imaging, especially since they are very rare and extremely difficult to precisely identify phenotypically. Furthermore, definitive HSC are classified into two sub-types: long term-HSC (LT-HSC) which are capable of contributing to hematopoiesis for potentially a lifetime; and short term-HSC (ST-HSC) whose reconstitution capabilities are limited to several weeks (Christensen and Weissman 2001). Each of these sub-types are phenotypically different, further adding to imaging difficulties. While HSC are known to circulate and reside in multiple locations, their primary site of localization is the bone marrow. Within the bone marrow, two main HSC niches have been described: the endosteal niche and the vascular niche (Kiel and Morrison 2008). Several studies have

identified cellular and soluble elements within these niches and have probed for the contribution of each of these elements towards HSC maintenance and function.

The endosteal niche consists of the endosteal surface which is primarily lined by osteoblasts and surrounded by hematopoietic cells. This suggests reciprocal communication between osteoblasts and hematopoietic cells including HSC. This notion is supported by many groups which have documented several factors secreted by osteoblasts that regulate hematopoiesis. These include hepatocyte growth factor which is important for the survival of hematopoietic progenitors (Taichman, Reilly et al. 2001); and angiopoietin and thrombopoietin (TPO) which are implicated in maintaining HSC quiescence (Arai, Hirao et al. 2004, Yoshihara, Arai et al. 2007). In fact, increasing evidence suggests that HSC residing next to the endosteal surface are quiescent and produce progenitors which migrate to the center of the bone marrow towards the blood vessels as they mature and differentiate (Nilsson, Johnston et al. 2001). Other studies in support of the endosteal niche demonstrate that post transplantation, HSC have a tendency to home to N-cadherin+ osteoblasts predominantly located in the trabecular bone (Nilsson, Johnston et al. 2001, Zhang, Niu et al. 2003, Xie, Yin et al. 2009). This tendency to home to the trabecular bone could be due to the increased production of C-X-C Motif Chemokine Ligand 12 (CXCL12) at this site post irradiation (Xie, Yin et al. 2009).

CXCL12 also known as stromal derived factor-1 (SDF1) is a chemoattractant primarily secreted by stromal cells (Aiuti, Webb et al. 1997, Lapidot, Dar et al. 2005, Sugiyama, Kohara et al. 2006) mainly endothelial and perivascular cells (Ding, Saunders et al. 2012, Ding and Morrison 2013, Greenbaum, Hsu et al. 2013). This ligand binds to C-X-C Motif Chemokine Receptor 4 (CXCR4) also known as fusin/CD184 which is a surface protein expressed on HSC (Mohle, Bautz et al. 1998, Zou, Kottmann et al. 1998, Aiuti, Taviani et

al. 1999, Sugiyama, Kohara et al. 2006). It is a known fact that CXCR4-CXCL12 chemokine signaling is important for the maintenance of the HSC pool (Aiuti, Webb et al. 1997, Zou, Kottmann et al. 1998, Sugiyama, Kohara et al. 2006, Xie, Yin et al. 2009) and that CXCL-12 abundant reticular (CAR) cells express high amounts of CXCL12 (Sugiyama, Kohara et al. 2006). CAR cells are an important part of the HSC niche and are located near sinusoidal endothelial cells as well as near the endosteum making it important for both vascular and endosteal niches (Sugiyama, Kohara et al. 2006).

Supporting the concept of a vascular niche, Kiel et al. revealed that HSC identified via the SLAM (signaling lymphocyte activation molecules) markers localized adjacent to the sinusoidal endothelium in the bone marrow (Kiel, Yilmaz et al. 2005). Adding to this, several factors including fibroblast growth factor-4 (FGF-4) and SDF1 are secreted within the vascular niche which support hematopoiesis (Avecilla, Hattori et al. 2004). It has also been demonstrated that disruption of this vascular niche by in vivo ablation of endothelial cells led to failure of hematopoiesis, in particular, thrombopoiesis (Avecilla, Hattori et al. 2004).

Since the bone is highly interconnected with vasculature, it is very difficult to differentiate between an endosteal and vascular niche. Nombela-Arrieta et. al combined both these niche concepts; and using laser scanning cytometry demonstrated that HSPC localize near the endosteum which is in close contact with bone marrow (BM) micro vessels (Nombela-Arrieta, Pivarnik et al. 2013). Furthermore, quiescent HSC associate with small arterioles ensheathed with NG2+ pericytes near the endosteal region; whereas HSC that have entered the cell cycle redistribute to leptin receptor (LEPR)+ perisinusoidal sites (Kunisaki, Bruns et al. 2013). Strangely, most of these localization studies are limited to the position of HSC relative to either the endosteum or the vasculature (Aiuti, Webb et al.

1997, Nilsson, Johnston et al. 2001, Zhang, Niu et al. 2003, Kiel, Yilmaz et al. 2005, Sugiyama, Kohara et al. 2006, Xie, Yin et al. 2009, Kunisaki, Bruns et al. 2013, Nombela-Arrieta, Pivarnik et al. 2013). Missing from these data are other cellular elements involved in HSC regulation within the niche. More comprehensive multi-dimensional imaging studies combining existing data with additional niche participants are warranted.

1.3 Cellular components participating in the hematopoietic niche

Several cellular niche components have been identified and examined for their role in the regulation of hematopoiesis. Some of them are mentioned below.

1.3.1 Osteoblasts

It is already established that HSC have a tendency to home towards the endosteum which is lined by osteoblasts (Nilsson, Johnston et al. 2001, Zhang, Niu et al. 2003, Xie, Yin et al. 2009, Kunisaki, Bruns et al. 2013, Nombela-Arrieta, Pivarnik et al. 2013). Due to the proximity of the bone and bone marrow, osteoblasts were one of the first stromal cells discovered as an important part of the hematopoietic niche. Early work on the role of osteoblasts in hematopoiesis established that these cells support human cord blood isolated CD34+ cells *in vitro* (Taichman and Emerson 1994, Taichman, Reilly et al. 1996). In fact, depletion of these osteoblasts in mice resulted in the loss of myeloid, lymphoid and erythroid progenitors in addition to the decrease in the number of HSC (Visnjic, Kalajzic et al. 2004). Since then, several researchers have worked to identify the molecular mediators through which these cells maintain hematopoietic function. One such group demonstrated that osteoblasts secrete hepatocyte growth factor which is important for the survival of hematopoietic progenitors (Taichman, Reilly et al. 2001). Another, administered the activation of parathyroid hormone (PTH) and its receptor (PTH1R) *in vivo* which resulted in increased bone anabolism and augmented HSC numbers (Calvi, Adams et al.

2003). Another group, conditionally depleted bone morphogenetic protein receptor 1A (BMPR1A) to demonstrate the importance of BMP signaling in regulating HSC numbers (Zhang, Niu et al. 2003). However, increase in HSC numbers does not necessarily correlate with increase in function (Lymperi, Horwood et al. 2007, Calvi, Bromberg et al. 2012, Yu and Scadden 2016). Functional transplantation studies used to determine whether HSC can engraft, that is reconstitute the entire bone marrow are required. This was demonstrated via specific depletion of osteocalcin expressing mature osteoblasts. This depletion led to the increase in HSPC numbers with no change in engraftment as demonstrated via primary and secondary transplantations (Yu, Saez et al. 2015). Another group used strontium to increase the numbers of a subgroup of osteoblasts but failed to record an increase in HSC numbers (Lymperi, Horwood et al. 2007). They hypothesized that this discrepancy was due to the failure to increase the number of N-cadherin+ osteoblasts indicating that certain groups of osteoblasts support hematopoietic function better than others (Zhang, Niu et al. 2003, Lymperi, Horwood et al. 2007).

In 2010, Chitteti et al. corroborated the importance of osteoblasts in the hematopoietic niche. Furthermore, this activity was dependent on Notch signaling and was suppressed by adipocytes (Chitteti, Cheng et al. 2010). On analyzing the maturational status of these osteoblasts; it was demonstrated that immature osteoblasts expressing high levels of Runx2 (Chitteti, Cheng et al. 2010) maintain the most robust hematopoietic enhancing activity (Chitteti, Cheng et al. 2010, Cheng, Chitteti et al. 2011). Phenotypically, these cells also expressed ALCAM (Activated Leukocyte Cell Adhesion Molecule) or CD166 which has been used during the last 10 years to identify immature osteoblasts. It was also demonstrated that CD166 knock out mice have decreased hematopoietic activity (Chitteti, Bethel et al. 2013, Chitteti, Cheng et al. 2013, Chitteti, Kobayashi et al. 2014). Conversely, mature osteoblasts which are Runx2^{low} and osteocalcin+ do not express CD166 (Chitteti,

Cheng et al. 2013). Interestingly, constitutive activation of PTH1R on terminally differentiated osteocytes caused an increase in bone mass but a decrease in HSC function (Calvi, Bromberg et al. 2012) further indicating the importance of immature osteoblasts in the hematopoietic niche.

Mature osteoblasts may not play a major role in HSC function, but they do have a role in hematopoiesis. Of note, depletion of osteocalcin expressing mature osteoblasts in mice causes a marked reduction in lymphopoiesis (Yu, Saez et al. 2015). This correlates with the fact that osteoblast lineage cells secrete CXCL12; and depletion of this chemokine causes a decrease in lymphoid progenitors (Greenbaum, Hsu et al. 2013). The same osteocalcin depleted mice even demonstrate compromised G-CSF induced HSPC mobilization (Ferraro, Lympieri et al. 2011). Overall, the maturational status of an osteoblast is important to determine its specific function in hematopoiesis.

Osteoblasts also secrete osteopontin which negatively regulates stem cell numbers and is important to maintain a quiescent stem cell pool. Osteopontin null mice show increased expression of stromal jagged-1 and angiopoietin-1 which elevates HSC numbers and reduces apoptosis (Stier, Ko et al. 2005). Osteoblasts even secrete TPO (Yoshihara, Arai et al. 2007) and angiopoietin (Arai, Hirao et al. 2004) which are important for HSC regulation. LT-HSC possess the thrombopoietin receptor and the Tie2 receptor which binds to TPO and angiopoietin, respectively. The signaling pathways thus activated maintain stem cell quiescence in the osteoblastic niche (Arai, Hirao et al. 2004, Yoshihara, Arai et al. 2007).

1.3.2 Megakaryocytes

Megakaryocytes are responsible for thrombopoiesis (Wright 1910), the process by which they form platelets which are responsible for the clotting of blood. However, in the early 2000s, megakaryocytes were found to have another important function. They are involved in osteoblast proliferation and suppression of osteoblast differentiation (Kacena, Shivdasani et al. 2004, Kacena, Gundberg et al. 2005, Ciovacco, Goldberg et al. 2009, Bethel, Srour et al. 2011, Cheng, Hooker et al. 2013, Cheng, Streicher et al. 2015, Alvarez, Xu et al. 2018). This was demonstrated by targeting GATA-1 and NF-E2 transcription factors which are involved in megakaryocyte differentiation. GATA-1 knockdown and NF-E2 deficient mice have increased megakaryocyte numbers and portray increased bone anabolism (Kacena, Shivdasani et al. 2004, Kacena, Gundberg et al. 2005). Since then the signaling pathways involved in this megakaryocyte function became an active area of investigation (Cheng, Hooker et al. 2013, Cheng, Streicher et al. 2015, Meijome, Baughman et al. 2016, Alvarez, Xu et al. 2018). By increasing osteoblast numbers, megakaryocytes are indirectly involved in regulating hematopoiesis. Furthermore, megakaryocytes tend to migrate to the endosteum post total bone marrow radioablation (Dominici, Rasini et al. 2009). This migration is based on thrombopoietin signaling as well as CD41 integrin-based cell adhesion (Olson, Caselli et al. 2013). Once they reach the endosteum, they participate in osteoblast proliferation through the increased expression of growth factors such as platelet derived growth factor- β (PDGF- β) and fibroblast growth factor-2 (FGF2). This proliferation of osteoblasts is important for HSC engraftment and to revert back to homeostatic conditions (Dominici, Rasini et al. 2009, Olson, Caselli et al. 2013).

Other mechanisms through which megakaryocytes directly support HSC maintenance have also been reported. Whole mount imaging demonstrated that HSC have a tendency

to localize adjacent to megakaryocytes in a non-random manner (Heazlewood, Neaves et al. 2013, Bruns, Lucas et al. 2014). Megakaryocytes also release several cytokines which are known to regulate hematopoiesis. Heazlewood et. al demonstrated that megakaryocytes secrete insulin growth factor-1 (IGF1) which in turn is important in increasing HSC numbers (Heazlewood, Neaves et al. 2013). They also release Platelet Factor-4 (PF4/CXCL4) (Bruns, Lucas et al. 2014, Norozi, Shahrabi et al. 2016), TPO (Nakamura-Ishizu, Takubo et al. 2014) and TGF- β (Zhao, Perry et al. 2014) all of which have been implicated in HSC quiescence.

Megakaryocytes, being the progeny of HSPC can also regulate hematopoiesis via self-regulation of their own proliferation. These cells release microparticles (different from exosomes) which can be endocytosed or directly fused into HSPC. Once fused, the RNA present in these microparticles can reprogram HSPC to specifically differentiate into functional megakaryocytes (Jiang, Kao et al. 2017). Through all the mechanisms mentioned above, megakaryocytes play an important role in maintaining the hematopoietic stem cell niche.

1.3.3 Macrophages

Macrophages are phagocytic immune cells known for their heterogeneity amongst different tissues (Cannon and Swanson 1992). Apart from the cartilage, resident macrophages in almost every tissue of the body are phenotypically identified (Davies and Taylor 2015). Amongst these tissue resident macrophages are three subsets that normally reside in close proximity in the bone marrow microenvironment called erythroblastic island macrophages (EIM), OM and bone marrow derived macrophages (BM M ϕ) (Kaur, Raggatt et al. 2017). Several roles for each of these subsets are already identified in hematopoiesis (Winkler, Sims et al. 2010, Chow, Lucas et al. 2011, Chow, Huggins et al. 2013, Chang,

Sengupta et al. 2014, Jacobsen, Forristal et al. 2014, Dutta, Hoyer et al. 2015, McCabe, Zhang et al. 2015, Hur, Choi et al. 2016, Lu, Chen et al. 2016, Mohamad, Xu et al. 2017, Kaur, Raggatt et al. 2018). However, recently, multiple groups have identified several subtypes of BM M ϕ and assigned to each individual subtype its own name or identity (Chow, Lucas et al. 2011, Chang, Sengupta et al. 2014, Jacobsen, Forristal et al. 2014, Hur, Choi et al. 2016, Mohamad, Xu et al. 2017, Kaur, Raggatt et al. 2018). This has led to confusion in the field with no generalized characterization of each of these subtypes. Below, I will describe the roles of each of the three broad subsets of macrophages and outline the dire need of a generalized, well characterized nomenclature system for these macrophages.

1.3.3.1 Erythroblastic island macrophages (EIM)

EIM are the central macrophages surrounded by erythroblasts in the erythroblastic islands which are essential for erythropoiesis (Bessis 1958). There are three main roles through which EIM support erythropoiesis. 1. Secretion of cytokines such as erythropoietin (EPO) without which erythropoiesis would fail (Rich, Vogt et al. 1988). 2. Recycling iron by incorporating it into ferritin which is essential for hemoglobin synthesis (Leimberg, Prus et al. 2008). 3. Phagocytosis of the nuclei which are extruded during the formation of reticulocytes (Toda, Segawa et al. 2014). Thus, EIM participate in the entire maturation process starting from the pro-erythroblast stage right up to their differentiation into mature enucleated erythrocytes. This was demonstrated by models involving depletion of EIM which led to total collapse of BM erythropoiesis (Jacobsen, Forristal et al. 2014). However, extramedullary erythropoiesis was capable of compensating for the loss in the number of erythrocytes; but it could not compensate for reduced hemoglobin levels indicating the importance of EIM in iron recycling (Ramos, Casu et al. 2013).

Phenotypic characterization of EIM identified that they express common macrophage markers such as F4/80, CD11b, Ly6G, VCAM-1 and CD169 (Jacobsen, Forristal et al. 2014). However, what sets them apart from other subsets of macrophages is their expression of ER-HR3 (Sonoda and Sasaki 2008). Not much is known about the function of this antigen, nevertheless, it may play some role in macrophage maturity (de Jong, Leenen et al. 1994).

EIM are particularly important during hematopoietic stress conditions. Loss of these macrophages before induced hemolytic anemia (Chow, Huggins et al. 2013) or administered exogenous EPO (Ramos, Casu et al. 2013) significantly impairs erythropoietic recovery. Also, depletion of these macrophages in polycythemia vera and β -thalassemia mouse models reduced impaired erythropoietic activity associated with these disease conditions (Ramos, Casu et al. 2013). This indicates that focusing on these macrophages could be an interesting futuristic therapeutic target for erythropoiesis related impairments.

1.3.3.2 Osteomacs (OM)

OM are bone resident macrophages, which form a canopy over the endosteal bone surface. They are currently characterized as CD45⁺F4/80⁺ cells which is the same definition as that of a BM M ϕ (Chang, Raggatt et al. 2008). In fact, one of the differentiating characteristic between these two subsets is their location; BM M ϕ are located towards the center of the bone marrow whereas OM are located at the endosteum (maximum of 2-3 cells away from the bone surface) (Chang, Raggatt et al. 2008, Batoon, Millard et al. 2017). OM express several common macrophage markers including F4/80, CD11b, CD68, Gr-1 and CSF1R. A similar CD68⁺ OM population has also been associated with human bone (Chang, Raggatt et al. 2008). Also, OM do not express tartrate resistant acid phosphatase

(TRAP) which is the identification marker of osteoclasts; which differentiate from macrophages and are separate from OM (Chang, Raggatt et al. 2008, Wu, Raggatt et al. 2013, Sinder, Pettit et al. 2015). Recently, OM have even been shown to express CD169 (Batoon, Millard et al. 2017, Mohamad, Xu et al. 2017) which to date has been associated with BM Mφ that are important for hematopoietic activity (Chow, Lucas et al. 2011, Chow, Huggins et al. 2013, Jacobsen, Forristal et al. 2014, Kaur, Raggatt et al. 2018). This phenotypic similarity drives the conundrum regarding which macrophage subset is important in the hematopoietic niche and increases the confusion in studies that affect many targets that are common to many macrophage types (such as CD169). This is especially important when CD169+ cells are depleted (Chow, Lucas et al. 2011, Chow, Huggins et al. 2013) thus attributing the function of CD169+ cells to macrophages in general and ignoring the fact that the described functions may be attributed to a certain subset of macrophages. These similarities between the two subsets will be further discussed in the next section.

Functionally, OM are well defined for their role in bone morphogenesis. It was demonstrated that OM promote bone anabolism, remodeling, mineralization, repair and regeneration (Chang, Raggatt et al. 2008, Pettit, Chang et al. 2008, Alexander, Chang et al. 2011, Wu, Raggatt et al. 2013, Millard, Pettit et al. 2015, Sinder, Pettit et al. 2015, Alexander, Raggatt et al. 2017, Batoon, Millard et al. 2017, Batoon, Millard et al. 2017, Kaur, Raggatt et al. 2017). However, not much is known about its role in hematopoiesis. Winkler et. al have shown that G-CSF administration which mobilizes HSPC from the bone marrow to the peripheral blood also caused the depletion of OM. This depletion of OM occurred parallel to the suppression of osteoblasts and HSC mobilization; thus, suggesting that disruption of OM from the endosteal niche was linked to HSC mobilization (Winkler, Sims et al. 2010). My own work in tandem with the laboratory has demonstrated that OM

interact with osteoblasts and megakaryocytes to maintain hematopoietic activity both *in vitro* and *in vivo*; and that this activity cannot be substituted by BM M ϕ (Mohamad, Xu et al. 2017).

1.3.3.3 Bone marrow derived macrophages (BM M ϕ)

There is a considerable phenotypic heterogeneity amongst BM M ϕ making their characterization extremely difficult. However, much is known about the role of these heterogenous populations in hematopoiesis. In 2011, Chow et. al used a CD169+ M ϕ depletion model to indicate the importance of macrophages in hematopoiesis. They demonstrated that loss of these macrophages led to reduced expression of CXCL12, kit ligand, VCAM1 and angiopoietin-1 in BM stromal cells; with a concomitant increase in HSC egress (Chow, Lucas et al. 2011). They further characterized these macrophages as drivers of erythropoiesis under homeostatic and hematopoietic stress conditions (Chow, Huggins et al. 2013). Another group identified the importance of CD169+ M ϕ in maintaining long-term reconstituting activity of HSC (Kaur, Raggatt et al. 2018). However, depletion of CD169+ M ϕ also depletes EIM and blocks erythropoiesis (Jacobsen, Forristal et al. 2014). Similarly, OM also express CD169 (Batoon, Millard et al. 2017, Mohamad, Xu et al. 2017) and CD169+ M ϕ depletion also leads to OM loss (Batoon, Millard et al. 2017). Thus, it is difficult to determine which subset of macrophages is responsible for maintaining the competence of the hematopoietic niche based on the CD169+ M ϕ depletion model as described by Chow et al, Chow and Lucas, and Kaur and Raggatt.

Moving away from CD169, Hur et. al, identified CD234/DARC+ macrophages to be important for hematopoiesis. LT-HSC express CD82 which is absent in other progenitors. Interactions between CD82 and CD234 cause the activation of TGF- β /SMAD-3 signaling pathways ultimately leading to cell-cycle inhibition and maintenance of quiescence in LT-

HSC. 10% of DARC+ M ϕ also expressed α -smooth muscle actin (α -SMA) and cyclooxygenase-2 (COX-2) (Hur, Choi et al. 2016). This subset of M ϕ share a functional overlap with another subset described by Ludin et al. This rare subpopulation of M ϕ is radiation resistant and found adjacent to HSPC (Ludin, Itkin et al. 2012). Under stress conditions, these M ϕ upregulate COX-2 and in turn prostaglandin-E2, which restricts the production of reactive oxygen species (ROS) and maintains stem cell quiescence (Ludin, Itkin et al. 2012, Porter, Georger et al. 2013). This regulation of HSPC quiescence is especially important during stress conditions to prevent the exhaustion of the stem cell population.

Circling back to interactions between different components of the niche, one such interaction exists between M ϕ and osteoblasts. Using p62 deficient mice, Chang et. al discovered a loss in the repression of osteoblast mediated NF- κ B signaling. This repression was based on direct cell-cell contact between M ϕ and osteoblasts and was dependent on the presence of p62; a regulator of autophagy. P62 deficient mice lose bone as well as osteoblast C-C motif chemokine ligand-4 (CCL4) expression resulting in HSPC egress (Chang, Sengupta et al. 2014).

Conversely, macrophages can even drive HSPC expansion and mobilization under stressful conditions. LECT-2 (Leukocyte Cell Derived Chemotaxin 2), a cytokine secreted by the liver into the blood is capable of binding to CD209a expressed by BM M ϕ . This causes a reduction in the tumor necrosis factor (TNF) mediated CXCR4-CXCL12 production causing HSPC mobilization (Lu, Chen et al. 2016). During hematopoietic stress caused by infection, a cytokine called Interferon- γ (IFN- γ) was also shown to act on M ϕ to negatively regulate HSC numbers and function (McCabe, Zhang et al. 2015). Furthermore, recent data suggests that alternative polarized M2 M ϕ promote, whereas, classical M1

M ϕ inhibit the self-renewal and expansion of HSC from mouse bone marrow (Luo, Shao et al. 2018). These studies indicate the importance of the various roles played by macrophages in the hematopoietic niche.

1.3.4 Other cellular components

There are several other cell types participating in the hematopoietic niche to maintain HSC function. These cell types are both non-hematopoietic as well as hematopoietic in origin. Mesenchymal stromal cells (MSC) which can differentiate into osteoblasts, adipocytes and chondrocytes are one of the active non-hematopoietic resident in the niche. It was demonstrated that intra-femoral injections of these MSC co-transplanted with HSC increased HSC self-renewal (Ahn, Park et al. 2010). Besides, an MSC subset defined as CAR cells are deemed essential for efficient retention of HSPC in the bone marrow (Ding, Saunders et al. 2012, Greenbaum, Hsu et al. 2013). Adipocytes on the other hand, even though they are MSC progeny are negative regulators of the hematopoietic niche. This has been demonstrated using A-ZIP/F 'fatless' mice which are incapable of making adipocytes and have accelerated marrow engraftment post irradiation compared to wild type mice (Naveiras, Nardi et al. 2009). The balance between MSC undergoing osteoblastogenesis versus adipogenesis is key in determining the fate of the hematopoietic niche.

Endothelial cells which are essential for vasculature are also an important part of the hematopoietic niche. They secrete paracrine factors such as stem cell factor (SCF) and CXCL12 to maintain hematopoiesis. Conditional depletion of these factors on Tie-2 endothelial cells are shown to reduce endogenous HSC numbers (Ding, Saunders et al. 2012, Greenbaum, Hsu et al. 2013). Additionally, *in vivo* ablation of endothelial cells disrupts thrombopoiesis (Avecilla, Hattori et al. 2004). On a different note, as described in

section 1.1, endothelial cell precursors play an important role in the ontogeny of HSC. Hemangioblasts, which are formed in the AGM have the capability to act as precursors for hemogenic endothelial cells. These cells are precursors for both HSC and endothelial cells. Hemogenic endothelial cells grow on the ventral wall of the aorta and bud off into HSC (North, De Bruijn et al. 2002, Lancrin, Sroczynska et al. 2009, Boisset and Robin 2010).

Neuronal and glial cells have also been implicated in stem cell maintenance via their impact on HSC mobilization. Convincing evidence exists regarding the sympathetic nervous system which controls the circadian rhythms of the body which in turn regulate CXCL12 production. This mechanism allows the nervous system to regulate HSC mobilization (Katayama, Battista et al. 2006, Mendez-Ferrer, Lucas et al. 2008). Furthermore, enzymatically truncated neurotransmitters such as neuropeptide Y are known to alter signaling in endothelial cells resulting in increased vascular permeability and HSPC egress (Singh, Hoggatt et al. 2017). Interestingly, non-myelinating Schwann cells are a major source of TGF- β in the bone marrow. Depletion of Schwann cells causes a loss in HSC quiescence and HSC numbers (Yamazaki, Ema et al. 2011). These data link the nervous system to HSC regulation in the bone marrow.

On the hematopoietic front, neutrophils are suggested to play a role in G-CSF induced HSC mobilization via their production of proteinases such as matrix metalloproteinase-9 (MMP9), neutrophil elastase and cathepsin G (Levesque, Takamatsu et al. 2001, Heissig, Hattori et al. 2002). It was hypothesized that neutrophil degranulation causes the release of these proteases which then cleaves stromal cells produced VCAM-1 and CXCL-12 leading up to HSPC mobilization. However, there is contradictory evidence regarding the same. Protease deficient mice were used to demonstrate that lack of the proteases

mentioned above did not affect G-CSF induced HSPC mobilization (Levesque, Liu et al. 2004). However, G-CSF does contribute to neutrophil expansion, which, through the increase of reactive oxygen species leads to the apoptosis of osteoblasts (Singh, Hu et al. 2012). Thus, G-CSF induced HSPC mobilization, neutrophil expansion and osteoblast apoptosis occur concomitantly, suggesting that neutrophils may have a protease independent role in G-CSF induced HSPC mobilization. Alternatively, neutrophil released proteases such as MMP9 are mechanistically involved in G-CSF independent HSPC mobilization induced by alternate mobilizers such as AMD3100 and GRO β (Hoggatt, Singh et al. 2018). Furthermore, there is evidence that IL-8 induced HSPC mobilization requires the activation of circulating neutrophils. This neutrophil regulation of HSPC mobilization is not dependent on degranulation and release of MMP9 (Pruijt, Verzaal et al. 2002). Other important players that are progeny of HSC are macrophages and megakaryocytes which have been discussed in the previous sections.

1.4 CD166 as a regulator of the hematopoietic niche

CD166 (ALCAM-Activated Leukocyte Cell Adhesion Molecule) is a transmembrane glycoprotein belonging to the immunoglobulin superfamily (Lehmann, Riethmuller et al. 1989). It is expressed both by mice and humans; and between them, their amino acid sequence is conserved by 93% (Bowen, Bajorath et al. 1997). CD166 is capable of mediating both homophilic interactions as well as heterophilic interactions with CD6 (Degen, van Kempen et al. 1998). It is found to be expressed on several hematopoietic cells including T cells (Zimmerman, Joosten et al. 2006), activated monocytes and macrophages (Masedunskas, King et al. 2006). It is even expressed on non-hematopoietic cells present in the niche such as osteoblasts, stromal cells and endothelial cells (Chitteti, Bethel et al. 2013). To date, this is the only marker which is identified to be expressed both on murine (Ohneda, Ohneda et al. 2001) and human HSC (Uchida, Yang et al. 1997);

bridging the gap between the two model systems (Chitteti, Cheng et al. 2010, Chitteti, Bethel et al. 2013, Chitteti, Kobayashi et al. 2014). In fact, using cell fractionation and CD166 knock out mice, it was demonstrated that the CD166+ fraction only, but not the CD166- fraction of murine HSC mediate robust engraftment in both primary and secondary transplants. The same results were observed while using the CD166+ fraction of human CD34+ cells, thus marking CD166 as an important molecular marker for HSC. Besides engraftment, CD166 is also demonstrated to play an important role during homing and recovery from hematopoietic stress (Chitteti, Kobayashi et al. 2014). This function is shown to be coupled with STAT3 activation.

CD166 is also expressed on several cells residing in the stem cell niche. It was demonstrated that CD166 expression on osteoblasts is inversely proportional to its maturity. Immature osteoblasts expressing higher CD166 maintain maximum hematopoietic enhancing activity compared to differentiated osteoblasts expressing lower levels of CD166 (Chitteti, Cheng et al. 2010, Chitteti, Cheng et al. 2013). Furthermore, MSC which can give rise to several mesodermal tissues also express CD166. In fact, CD166 acts as an accelerant of bone morphogenesis when added to MSC undergoing osteogenic differentiation (Bruder, Ricalton et al. 1998). In 2001, Ohneda et. al demonstrated that stromal cells and yolk sac endothelial cells express CD166. He also went on to demonstrate the importance of the expression of this marker to mediate embryonic hematopoiesis and vasculogenesis (Ohneda, Ohneda et al. 2001).

Normal expression of CD166 is important for the hematopoietic niche. However, aberrant expression of the same can give rise to osteosarcomas, melanomas, pancreatic cancers etc. (Degen, van Kempen et al. 1998, Kristiansen, Pilarsky et al. 2003, Federman, Chan et al. 2012). Even in the hematopoietic system, CD166 is overexpressed in B-lymphomas

(Zhang, Slaughter et al. 1995) and Hodgkin-lymphomas (Ma, Visser et al. 2008). Also, previous members in my laboratory have worked on the importance of CD166 expression for the prognosis of multiple myeloma. Osteolytic lesions indicate a poor prognosis of multiple myeloma. It was demonstrated that CD166+ myeloma cells alter bone remodeling by inhibiting osteoblastogenesis and increasing osteoclastogenesis. CD166 acts as a driver in homing of these multiple myeloma cells, thus guaranteeing its progression (Xu, Mohammad et al. 2016). These studies rationalize CD166 as an important therapeutic target for the possible treatment of multiple cancers.

1.5 Embigin as a regulator of the hematopoietic niche

Embigin is a transmembrane glycoprotein (gp70) belonging to the immunoglobulin superfamily (Huang, Ozawa et al. 1990, Huang, Ozawa et al. 1993). It is expressed on several hematopoietic cells including bone marrow progenitors, T cells and several myeloid cells; and is specifically repressed by Pax5 which is expressed on B cells (Pridans, Holmes et al. 2008). Functionally, embigin is essential for the expression of monocarboxylate transporter-2 on the plasma membrane. This transporter is important for the exchange of protons during anaerobic respiration in neurons (Wilson, Kraus et al. 2013). In fact, embigin is shown to be involved in neuromuscular synapse formation (Lain, Carnejac et al. 2009).

In a report by Silberstein et al., osteolineage cells proximal and distal to HSPC were isolated for further characterization of their mRNA profile. Proximal osteolineage cells were defined as the nearest cell within two cell diameters of HSPC; and were runx2+, osterix+, col1a+, osteopontin low and osteocalcin low. Distal osteolineage cells were defined as cells which were at least five cell diameters away from HSPC. Furthermore, proximal osteolineage cells had increased mRNA expression of embigin, angiogenin and

IL-18 compared to distal osteolineage cells. Silberstein et al. went on to demonstrate how angiogenin regulates LT-HSC quiescence, self-renewal and myeloid proliferation; whereas IL-18 regulates ST-HSPC quiescence. Blocking embigin in the hematopoietic niche results in loss of quiescence with a corresponding increase in the frequency of LT-HSCs, ST-HSCs, as well as MPPs (Silberstein, Goncalves et al. 2016). Embigin, being a cell adhesion molecule (Huang, Ozawa et al. 1993), even causes a loss in HSPC localization (Silberstein, Goncalves et al. 2016). Overall, this was the first group implicating embigin as a regulator of hematopoiesis. However, the osteolineage cells in the hematopoietic niche responsible for these effects of embigin are still relatively unknown and were poorly defined in the studies of Silberstein et. al. (Silberstein, Goncalves et al. 2016).

1.6 Significance of the hematopoietic niche

Networking between HSC and cells of the hematopoietic niche is critical for the maintenance of stem cell renewal and function. HSC maintenance in the hematopoietic niche is considered to be the product of intimate interactions between cellular and soluble elements of the niche and stem cells. Crosstalk between these niche elements; especially OM, osteoblasts and megakaryocytes is essential for the maintenance of the niche (Mohamad, Xu et al. 2017). If any of the niche components is functionally missing or cannot interact with other critically relevant components, it would hinder HSC from attaining maximal function and also compromise the hematopoietic niche (Visnjic, Kalajzic et al. 2004, Winkler, Sims et al. 2010, Chow, Huggins et al. 2013). Diabetes is an example of a disease which causes a major alteration in the hematopoietic niche. It affects BM architecture and function by altering both the endosteal and vascular niche. This leads to impaired HSPC mobilization and causes a decrease in the circulating pool of regenerative HSPC (Fadini, Ferraro et al. 2014). A compromised niche also results from diseased

conditions such as osteoporosis. Such alterations cause genetic mutations and reorganize the niche which could lead to malignancies and/or hematopoietic disorders. A befitting example of a genetic mutation disrupting the hematopoietic niche is that of mice deficient in the retinoblastoma gene or the retinoic acid receptor (Walkley, Olsen et al. 2007, Walkley, Shea et al. 2007). These genetic changes alter the BM microenvironment leading to myelodysplasia. Another example is the activation of β -catenin (Kode, Manavalan et al. 2014) or PTH receptor (Krause, Fulzele et al. 2013) in osteoblasts which can induce acute myelogenous leukemia in mouse transplantation models. Alternatively, abnormal upregulation of CD166 in primary bone marrow cells is a hallmark of multiple myeloma. As mentioned before, CD166 upregulation in multiple myeloma cells promotes osteoclastogenesis and inhibits osteoblastogenesis thus disrupting the hematopoietic niche (Xu, Mohammad et al. 2016). Such examples dictate that the dysregulation of the hematopoietic niche could be devastating leading to malignancies such as leukemia and lymphomas amongst others.

Another reason for a compromised niche is aging. With age, there is an increased number of phenotypically defined HSC both in human (Pang, Price et al. 2011) as well as C57BL/6 mice (Rossi, Bryder et al. 2005). However, the increased number of HSC appear to be dysfunctional with reduced self-renewing capacity (Janzen, Forkert et al. 2006) and increased myeloid skewing (Gekas and Graf 2013). One of the reasons for this change are age-induced alterations in the hematopoietic niche. This includes decreased bone formation, increased adipogenesis and changes in the transcriptional regulation of HSC (Bethel, Chitteti et al. 2013, Latchney and Calvi 2016). Increased adipogenesis is inversely correlated with CXCL12 expression. Decreased CXCL12 expression causes increased mobilization of HSC to the peripheral blood (Tuljapurkar, McGuire et al. 2011). Changes

in the hematopoietic niche with age also promote progression of leukemias (Vas, Wandhoff et al. 2012).

Another significant focus of hematopoietic niche research is bone marrow transplantation. Currently, bone marrow transplantation is used as a mode of treatment for several blood cancers and genetic disorders. My work involves identifying the molecular pathways through which OM maintain its function in the niche. The ultimate objective is to effectively use modulators to substitute for OM activity and enhance HSC function leading to increased efficiency of bone marrow transplantations. The premise that OM are important residents of the hematopoietic niche is important in understanding the crosstalk between cellular components within the niche; and is also an unexplored pathway critical to the maintenance of hematopoiesis.

CHAPTER TWO: Methods

2.1 Mice

C57BL/6J mice which were 2-3 day old in age were used to prepare neonatal calvarial cells (NCC) which consist of OM and osteoblasts. The long bones of the same mice were used to prepare neonatal bone marrow (NBM) from which bone marrow-derived macrophages (BM M ϕ) were isolated. Certain experiments required the isolation of CD166 knockout OM. CD166 KO mice on a C57BL/6 background were used to prepare the neonatal calvarial cells from which CD166 KO OM were isolated. All megakaryocytes were prepared from fetal livers. C57BL/6J mice which were 8-12 wk in age were used for the isolation of adult OM, BM M ϕ and LSK cells. Competitive repopulation assays were performed using C57BL/6J mice as donors, BoyJ mice as competitors and C57BL/6J X BoyJ F1 mice as recipients. Fgd5 mice (8-12 wk in age) (courtesy of Dr. Louis Pelus, Indiana University) were used to perform 3D tissue cytometry. All mice were bred and housed at Indiana University School of Medicine.

2.2 Cells

Cells were prepared as described below. These protocols are available with more details in Methods in Molecular Biology (Ghosh, Mohamad et al. 2019).

2.2.1 Preparation of fresh neonatal calvarial cells

Calvariae from 2-3 day old pups were dissected and all associated soft tissues were removed. These calvariae were then pretreated with 4mM EDTA in phosphate buffer saline (PBS) for 10 mins at 37°C followed by a PBS wash. The pretreatment step was repeated twice. The pretreated calvariae were then digested using 5ml of collagenase,

type 2 (Worthington Biochemicals, Lakewood NJ). The first two digestions were performed for 10 mins at 37°C in a water bath shaker. The supernatant from both these digestions was discarded. The next three digestions were performed for 15 mins at 37°C in a water bath shaker. The supernatant from each of these digestions was transferred to a tube containing 25ml of complete α -MEM medium (α -MEM+ 10% fetal bovine serum +1% penicillin/streptomycin). At the end of the three digestions, the tube containing the digestion supernatant and complete α -MEM medium was centrifuged at 2000 rpm for 6 mins at 4°C. The cells in the pellet are neonatal calvarial cells. The pellet was resuspended in 10ml of complete α -MEM medium and the cells were counted using a hemocytometer. These NCC are 90-95% osteoblasts or osteoblast precursors and ~5% OM.

2.2.2 Preparation of fresh neonatal bone marrow

The same 2-3 day old decapitated pups which were used to make NCC were also used to make NBM. The hind limbs from these pups were dissected and kept in Iscove's Modified Dulbecco's Medium (IMDM). Using sterile forceps, the skin was removed, and sterile gauze was used to manually separate muscle from bone. The bone, once separated from muscle, was cut into small pieces and transferred to a sterile mortar containing 2-3ml of IMDM. Next, a sterile pestle was used to gently crush the bone and release the marrow from within the bone. The supernatant accumulated in the mortar was transferred to a 50ml tube. Fresh 2-3ml IMDM was again added to the mortar and the bones were crushed gently once more to further release the marrow. The bones were crushed for a total of 3 rounds and the supernatant from each round was transferred to the same 50ml tube. The collected supernatant was centrifuged at 1800 rpm for 10 mins at 4°C. Once centrifuged, the supernatant was discarded, and the cell pellet was subjected to RBC lysis. 2ml of RBC lysis buffer (Invitrogen, Carlsbad, CA) was added to the cell pellet followed by incubation at room temperature for 3-4 mins. To stop the RBC lysis,

10ml of complete IMDM medium (IMDM+ 10% fetal bovine serum +1% penicillin/streptomycin +1% glutamax) was added to the cells. The tube was centrifuged, and the pellet was reconstituted in 10ml complete IMDM medium. Total cell counts were calculated using a hemocytometer.

2.2.3 Preparation of fetal liver-derived megakaryocytes

Megakaryocytes were prepared from murine fetal livers as previously described (Kacena, Shivdasani et al. 2004, Kacena, Eleniste et al. 2012). Fetuses were dissected from pregnant mice on E13-15. The livers were removed and made into a single cell suspension using first an 18 gauge followed by 20 and 23 gauge needles. Cells were washed for a total of two times using complete Dulbecco's Modified Eagle Medium (DMEM) (DMEM+ 10% fetal bovine serum +1% penicillin/streptomycin +1% murine thrombopoietin). Washed cells were cultured in complete DMEM medium in 10cm culture dishes (5 fetal livers/ dish). Cells became confluent within 3-5 days of culture. At this point albumin gradients were set up to separate megakaryocytes from lymphocytes and other cells. The bottom layer of the gradient consisted of 3% albumin in PBS (bovine albumin, protease-free and fatty acid-poor, Serological Proteins Inc., Kankakee, IL); the middle layer was 1.5% albumin in PBS, and the top layer was media containing the cells to be separated. The cells were sedimented through the layers at 1 x g for ~90 mins. The megakaryocyte rich fraction was sedimented to the bottom of the tube. These cells were collected and then used for tissue culture experiments.

2.2.4 Preparation of 8-12 wk bone marrow

To isolate bone marrow, hind limbs (2 femurs and 2 tibias) from 8-12 wk old C57BL/6J mice were dissected and stored in a sterile tissue culture plate containing 10ml IMDM. A pair of forceps and a sterile gauze were then used to strip the muscle off these bones.

The stripped bones were transferred to a new tissue culture plate containing IMDM. Using a 10ml syringe with a 25 gauge needle, complete IMDM medium was aspirated. This syringe containing IMDM was then inserted into the stripped bones to flush the bone marrow from within. The flushing process was repeated until all the bone marrow was released at which point the bone changed color from red to pale. The bone marrow was prepared into a single cell suspension by repeated aspiration, collected in 50ml tubes, and was centrifuged at 1800 rpm for 10 mins at 4°C. The supernatant was discarded, and the cell pellet was resuspended in 2ml of RBC lysis buffer which was incubated at room temperature for 3-4 mins. To stop the RBC lysis, 10ml of complete IMDM medium was added to the tube followed by centrifugation. The cell pellet was resuspended in 10ml of complete IMDM medium and counted using a hemocytometer. This bone marrow preparation was used to isolate bone marrow macrophages from adult and for flow cytometric analysis.

Bone marrow was lineage depleted to isolate LSK cells for colony forming assays and competitive repopulation assays. MagCelect™ Mouse Hematopoietic Cell Lineage Depletion Kit from R&D Systems (Minneapolis, MN) was used to isolate lineage depleted cells. Briefly, 100 million RBC lysed bone marrow cells were resuspended in 5ml of 1X MagCelect Buffer. Then, 50µl of Blocking Reagent-1 was added to these cells followed by incubation at 4°C for 15 mins. After the blocking step, 100µl of Mouse Cell Lineage Depletion Biotinylated Antibody Cocktail was added and incubated at 4°C for 15 mins. Excess antibody was washed away by adding 10ml of 1X MagCelect Buffer followed by centrifugation. The supernatant was discarded and 150µl of Streptavidin Ferrofluid was added to the cell pellet which was again incubated at 4°C for 15 mins. At the end of the incubation period, the volume was brought up to 2ml and those 2ml were transferred to a 5ml round bottom tube. The tube was placed in a magnet (Stemcell Technologies,

Vancouver, Canada) designed to accommodate 5ml tubes. Once in the magnet the tube was incubated at room temperature for 6 mins. Magnetically tagged lineage positive cells migrated towards the walls of the tube leaving the lineage negative cells in suspension in the supernatant. At the end of the 6 min incubation, the supernatant was carefully removed and transferred to a new tube. When required, a second magnetic separation was performed. Lineage depleted cells were counted using a hemocytometer and stained for flow cytometric sorting to isolate LSK cells.

2.2.5 Preparation of 8-12 wk digested bone

Long bones from 8-12 wk mice, which were previously flushed as described above, were used to obtain digested bone. Flushed bones were cut into small pieces approximately 1mm long; and the cut pieces were transferred to a 15ml tube containing 5ml of sterile PBS. Bones from around 1-3 mice could be transferred to the same 15ml tube. The tube was thoroughly vortexed for 30 secs after which the PBS supernatant was discarded. The bones were then subjected to digestion by adding 2ml of collagenase for 15 mins at 37°C in a water bath shaker. For optimum results, the tube was vortexed every 5 mins. At the end of the first digestion, the supernatant was transferred to a 50ml tube through a 70µm cell strainer. To stop the digestion, 5ml of complete αMEM medium (αMEM +10% fetal bovine serum +1% penicillin/streptomycin +1% glutamax) was added and the tube was kept on ice. A total of 5 such digestions were performed. The combined supernatant from these 5 digestions was transferred to the same 50ml tube containing complete αMEM medium. At the end of the digestions, the 50ml tube was centrifuged at 1800 rpm for 10 mins at 4°C. The supernatant was discarded, and the cells were resuspended in 10ml of complete αMEM medium. Total cell counts were calculated using a hemocytometer. Single cell preparation from digested bone was processed to obtain adult OM and osteoblasts by cell sorting and as described below.

2.3 Cell staining, flow cytometry and cell sorting

Cells were washed with sterile cell stain wash (1% Bovine Serum in 1X PBS) at 1800 rpm for 10 mins at 4°C. Supernatant was discarded and the cell pellet was stained with the appropriate antibodies listed in Table 2.1. OM from NCC or 8 wk digested bone, as well as BM Mφ from NBM and 8 wk bone marrow were identified as CD45+F4/80+. Neonatal osteoblasts were identified as CD45-F4/80- whereas, 8 wk osteoblasts were lineage (Ter119, CD31, Sca-1)-CD45-F4/80-. Adult 8 wk bone marrow was also stained to sort for LSK cells which were Lin-Sca1+ckit+. The lineage cocktail for the LSK cells consisted of CD4, CD45R, CD3, Gr-1 and Ter-119. The other antibodies listed in Table 2.1 were all used for cell analysis. All antibodies were purchased from Biolegend (San Diego, CA) except for CD166 and Embigin which was purchased from eBiosciences (San Diego, CA) and CD110 from Immuno-Biological Laboratories, Japan. To stain for the respective experiments, 0.5-1µg of antibody was added per million cells. Cells were then incubated for 15 mins at 4°C after which they were washed with 2ml of cell stain wash. The supernatant was discarded, and the pellet was resuspended in stain wash as 10 million cells/ml. BD SORP Aria, Facs Aria and Facs Fusion were used to sort cells. LSR II, FACS Fortessa and FACS X20 were used for cell analysis.

Table 2.1 List of fluorophore conjugated antibodies used in this study.

Antibody	Fluorophore	Clone
CD45	FITC/ PE-Cy7/ Pacific Blue	30-F11
F4/80	APC	BM8
CD11b	PE/ APC-Cy7	M1/70
CD14	PE	rmC5-3
CD31	PE/ FITC	MEC 13.3
CD150	PE	TC15-12F12.2
CD68	PE/ Percp-Cy5.5	FA-11
CD34	PE	MEC14.7
CD169	BV605	3D6.112
Ly6G	PE-Texas Red	1A8
Mac2	AF488	M3/38
CD166	PE	eBioALC48
CSF1R	PE-Cy7	AFS98
CD110	Biotin	AMM2
Streptavidin	Pacific Blue	
Lineage Cocktail (LSK)	FITC/ PE	
Sca-1	FITC/ PE	D7
c-kit	APC	2B8
Ter-119	PE/ FITC	TER-119
CD41	FITC/ PE/ Biotin	MWReg30
CD45.1	FITC	A20
CD45.2	APC	104
Embigin	PE	G7.43.1

2.4 Phagocytosis assay

Phagocytosis assay was performed using pHrodo™ Red BioParticles® (Life Technologies, Carlsbad, CA). Briefly, digested bone and bone marrow were sorted using CD45 and F4/80 to isolate adult OM and BM Mφ respectively. These cells were resuspended as 75,000-100,000 cells per 100µl of complete αMEM medium (+10ng/ml of MCSF1). Cells were then cultured in a 96-well plate overnight at 37°C. This step was performed to let the macrophages adhere to the tissue culture plate. The next day, pHrodo™ Red BioParticles® were resuspended in 2ml of live imaging solution (Thermo Scientific, Waltham, MA). After resuspension, this solution contained 1mg/ml of lyophilized *E. coli*. The suspension was sonicated for 5 mins until all the fluorescent particles were homogenously dispersed.

After the cells adhered to the tissue culture plate, supernatant media from each of the wells was removed. Three of the OM wells and three of the BM Mφ wells were supplemented with 100µl of complete αMEM medium and used as a negative control. The remaining three OM wells and three BM Mφ wells were supplemented with 100µl of the pHrodo Bioparticle solution. The culture plate was incubated at 37°C for 1–2 hours to allow phagocytosis and acidification to reach its maximum. Post incubation, cells were collected and analyzed using a flow cytometer. Red BioParticles were excited with 488nm and emission was collected at 575nm. Images of the same were collected using ImageStream (Amnis, Seattle, WA).

2.5 Single cell qRT-PCR

2.5.1 Data collection

The procedure for data collection for single cell qRT-PCR has been previously described (Anjanappa, Cardoso et al. 2017). The C1 Single-Cell Auto prep System (Fluidigm, San

Francisco, CA) was used for capturing single cells and preparing cDNA followed by fast gene expression analysis using EvaGreen on the BioMark HD System (Fluidigm). Instructions for the same are provided online (PN 100-4904 I1). Briefly, a pool of 100 μ M primers (Fluidigm) were prepared, which was followed by preparation of the lysis final mix, reverse transcription final mix and preamp final mix. Each mix was prepared as per manufacturer's instructions (Fluidigm). Next, the size of OM and BM M ϕ was measured on an automated cell counter (Countess, Invitrogen) to determine the C1 chip needed to capture single cells. Based on the sizing, a C1 Integrated Fluidic Circuit chip (IFC) for PreAmp (10-17 μ m) for OM and a C1 IFC for PreAmp (5-10 μ m) for BM M ϕ was primed. To prime the IFC chip, 200 μ l of the C1 harvest reagent was pipetted at the center of the IFC chip and 20 μ l of the same into each of the wells located to the sides. 20 μ l of the preloading reagent was added in the purple inlet, 15 μ l of blocking reagent in the white inlet and 20 μ l of cell wash buffer in the grey inlets followed by running it on the STA: Prime program on the C1.

Simultaneously, cells were resuspended to a concentration of 200,000 cells/ml. These resuspended cells were mixed with the suspension reagent in a 3:2 ratio to prepare the final cell mix which was loaded onto the primed IFC. The IFC was placed onto the C1 and run using the STA: Cell Load script to capture single cells. The single cells were viewed under the microscope to identify and exclude capture sites which were empty, had 2 cells in 1 site or had debris. The IFC chip with the captured single cells was then loaded with 7 μ l of lysis final mix, 7 μ l of RT final mix and 24 μ l of PreAmp final mix. This was again placed into the C1 system to run the STA: PreAmp script. At the end of this program, the mRNA from the single cells was reverse transcribed into cDNA and pre-amplified into the product that would finally be subjected to gene expression analysis.

The BioMark HD system (Fluidigm) (protocol 68000088 K1) was used to perform 90 individual qRT-PCR reactions on the harvested product from every single cell captured on the IFC. A 96.96 dynamic array IFC was primed using the Prime (136X) script on the Juno system (Fluidigm). Next, the harvested product was combined with 2X SsoFast EvaGreen Supermix (Bio-Rad, Hercules, CA) and 20X DNA binding dye sample loading reagent (Fluidigm, #100-3738) to prepare the sample pre-mix. This pre-mix was then loaded on one side of the primed IFC BioMark chip. On the other side of the same chip, the assay mix which contained 2X loading reagent, 1X DNA suspension buffer and 100 μ M each of mixed forward and reverse primers was loaded. The Juno system was used to distribute the assay mix and the sample pre-mix into individual reaction chambers inside the IFC. The IFC was then transferred to the BioMark HD where individual gene expression was quantified at the single cell level.

2.5.2 Data analysis of single cell qRT-PCR

Singular Analysis Toolset available on the Fluidigm website was used to analyze the data files generated using the BioMark HD System. This toolset was only compatible when used with the software R (Version 3.0.2). Principal component analysis plots were used to determine outliers within the single cell OM group and single cell BM M ϕ group. Differentially expressed genes were identified between OM and BM M ϕ using one-way ANOVA. Violin plots and heat maps were created to further compare the two cell types.

2.6 Single cell mRNA sequencing

2.6.1 Data collection

Single cell mRNA sequencing (scRNA-seq) was performed on OM cultured in the presence and absence of megakaryocytes. Briefly, 100,000 NCC (resuspended in complete α MEM) were cultured with or without 50,000 megakaryocytes for 16 hrs in a 12

well plate. After culture, the cells were trypsinized and stained for CD45 and F4/80. OM from each of these two groups were sorted out using flow cytometry (CD45+F4/80+) and these OM from NCC and NCC +megakaryocytes were analyzed for differential gene expression analysis. To do so, sorted cells from each group were suspended in PBS at a final cell density of 300,000 cells/ml. The cell suspension was then dispensed into individual medium sized IFC chips of the Fluidigm C1 Single-Cell Auto Prep System for scRNA-seq (Fluidigm Corporation) (Zhang, Ghosh et al. 2019). The principle and procedure for the single cell capture was almost the same as the one described above for the single cell qRT-PCR. mRNA was isolated from the single cells that were captured, which was followed by cDNA synthesis using the protocol for the Clontech SMART-Seq v4 Ultra Low Input RNA Kit for Fluidigm C1 System. Furthermore, cDNA was quantified using the PicoGreen Kit (Thermo Fisher); and up to 0.4ng of the quantified cDNA was used for library preparation and indexing using the Nextera XT DNA Library Prep Kit (Illumina, Inc., San Diego, CA). Quality of the libraries was assessed by the Qubit and Agilent Bioanalyzer after which 5µl of 4nM pooled libraries were used for 150b paired-end sequencing on NextSeq 500.

2.6.2 scRNA-seq data analysis

Raw fastq files of the scRNA-seq data were mapped to mm10 mouse genome by using STAR pipeline [23104886]. Cells with observed genes smaller than 500 and larger than 8000, and cells with more than 10% reads mapped to mitochondrial genes were excluded from further analysis. 21 OM sorted from cultured NCC, and 24 OM sorted from cultured NCC+ megakaryocytes were retained. Cell type cluster analysis were conducted by using Seurat with default parameters [25867923]. Differential gene expression analysis were conducted by an in-house method LTMG-DGE [<https://academic.oup.com/nar/advance-article/doi/10.1093/nar/gkz655/5542876>] with $p < 0.001$ as significance cutoff.

2.7 Mass cytometry (CyTOF)

2.7.1 Custom conjugation of CyTOF antibodies

The antibodies used in this study, along with their clones are listed in Table 2.2. All pre-conjugated antibodies and most custom conjugated antibodies were purchased from DVS sciences, Fluidigm. Certain antibodies (6 of the 30) were conjugated in house using the Maxpar Antibody Labeling kit (Fluidigm). The main components of the kit were the lanthanide solution which consisted of the metal that needed to be conjugated to the antibody; and the Maxpar Polymer which formed the link between the metal and the antibody.

Step 1: The protocol began by resuspending the polymer with 95 μ l of L-buffer. Next, 5 μ l of lanthanide metal solution was added to the same tube; after which the tube was incubated at 37°C for 30-40 mins in a water bath.

Step 2: Simultaneously, 100 μ g of the desired antibody was added in up to 400 μ l of R-buffer to a 50kDa column filter. This was centrifuged at 12,000 x *g* for 10 mins at room temperature. The flow-through in the column was discarded and 100 μ l of 4mM TCEP-R-buffer (Thermo Scientific) was added to the antibody in the filter. This was followed by incubating the tube at 37°C for 30 mins in a water bath (Do not exceed 30 mins!!)

Step 3: Next, 200 μ l of L-buffer was added to a 3kDa filter. The tube from step 1 which contained the polymer and lanthanide solution was transferred to the same 3kDa filter. The tube was centrifuged at 12,000 x *g* for 25 mins at room temperature; and further washed with 400 μ l of C-buffer for 30 mins.

Step 4: The 50kDa filter containing the partially reduced antibody was retrieved and the filter was washed twice with 400µl of C-buffer at 12,000 x *g* for 10 mins at room temperature.

It is imperative that step 3 and step 4 are completed at the same time.

Step 5: The lanthanide loaded polymer was resuspended in 60µl of C-buffer and transferred to the 50kDa filter containing the partially reduced antibody. To let the conjugation occur, the filter was incubated at 37°C for 90 mins.

Step 6: The conjugation mixture was washed for a total of 4 times using 400µl of W-buffer after which the yield of the conjugated antibody was determined using a nanodrop (Thermo Scientific). The antibody was resuspended at 0.5µg/µl in antibody stabilizer (CANDOR Bioscience, Germany) with 0.05% sodium azide.

Each of the 30 antibodies was titrated to determine optimal concentration to label NCC and NBM.

2.7.2 Staining protocol for cell surface and intracellular antibodies

Four groups of cells were stained and analyzed for CyTOF. For the first two groups, freshly processed NCC and NBM were analyzed to phenotypically differentiate OM from BM Mφ. The second aim was to differentiate OM cultured in the presence and absence of megakaryocytes. To do this, 1 million NCC (resuspended in complete αMEM) were cultured per well in a 6 well plate. Half of these wells were cultured in the presence of 500,000 megakaryocytes per well and the other half were cultured in the absence of megakaryocytes. Cells were cultured for a total of 2 days at 37°C. On the day of CyTOF

stain, fresh NCC and NBM were plated in a 6 well plate (2-3 million cells/well) and all 4 groups were treated with 10ug/ml of Brefeldin A (Sigma-Aldrich, St. Louis, MO) in a 37°C incubator for 3 hrs to inhibit protein transport. Following stimulation with Brefeldin A, 3.5 million cells were resuspended in 400µl of PBS and transferred to a 5ml round bottom tube. These cells were stained with 0.4µl of Cell-ID Cisplatin viability dye (DVS Sciences, Fluidigm) for 2 mins at room temperature. Cells were washed at 1800 rpm for 10 mins at 4°C using 2ml of stain wash (0.1% BSA, 0.1% Na-Azide, 10nM EDTA in 1X PBS). The supernatant was discarded, and 1µl of Fc-Receptor blocking solution (Biolegend) was added to the cell pellet for 5 mins. Following the block, cells were stained with a master mix of primary fluorophore antibodies (refer Table 2.2) at 4°C for 20 mins. Cells were washed using stain wash and then stained with a master mix containing extracellular metal-labeled antibodies (refer Table 2.2) at 4°C for 30 mins. After surface staining, cells were washed using stain wash and then fixed with 1ml of 1.5% formaldehyde for 30 mins at room temperature. Two 10 min washes with Maxpar Perm-S Buffer (DVS Sciences, Fluidigm) were performed to permeabilize cells. Next, cells were stained with a master mix containing intracellular metal-labeled antibodies at 4°C for 30 mins. Following incubation, cells were washed using stain wash and incubated overnight in 1:1000 Cell-ID Intercalator-Ir diluted in Maxpar Fix and Perm buffer (DVS, Sciences, Fluidigm). The next day, the cells were washed once with stain wash and twice with Millipore water followed by resuspension in 1X EQ Calibration beads (DVS, Sciences, Fluidigm). Samples were acquired on a CyTOF 2 mass cytometer (DVS, Sciences, Fluidigm). The bead signature was used to normalize raw CyTOF data before analysis on Cytobank software.

2.7.3 ViSNE analysis of normalized CyTOF events

The exported files were gated on singlet viable cells based on DNA labeling with iridium (Ir191/193), event length and cisplatin (Pt195). NCC and NBM samples were then gated

on CD45+F4/80+ cells to identify OM and BM M ϕ respectively. These gated CD45+F4/80+ cells were used to make viSNE plots and heatmaps on Cytobank software. Each antibody was further annotated on the viSNE plots to determine phenotypic differences between OM and BM-derived macrophages. The scale is the mean marker intensity of arcsinh transformed values.

Table 2.2 List of metal conjugated CyTOF antibodies used in this study.

Antibody	Metal	Extra/Intracellular	Clone
CD45	147Sm	Extracellular	30-F11
CD14	156Gd	Extracellular	Sa 14-2
CD166	151Eu	Extracellular	eBioALC48
CD11b	154Sm	Extracellular	M1/70
CD169	170Er	Extracellular	3D6.112
CD206	173Yb	Extracellular	C068C2
CD41	143Nd	Extracellular	MWReg30
Mac2	153Eu	Extracellular	M3/38
CD86	172Yb	Extracellular	GL1
F4/80	146Nd	Extracellular	BM8
Ly6G-FITC (Anti-FITC metal)	144Nd	Extracellular	1A8
Embigin-PE (Anti-PE metal)	145Nd	Extracellular	G7.43.1
VCAM1-APC (Anti-APC metal)	176Yb	Extracellular	429 (MVCAM.A)
CSF1R	152Sm	Extracellular	AFS98
VEGFR3	160Gd	Extracellular	Custom Clone
CD130	166Er	Extracellular	4H1B35
CD143	155Gd	Extracellular	Custom Clone
SDF1	165Ho	Intracellular	79018
PDGF- β	169Tm	Intracellular	Polyclonal
MCP1	171Yb	Intracellular	2H5

Antibody	Metal	Extra/Intracellular	Clone
TGF- β	164Dy	Intracellular	TW7-16B4
FGF2	141Pr	Intracellular	MC-GF1
IGF1	174Yb	Intracellular	Polyclonal
IL-18	159Tb	Intracellular	12E7.1
TNF- α	162Dy	Intracellular	MP6-XT22
pSTAT3	158Gd	Intracellular	4/P-STAT3
Ikzf1	175Lu	Intracellular	2A9
Lmo-2-Biotin (Anti-Biotin metal)	150Nd	Intracellular	aa35-84
Fli-1	149Sm	Intracellular	Polyclonal
PF-4	142 Nd	Intracellular	RM0210-14M15

2.8 Quantitative global proteomic comparison of protein levels in OM obtained from fresh NCC and NCC cultured in the absence and presence of megakaryocytes

Three groups of cells were quantitatively compared for their protein levels using three biologically distinct replicate cell cultures for each group. Briefly, the groups are-1) fresh OM sorted from NCC (from now on will be referred to as “Fresh NCC”); 2) OM sorted from cultured NCC in the absence of megakaryocytes (from now on will be referred to as “NCC”); and 3) OM sorted from cultured NCC in the presence of megakaryocytes (from now on will be referred to as “NCC+MK”). Sample preparation, mass spectrometry analysis, bioinformatics and data evaluation were performed in collaboration with the Proteomics Core Facility at the Indiana University School of Medicine (IUSM), 635 Barnhill Drive, Medical Science Building 0034, Indianapolis, IN 46202-5122, U.S.A. Methods described below in brief were adaptations from literature reports published elsewhere (Mosley, Florens et al. 2009, Mosley, Sardiou et al. 2011, Smith-Kinnaman, Berna et al. 2014, Wijeratne, Xiao et al. 2018, Yamamoto, Bone et al. 2019) and vendor provided protocols.

2.8.1 Cell lysis, protein assay and proteolytic digestion

Pelleted cells mobilized in 8M urea in 100mM Tris.HCl (25µL) in 1.5mL Micro Tubes (TPX Plastic for Sonication from Diagende Inc.) were subjected to sonication using a Bioruptor® sonication system from Diagende Inc. USA, North America with 30 secs/30 secs on/off cycles for 15 mins in a cold water bath kept at 4°C. Protein concentrations of each sample was then determined using a Bradford protein assay (BioRad) and colorimeter-EPOCH|2 (BioTek Instruments, Inc., Winooski, VT 05404-0998, U.S.A.) employing vendor provided protocols. Protein samples in equal amounts (2.5µg) were next subjected to reduction of Cys-Cys bonds of proteins with 5mM tris(2-carboxyethyl)phosphine hydrochloride (TCEP), and alkylation with 10mM chloroacetamide (CAM) to protect the reduced Cys residues, followed by dilution of the solution to archive 2M urea concentration using 100mM Tris.HCl. Overnight proteolytic digestion using 0.2µg Trypsin/Lys-C Mix Mass Spectrometry Grade for each sample (Promega Corporation, Madison, WI 53711-5399, U.S.A.) was then carried out as described (Mosley, Florens et al. 2009, Mosley, Sardi et al. 2011, Smith-Kinnaman, Berna et al. 2014) to derive peptides.

2.8.2 “De-salting” of peptides from other low molecular weight organic matter and salts

Resulting peptides were “de-salted” using Sep-Pak® Vac 1cc C18 Cartridges, 50mg Sorbent per Cartridge, 55-105µm Particle Size (Waters Corporation Milford, MA 01757, U.S.A.) employing a vacuum manifold (Waters Corporation Milford, MA 01757, U.S.A.). Briefly, columns adapted onto the extraction manifold were first washed sequentially with (1) ACN (500µL)-two times, (2) ACN/H₂O 70/30 (v/v; 0.1% FA; 200µL)-one time, and (3) MS-grade water (500µL)-two times. Peptides from each “digestion” solution were then subjected to immobilization on C18 material by a gentle application of vacuum into the extraction manifold vacuum chamber to move each solution three times by collecting the

“flow-through” fractions and running them again on to the same column. Next, the peptide-bound C18 columns were washed with 500 μ L of MS-Grade H₂O and then eluted by passing 150 μ L of ACN/H₂O 70/30 (v/v; 0.1% FA) three times. All elution fractions were collected into 1.5mL eppendorf tubes and subjected to complete dryness using a speed vacuum system.

2.8.3 Tandem Mass Tags (TMT) based peptide labelling, reaction quenching and mixing

The respective dried samples were then subjected to TMT (Tandem Mass Tags) based labelling using a tenplex kit (TMT10plex™ Isobaric Label Reagent Set, 8 x 0.2mg; lot no. UC276347). The TMT channels-TMT126, TMT127N, TMT127C, and TMT128N, were employed for the labelling of four “NCC” samples; the TMT channels-TMT128C, TMT129N, and TMT129C were employed for the labelling of three “NCC+MK” samples and the TMT channels-TMT130N, TMT130C, and TMT131 were employed for the labelling of three “Fresh NCC” samples. Briefly, each dried sample was reconstituted in 100 μ L of 50mM triethylammonium bicarbonate (TEAB) and dry labelling reagents were dissolved in 40 μ L of acetonitrile (ACN). Reconstituted peptide solution were then moved to the respective labelling reagent-vials and kept at room temperature for overnight to label the peptides. Labelling reaction was next quenched by adding 8 μ L of 5% hydroxylamine and keeping the reaction mixture at room temperature for more than 15 mins. Labelled peptide solutions were then mixed together and subjected to complete dryness in a speed vacuum system.

2.8.4 “De-salting” of labelled peptide mixtures

Dried labelled peptide mixture was reconstituted in 200 μ L of 0.1% FA (Formic Acid) and subjected to the above mentioned desalting procedure described in **2.8.2**. The desalted,

eluted mixture that carries a higher percentage of acetonitrile was again subjected to complete dryness using a speed vacuum system prior to the below explained nano-LC-MS/MS analysis.

2.8.5 Nano-LC-MS/MS analysis

Nano-LC-MS/MS analyses were performed on an Orbitrap Fusion™ Lumos™ mass spectrometer (Thermo Fisher Scientific) coupled to an EASY-nLC™ HPLC system (Thermo Scientific). Labelled, mixed, and dried peptide samples were reconstituted in 0.1% formic acid (12µL) and 5µL equivalent volume was loaded (i.e. two technical replicate analyses) onto a reversed phase PepMap™ RSLC C18 column (2µm, 100Å, 75µm x 50cm) with Easy-Spray tip at 750 bar applied maximum pressure. The peptides were eluted using a varying mobile phase (MP) gradient from 94% phase A (FA/H₂O 0.1/99.9, v/v) to 28% phase B (FA/ACN 0.4/99.6, v/v) for 160 mins.; from 28% phase B to 35% phase B for 5 mins; from 35% phase B to 50% phase B for 14 mins to ensure elution of all peptides; and bringing down the MP-composition to 10% phase B for 1 min. at 400nL/min to bring the MP-composition to higher % of phase A. Nano-LC mobile phase was introduced into the mass spectrometer using an EASY-Spray™ Source (Thermo Scientific™). During peptide elution, the heated capillary temperature was kept at 275°C and ion spray voltage was kept at 2.5kV. The mass spectrometer method was operated in positive ion mode for 180 mins having a cycle time of 4 secs. MS data was acquired using a data-dependent acquisition method that was programmed to have 2 data dependent scan events following the first survey MS scan. During MS_n level 1, using a wide quadrupole isolation, survey scans were obtained with an Orbitrap resolution of 60 k with vendor defined parameters—m/z scan range, 400-1500; maximum injection time, 50; AGC target, 4E5; micro scans, 1; RF Lens(%), 30; “DataType”, profile; Polarity, Positive

with no source fragmentation and to include charge states 2 to 6 for fragmentation. Dynamic exclusion for fragmentation was kept at 60 secs.

During MSⁿ level 2, following vendor defined parameters were assigned to isolate and fragment the selected precursor ions. Isolation mode = Quadrupole; Isolation Offset = Off; Isolation Window = 1; Multi-notch Isolation = False; Scan Range Mode = Auto Normal; First Mass = 100; Activation Type = HCD; Collision Energy Mode = Fixed; Collision Energy (%) = 36 for the 1st replicate and 37 for the second replicate MS analysis; Detector Type = Orbitrap; Orbitrap Resolution = 50k; Data type = Centroid; Polarity = Positive; Source Fragmentation = False. The data were recorded using Thermo Scientific Xcalibur (4.1.31.9) software (Copyright 2017 Thermo Fisher Scientific Inc.).

2.8.6 Data analysis

Resulting RAW files were analyzed using Proteome Discover™ 2.2 (Thermo Scientific). A specific TMT 10plex quantification method was formulated using the tools available in Proteome Discover™ 2.2 to account for isotopic impurity levels provided by vendor (lot no. UC276347). The MS/MS spectra were searched against *in silico* tryptic digest of a *Mus musculus* proteins database (FASTA format) downloaded from the UniProt sequence database (v. June 2017) using the SEQUEST HT search engine. In order to carry out the search, following specific search parameters were applied to vendor provided “processing” and “consensus” workflow templates that correspond to Thermo “Fusion” instruments: Trypsin as the proteolytic enzyme; searched for peptides with a maximum number of 2 missed cleavages; precursor mass tolerance of 10ppm; and a fragment mass tolerance of 0.6Da. Static modifications used for the search were, 1) carbamidomethylation on cysteine(C) residues; 2) TMT sixplex label on lysine (K) residues and the N-termini of peptides. Dynamic modifications used for the search were oxidation of methionines and

acetylation of N-termini. Percolator False Discovery Rate was set to a strict setting of 0.01 and a relaxed setting of 0.05. Values from both unique and razor peptides were used for quantification. Peptides were normalized in Proteome Discover™ 2.2 (Thermo Scientific) using the “total peptide amount” option. Resulting “grouped” abundance values for each sample type; “abundance ratio” values; and respective “p-values (ANOVA)” from Proteome Discover™ were exported to Microsoft Excel and then to JMP® Pro 14.0.0 (64 bit), Copyright © 2018 SAS Institute Inc. to construct “Distribution” plots and “Volcano Plots” to screen out statistically increased or decreased proteins for each global proteomic comparison performed.

2.9 3D Tissue cytometry

3D tissue cytometry was used to determine the spatial location of OM, osteoblasts and megakaryocytes in relation to HSC. Fgd5 mice (8-12 wk in age) (courtesy of Dr. Louis Pelus, Indiana University) which are GFP+ for HSC and endothelial cells were used. These mice were anesthetized and fixative perfused using 4% paraformaldehyde to clear the RBCs from the blood stream. Next, mice were sacked, and the femur and tibia were dissected. Muscle from the hind limbs was stripped after which the bones were fixed overnight in 10% neutral buffer formalin, then transferred to 70% ethyl alcohol. Bones were then placed in decalcification buffer (10% EDTA, pH7.4) for two weeks, after which they were paraffin embedded. A microtome was used to make 25 micron sections. These sections were then stained for imaging.

To stain these sections, the paraffin embedding was first removed by incubating the sections in xylene (Honeywell Research Chemical, Mexico City, Mexico) for 10 mins at room temperature. This step was repeated thrice altogether and was followed by 5 mins incubation each in 100% ethyl alcohol, 95% ethyl alcohol, 75% ethyl alcohol, 50% ethyl

alcohol and 25% ethyl alcohol. The sections were washed twice in PBS for 5 mins at room temperature to get rid of the ethyl alcohol. Antigen retrieval was performed by incubating the sections in citrate buffer (10mM Citric Acid, 0.05% Tween-20, pH6.0) overnight in a 60°C water bath. The next day, the sections were washed twice in PBS at room temperature for 10 mins; followed by blocking the tissue in blocking buffer (5-10% BSA, 0.1% Tween-20 in PBS) at 4°C, overnight on a rotary shaker. On day 3, sections were incubated with F4/80 primary antibody at 4°C, overnight on a rotary shaker. The sections were washed with PBS (4 times for 30 mins at room temperature) and then incubated with AF647 anti-rat IgG (against F4/80) at 4°C, overnight on a rotary shaker. Next, the sections were incubated overnight with fluorophore conjugated antibodies CD45 AF594 and CD41 AF405. All antibodies were used at a concentration of 1µg in 200µl blocking buffer. On the final day of staining, cells were washed four times in PBS (30 mins each, room temperature), incubated with DAPI at a ratio of 1:10,000 and finally mounted with a cover slip using an oil based mounting media. Images were captured using a confocal microscope (Leica) which included 2-photon mode.

2.10 qRT-PCR

qRT-PCR was performed to quantify the mRNA expression of several genes. To begin with, 100,000-200,000 cells were collected through cell sorting. These cells were subjected to an RNA extraction process using the RNeasy® Plus Micro Kit (Qiagen, Germany). Briefly, cells were lysed in 35µl of RLT buffer containing 10µl of β-mercaptoethanol. The lysate was transferred to a QIAshredder spin column and centrifuged at full speed for 2 mins. The supernatant was then pipetted onto a gDNA Eliminator spin column and centrifuged at full speed for 30 secs. Next, 350µl of 70% ethanol was added to the flow through from the previous step and the entire volume was transferred to a RNeasy MinElute spin column which was centrifuged at full speed for 15

secs. The flow through was discarded and the column was washed with 700µl RW1 buffer followed by a wash using 500µl of RPE buffer. Finally, 500µl of 80% ethanol was added to the spin column and centrifuged at full speed for 2 mins. RNA was collected in 14µl of RNase-free water and the concentration was measured using a nanodrop (Thermo Scientific).

Transcriptor First Strand cDNA Synthesis Kit (Version 6.0, Roche, Basel, Switzerland) was used to convert mRNA into cDNA. Briefly, 200ng of mRNA was added to a PCR tube along with 2µl of Random Hexamer Primer. Total volume was brought up to 13µl using PCR-grade water. The template-primer was denatured by heating the PCR tube for 10 mins at 65°C in a thermocycler (Bio-Rad). The following was added to this tube: 4µl of reverse transcriptase reaction buffer, 0.5µl of RNase inhibitor, 2µl of deoxynucleotide mix and 0.5µl of reverse transcriptase. The reaction was run at 25°C for 10 mins followed by 60 mins at 50°C. The enzyme was inactivated by heating the tube at 85°C for 5 mins, followed by cooling the tube at 4°C. The synthesized cDNA was diluted to a total volume of 100µl.

To quantify the gene expression using qRT-PCR, a reaction tube was prepared containing 12.5µl of 1X Power Sybr Green Master Mix (Applied Biosystems®, Foster City, CA), 1µl of 10µM forward primer, 1µl of 10µM reverse primer, 5.5µl of molecular biology grade water and 5µl of respective cDNA. The total volume for each reaction was 25µl. qRT-PCR was performed using an ABI Prism 7300 (Applied Biosystems). The machine was run using a standard protocol with 40 cycles. Each cDNA sample was run in triplicate. The average Ct value of the three replicates was calculated and normalized to GAPDH. The list of genes quantified, and their primers are given below in Table 2.3.

Table 2.3 List of qRT-PCR primers for genes investigated in this study.

Gene	Primers (5'-3')
PF4	F- CTCATAGCCACCCTGAAGAATG R- AGGCAGCTGATACCTAACTCT
Embigin	F- ATCGCTTACGTGGGGGATTC R- AGCGTCAATGGGAACCTGTG
Fli-1	F- AGTTCACTGCTGGCCTATAAC R- TTATTGTTCCATGCTCCTCTCC
Lmo-2	F- CTACAAGCTGGGACGGAAAT R- CCCGCATCGTCATCTCATAG
Ikzf1	F- TTGTGGCCGGAGCTATAAAC R- TGCCATCTCGTTGTGGTTAG
Runx2	F- CGACAGTCCCAACTTCCTGT R- CGGTAACCACAGTCCCATCT
Osterix	F- CCCTTCTCAAGCACCAATGG R- AGGGTGGGTAGTCATTTGCATAG
Col1a1	F-CAGGGAAGCCTCTTTCTCCT R-ACGTCCTGGTGAAGTTGGTC
Osteopontin	F- ACTCCAATCGTCCCTACAGTCG R- TGAGGTCCTCATCTGTGGCAT
Osteocalcin	F - AAGCAGGAGGGCAATAAGGT R- TTTGTAGGCGGTCTTCAAGC
Angiogenin	F- AGCGAATGGAAGCCCTTACA R- CTCATCGAAGTGGACAGGCA
IL-18	F- ATGCTTTCTGGACTCCTGCC R- ATTGTTCCCTGGGCCAAGAGG
GAPDH	F- CGTGGGGCTGCCCAGAACAT R- TCTCCAGGCGGCACGTCAGA

2.11 shRNA knockdown

shRNAs were purchased and tested from Millipore-Sigma to achieve embigin lentiviral knockdown. Two of the 5 shRNA gave sufficient knockdowns. The first one was CCGGGCACAGAAGTAGCTTTATGAACTCGAGTTCATAAAGCTACTTCTGTGCTTTTT G which targets the 3'UTR region of embigin; and the second one was CCGGCGGGTGAAGTTCATCAATACTACTCGAGTAGTTGTATTGAAGTCACCCGTTTTT G which targets the coding region. All shRNAs were cloned into a pLKO.1-CMV-tGFP vector and were custom made by Sigma. HEK293T cells acquired by the American Type Culture Collection (ATCC) were used to make the virus. These cells were cultured in 10cm dishes containing 10ml of complete IMDM medium. Once the cells reached 70% confluency, they were ready for transfection. 5-8 million cells were transfected by a calcium phosphate-HEPES-buffered saline method (Layer, Alford et al. 2016). 1pmol pLKO.1-CMV-tGFP vector, 2pmol pMD-2, and 2pmol pSPAX2 (packaging plasmids courtesy of Dr. Justin Layer, Indiana University) plasmid constructs were used to derive virus. Following 12-18 hrs post transfection, medium was aspirated and replaced with 6ml of fresh complete IMDM. Virus was harvested at 24 hrs and 48 hrs. Virus titers were estimated by analyzing GFP from serially diluted virus used to transduce Jurkat cells.

Spinfections were performed to transduce NCC with lentivirus. Briefly, NCC were resuspended in complete α MEM medium (750,000cells/ml) and then 1ml was plated per well in a 6 well plate. To achieve a multiplicity of infection of 1 to 2, either 500 μ l of shRNA containing lentivirus or empty vector lentivirus was added to each well. Around 2-3 wells were plated as no virus controls. Also, 4 μ g/ml of polybrene was added to the wells containing virus to increase the efficiency of transduction. These 6 well plates were centrifuged at 1800 rpm for 45 mins to perform the spinfection. Post spinfection, the medium containing virus was removed, and 1ml of fresh complete α MEM medium was

added. The cells were incubated at 37°C for 6 hrs followed by a 2nd spinfection. A total of 4 spinfections were performed to transduce the cells with lentivirus. Post transduction, megakaryocytes were added to the NCC to help them recover and proliferate. These cells were cultured for 7 days at 37°C to achieve maximal knockdown. On day 7, cells were sorted for GFP+embigin- OM and osteoblasts (Knockdown cells), as well as GFP+embigin+ OM and osteoblasts (empty vector control). Transduction efficiency was ~15-40% depending on the shRNA used. Of these transduced cells, 50-80% underwent embigin knockdown. These cells were used to perform colony forming assays.

2.12 Colony forming assays

Colony forming assays were performed to test the functionality of progenitor cells *in vitro*. Cultures were set up using 40,000 NCC cells/ well in a 12 well plate or 20,000 cells/ well in a 24 well plate. While using sorted neonatal OM and osteoblasts, cells were reconstituted based on the percentage of each group of cells on the day of the experiment. On an average, the cells were reconstituted as 3-5% OM and 95-97% osteoblasts. If adult cells, were used, OM and osteoblasts were reconstituted in a 1:1 ratio. When these assays were performed in the presence of megakaryocytes, 20,000 megakaryocytes were added per well in a 12 well plate or 10,000 cells/well in a 24 well plate. Cells were incubated at 37°C in 500-750µl of complete αMEM medium. NCC were able to form a monolayer overnight; whereas adult OM and osteoblasts required incubation in 3% O₂ for 1 week to form a monolayer. Once the monolayer was formed, each well was supplemented with 1000 LSK cells in a 12 well plate or 500 LSK cells in a 24 well plate. To each well, 500-750µl of complete IMDM medium was added supplemented with a cytokine cocktail containing 10ng/ml IL3, 10ng/ml SCF, 20ng/ml TPO, 25ng/ml Flt3, 25ng/ml IL-6 and 25ng/ml IGF1. LSK cells were maintained for 1 week in culture alone or with other cell

types before being processed for colony forming assays or for competitive repopulation assays.

For colony forming assays, cultured LSK cells were trypsinized and collected from each well. The cells were washed, the supernatant discarded, and the pellet resuspended in 3ml of complete IMDM medium. Cells from each well were counted using a hemocytometer. 3500 cultured LSK cells from each group were replated in 3.5ml of methylcellulose (#GF M3434, Stemcell Technologies) contained in a 15ml tube. The tube was vigorously vortexed for approximately 30 secs to mix the cells and the methylcellulose; after which the tube was allowed to stand for 5-10 mins. Using an 18 gauge needle and a 3ml syringe, 3ml of the concoction were aspirated and 1ml each was transferred in three 35mm tissue culture plates. The plates were incubated at 37°C for 1 wk in a humidified environment after which number of colonies were counted using an inverted microscope.

To better identify BFU-E and CFU-GEMM colonies, plates were stained with benzidine which stains hemoglobin blue. Briefly, 3 μ l of 50% hydrogen peroxide was added to 1ml of benzidine stain stock (0.2% benzidine dihydrochloride in 0.5M acetic acid). 0.5ml of this stain was immediately layered onto the methylcellulose dish. BFU-E and CFU-GEMM colonies which contain erythroid cells turn blue within 5 mins of incubation at room temperature.

2.13 Competitive repopulating assays

Competitive repopulating assays were performed to determine HSC functionality *in vivo*. Cultures were set up as described in the previous section. Donor LSK cells which were used fresh as well as cultured under different conditions were obtained from C57BL/6J

(CD45.2) mice; competitor bone marrow was obtained from BoyJ (CD45.1) mice and BoyJ X C57BL/6J F1 (CD45.1 and CD45.2) progeny were utilized as recipients. All procedures were approved by the Institutional Animal Care and Use Committee of the Indiana University School of Medicine and followed National Institutes of Health guidelines. Recipients received 1100cGy (750 and 350 cGy, split dose, 4hrs apart) before tail vein injection of test cells in 200µl of PBS. Freshly isolated 100,000 cells of BoyJ bone marrow was combined with either 1000 fresh LSK cells or progeny of cultured 1000 LSK cells (obtained from individual groups in the cultures mentioned above) as test cells. For test cells, all culture wells belonging to the same group were collected, mixed and then divided amongst recipients. Peripheral blood was assessed monthly to analyze percentage chimerism. Four months post primary transplantation, bone marrow from recipient mice was isolated and analyzed for percent engraftment via staining with CD45.1 and CD45.2. If secondary transplants were performed, half the bone marrow content of a femur from primary transplanted recipient was transplanted into lethally irradiated new F1 recipient mice.

2.14 Recombinant, block and other proteins

Several recombinant proteins were used to determine the molecular mediators through which OM enhance hematopoietic function. These recombinant proteins were 1µg/ml rmCD166 (R&D systems), 1µg/ml rmEmbigin (Cusabio Technology, Tokyo), 1µg/ml rmMac2 (In-house), 10ng/ml IL-10 (Biolegend), 25ng/ml IL-18 (R&D Systems), 25ng/ml Angiogenin (RayBiotech, GA), 10ng/ml MCSF (Pepro Tech Rocky Hill, NJ) and 25ng/ml Lcn2 (Biolegend). Surface proteins such as rmCD166, rmEmbigin and rmMac2 were reconstituted in PBS and coated on 24 well plates overnight at 4°C. The next day, the plates were washed with PBS and then coated with 2% low fat milk to prevent non-specific binding. Plates were incubated at room temperature for 30 mins after which they were

washed twice with PBS. Coated plates were used to perform certain colony forming experiments.

For one of the colony forming experiments, an embigin blocking antibody provided by eBiosciences was used to block surface embigin on OM and osteoblasts.

2.15 Statistical analysis

Data has been presented as the mean \pm standard deviation unless otherwise indicated. All experiments except the single cell genomics and competitive repopulating assays were repeated a minimum of 3 independent times. Statistical differences were determined using Student's t-test or One-way Anova test followed by a Tukey Kramer post hoc analysis as indicated where appropriate. Significance was set at a p-value of 0.05.

CHAPTER THREE: Characterization of osteomacs and their phenotypic and functional differences from bone marrow derived macrophages

3.1 Introduction

Macrophages are phagocytic immune cells known for their heterogeneity amongst different tissues. Apart from the cartilage, resident macrophages in almost every tissue of the body have been phenotypically identified. Amongst these tissue resident macrophages are two subsets that normally reside in close proximity in the bone marrow microenvironment called osteomacs (OM) and bone marrow derived macrophages (BM M ϕ). OM are bone resident macrophages, found lining the endosteal bone surface currently characterized as CD45+F4/80+ cells (Chang, Raggatt et al. 2008). Functionally, they are critical for promoting bone anabolism, remodeling, repair, and regeneration (Chang, Raggatt et al. 2008, Alexander, Chang et al. 2011, Guihard, Danger et al. 2012, Wu, Raggatt et al. 2013, Cho, Soki et al. 2014, Raggatt, Wullschleger et al. 2014, Sinder, Pettit et al. 2015, Vi, Baht et al. 2015, Alexander, Raggatt et al. 2017, Batoon, Millard et al. 2017, Batoon, Millard et al. 2017, Kaur, Raggatt et al. 2017). On the other hand, BM M ϕ are found in the bone marrow cavity among other hematopoietic cells; and are similarly characterized as CD45+F4/80+ cells. Some subsets of macrophages have also been implicated in promoting erythropoiesis, HSC mobilization and HSC engraftment (Winkler, Sims et al. 2010, Chow, Lucas et al. 2011, Hoggatt and Pelus 2011, Ludin, Itkin et al. 2012, Chow, Huggins et al. 2013, Chang, Sengupta et al. 2014, Heazlewood, Oteiza et al. 2014, Jacobsen, Forristal et al. 2014, Dutta, Hoyer et al. 2015, Jacobsen, Perkins et al. 2015, McCabe, Zhang et al. 2015, Hur, Choi et al. 2016, Qiao, Liu et al. 2018); whereas other subsets negatively regulate HSC numbers and function (McCabe, Zhang et al. 2015, Luo, Shao et al. 2018). Since both OM and BM M ϕ are considered as residents of the

hematopoietic niche, it is difficult to attribute which macrophage subset is responsible for supporting hematopoietic function. In this chapter, calvariae-resident OM are defined and characterized; and distinguishing phenotypic and functional attributes between them and BM M ϕ are demonstrated.

3.2 Characterization of osteomac origin and phenotypic expression of surface markers

Consistent with a previous study (Chang, Raggatt et al. 2008), the analysis of freshly isolated neonatal calvarial cells (NCC) led to the identification of a CD45⁺F4/80⁺ subpopulation of cells, that share multiple characteristics with OM. Further analysis of these cells revealed that they express classical macrophage markers such as CD11b, CD14 and CD68 (Figure 3.1, NCC). However, they do not express endothelial markers such as CD31; nor hematopoietic stem cell markers such as CD150 and CD34 (Figure 3.1). Since megakaryocytes promote *in vitro* and *in vivo* osteoblast expansion (Kacena, Shivdasani et al. 2004, Kacena, Gundberg et al. 2005, Ciovacco, Goldberg et al. 2009, Ciovacco, Cheng et al. 2010, Kacena, Eleniste et al. 2012, Cheng, Hooker et al. 2013, Cheng, Streicher et al. 2015, Alvarez, Xu et al. 2018), the impact of megakaryocyte stimulation on NCC was examined. When cultured alone for 7 days, NCC increased in numbers but the percentage of OM remained relatively unchanged or declined (Figure 3.1, middle panel). On the other hand, NCC cocultured with megakaryocytes displayed an almost 4-fold increase in the percentage of OM (Figure 3.1, right panel). This indicates that megakaryocytes promote OM proliferation *in vitro*.

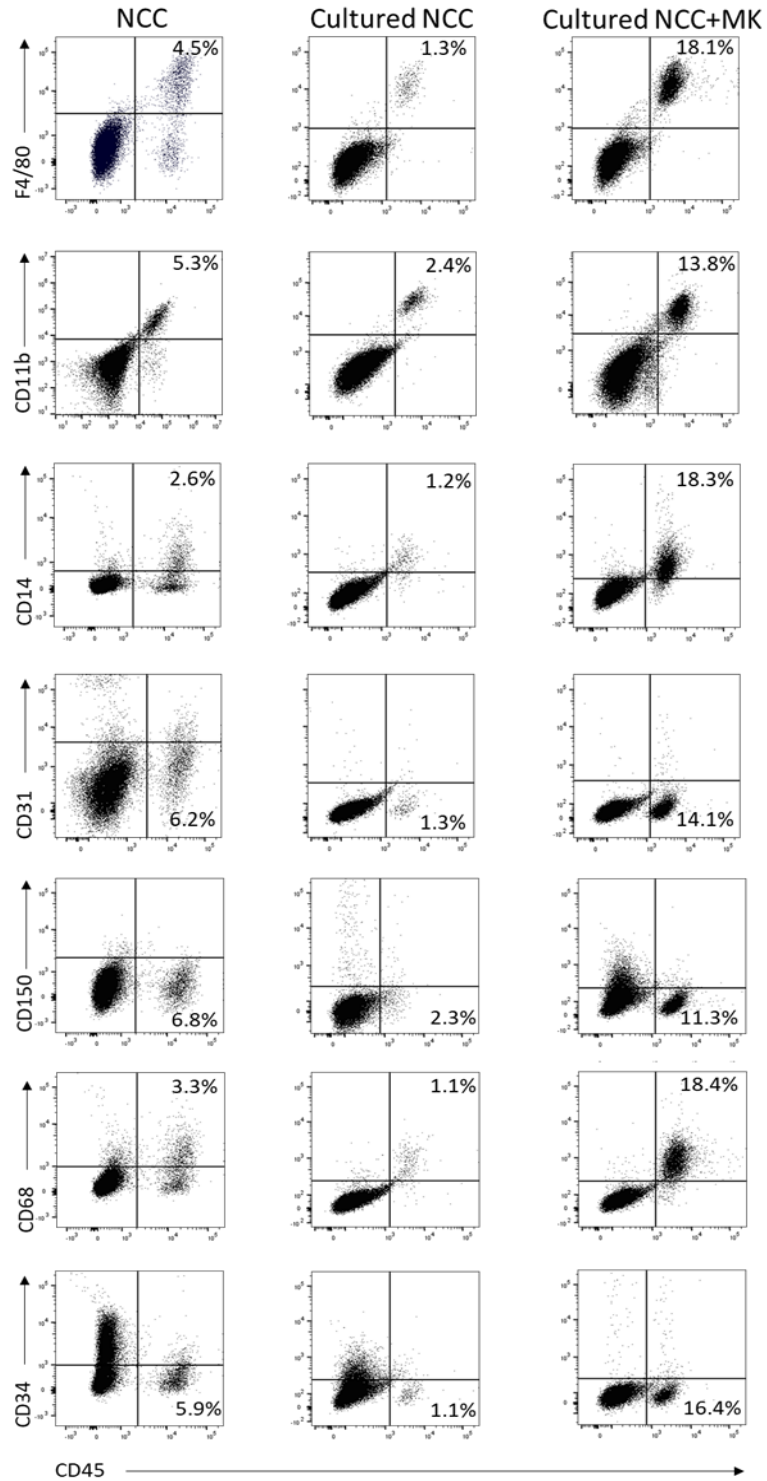


Figure 3.1 **Phenotypic characterization of fresh and cultured osteomacs.** Representative flow cytometric data of freshly isolated NCC (left column), NCC cultured for 1 week in the absence (middle column) or presence (right column) of megakaryocytes (MK). N=3

Since OM are bone resident macrophages, the next focus was to determine whether they originate from progenitors produced during embryonic development or circulating monocytes derived from HSC (Yona, Kim et al. 2013, McGrath, Frame et al. 2015). To do so, a competitive repopulation assay was performed; where 1000 donor LSKs (C57BL/6J mice which are CD45.2+) and 100,000 competitor bone marrow cells (BoyJ mice which are CD45.1+) were co-transplanted into irradiated (900cGy) F1 recipients (Mice which are CD45.1+CD45.2+). A total of 18 F1 mice were transplanted. Every month, for a total of 4 months, 4-5 mice were sacrificed and the hind limbs were dissected to obtain digested bones (previously flushed) which were analyzed for CD11b+F4/80+ macrophages (Figure 3.2A). These cells were then gated on CD45.1 and CD45.2 to obtain OM and determine their source of origin. Interestingly, it was observed that 5-30% of host OM (CD45.1+CD45.2+) survive irradiation (Figure 3.2B) right up to four months post transplantation. However, the data demonstrate that donor LSK cells could also differentiate into OM. It was observed that on an average 35-60% OM (CD45.2) originate from donor cells suggesting that OM are myeloid cells originating from HSC. These data and the design of the transplantation studies makes it difficult to reach a definitive answer concerning whether OM are totally HSC-derived or whether a subset is derived embryonically and cannot be replaced by transplantation.

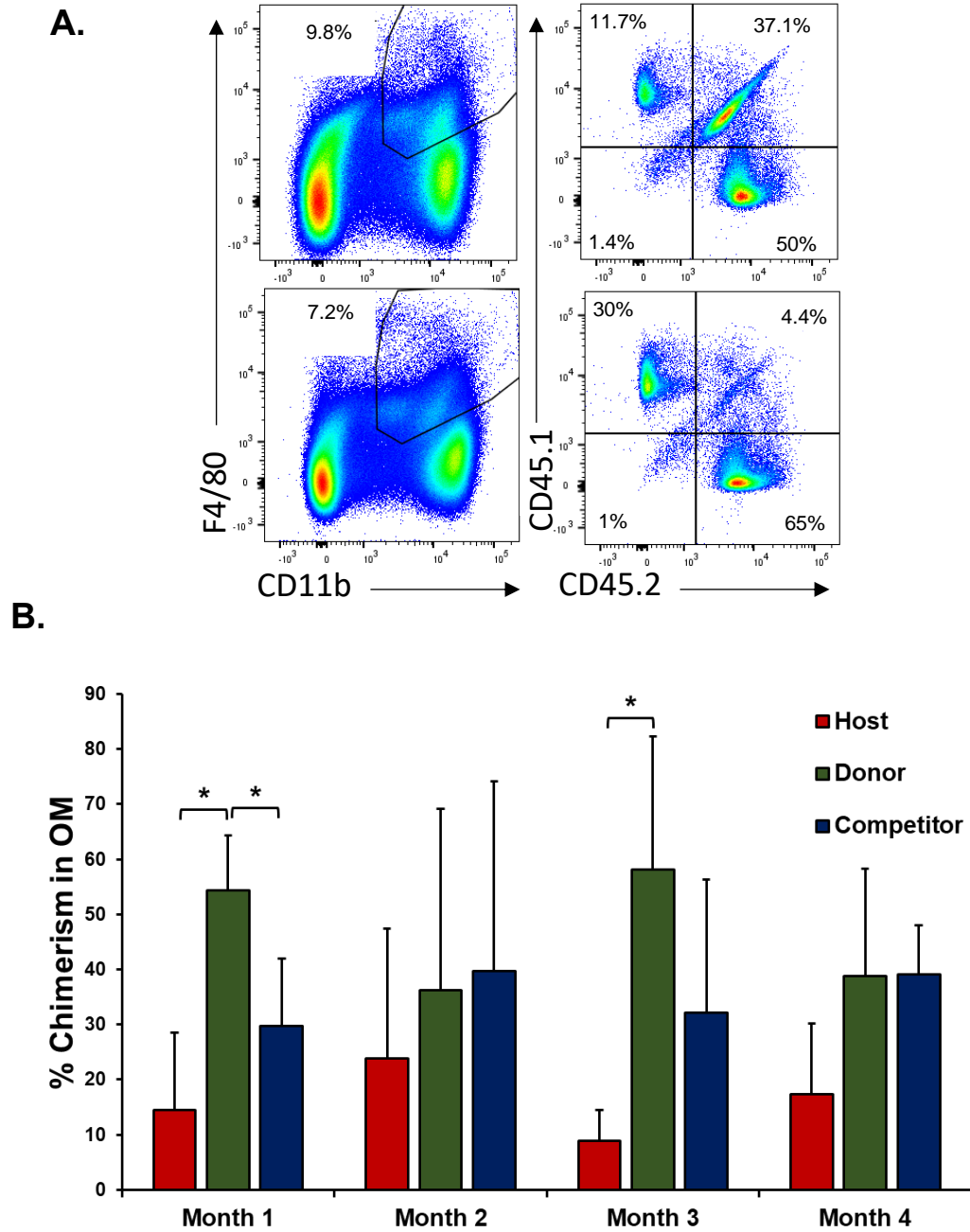


Figure 3.2 **OM are radioresistant and are derived from HSC.** 1000 LSK cells from C57BL/6 (CD45.2) mice and 100,000 bone marrow cells from BoyJ (CD45.1) mice were co-transplanted in (900cGy) CD45.1/CD45.2 F1 recipients via tail vein injection. (A) Representative flow cytometry data from two mice outlining the gating were used to determine percent chimerism in CD11b+F4/80+ OM. (B) Monthly data demonstrating percent chimerism in OM post transplantation. * $p < 0.05$ 1-way ANOVA.

3.3 CD166 and CSF1R co-expression distinguish between OM and BM M ϕ from neonatal and adult donors

Since OM and BM M ϕ both are characterized as CD45+F4/80+ cells, the next goal was to examine phenotypic differences between OM contained in NCC and their CD45+F4/80+ BM M ϕ from age matched counterparts collected from the long bones of neonatal pups. To identify possible developmental changes in the phenotypic makeup of BM M ϕ , bone marrow (BM) cells collected from the long bones of 8 wk-old mice were analyzed. Also, to confirm that OM are osteolineage-associated macrophages (present in the bones of neonatal and adult mice) with a unique identity, digested bones (previously flushed) from 8 wk-old mice were analyzed. The analysis showed that cells from all four sources demonstrate positive expression patterns for CD45, F4/80, CD169, CD11b, CD68, Ly6G and Mac-2 (Figure 3.3). However, only a subset of OM analyzed from NCC and 8 wk digested bone co-expressed CD166 and CSF1R. This co-expression was seen in the Ly6G+Mac-2+ as well Ly6G+Mac-2- subfractions of OM. BM M ϕ from both NBM and 8 wk flushed BM expressed CSF1R but not CD166. Interestingly, the expression of CD169, a known macrophage marker (Chow, Lucas et al. 2011, Chow, Huggins et al. 2013, Jacobsen, Forristal et al. 2014, Batoon, Millard et al. 2017) did not discriminate between OM and BM M ϕ since both groups of cells expressed this marker (Figure 3.3). In fact, in the example shown in Figure 3.3, a higher percentage of neonatal OM expressed CD169 than that detected among neonatal BM M ϕ . However, the expression was similar on adult donor cells. CD169 macrophages have previously been implicated in promoting erythropoiesis and long-term hematopoietic stem cell engraftment (Chow, Lucas et al. 2011, Chow, Huggins et al. 2013, Jacobsen, Forristal et al. 2014, Kaur, Raggatt et al. 2018). This data indicates that irrespective of the developmental stage, a subfraction of OM both from neonatal and adult donors co-express CD166 and CSF1R; and this co-expression is not detected on BM M ϕ .

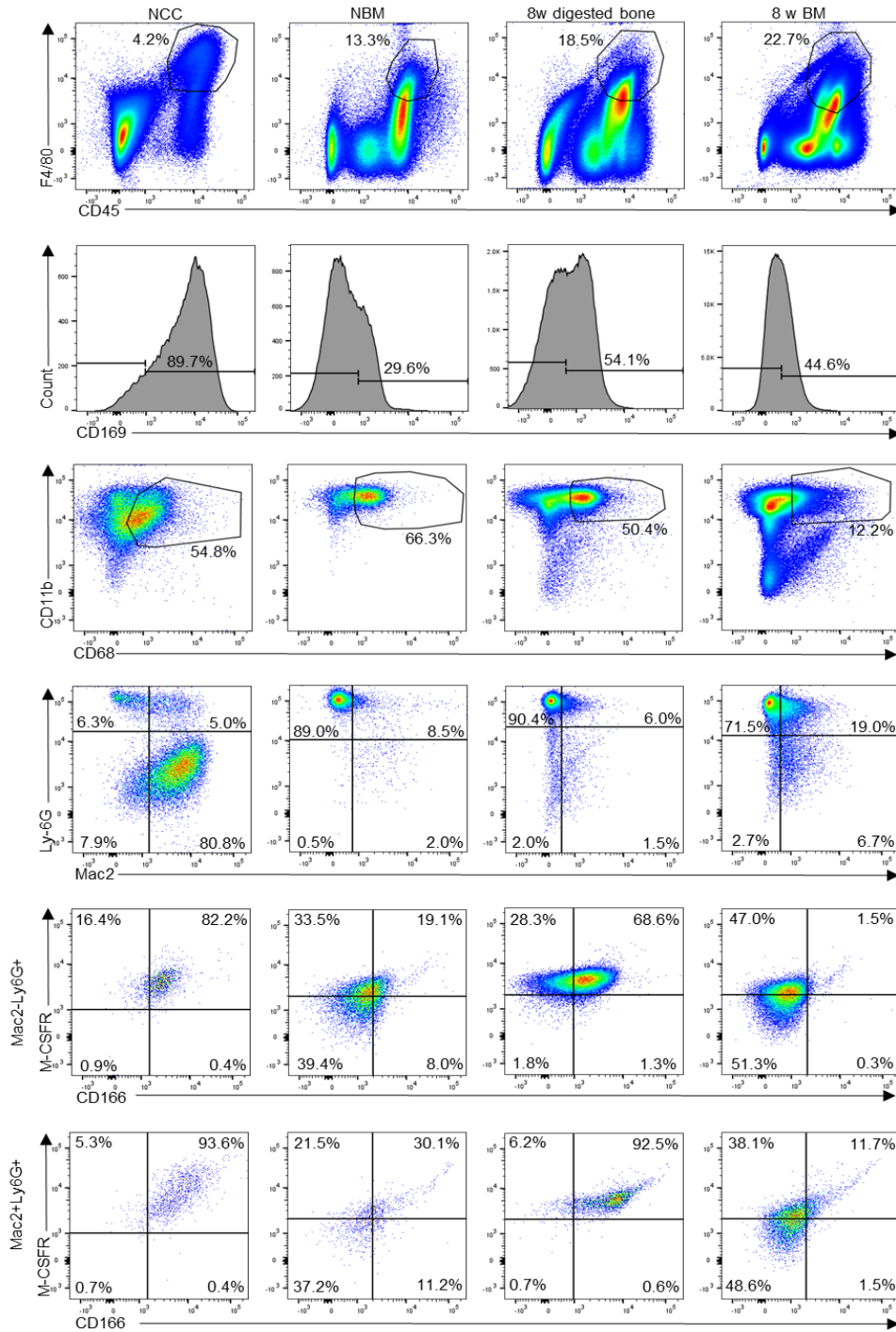


Figure 3.3 **Phenotypic analysis of OM and BM Mφ derived from neonatal and adult donors.**

Nine color flow cytometric analysis of freshly isolated NCC and NBM; as well as 8 wk digested long bones (flushed then digested) and 8 wk flushed BM. All gates were based on fluorescence minus one (FMO) controls. Gating proceeded from top to bottom in each column. N=4-6

3.4 Single cell genomics identifies transcriptional changes between neonatal OM and BM M ϕ

The BioMark HD microfluidic platform was used to examine global differences between OM isolated from fresh NCC and their BM counterparts derived from neonatal long bones. First, 70 freshly isolated single OM and 96 single BM M ϕ were captured using the C1 integrated fluidic circuit. The cDNA from these cells was analyzed by qRT-PCR to quantify the expression of 90 genes. As observed in the violin plots (Figure 3.4A), 48 of the 90 total genes analyzed, were significantly different between the two cell types. The data indicated adiponectin (ADIPOQ) to be upregulated in BM M ϕ with minimal mRNA expression in OM. On the other hand, the thrombopoietin receptor (CD110 or MPL) and bone morphogenetic protein-2 (BMP-2) were upregulated in OM with minimal to no mRNA expression in BM M ϕ . Raw data for the significantly different genes has been shown in Figure 3.4B. To confirm these changes at the proteomic level, CD45+F4/80+ cells from both sources were gated and analyzed for the expression of CD110. Figure 3.4C demonstrates that CD110 expression was unique to OM, indicating it to be a novel surface marker on neonatal OM. Due to the lack of a verified and dependable flow cytometry antibody, it was not possible to confirm the change in adiponectin and BMP-2 expression at the protein level.

A.

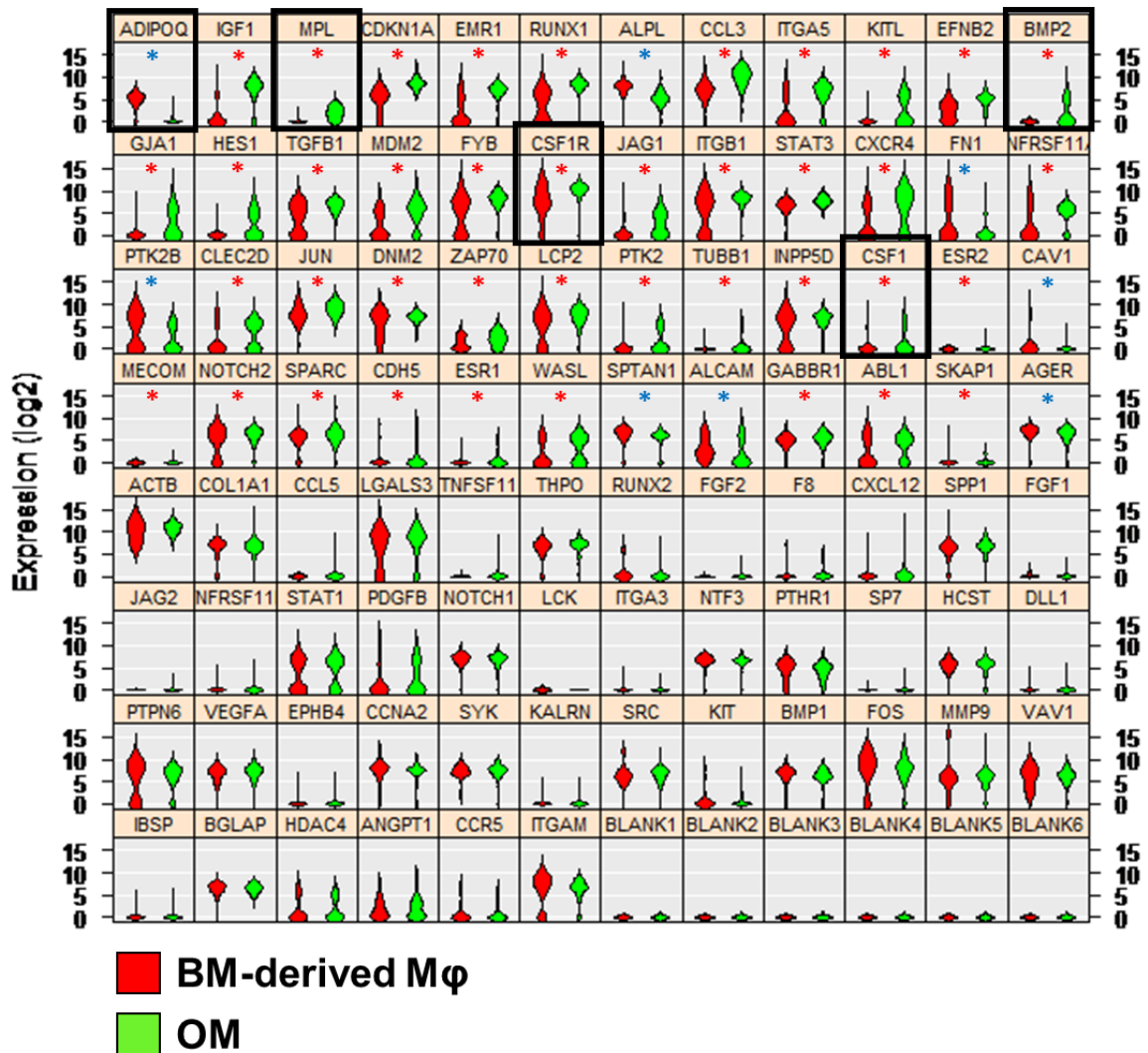
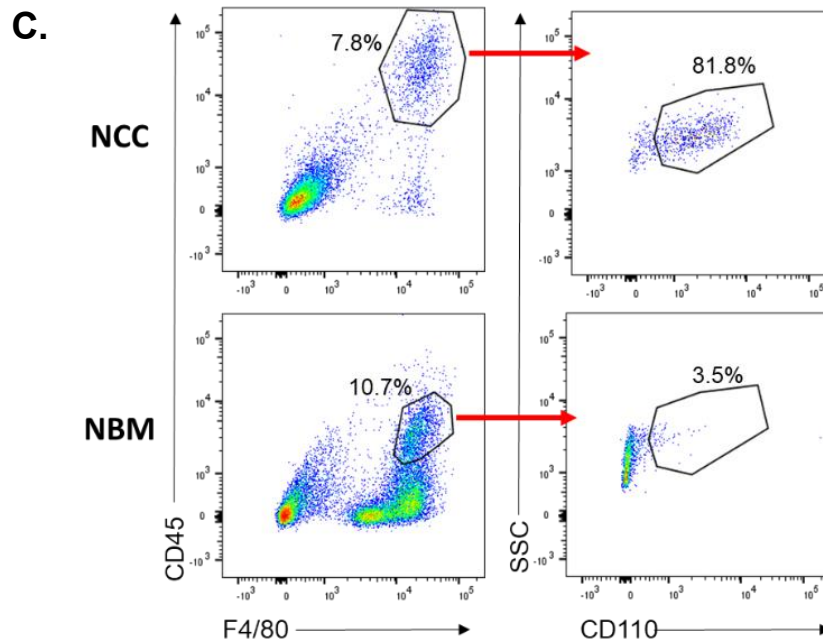


Figure 3.4 **CD110/MPL differentiates OM from BM Mφ in neonates.** (A) Freshly isolated 70 single OM and 96 single BM Mφ were captured using the C1 integrated fluidic circuit. The cDNA from these cells was analyzed by qPCR with the primers of 90 genes using the BioMark HD platform. Data have been represented using violin plots in (A). Blue asterisk (*) indicates downregulation of that gene in OM whereas red asterisk (*) indicates upregulation. $p < 0.05$. Raw data for the 48 significantly different genes have been shown in (B). (C) Flow cytometric analysis (representative data) of freshly isolated neonatal cells (NCC) and freshly isolated neonatal bone marrow (NBM) using CD45, F4/80, and CD110 antibodies. $N = 3$.

B.

Gene	p-value	BM Mφ Avg	OM Avg	Gene	p-value	BM Mφ Avg	OM Avg
ADIPOQ	2.27E-40	4.89	0.49	PTK2B	0.00012	4.46	2.26
IGF1	6.08E-30	1.22	7.36	CLEC2D	0.00022	1.57	3.41
MPL	2.29E-23	0.07	1.98	JUN	0.00024	7.72	9.03
CDKN1A	4.81E-19	5.07	8.60	DNM2	0.00041	5.70	7.10
EMR1	5.52E-16	2.56	6.69	ZAP70	0.00047	1.49	2.39
RUNX1	1.63E-15	4.13	8.12	LCP2	0.0006	5.39	7.17
ALPL	1.76E-15	7.75	5.20	PTK2	0.00064	0.62	1.93
CCL3	7.09E-15	6.82	10.08	TUBB1	0.0009	0.08	0.83
ITGA5	4.35E-12	2.50	6.30	INPP5D	0.00112	4.91	6.54
KITL	6.66E-12	0.18	2.85	CSF1	0.0018	0.54	1.71
EFNB2	1.11E-11	2.64	4.85	ESR2	0.00402	0.00	0.22
BMP2	2.79E-10	0.00	2.06	CAV1	0.00571	1.08	0.12
GJA1	1.02E-09	0.39	3.01	MECOM	0.00818	0.00	0.13
HES1	1.10E-08	0.53	2.73	NOTCH2	0.00884	4.92	6.08
TGFB1	4.16E-08	4.03	6.53	SPARC	0.00987	5.22	6.16
MDM2	6.25E-08	2.69	5.42	CDH5	0.01164	0.17	0.89
FYB	8.81E-08	5.13	8.07	ESR1	0.01268	0.14	0.62
CSF1R	8.26E-07	7.38	9.98	WASL	0.01307	2.16	3.31
JAG1	8.98E-07	0.90	2.83	SPTAN1	0.01431	6.36	5.61
ITGB1	1.45E-06	5.54	8.14	ALCAM	0.02113	3.28	2.24
STAT3	1.76E-06	6.52	7.72	GABBR1	0.02662	4.83	5.37
CXCR4	2.47E-06	2.91	6.02	ABL1	0.03435	2.79	3.83
FN1	6.02E-06	3.70	0.90	SKAP1	0.03541	0.09	0.37
TNFRSF11A	2.79E-05	2.81	5.11	AGER	0.04108	6.78	6.18



3.5 Single cell CyTOF analysis reveals a novel set of markers expressed on neonatal OM

Single cell mass cytometry analysis (CyTOF) was used to further distinguish between neonatal OM and BM M ϕ . The advantage of using CyTOF over flow cytometry were the absence of single color and FMO controls required to perform multi-color flow cytometric analysis; and the absence of compensation issues involved in flow cytometry. Also, CyTOF allows the use of complex algorithms such as ViSNE to understand the heterogeneity within populations in a more efficient manner.

OM and BM M ϕ were analyzed using simultaneously a panel of 17 surface and 13 intracellular antibodies (Figure 3.5A). The panel of 30 antibodies was designed based on previous literature pertaining macrophage expression markers and regulators of hematopoiesis. The expression of several intracellular markers such as platelet factor-4 (PF4), stromal derived factor-1 (SDF1), and platelet derived growth factor- β (PDGF- β) were upregulated in OM compared to BM M ϕ (Figure 3.5B). Interestingly, these proteins were previously implicated in regulating hematopoiesis (Leveen, Pekny et al. 1994, Aiuti, Webb et al. 1997, Dominici, Rasini et al. 2009, Bruns, Lucas et al. 2014, Lim, Esain et al. 2016). This indicates the possibility of different functional roles between OM and BM M ϕ in the hematopoietic niche. To determine the individual functional roles of each of these cells in the hematopoietic niche is an important topic which will be covered in the next section.

In my hands and with these two cell types, staining for intracellular markers reduced the expression of certain key surface markers such as CD166 and CD169. This reduction in expression of certain surface markers could be due to the permeabilization step involved in the staining of intracellular markers. Therefore, studies were performed on OM and BM

M ϕ using a subgroup of 17 surface markers from the panel. Initial analysis of these data revealed the heterogeneity of OM and BM M ϕ (Figure 3.6A). FlowSOM was used to identify unbiased subpopulations/clusters (7 in OM and 6 in BM M ϕ) based on the 17 surface antibodies. Each cluster was then phenotypically characterized based on the same panel of surface markers. Only 1 small cluster overlapped between OM and BM M ϕ (group of cells designated teal in color in Figure 3.6A) indicating that these two cell sources are phenotypically very different.

Consistent with previous characterization (Alexander, Chang et al. 2011), OM were Mac-2 low and expressed macrophage markers such as CD11b, CD14, CSF1R and CD169 (Figure 3.6B). In fact, expression of CD14 and CD169 was upregulated in OM compared to BM M ϕ . CD166, a marker important for the hematopoietic niche (Chitteti, Cheng et al. 2010, Chitteti, Bethel et al. 2013, Chitteti, Cheng et al. 2013, Chitteti, Kobayashi et al. 2014) was also upregulated (Figure 3.6C). Also, the two cell sources were analyzed for expression of CD86 (M1 macrophage marker) and CD206 (M2 macrophage marker). Neonatal OM uniquely co-expressed CD86 and CD206 (Figure 3.4E), whereas BM M ϕ expressed CD86 with low or undetectable expression of CD206. Altogether, the single cell data identified the unique expression of CD166, CD110 and CD206 on neonatal OM.

Next, a four-color flow cytometry analysis was performed to identify the percentage of OM and BM M ϕ which are CD206+CD80+. The analysis of CD80 was due to preliminary single cell RNA sequencing data performed in the laboratory using 8 wk OM and BM M ϕ . As seen in Figure 3.7A, ~85-90% of neonatal OM co-express CD80 and CD206. However, a fraction of BM M ϕ also expressed CD80, but not CD206. These data demonstrate that the unique expression of CD80 and CD206 on OM from neonatal pups can be used for future experiments to separate them from age matched contaminating BM M ϕ . Interestingly,

these two surface markers lose expression during development. As seen in Figure 3.7B ~45-55% of OM obtained from 3 wk calvarial cells and ~10-20% of OM obtained from 3 wk digested bones co-express CD80 and CD206. Similarly, ~35-40% of OM obtained from 8 wk calvarial cells and ~10-20% of OM obtained from 8 wk digested bones co-express CD80 and CD206 (Figure 3.7C), indicating the loss of co-expression of these markers on OM during aging or through development.

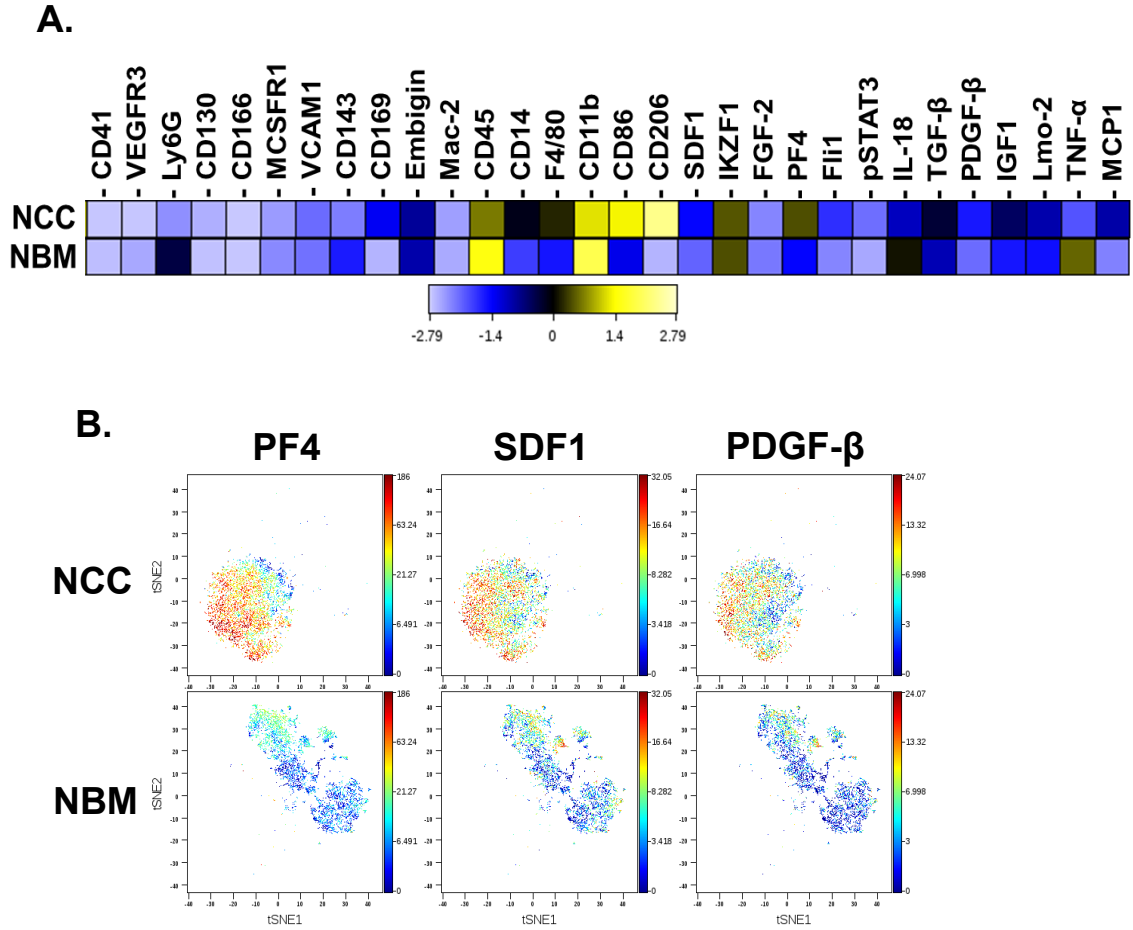


Figure 3.5 **Differential expression patterns of surface and intracellular antigens on OM and BM Mφ from neonates.** Single cell suspensions of NCC and NBM were analyzed using a panel of 30 surface and intracellular antibodies. Data were gated on CD45+F4/80+ cells to indicate OM in NCC (upper panel) and BM Mφ in NBM (lower panel). (A) Representative Heat map and (B) ViSNE plots indicating intracellular differences of several proteins between the two cell types. N=3-7

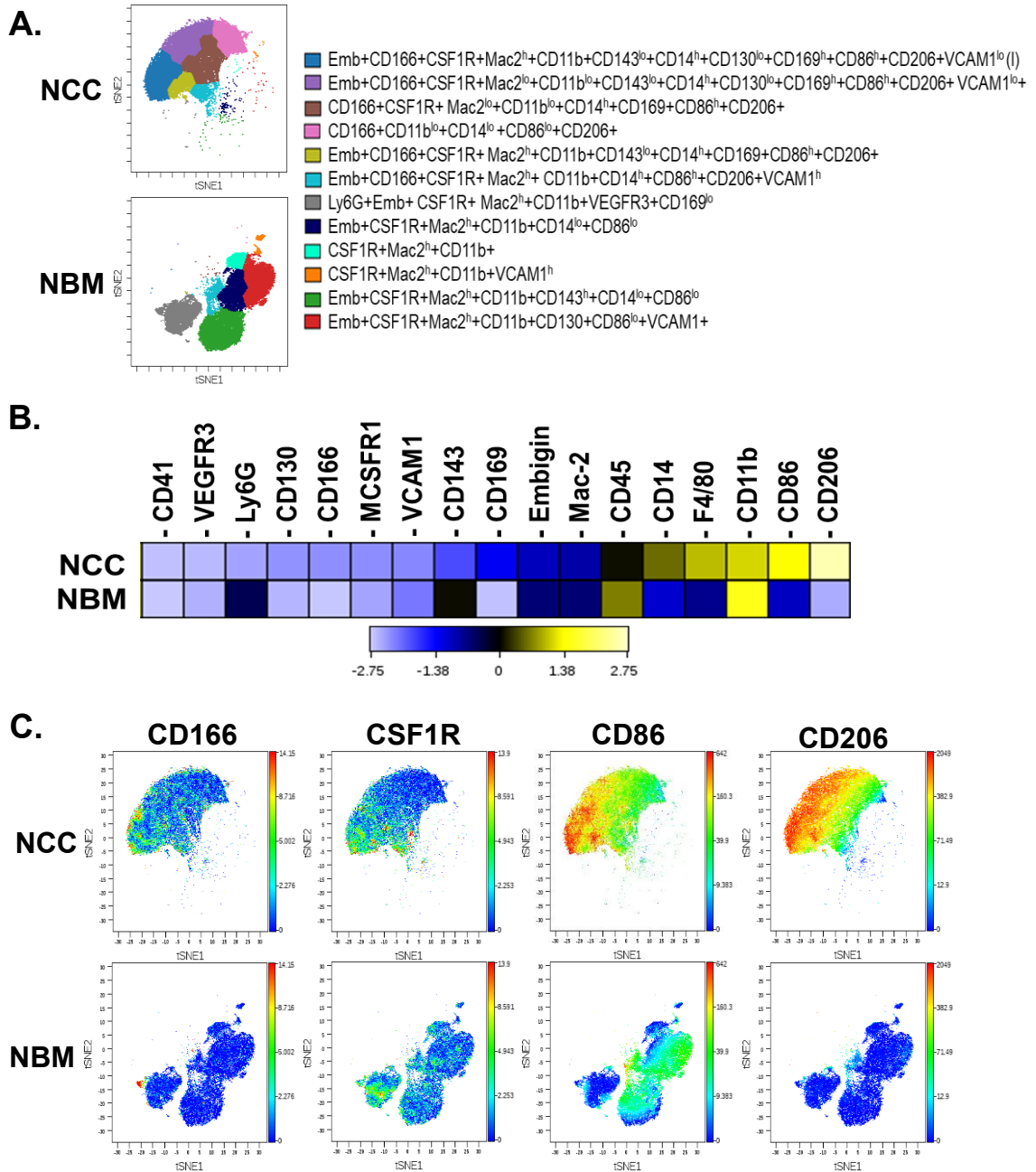
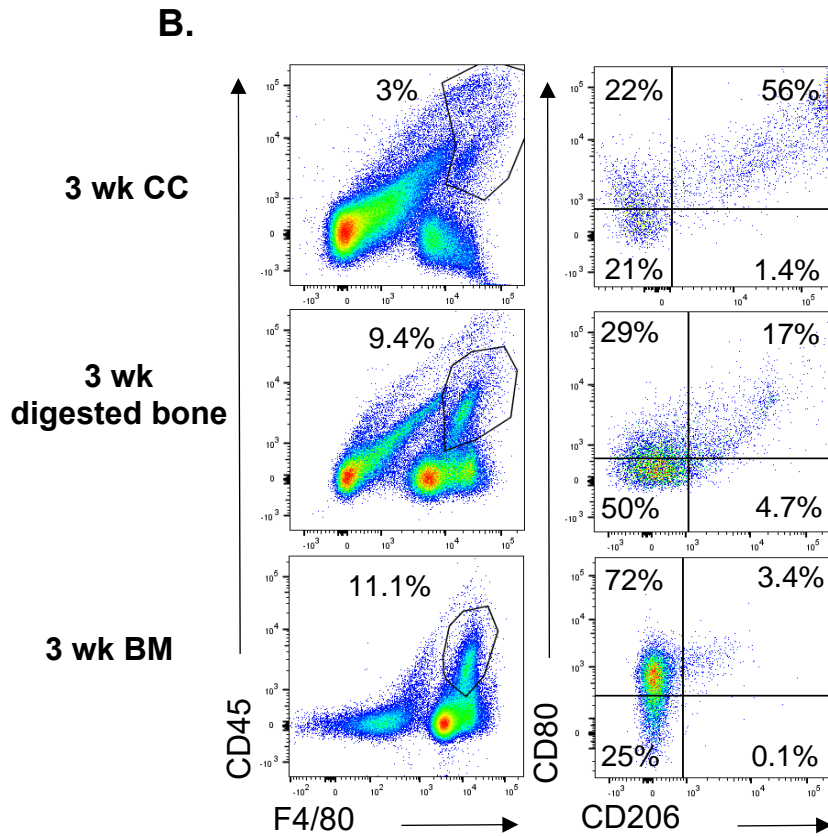
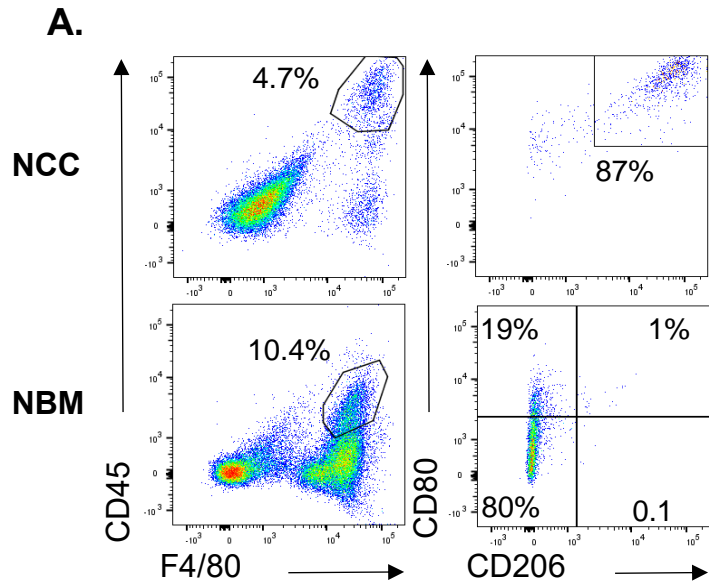


Figure 3.6 **Multidimensional CyTOF analysis of OM and BM Mφ from neonates.** Single cell suspensions of NCC and NBM were analyzed using a subpanel of 17 surface antibodies. Data were gated on CD45+F4/80+ cells to indicate OM in NCC (upper panel) and BM Mφ in NBM (lower panel). (A) Representation of the heterogeneity observed within subpopulations of OM and BM Mφ. Each subpopulation was characterized depending on their expression of the surface markers. (B) Heat map and (C) ViSNE plots indicating individual surface differences between OM and BM Mφ. N=3-6.



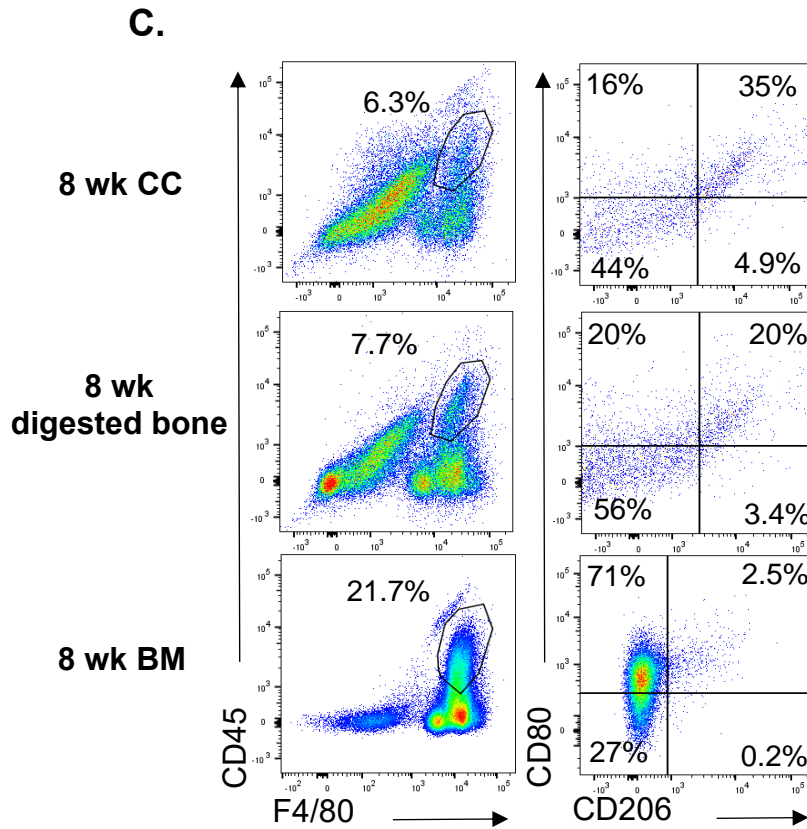


Figure 3.7 **Developmental loss of CD206 expression on OM.** Four color flow cytometric analysis of (A) freshly isolated NCC and NBM, (B) 3 wk digested calvarial cells (CC), digested long bones (flushed then digested) and bone marrow and (C) 8 wk digested CC, digested long bones (flushed then digested) and bone marrow. Cells were gated on CD45+F4/80+ macrophages which were further gates on CD80 and CD206. N=3

3.6 OM are a subset of macrophages that phagocytose and differentiate into osteoclasts

Phagocytosis assays were performed to identify whether OM can phagocytose similar to other macrophage subtypes and might therefore possibly have an immune function. PE-conjugated *E.coli* BioParticles were used to activate OM and induce phagocytosis. Flow cytometry results indicate that both OM and BM M ϕ fluoresce in the PE channel illustrating that both cell types phagocytose (Figure 3.8A). Images of the same demonstrate that these BioParticles were intracellular in both OM and BM M ϕ , indicating their engulfment (Figure 3.8B). These data show that OM can functionally phagocytose foreign particles similar to BM M ϕ .

Since macrophages act as osteoclast progenitors; and several phenotypic and functional similarities exist between OM and BM M ϕ ; the next goal was to determine if OM may also differentiate into osteoclasts. The data in Figure 3.9A (Mohamad, Xu et al. 2017) demonstrate that culturing OM with RANKL and M-CSF can induce their differentiation into multinucleated osteoclasts that express TRAP. In addition, these osteoclasts were functional since they were capable of resorbing dentin and forming resorption pits (Figure 3.9B) (Mohamad, Xu et al. 2017). This suggests that contrary to previous published data (Chang, Raggatt et al. 2008), OM are osteoclast progenitors which can differentiate into functional osteoclasts.

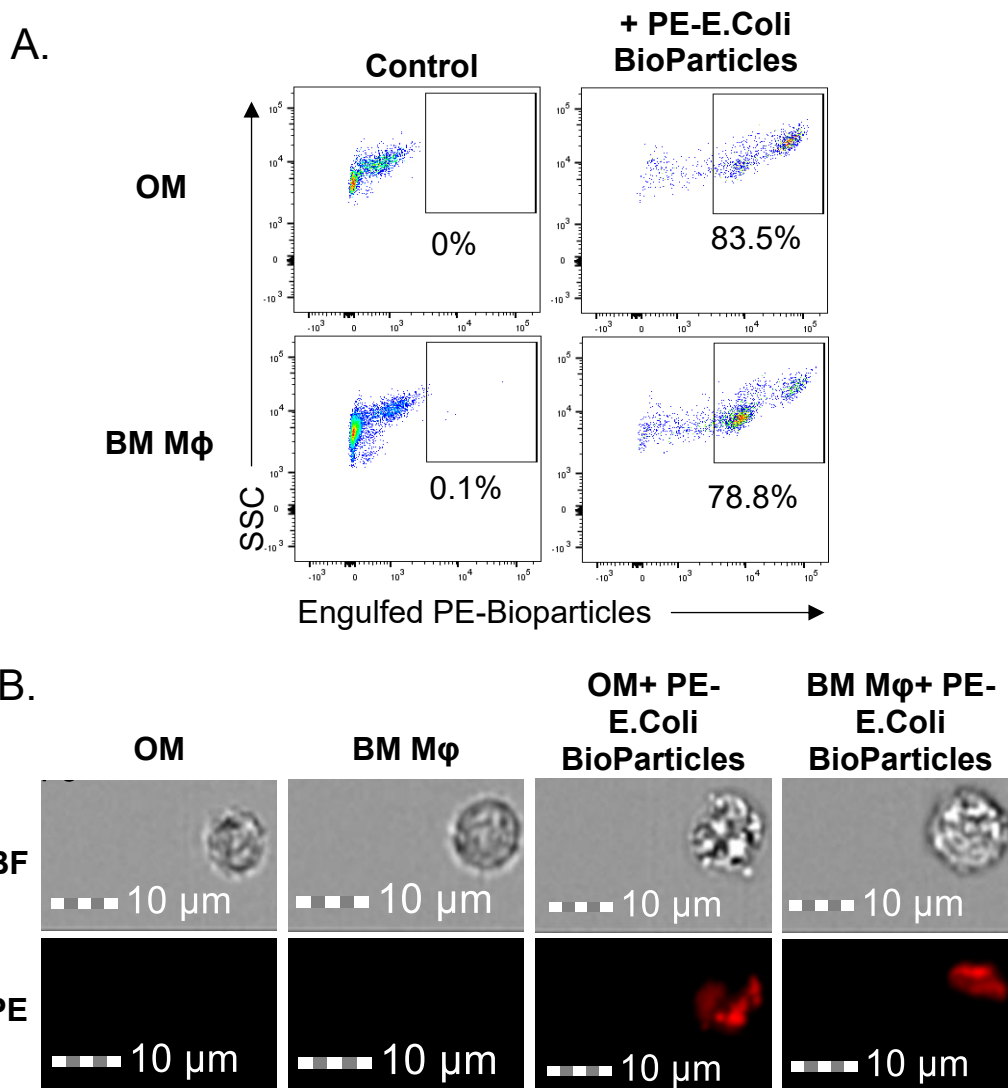
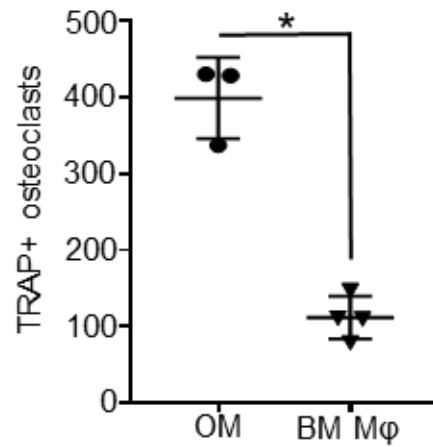


Figure 3.8 **OM perform phagocytosis comparable to BM Mφ.** 8 wk digested long bones (flushed then digested) and 8 wk flushed BM were processed to isolate OM and BM Mφ, respectively, that were collected through flow sorting. 75,000 cells from each group were cultured per well in a 96-well plate for 24 hrs. The next day, cells were incubated with 100μL of PE conjugated *E. coli* BioParticles for 1 hr after which they were analyzed for phagocytosis. (A) Representative dot plots (N=3) and (B) images (N=2 independent experiments) indicating both OM and BM Mφ phagocytose PE conjugated *E. coli*. The top row in (B) are bright field (BF) images of cells whereas the bottom row represents cells that have engulfed the PE conjugated BioParticles.

A.



B.

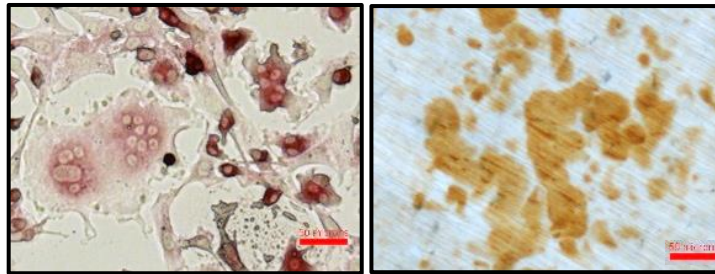
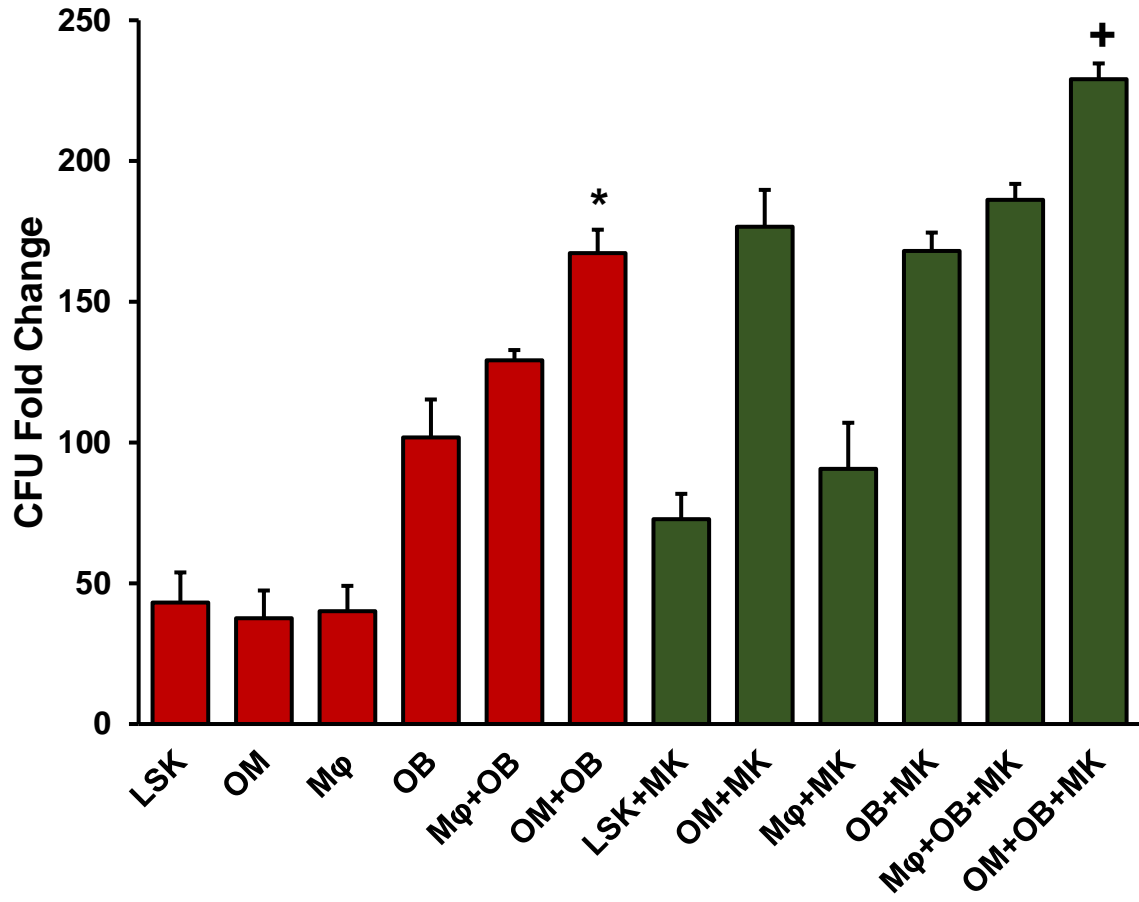


Figure 3.9 **OM can differentiate into functional osteoclasts.** (A) CD45+F/480+ OM from NCCs or BM Mφ from NBM were cultured with RANKL and M-CSF to induce osteoclast formation. TRAP+ osteoclasts with less than or equal to 3 nuclei were quantified. * $p > 0.05$. (B) Osteoclasts formed from the calvariae-derived (left panel) OMs were replated on dentin, and resorption pits were stained after 3 days (right panel). Representative images of TRAP1 osteoclasts and resorption pits formed by these cells are shown. Slides were stained as described in (Mohamad, Xu et al. 2017). Scale bar indicates 50mm.

3.7 OM, osteoblast and megakaryocyte interactions are essential for maintaining murine hematopoietic stem cell function

Since NCC mediate hematopoietic enhancing activity (Chitteti, Cheng et al. 2010), it was important to examine whether the OM and/or osteoblast subfraction of NCC were responsible for mediating this activity. As seen in Figure 3.10A, when OM were cultured with LSKs in the absence of osteoblasts, they were incapable of maintaining hematopoietic activity higher than the LSK control. On the other hand, osteoblasts alone were capable of expanding CFU fold change but not to the same level as that observed when osteoblast were mixed with OM. CFU fold change was significantly increased when both OM and osteoblasts were co-cultured; and this activity was further augmented by the addition of megakaryocytes to the mix. The CFU fold change of OM cultured with osteoblasts in the absence or presence of megakaryocytes was always higher compared to the CFU fold change of the LSK control. However, regardless of whether megakaryocytes were added to the co-cultures, BM M ϕ were unable to substitute for OM to support hematopoiesis. These data demonstrate that while osteoblasts can mediate the previously reported hematopoiesis enhancing activity (Chitteti, Cheng et al. 2010), OM are required for maximal hematopoiesis enhancing activity promoted by NCC. Promotion of hematopoiesis enhancing activity was not restricted to OM isolated from neonatal calvariae since OM collected from long bones of adult mice mediated the same activity (Figure 3.10B). Together, the data indicate that OM, osteoblast and megakaryocyte interactions are important for maintaining hematopoietic stem cell activity and that OM cannot be substituted by BM M ϕ to maintain this function in the hematopoietic niche.

A.



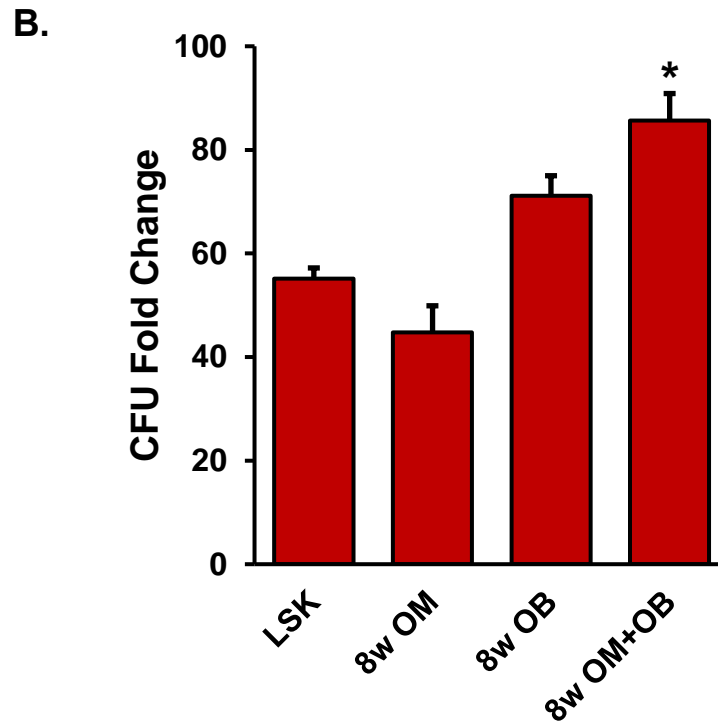


Figure 3.10 **OM are bone-resident macrophages that are functionally different from BM-derived M ϕ .** (A) Co-cultures of NCC-derived osteoblasts (OB) mixed with either the original number of OM contained in freshly isolated NCC (OM+OB) or a complimentary number (equivalent to the original number of OM in NCC) of BM-derived CD45+F4/80+ macrophages (M ϕ +OB) were established. LSK cells were added with (green bars) or without (red bars) megakaryocytes (labeled in this Figure as MK) and LSK progeny were assessed for CFU content on day 7. CFU fold-increase was calculated relative to that obtained from 250 fresh LSK. * $p < 0.001$ vs LSK, OM, M ϕ , OB and M ϕ +OB; + $p < 0.001$ vs OM+OB, LSK+MK, OM+MK, M ϕ +MK, OB+MK and M ϕ +OB+MK, One-way Anova. (B) Long bones from adult mice were flushed, then digested with collagenase to obtain a cell population containing OM and osteoblasts (OB). OM and OB were purified by sorting. Sorted cells were cultured alone or co-cultured in a 1:1 ratio for 7 days. These cultures were then seeded with LSK and assayed 7 days later for their CFU content. CFU fold increase was calculated relative to that obtained from 250 fresh LSK cells. * $p < 0.01$ compared to LSK, 8w OM and 8w OB, One-way Anova.

3.8 Discussion

In this chapter, calvariae-resident macrophages called OM were characterized and shown to be phenotypically and functionally different from BM M ϕ . OM, which were first defined in 2008 (Chang, Raggatt et al. 2008), are identified as F4/80+ macrophages that line the endosteum. Through the work in this chapter, OM were further characterized; and it was shown that in addition to F4/80, they express other classical macrophage markers such as CD11b, CD14, CD68 and Mac-2 (Figure 3.1 and Figure 3.3). Interestingly, all these markers are common between OM and BM M ϕ which are also defined as CD45+F4/80+ cells. Similar to BM M ϕ , OM possess the functional capability of phagocytosis, marking them as part of the immune system (Figure 3.8). Although no previous data demonstrated that OM phagocytose, there have been instances of correlation between OM and efferocytosis of apoptotic cells within the bone (Cho, Soki et al. 2014, Sinder, Zweifler et al. 2017). Data in Figure 3.8 further strengthen this analogy and identify OM as possessing the most classical function of macrophages, which is phagocytosis.

Another important function of BM M ϕ is their ability to differentiate into osteoclasts. However, previous reports have mentioned that OM do not act as osteoclast precursors (Chang, Raggatt et al. 2008). Contrary to these data, it was demonstrated that OM are able to differentiate into TRAP+ osteoclasts when cultured in the presence of MCSF-1 and RANKL (Figure 3.9A) (Mohamad, Xu et al. 2017). Furthermore, these osteoclasts resorbed dentin (Figure 3.9B). Although it remains possible that different OM subpopulations were used by the independent laboratories, carefully controlled and optimized culture conditions are also necessary to induce osteoclast differentiation, which could possibly explain the differing results. Whether only a subpopulation of OM differentiated into osteoclasts is also not defined at present. Interestingly, OM but not BM M ϕ differentiated into osteoclasts in the absence of MCSF-1 (Data not shown). These

findings correlate with the single cell qPCR data where it was demonstrated that OM express significantly higher MCSF-1 mRNA compared to BM M ϕ (Figure 3.4A and B).

In the past decade, several groups have demonstrated various tissue resident macrophages including BM M ϕ as being resistant to radioablation (Haniffa, Ginhoux et al. 2009, Hashimoto, Chow et al. 2011, Winkler, Pettit et al. 2012, Kaur, Raggatt et al. 2018). In this study, the CD45.1/CD45.2 system was used, where donor cells express the CD45.2 allele, and recipients express both CD45.1 and CD45.2. The transplant data demonstrate that a percentage of OM in recipient mice survive post irradiation. However, this radioresistant population eventually depletes and is replaced by donor OM derived from HSC (Figure 3.2). This answers a second question regarding OM origin. Several reports have identified that fetal-derived macrophage progenitors are responsible for maintaining several tissue resident macrophages in adult hematopoiesis (Schulz, Perdiguero et al. 2012, Yona, Kim et al. 2013). The transplant data in Figure 3.2 demonstrate that OM are radioresistant myeloid cells which can originate from HSC.

All characteristics discussed above, are phenotypic and functional similarities between OM and BM M ϕ . The similarities as well as the differences between neonatal and adult OM and BM M ϕ are summarized in Table 3.1. Next, a series of experiments were designed, which included multi-color flow cytometry, single cell genomics and single cell proteomics, to determine phenotypic differences between the two neonatal subsets. Each of these experiments was designed to include maximum novel expression markers which could help characterize OM and distinguish them from BM M ϕ . Through these studies, a subfraction of neonatal OM was identified which was CD166 and CSF1-R positive (Figure 3.3) and was phenotypically distinct from neonatal BM M ϕ . Interestingly, the same subfraction of OM was present not only in neonatal calvariae, but also in the long bones

of adult mice. This indicates that OM are not a developmentally unique cell type present only in neonatal calvariae. In fact, OM from both neonates and adults are also functionally similar in that they interact with osteoblasts to enhance hematopoietic activity (Figure 3.10). This hematopoietic activity of OM could not be substituted by BM M ϕ . It was previously demonstrated that CD166 is a critical mediator of the hematopoietic niche (Chitteti, Cheng et al. 2010, Chitteti, Cheng et al. 2010, Chitteti, Bethel et al. 2013, Chitteti, Cheng et al. 2013, Chitteti, Kobayashi et al. 2014). Since this marker is present on OM and not on BM M ϕ , it is possible to hypothesize that CD166 may be one of the molecular mediators through which OM enhance hematopoietic function. This premise will be covered in the upcoming chapters.

Through the multi-color flow cytometry studies and CyTOF, it was also shown that neonatal OM express CD169 at a higher level than their bone marrow counterpart; whereas adult OM and BM M ϕ express similar levels of CD169 (Figure 3.3, Figure 3.6). This illustrates that CD169 is not a distinguishing marker between various subsets of macrophages. However, CD169 has been implicated as an important identifying marker for BM M ϕ resident in the hematopoietic niche (Chow, Lucas et al. 2011, Chow, Huggins et al. 2013). Furthermore, depletion of CD169+ macrophages causes loss of both OM lining the endosteum and BM M ϕ lodged within the center of the bone marrow (Batoon, Millard et al. 2017). This makes it difficult to determine which subset of macrophages is essential for hematopoietic function. Hence, it is important to identify a novel marker distinguishing adult OM from BM M ϕ . Current studies have identified CD166 as a distinguishing marker between adult OM and BM M ϕ , but it only expressed on a small subset of OM.

Single cell studies have further helped identify several phenotypic differences between neonatal OM and BM M ϕ including expression of CD110, CD206, CD86 and CD80 (Figure 3.4, 3.5, 3.6, 3.7). Interestingly, previous data bifurcate CD86 macrophages as M1 subtype and CD206 macrophages as M2 (Hume 2015, Huang, Feng et al. 2019). However, OM are unique since they co-express both CD86 and CD206 on their surface (Figure 3.6). There is a possibility that these macrophages are at an earlier phase of differentiation and lose expression of either CD86 or CD206 with development. This finding was not further explored. Also, OM express CD80 which is an important co-stimulatory marker on T cells (Sabzevari, Kantor et al. 2001). It was demonstrated that almost all CD80+CD206+ cells in neonatal calvarial cells are CD45+F/480+ (Figure 3.7A). For future studies, CD206 and CD80 could be used as two distinct markers that discriminate OM from contaminating macrophages within the neonatal calvariae. Interestingly, CD80 and CD206 expression patterns of OM in 3 wk and 8 wk old mice was also analyzed (Figure 3.7B and C). A decline in the expression pattern of both CD206 and CD80 on OM was observed with age. Furthermore, the decline was faster in OM isolated from long bones as compared to OM obtained from calvarial cells. On the other hand, BM M ϕ gain expression of CD80 with development. CD80 being a marker of T-cells and in turn the immune system (Sabzevari, Kantor et al. 2001), there is the possibility that as the immune system is exposed to various foreign antigens and develops, immune cells such as BM M ϕ , these gain CD80 expression with time. This is an interesting avenue which could be explored in future research. Nonetheless, CD206 and CD80 which are excellent distinguishing markers between neonatal OM and BM M ϕ , are only expressed on a subset of OM in adults. It is critical to identify a distinguishing marker between adult OM and BM M ϕ so that genetic models can be used to define their individual function *in vivo* in the hematopoietic niche.

Overall, these studies suggest that even though OM phagocytose (Figure 3.8) and act as osteoclast progenitors (Figure 3.9) (Mohamad, Xu et al. 2017) similar to BM M ϕ ; they are phenotypically and functionally very distinct from their BM counterparts (Table 3.1). These investigations extend the definition of OM and describe novel surface markers such as CD166, CD110, CD206 and CD80 which distinguish neonatal OM from BM M ϕ . Furthermore, the importance of networking between OM, osteoblasts and megakaryocytes in enhancing hematopoietic function is described. Detailed analysis of the crosstalk between these cells and the molecular mediators through which OM maintain hematopoiesis will be covered in the upcoming chapters.

Table 3.1 **Summary of similarities and differences between OM and BM M ϕ .**

Characteristic	Neonatal OM	Neonatal BM Mϕ	Adult OM	Adult BM Mϕ
Expression of surface markers:				
• CD45	++	++	++	++
• F4/80	+++	++	++	++
• CD11b	+++	+++	+++	+++
• CD68	+	+	+	+
• Ly6G	++	+++	+++	+++
• Mac-2	+	+	+++	++
• CSF-1R	+++	++	+++	+++
• CD14	+++	++	++	++
• CD169	+++	++	++	++
• CD166	++	-	++	+
• CD110	+++	-	N/D	N/D
• CD206	+++	-	+	-
• CD86	+++	+	+	+
• CD80	+++	++	++	+++
Expression of intracellular markers:				
• SDF-1	+++	+	N/D	N/D
• PF-4	+++	+	N/D	N/D
• PDGF- β	+++	+	N/D	N/D
• MCP-1	+++	-	N/D	N/D
• TNF- α	+	++	N/D	N/D
Resistance to radioablation	N/D	N/D	Yes	Yes
Megakaryocyte induced proliferation	Yes	No	Yes	N/D
Phagocytic Capability	Yes	Yes	Yes	Yes
Precursor for osteoclast differentiation	Yes	Yes	Yes	Yes
Size	~10-15 micron	~8-10 micron	N/D	N/D
Interacts with osteoblasts and megakaryocytes to enhance hematopoietic activity	Yes	No	Yes	No

CHAPTER FOUR: Megakaryocytes interact with osteomacs and osteoblasts to regulate murine hematopoiesis

4.1 Introduction

Megakaryocytes are hematopoietic myeloid cells whose primary function is to produce platelets that are critical for blood clotting. Megakaryocytes are also known to play key roles in skeletal homeostasis and hematopoiesis. In skeletal homeostasis, they regulate osteoblast proliferation and suppress osteoblast differentiation (Kacena, Shivdasani et al. 2004, Kacena, Gundberg et al. 2005, Ciovacco, Goldberg et al. 2009, Bethel, Srour et al. 2011, Cheng, Hooker et al. 2013, Cheng, Streicher et al. 2015, Alvarez, Xu et al. 2018). It was previously demonstrated that megakaryocytes increase OM numbers that are contained within NCC (Mohamad, Xu et al. 2017) (Figure 3.1). Also, OM, osteoblasts and megakaryocytes are all part of the hematopoietic niche. However, the relative location of these cells with respect to each other and also in relation to HSC is not clear. Several groups have indicated that quiescent HSC are found near the endosteum; and localize adjacent to megakaryocytes in a non-random manner (Nilsson, Johnston et al. 2001, Heazlewood, Neaves et al. 2013). Detailed multi-dimensional imaging studies combining existing data with additional niche participants are warranted.

Maintenance of HSC function is an orchestrated event between multiple cell types. Crosstalk between these cell types is an essential part of HSC regulation. Previous data has demonstrated the importance of NCC, which consist of OM and osteoblasts, in maintaining hematopoietic function (Chitteti, Cheng et al. 2010). Also, in chapter three, it was demonstrated that the hematopoietic enhancing function of NCC is further augmented

in the presence of megakaryocytes (Mohamad, Xu et al. 2017). This is not the first instance where megakaryocytes have been implicated in hematopoiesis. In 2009, Dominici et al. illustrated that megakaryocytes migrate to the endosteum post lethal radioablation. Once at the endosteum, they release growth factors such as PDGF- β and FGF-2 which accelerate osteoblast proliferation and in turn enhance hematopoietic function (Dominici, Rasini et al. 2009, Olson, Caselli et al. 2013). Interestingly, megakaryocytes can also directly regulate HSC pool size via direct secretion of factors such as CXCL4 and IGF-1 (Heazlewood, Neaves et al. 2013, Bruns, Lucas et al. 2014).

This chapter is focused on understanding the relative location of HSC, OM, osteoblasts and megakaryocytes within the hematopoietic niche. Previously, the importance of crosstalk between OM, osteoblasts and megakaryocytes in maintaining hematopoietic function was established. In this chapter, the essential role of megakaryocytes in maintaining hematopoiesis is discussed; and the importance of physical interactions between OM, osteoblasts and megakaryocytes in maintaining hematopoietic function is determined.

4.2 Crosstalk between OM, osteoblasts and megakaryocytes is essential to maintain murine hematopoiesis

It was previously established that immature osteoblasts support the most robust hematopoietic activity (Cheng, Chitteti et al. 2011, Chitteti, Cheng et al. 2013) and that osteoblasts lose this potential as they differentiate in culture (Chitteti, Cheng et al. 2010, Cheng, Chitteti et al. 2011, Chitteti, Cheng et al. 2013). Also, megakaryocytes have the potential to suppress osteoblast differentiation (Ciovacco, Cheng et al. 2010). Hence, the next study was to examine if megakaryocytes can augment osteoblast-mediated hematopoiesis enhancing activity via their interactions with OM. Unsorted NCC, sorted osteoblasts (CD45-F4/80-), or OM from C57BL/6 mice (CD45.2) were used for these assays. NCC were cultured fresh (NCC) or were maintained for 1 wk without (1 wk NCC) or with megakaryocytes (1 wk NCC+MK) prior to their use in culture (Figure 4.1A). The hypothesis being that cultured 1 wk NCC would have a higher number of differentiated osteoblasts; whereas the presence of megakaryocytes with NCC (1 wk NCC+MK) would suppress osteoblast differentiation and thus 1 wk NCC+MK will enhance hematopoiesis at the same level as fresh NCC. Similarly, cultures of osteoblasts (designated in Figure 4.1A as OB) and OM with megakaryocytes (1 wk OB+MK and 1 wk OM+MK, respectively) were established. At the 1 wk time point, cultures were seeded with freshly sorted BoyJ-derived (CD45.1) LSK cells. Cells were harvested 7 days later and assayed for CFU (Figure 4.1A). Consistent with previous findings, NCC maintained in culture for 1 wk (1 wk NCC) provided a significantly decreased level of hematopoiesis enhancing activity relative to fresh NCC. Megakaryocytes promoted the hematopoiesis enhancing activity of 1 wk NCC (1 wk NCC+MK) as evidenced by similar CFU counts compared to fresh NCC cultures. Interestingly, the megakaryocyte-enhanced activity was lost when OM were removed from NCC by cell sorting (1 wk OB+MK), suggesting that osteoblasts, OM, and megakaryocytes cooperate to promote hematopoietic progenitor and HSC function and

that megakaryocytes can delay or suppress osteoblast differentiation thus preserving their hematopoiesis enhancing potential. Data depicting the breakdown of the CFU subtypes based on lineage in these clonogenic assays are shown in Figure 4.1 B, C and D. The multi-lineage data suggests that crosstalk between OM, osteoblasts and megakaryocytes affect the CFU fold change at the granulocyte-monocyte level.

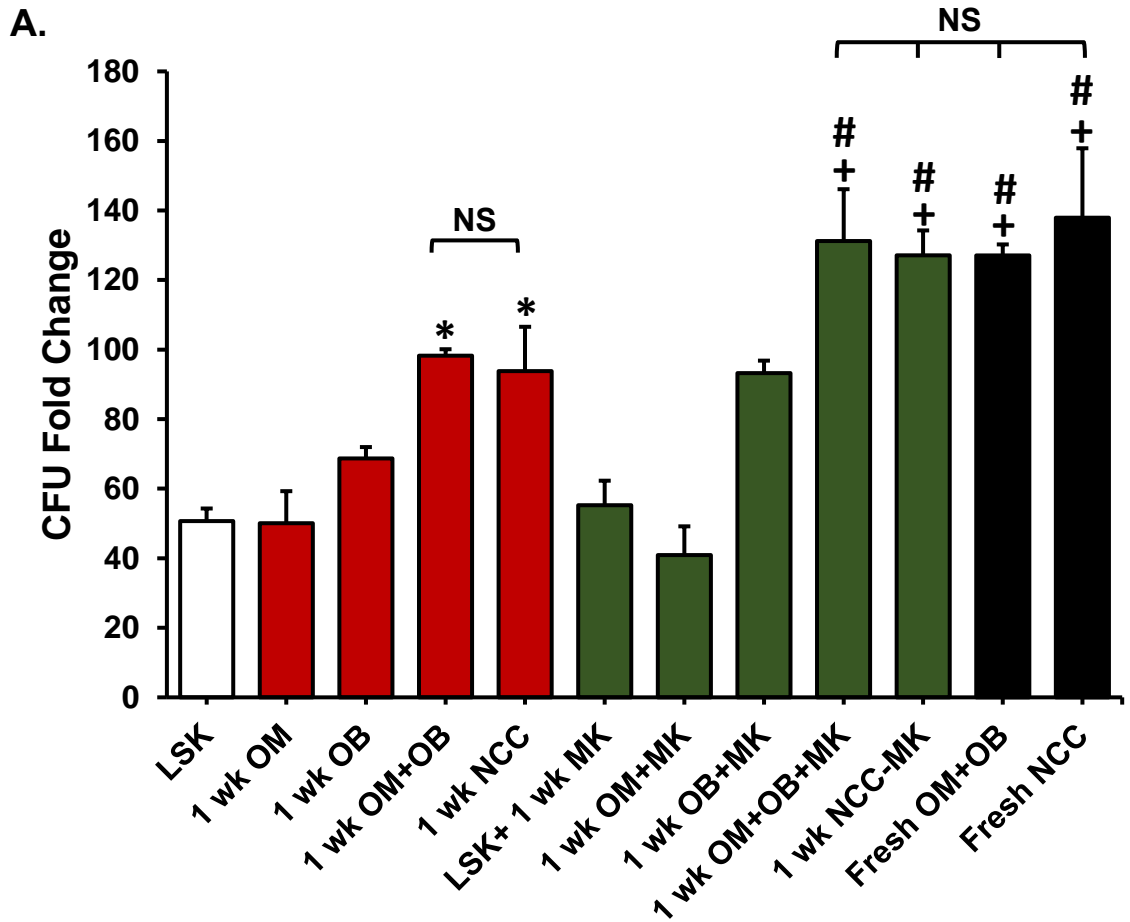
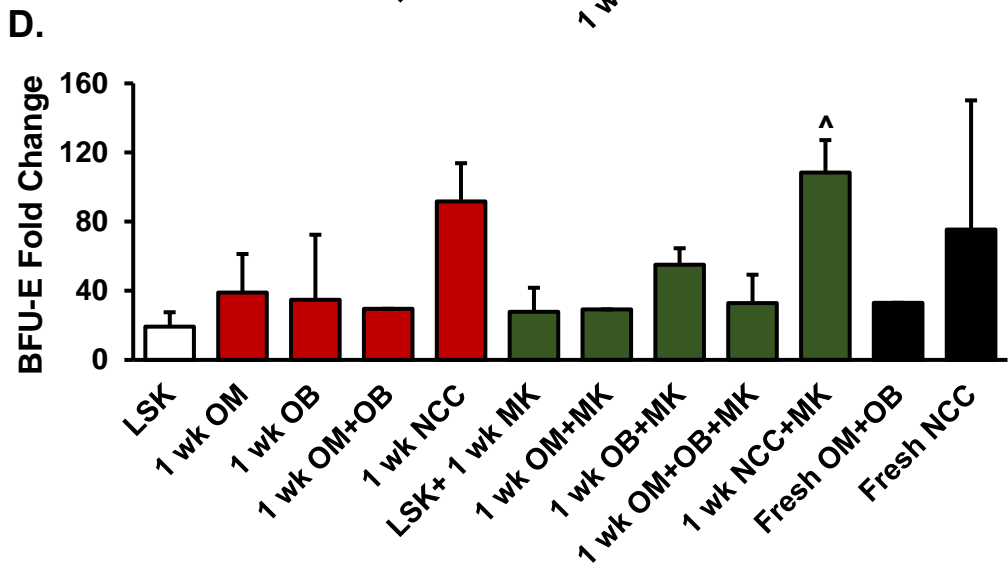
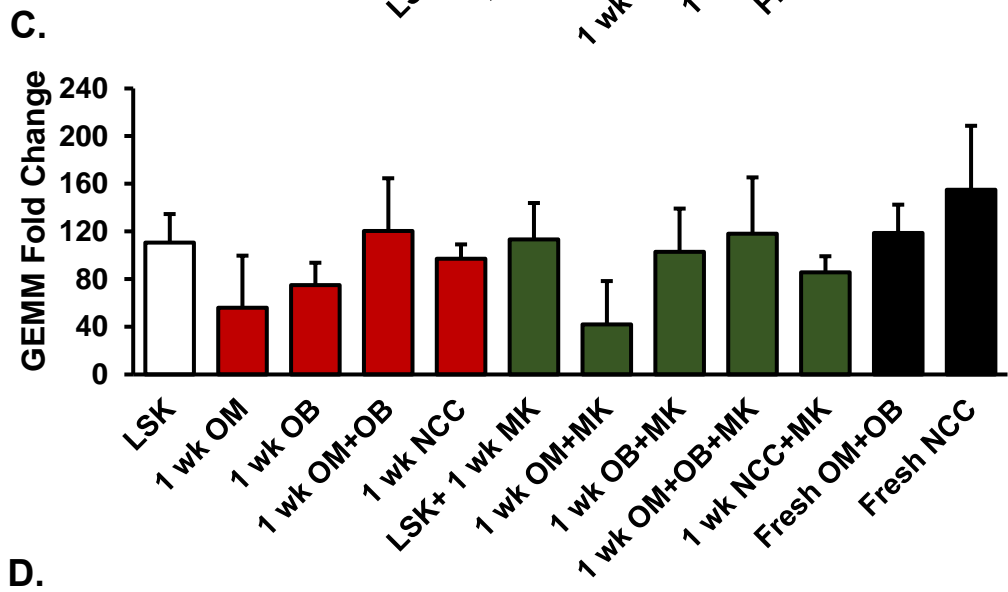
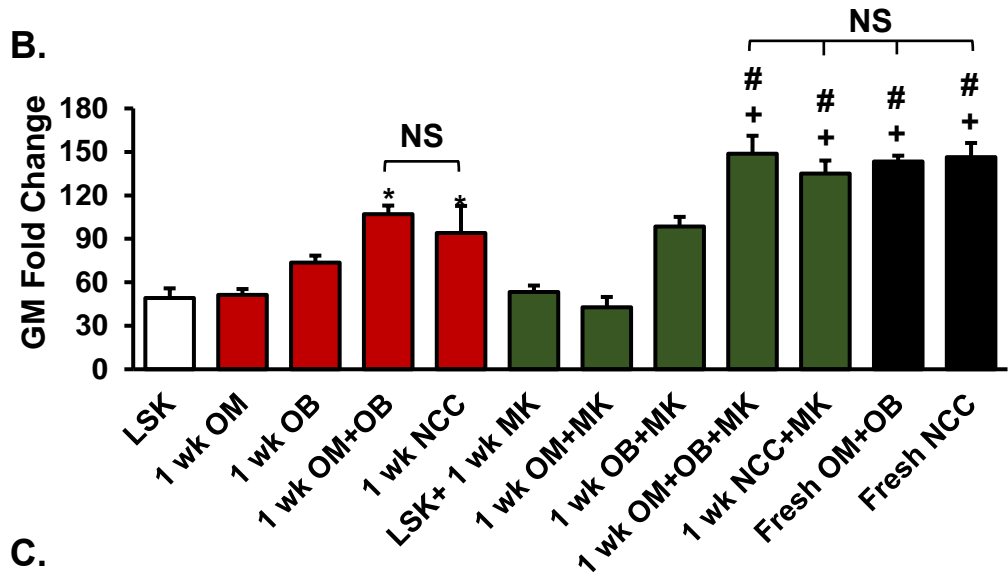


Figure 4.1 **Effect of megakaryocytes on OM and osteoblast function.** Neonatal OM and OB were co-cultured for 1 week in the absence (red bars) or presence (green bars) of MK. At the end of the week, additional control groups of fresh OM+OB and fresh NCC were plated. LSK cells were added to each of these groups and progenitor assays were performed on day 7 (14 days total after the establishment of the first series of cultures). CFU fold change was determined relative to 250 fresh LSK cells. Multilineage analysis was performed to identify the distribution of GM (B), GEMM (C) and BFU-E (D) colonies. N=One of three independent experiments performed in triplicates. NOTE: Each graph has been set with a different scale on the y-axis. * $p < 0.05$ vs LSK, OM and OB, + $p < 0.005$ vs LSK+MK, OM+MK, OB+MK, # $p < 0.05$ vs OM+OB, ^ $p < 0.05$ vs MK, OM+MK, OM+OB; One Way Anova.



In vitro observations were validated in competitive repopulation assays (Mohamad, Xu et al. 2017). Culture conditions were maintained similar to the previous CFU experiment. LSK cells (CD45.2) from each culture condition along with competitor cells (CD45.1) were co-transplanted into lethally irradiated F1 mice (CD45.1/CD45.2). Kinetics of chimerism in primary recipients over a period of 4 months are shown in Figure 4.2. LSK cells maintained for 1 wk in NCC+MK cultures retained the highest level of repopulating activity relative to fresh LSK cells (Figure 4.2A) suggesting that megakaryocytes were able to relatively reverse the decline in the hematopoiesis enhancing activity of NCC cultured alone without megakaryocytes (1 wk NCC). Secondary transplantation data (Figure 4.2B) demonstrated again that 1 wk NCC cultured with megakaryocytes (1 wk NCC+MK) retained a robust hematopoiesis enhancing activity relative to LSK cells cultured with NCC maintained alone for 1 wk. Neither osteoblasts nor OM alone sustained the marrow repopulating potential of LSK cells suggesting that the previously documented hematopoiesis enhancing activity of NCC (Chitteti, Cheng et al. 2010) is synergistically mediated by osteoblasts and OM. Overall, these data establish the importance of crosstalk between OM, osteoblasts and megakaryocytes to form a novel network in supporting HSC function.

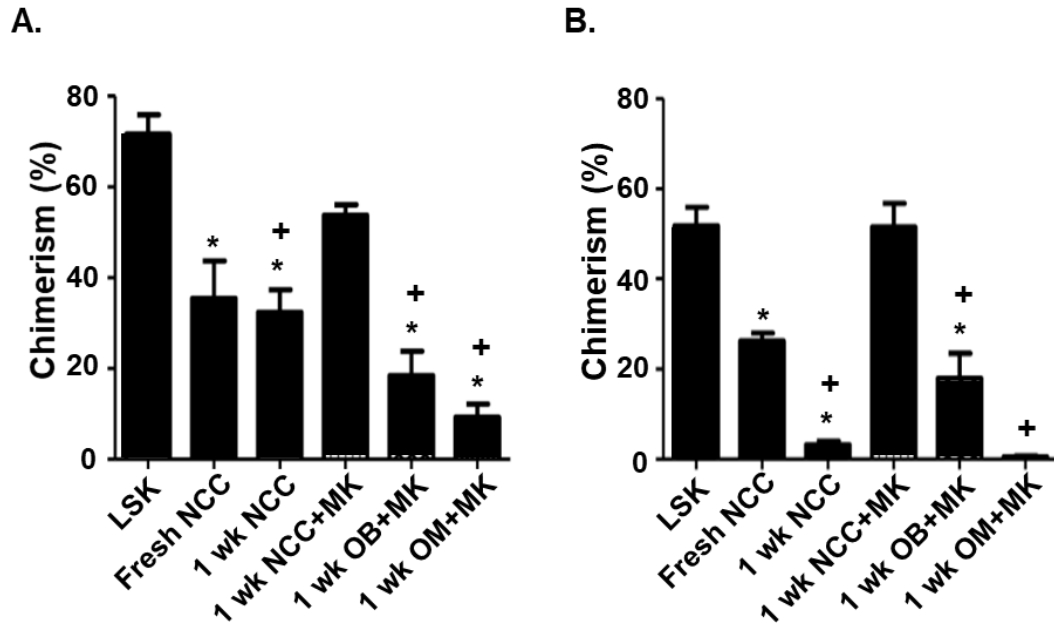


Figure 4.2 *In vivo* assays of cells maintained *in vitro* with NCC or sorted fractions of NCC. Progeny of 1000 LSK cells from C57BL/6 (CD45.2) mice, which were cocultured for 5 days with each group of cells identified in Figure 4.1A, were transplanted in a competitive repopulation assay with 100,000 BoyJ (CD45.1) cells via tail vein injection in lethally irradiated (split dose of 650 and 350 cGy) CD45.1/CD45.2 F1 recipients. Freshly isolated LSK cells from BoyJ mice were used as control. (A) Chimerism in the BM of primary recipients at 4 months post transplantation. (B) At 4 months post-primary transplantation, halves of femurs from primary recipients were transplanted into lethally irradiated secondary recipients. Chimerism in secondary recipients at 3 months post transplantation is shown in (B). * $p < 0.05$ vs LSK group, + $p < 0.05$ vs 1w NCC+MK group, 1-way ANOVA (Mohamad, Xu et al. 2017)

4.3 Early stage megakaryocytes are functionally important for OM proliferation

The evolution of megakaryocytes begins with a megakaryocyte progenitor which differentiates into a megakaryoblast (CD41-CD61+). These megakaryoblasts act as precursors for immature megakaryocytes (CD41+CD49d+) which then differentiate into mature megakaryocytes (CD41+CD49b+). Mature megakaryocytes are the cells that ultimately differentiate into platelets (Ciovacco, Cheng et al. 2010). Based on this process, the goal was to determine whether megakaryocytes at a particular stage of differentiation are responsible for OM proliferation. To do so, whole fraction megakaryocytes were flow sorted to isolate megakaryoblasts, immature megakaryocytes and mature megakaryocytes. Each of these three groups was then cultured with NCC in a 1:2 ratio. On day 6 of culture, cells were analyzed for OM expansion. As expected from earlier results (Figure 3.1), an increase in OM numbers and percentage was observed when NCC were cultured in the presence of unsorted megakaryocytes (Figure 4.3, top panel). The data consistently demonstrated that megakaryoblasts increase or maintain OM numbers in culture, whereas, OM numbers decline when cultured with mature megakaryocytes (Figure 4.3, bottom panel). These data indicate that most likely OM expand in numbers when cultured with immature megakaryocytes (megakaryoblasts and immature megakaryocytes). Furthermore, it suggests that mature megakaryocytes fail to sustain OM expansion.

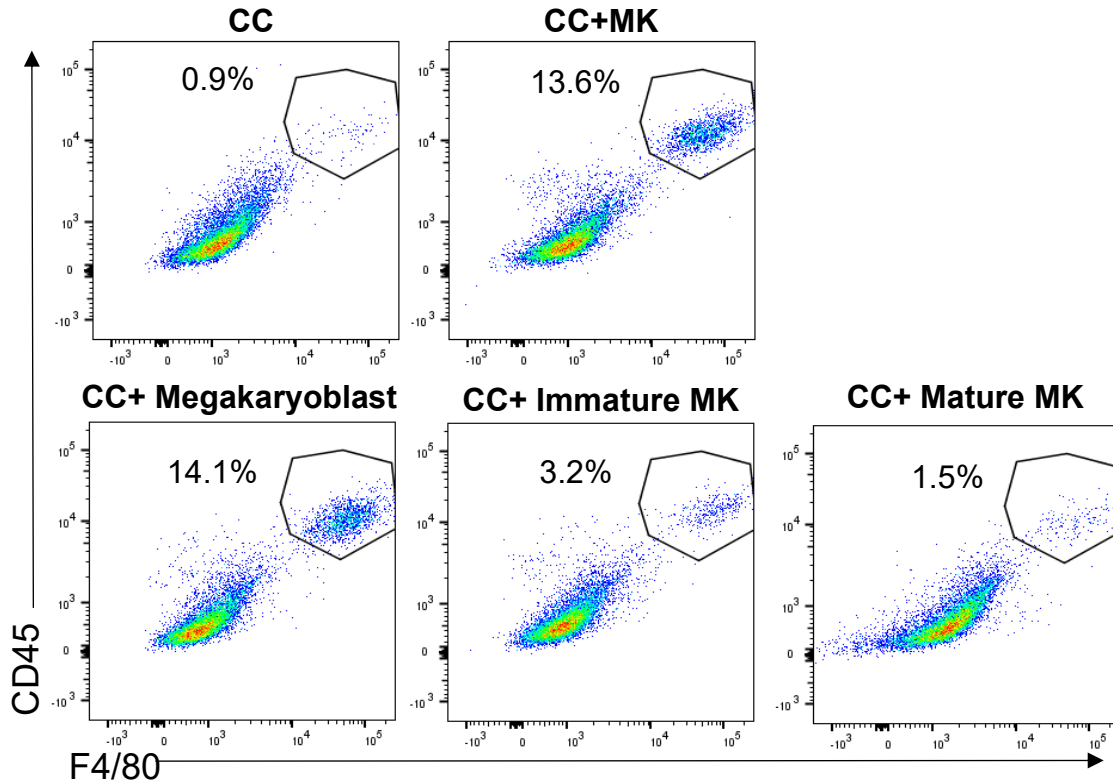


Figure 4.3 **Early stage megakaryocytes promote OM proliferation *in vitro*.** (Top Panel) NCC were cultured for 6 days in the absence or presence of megakaryocytes (MK). (Bottom Panel) Megakaryocytes were sorted into CD61+CD41⁻ megakaryoblasts, CD41+CD49d⁺ immature MK and CD41+CD49b⁺ mature MK. NCC were cultured for 6 days with each of these subgroups of MK. On day 6, cells were stained with CD45 and F4/80 to identify % increase in OM. N=3

4.4 Direct interactions between OM, osteoblasts and megakaryocytes are essential for maintaining hematopoiesis

Next, to determine the importance of direct contact between OM, osteoblasts and megakaryocytes in maintaining OM proliferation, NCC were cultured in the absence or presence of megakaryocytes for 4-6 days. To eliminate contact between NCC and megakaryocytes, 1-micron transwell system was used to separate the two types of cultured cells. The small pore size of the transwell even prevented platelets which are a maximum of 2-3 microns in size (Krishnegowda and Rajashekaraiah 2015) from coming into direct contact with NCC. On analyzing the data, OM failed to expand in numbers when NCC were physically separated from megakaryocytes (Figure 4.4). This indicates that OM need to be in direct contact with megakaryocytes for them to increase in numbers.

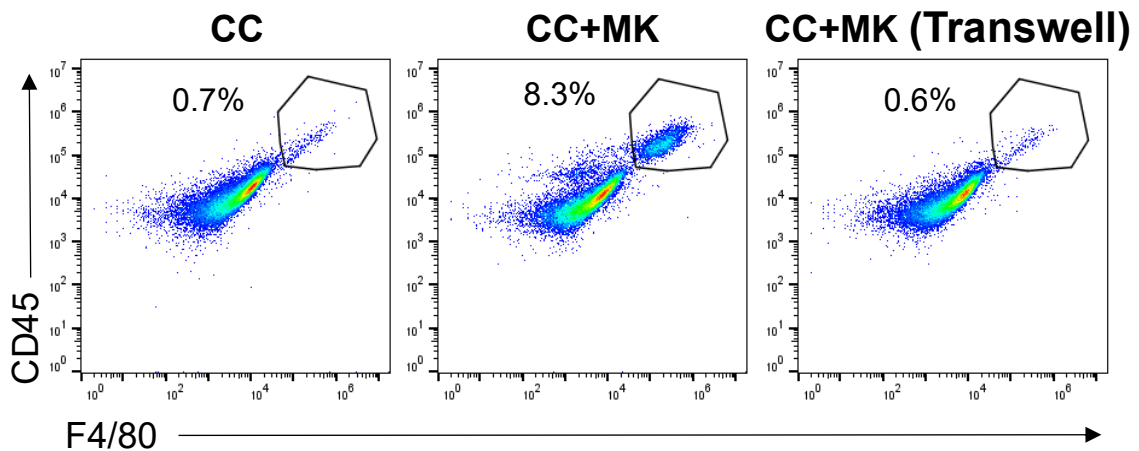


Figure 4.4 **Direct interaction is required for megakaryocytes to enhance OM numbers.** NCC were cultured for 6 days in the absence or presence of megakaryocytes (MK). An additional culture condition was maintained wherein a 1-micron transwell was placed above NCC creating a barrier between NCC and MK. On day 6 of culture, cells were collected and stained for CD45 and F4/80 to identify % increase in OM. N=2

Furthermore, these studies were expanded to determine whether direct contact between the three cell types is essential to maintain hematopoiesis. Sorted OM and osteoblasts (labeled as OB in Figure 4.5) were reconstituted and cultured in the absence (OM+OB) or presence (OM+OB+MK) of megakaryocytes, with a 0.4-micron transwell placed above OM+OB cultures to prevent direct contact with megakaryocytes. The next day, cultures were seeded with freshly sorted LSK cells that were placed in the lower chamber in direct contact with OM+OB but not with megakaryocytes in the upper chamber. Cells were harvested 7 days later and assayed for CFU. As seen in Figure 4.5, in the absence of a transwell, OM+OB maintained hematopoietic enhancing activity; and this activity was augmented when megakaryocytes were added in culture. However, when a transwell membrane separated megakaryocytes from OM+OB, the latter failed to augment the CFU fold change beyond what was observed with OM+OB cultured in the absence of megakaryocytes. Interestingly, placing a transwell above OM+OB+MK cultures wherein all the cells were in direct contact (OM+OB+MK (T)), also caused a decline in CFU activity. These data suggest, that this decline in CFU fold change might be due to alterations in oxygen exchange and/or changes in cellular waste in the medium due to the placement of the membrane in the transwell system.

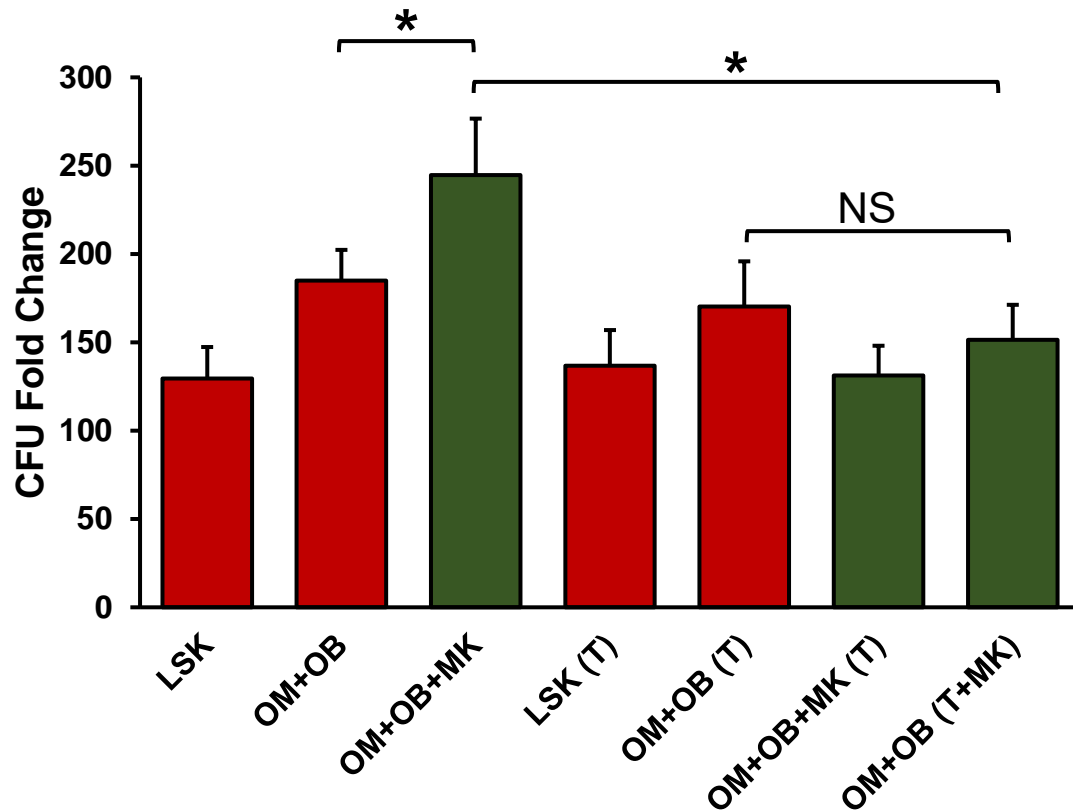


Figure 4.5 **Direct interactions between OM, osteoblasts and megakaryocytes are important to maintain hematopoietic enhancing activity.** Neonatal OM and osteoblasts (OB) were co-cultured for 1 day in the absence (red bars) or presence (green bars) of megakaryocytes (MK). In the groups labeled (T), a 0.4-micron transwell was added above the cultures. In the group labeled (T+MK), MK were added on the transwell separating them from OM and OB. LSK cells were added below the transwell to each of these groups and progenitor assays were performed on day 7. CFU fold change was determined relative to 250 fresh LSK cells. N=One of three independent experiments performed in triplicates. * $p < 0.05$ for OM+OB+MK vs all other groups, One Way Anova.

4.5 3D tissue cytometry helps define the spatial localization of OM, osteoblasts and megakaryocytes relative to HSC in the hematopoietic niche

The previous data (Figure 4.4 and 4.5) indicate that direct contact is required between OM, osteoblasts and megakaryocytes to maintain hematopoiesis. Therefore, the next goal was to understand the spatial relationship of these three cell types with respect to HSC in the hematopoietic niche. The use of confocal microscopy allows for the collection of large 3D datasets which preserve the spatial relationship between cells and allows for the quantitation of various cell types within this spatially conserved intact tissue. This process is referred to as 3D tissue cytometry. It has been successfully developed and used in the field of immunology, for example, to measure distances between various immune cells in intact kidney tissue (Winfrey, Khan et al. 2017) and recently in the bone marrow (Coutu, Kokkaliaris et al. 2017). Therefore, 3D tissue cytometry was performed to understand the spatial location of HSC, OM, osteoblasts and megakaryocytes in the hematopoietic niche. Fgd5 reporter mice were used to identify GFP+ HSC and GFP+ vasculature.

Cells were stained with anti-F4/80 antibody to identify macrophages in the bone marrow. Based on the anatomic location of F4/80+ macrophages, OM were identified as F4/80+ macrophages located at or near the endosteum (maximum of 2-3 cells away); whereas, BM M ϕ were F4/80+ macrophages located towards the center of the marrow away from the endosteum. Megakaryocytes were stained with an anti-CD41+ antibody. However, the CD41 antibody was conjugated to the AF405 fluorophore which was detected in the same channel as DAPI (a nuclear stain). A nuclear stain is always required in the 3D cytometry setting to identify all the cells observed in a given field of observation. Hence megakaryocytes were recognized partly based on their CD41 staining; and partly on their unique multi-lobulated nucleus which was easily identifiable. Finally, a 2 photon microscope was used to image the bone and ultimately identify osteoblasts.

As expected, majority of GFP+ HSC were located within the growth plate (Ellis, Grassinger et al. 2011). Interestingly, in the epiphysis as well as the diaphysis, multiple fields were observed wherein all four cell types were in close proximity to each other. Representative images are shown in Figure 4.6 B and C. Also, a mosaic encompassing the entire 25 micron section of the femur was captured (Figure 4.6A). Ongoing studies using the mosaic, involve determining the number of HSC, OM, osteoblasts and megakaryocytes within the whole volume of the unperturbed bone marrow; and using those data to compare the relative number and location of cells in a stressed or aged bone marrow. Altogether, these initial data suggest intimate spatial interactions between HSC, OM, osteoblasts and megakaryocytes in the unperturbed bone marrow.

A.

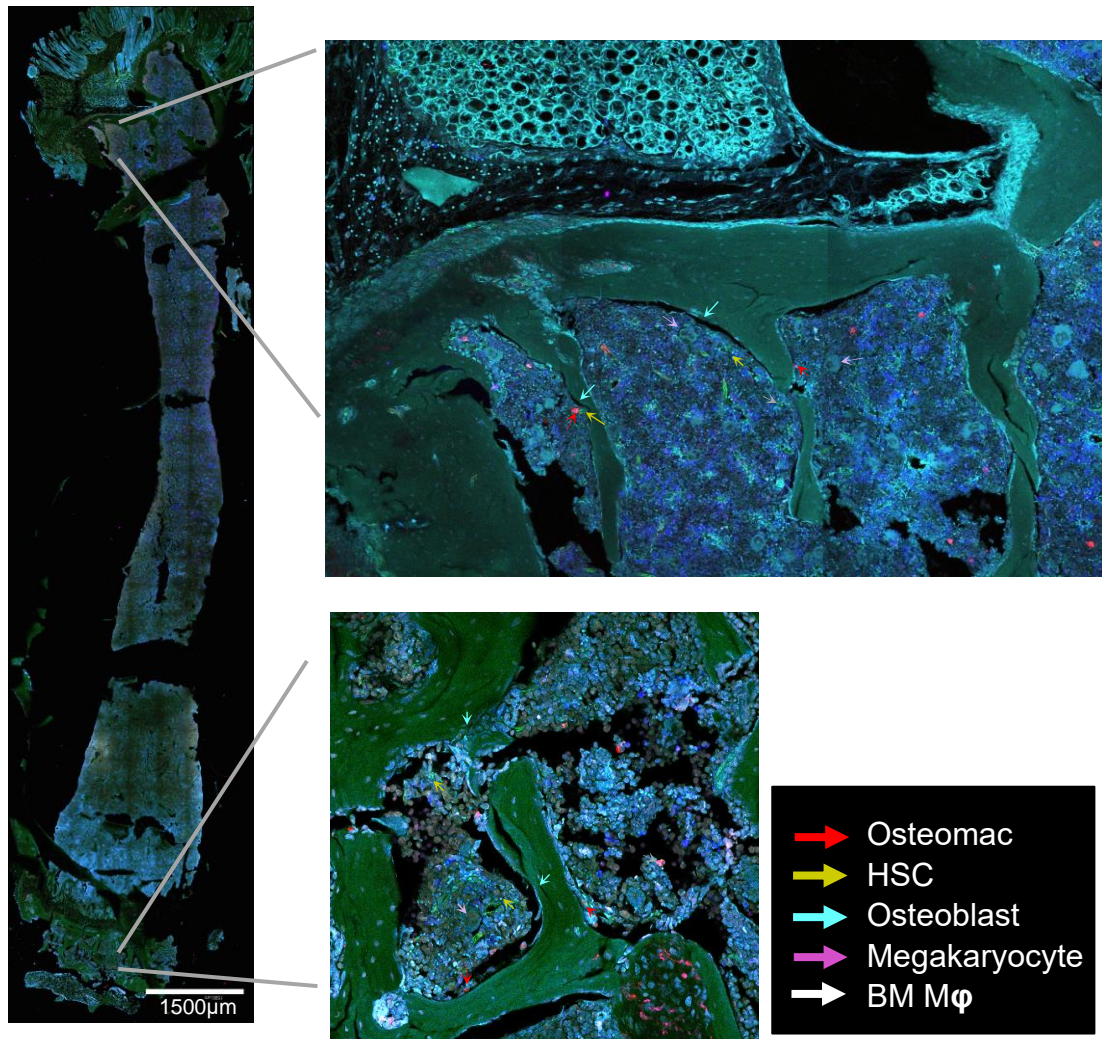
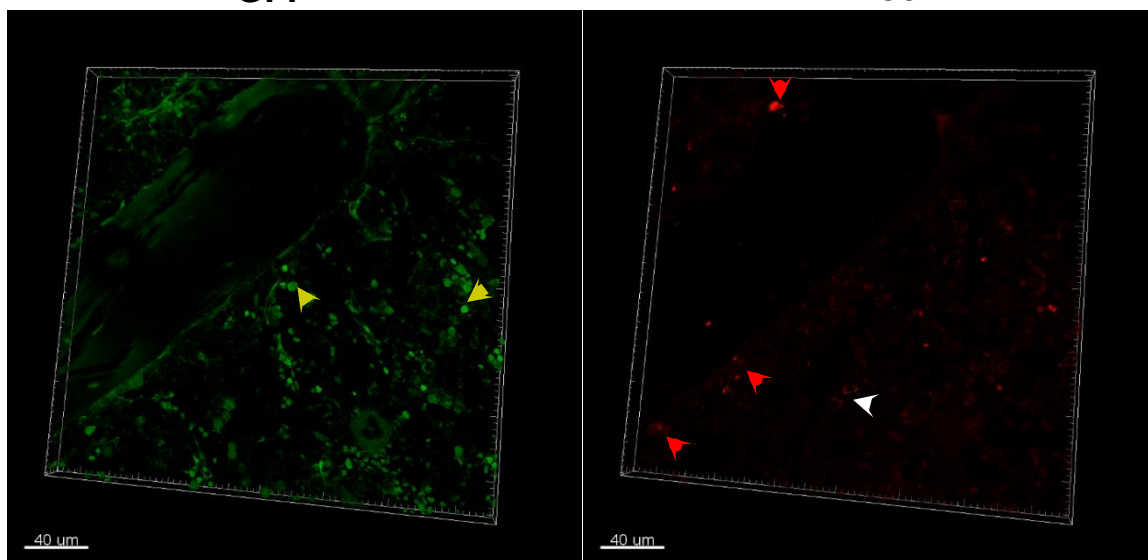


Figure 4.6 **Use of 3D cytometry to determine localization of hematopoietic niche residents.** 25-micron sections of *Fgd5* mice were used to stain for 3D tissue cytometry. HSC (yellow arrow) were GFP+, OM (red arrow) and BM Mφ (white arrow) were F4/80+ (AF647), megakaryocytes (purple arrow) were multi-lobulated and CD41+ (AF405). Osteoblasts (blue arrow) were imaged using the second harmonic signal (SHG). (A) Mosaic of the entire femur. (B) (C) 3D z-stack images of 25-micron sections.

B.

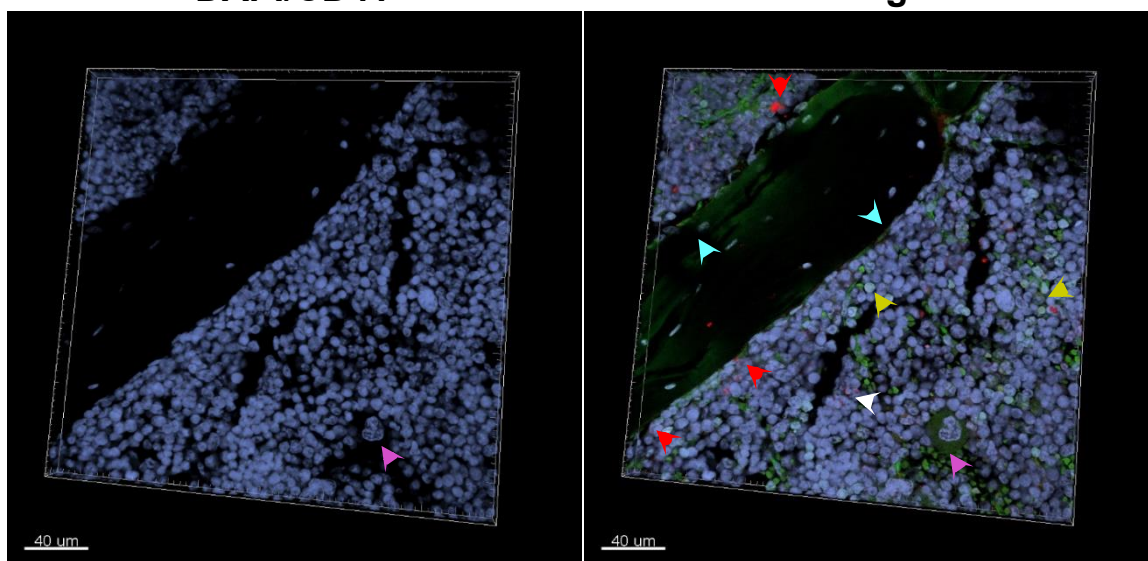
GFP+

F4/80+



DAPI/CD41

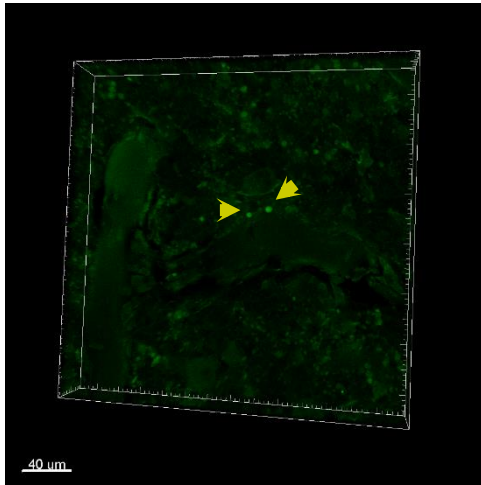
Merged



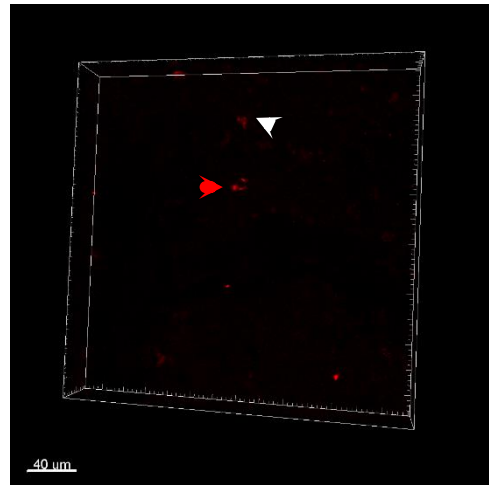
- Osteomac
- HSC
- Osteoblast
- Megakaryocyte
- BM Mφ

C.

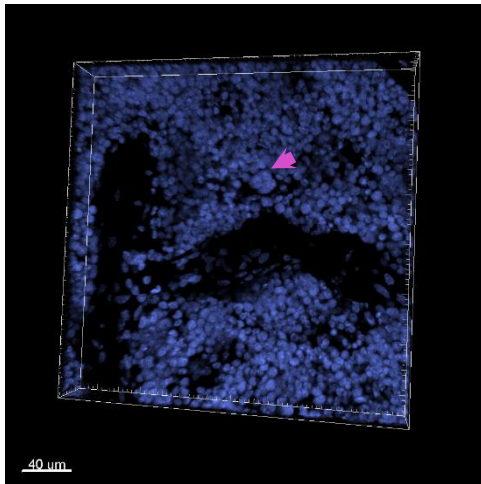
GFP+



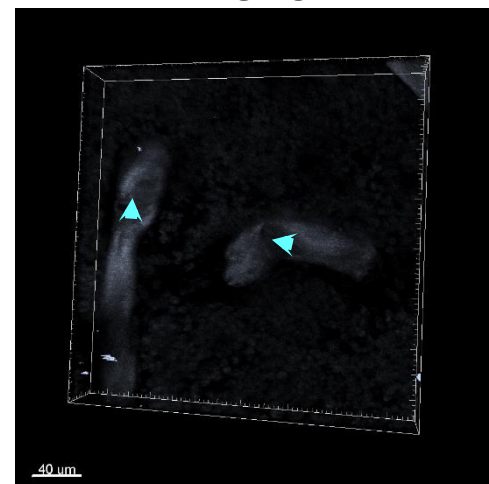
F4/80



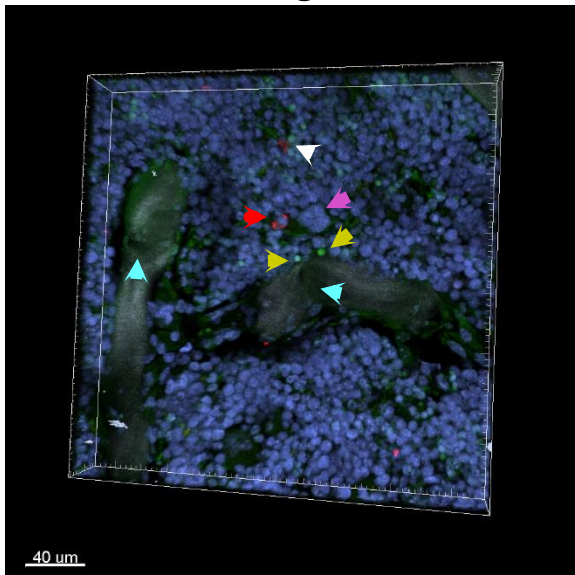
DAPI/CD41+



SHG



Merged



-  Osteomac
-  HSC
-  Osteoblast
-  Megakaryocyte
-  BM Mφ

4.6 Discussion

In this chapter, the importance of megakaryocytes in the hematopoietic niche was demonstrated. To begin with, the spatial localization of HSC, OM, osteoblasts and megakaryocytes was identified. HSC are known to localize adjacent to megakaryocytes in a non-random fashion (Heazlewood, Neaves et al. 2013). Also, HSC have the tendency to migrate to the endosteum to retain their quiescence (Nilsson, Johnston et al. 2001, Zhang, Niu et al. 2003, Xie, Yin et al. 2009). Previous studies illustrating HSC localization have always been focused on its location near the endosteum or the vasculature (Aiuti, Webb et al. 1997, Nilsson, Johnston et al. 2001, Zhang, Niu et al. 2003, Kiel, Yilmaz et al. 2005, Sugiyama, Kohara et al. 2006, Xie, Yin et al. 2009, Kunisaki, Bruns et al. 2013, Nombela-Arrieta, Pivarnik et al. 2013). The 3D tissue cytometry data in Figure 4.6 support these concepts, and furthermore provide additional information regarding the proximity of OM relative to the cell types mentioned above. Through ongoing studies, it was observed that HSC, OM, osteoblasts and megakaryocytes tend to co-localize in close proximity within the hematopoietic niche (Figure 4.6). However, these studies are at early stages. One of the technical difficulties in these studies include getting sections with bone marrow intact and attached to bone. This is because bone marrow easily sloughs off, giving cracked sections. Also, the current sections are only 25 microns in width. To truly understand the complexity of the niche, imaging whole femurs will be necessary. Furthermore, an additional technical problem to overcome is due to autofluorescence of bone. To overcome this obstacle, clearing the bone will be required to better visualize bone marrow architecture; a concept recently developed for other tissues (Li, Germain et al. 2017). Though these studies are incomplete, future studies will establish relative numbers of these four cell types in whole unperturbed bone marrow. The use of 3D technology to establish such correlations between cells has previously been developed at Indiana University (Winfree, Khan et al. 2017). Once complete, the changes in localization

that occur within a stressed hematopoietic niche will be determined. It is well established that age stresses the hematopoietic niche and slows down hematopoiesis (Rossi, Bryder et al. 2005, Janzen, Forkert et al. 2006, Gekas and Graf 2013). It will be interesting to determine whether changes in localization, occur with age correlating to loss in hematopoietic function.

However, HSC are dynamic in nature. Hence, the close proximity of HSC to OM, osteoblasts and megakaryocytes is not sufficient to suggest functional correlation. To that end, in vitro and in vivo data was established to determine the importance of crosstalk between OM, osteoblasts and megakaryocytes in maintaining hematopoietic function. These data demonstrate that OM and osteoblasts enhance hematopoietic activity, and megakaryocytes further augment this function (Figure 3.9A). Since immature osteoblasts best support hematopoietic enhancing activity (Chitteti, Cheng et al. 2010, Cheng, Chitteti et al. 2011, Chitteti, Cheng et al. 2013), this suggests the possibility that megakaryocytes might be suppressing osteoblast differentiation to maintain hematopoiesis. This is supported by the data in Figure 4.1 and 4.2, which show that fresh NCC, which consist of immature osteoblasts, maintain hematopoiesis similar to NCC cultured in the presence of megakaryocytes. Furthermore, megakaryocytes might also be supporting hematopoiesis through pathways involving OM. Since megakaryocytes increase OM numbers in NCC cultures, there is a possibility that they may also regulate expression of certain molecules on OM which in turn maintain hematopoietic function. This topic will be covered in more detail in the next chapter.

The next important question that was addressed was whether direct interactions are required between HSC, OM, osteoblasts and megakaryocytes or whether megakaryocytes might be working in a paracrine fashion to release cytokines or growth

factors that help OM and osteoblasts maintain hematopoiesis. Previous studies have demonstrated that megakaryocytes release growth factors such as FGF2 and PDGF- β to increase osteoblast proliferation post hematopoietic stress (Dominici, Rasini et al. 2009, Olson, Caselli et al. 2013). Also, previous reports have demonstrated that megakaryocytes themselves release several cytokines which directly regulate HSC pool size and quiescence (Heazlewood, Neaves et al. 2013, Bruns, Lucas et al. 2014, Nakamura-Ishizu, Takubo et al. 2014, Zhao, Perry et al. 2014). Therefore, it is important to understand whether megakaryocytes require direct physical contact with OM and OB to mediate hematopoietic function. The studies in Figure 4.4 illustrate, that OM also require physical contact with megakaryocytes to increase their proliferation. The observed increase in OM numbers was more robust when it was induced by megakaryocytes that are at early stages of differentiation (Figure 4.3). Furthermore, direct contact is also essential for megakaryocytes to augment OM and osteoblast mediated hematopoiesis (Figure 4.5). This is different from previous reports that demonstrate the importance of megakaryocyte secreted cytokines in direct regulation of HSC pool size and quiescence (Heazlewood, Neaves et al. 2013, Bruns, Lucas et al. 2014, Nakamura-Ishizu, Takubo et al. 2014, Zhao, Perry et al. 2014). This difference could be due to the different experimental procedures employed by different laboratories. For example, the report described by Dominici et al., is based on the migration of megakaryocytes to the endosteum post radioablation and the release of growth factors that catalyze osteoblast proliferation (Dominici, Rasini et al. 2009, Olson, Caselli et al. 2013). Since the megakaryocytes release the growth factors only after migrating to the endosteum, there is a possibility that direct contact between osteoblasts and megakaryocytes is necessary for the regulation of osteoblast proliferation. Also, Bruns et al., demonstrated the role of megakaryocytes in regulating HSC quiescence through CXCL4 secretion (Bruns, Lucas et al. 2014). They used two main pieces of data to verify this hypothesis. The first was depletion of megakaryocytes which resulted in loss

of HSC function. This fits with the data in Figure 4.1 and 4.2 where it was demonstrated that maximal hematopoietic enhancing activity is achieved only in the presence of megakaryocytes which interact with OM and osteoblasts. The second result was that megakaryocytes secrete CXCL4 and that CXCL4^{-/-} mice exhibit decreased HSC quiescence. The catalyst which activates the megakaryocyte secretion of CXCL4 is still unknown. Therefore, the possibility remains that direct interactions between OM, osteoblasts and megakaryocytes may be required to induce the secretion of CXCL4 by megakaryocytes.

Studies in this chapter demonstrate the importance of direct interactions between OM, osteoblasts and megakaryocytes to mediate hematopoietic function and maintain the competence of the hematopoietic niche. These findings help establish correlations between hematopoietic function and the close proximity of these cell types. These data suggest that hematopoiesis is best maintained when the four cell types interact as shown in Figure 4.7. It is postulated that as these cells 'age' or are compromised upon stress, their interactions are disrupted, and HSC begin to lose function leading to a compromised niche (Figure 4.7). Further detailed analyses are required to molecularly define how these cell types interact together.

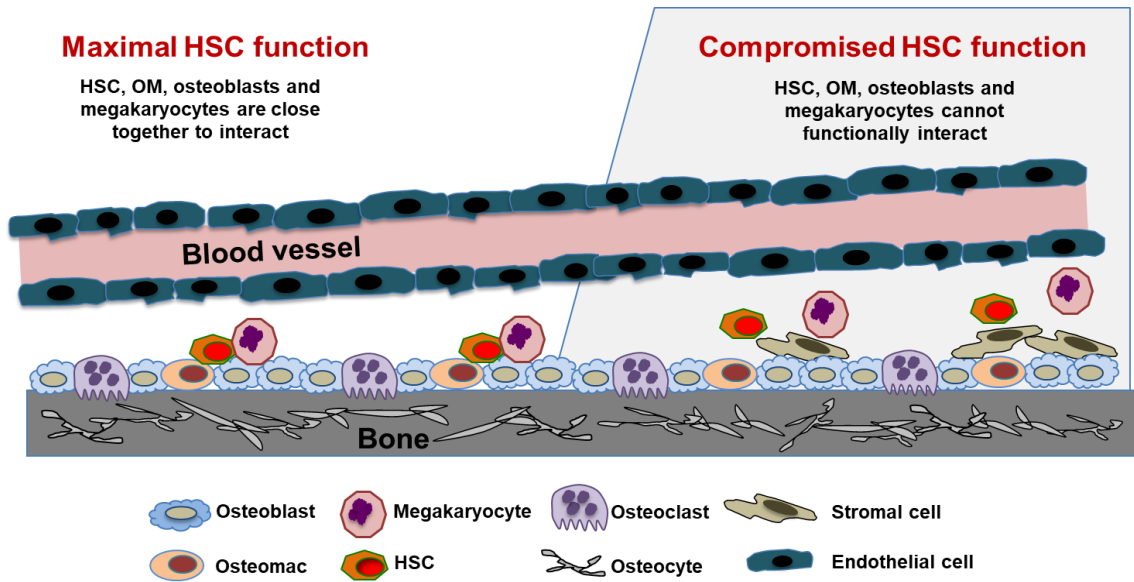


Figure 4.7 **Model depicting functional interaction between OM, osteoblasts and megakaryocytes.** Crosstalk between OM, osteoblasts and megakaryocytes are essential to maintain maximal hematopoietic function (left). Disruption in the functional interaction between these three cell types leads to a compromised hematopoietic niche (right).

CHAPTER FIVE: CD166 and embigin are molecular mediators through which OM maintain hematopoietic function

5.1 Introduction

Networking between HSC and cells of the hematopoietic niche is important to maintain hematopoiesis. Amongst the cell groups of the niche involved in this process are a group of bone-resident macrophages known as osteomacs (OM). Previously, it was demonstrated that OM and osteoblasts contained within NCC are critical to maintain hematopoietic function (Chitteti, Cheng et al. 2010, Mohamad, Xu et al. 2017). Additionally, interactions between NCC and megakaryocytes further enhance this hematopoietic activity (Figure 4.1, 4.2). However, the molecular pathways through which this crosstalk occurs and in turn enhances hematopoietic activity are still unknown.

CD166 (ALCAM-Activated Leukocyte Cell Adhesion Molecule) is a transmembrane glycoprotein belonging to the immunoglobulin superfamily (Lehmann, Riethmuller et al. 1989). It is capable of mediating both CD166-CD166 homophilic interactions as well as heterophilic interactions with CD6 (Degen, van Kempen et al. 1998). Recently, CD85k has been identified as a ligand which binds to CD166 and in turn blocks tumor growth in CD166+ tumor cell lines (Xu, Chang et al. 2018). In hematopoiesis, CD166 is an important functional marker of HSC and is critical for the competence of the niche (Chitteti, Cheng et al. 2010, Chitteti, Bethel et al. 2013, Chitteti, Cheng et al. 2013, Chitteti, Kobayashi et al. 2014). Previous work in my laboratory demonstrated that CD166 expression on osteoblasts is inversely proportional to their maturity (Chitteti, Cheng et al. 2010, Chitteti, Cheng et al. 2013). Immature osteoblasts expressing higher CD166 maintain maximum

hematopoietic enhancing activity compared to differentiated osteoblasts expressing lower CD166. Furthermore, CD166 through a mechanism likely involving STAT3 activation, plays an important role in homing and recovery from hematopoietic stress (Chitteti, Kobayashi et al. 2014). Besides HSC and osteoblasts, CD166 is also expressed on several other niche residents such as mesenchymal stem cells, endothelial cells and OM (Chitteti, Bethel et al. 2013, Mohamad, Xu et al. 2017).

Expression of embigin on hematopoietic cells such as bone marrow progenitors, T cells, B cells and several myeloid cells has been previously reported (Pridans, Holmes et al. 2008). Embigin, which is a transmembrane glycoprotein belonging to the immunoglobulin superfamily (Huang, Ozawa et al. 1990, Huang, Ozawa et al. 1993) is an ion transporter essential for the exchange of protons during anaerobic expression in neurons (Wilson, Kraus et al. 2013). Recently, it was reported that blocking embigin in the hematopoietic niche resulted in loss of quiescence with a corresponding increase in the frequency of LT-HSCs, ST-HSCs, as well as MPPs (Silberstein, Goncalves et al. 2016). Embigin, being a cell adhesion molecule (Huang, Ozawa et al. 1993), even caused a loss in HSPC localization (Silberstein, Goncalves et al. 2016). However, the cellular elements in the niche responsible for this hematopoietic function are still unknown.

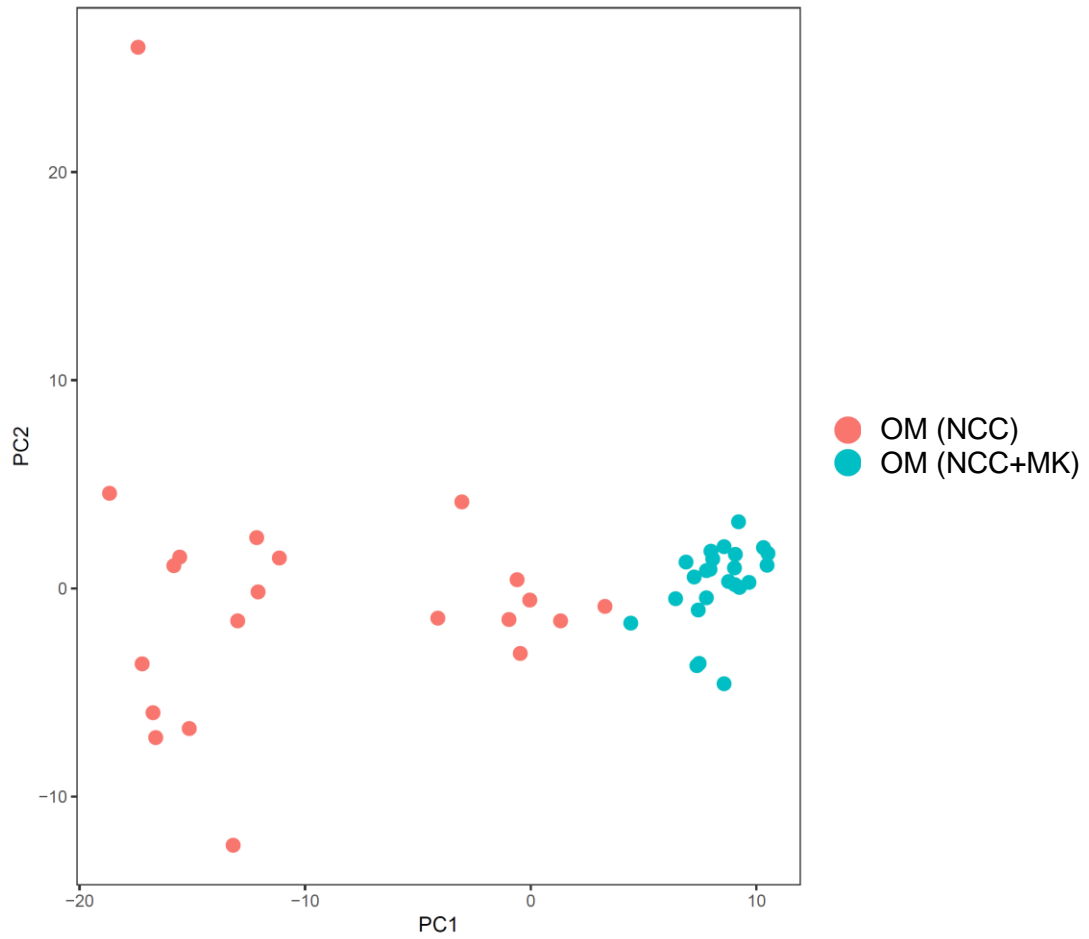
In this chapter, it is demonstrated that crosstalk between OM, osteoblasts and megakaryocytes is required for the upregulation of CD166 and embigin expression on OM. Once activated, these molecular mediators are partially responsible for OM arbitrated maintenance of hematopoietic function. Moreover, recombinant CD166 and embigin can be used to partially substitute for OM activity *in vitro*. Together, the data once again demonstrate the importance of CD166 for the hematopoietic niche; and introduce embigin expression on OM as a regulator of hematopoietic function.

5.2 Single cell mRNA sequencing identified several targets through which OM potentially maintain hematopoietic function

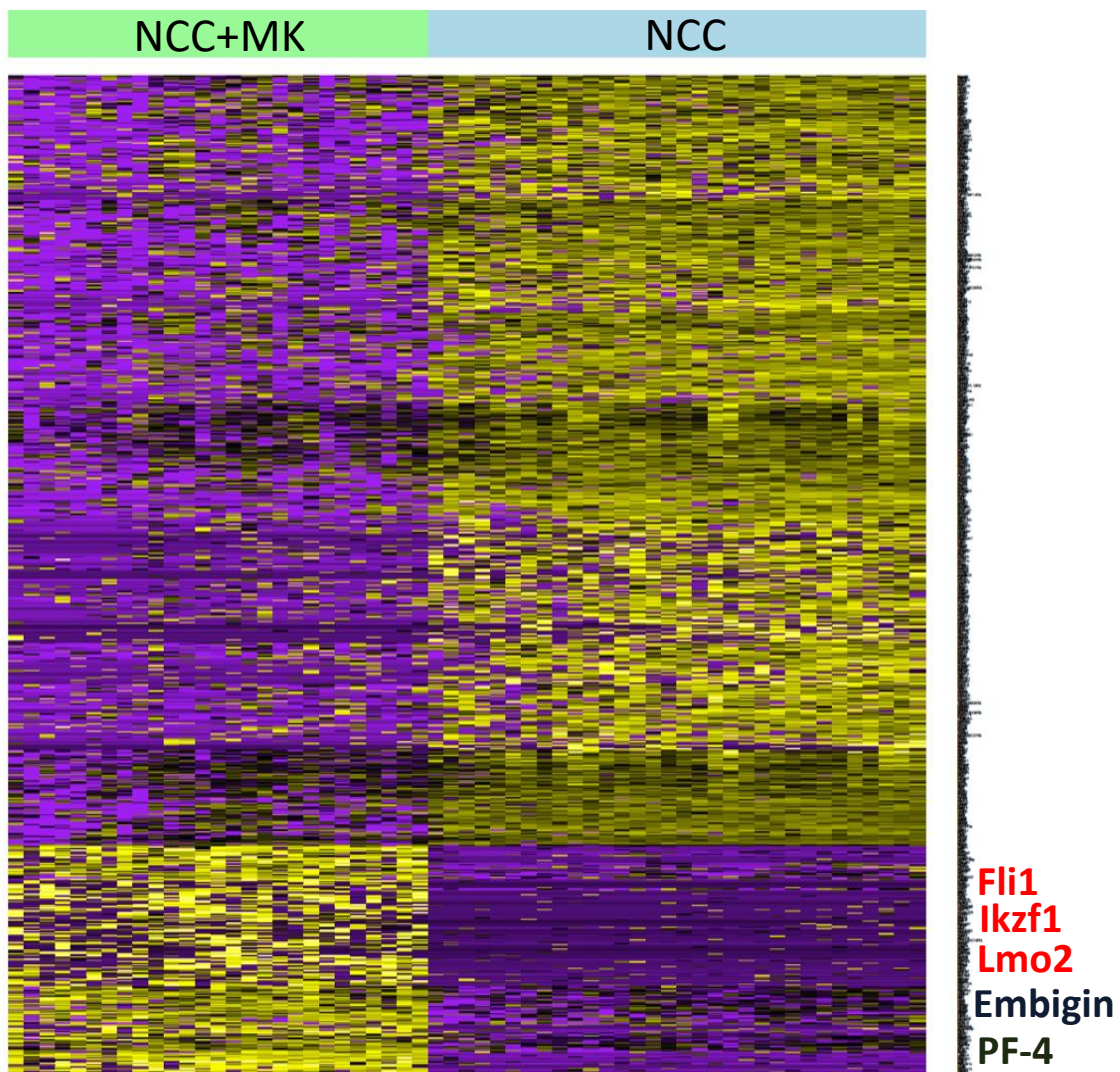
Single cell mRNA sequencing was performed to identify the molecular pathways through which OM interact with osteoblasts and megakaryocytes to maintain hematopoietic function. These single cells studies are highly beneficial over bulk genomics wherein quantification of target genes is averaged; and heterogeneity within populations is left unaccounted. Briefly, 100,000 NCC which consist of OM (~5%) and osteoblasts were cultured for 16 hrs in the absence or presence of 50,000 megakaryocytes. OM from these groups were sorted at the end of the 16 hrs incubation and subjected to single cell mRNA sequencing. Depending on the group from which the OM were sorted, data in the figures have been labeled as NCC or NCC+MK. From each group, 24 cells were sequenced and analyzed. 21 OM from NCC and 24 OM from NCC+MK passed quality check and were used for differentially expressed gene analysis. Comparisons identified 1008 genes as significantly expressed between the two groups. Multidimensional scaling (MDS) plot of top-2 principal components (PCs) of significantly expressed genes suggest a difference between OM obtained from NCC and NCC+MK (Figure 5.1A). Next, a heat map was plotted to identify target genes potentially implicated in the hematopoiesis enhancing activity of OM (NCC+MK) (Figure 5.1B). A total of 299 genes were upregulated in OM obtained from NCC+MK compared to those obtained from NCC, whereas, 709 genes were downregulated. Of note, embigin and PF-4, both of which have been implicated in hematopoiesis (Bruns, Lucas et al. 2014, Silberstein, Goncalves et al. 2016), were upregulated when OM were cultured with megakaryocytes. Lmo-2, Fli-1 and Ikzf-1 which are part of the HSC differentiation pathway (Zhu, Traver et al. 2005, Ferreiros-Vidal, Carroll et al. 2013, Malinge, Thiollier et al. 2013, Smeets, Chan et al. 2013, Pimkin, Kossenkov et al. 2014) were also upregulated. Single cell mRNA sequencing results were validated via qPCR (Figure 5.1C). These single cell genomics data demonstrate the

upregulation of genes such as embigin, PF-4, Fli-1, Lmo-2 and Ikzf-1 when OM contained within NCC were cultured in the presence of megakaryocytes. These targets could act as molecular mediators through which OM maintain HSC function.

A.



B.



Color Key



-1 0 1
Row Z-Score

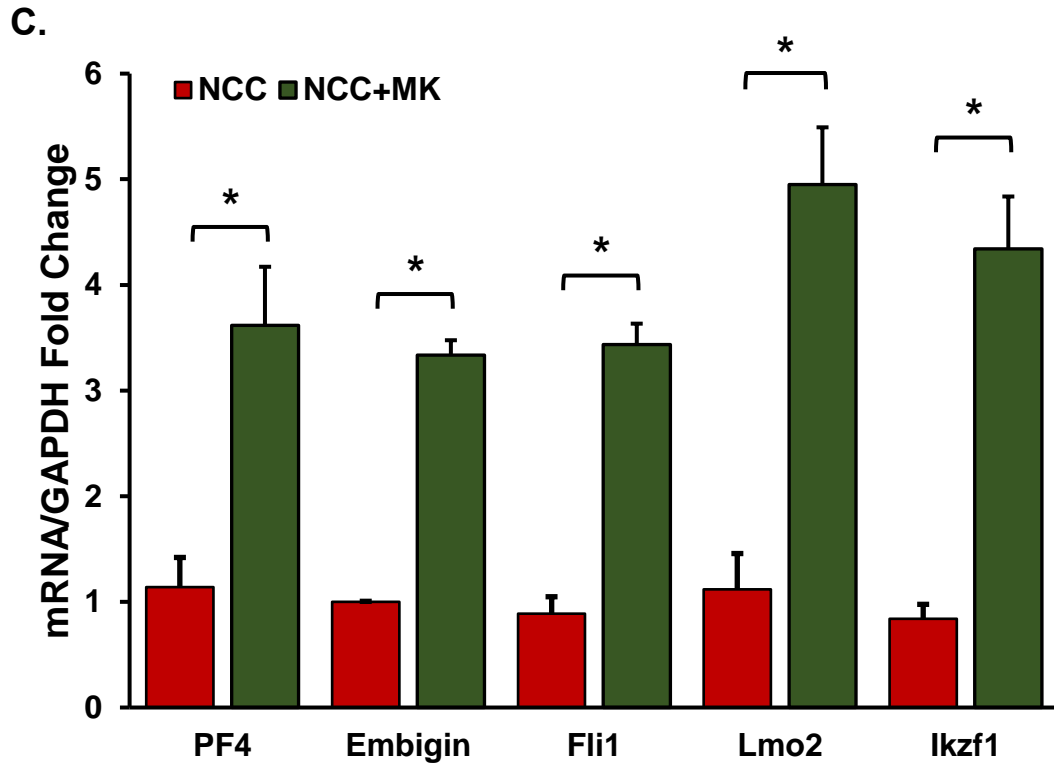


Figure 5.1 **Single cell mRNA sequencing of OM sorted from NCC and NCC+MK.** Neonatal calvarial cells (NCC) were cultured for 16 hrs in the absence (NCC) or presence of megakaryocytes (NCC+MK). OM were sorted from these two groups and then subjected to single cell capture. From each NCC and NCC+MK 24 OM underwent single cell mRNA sequencing. (A) PCA plot and (B) heat map of the differentially expressed genes in OM obtained from NCC and NCC+MK. (C) qPCR of target genes to validate single cell mRNA sequencing. N=3; $p > 0.05$, One Way Anova.

5.3 Quantitative comparison of protein levels using TMT based peptide labeling and LC-MS/MS

To determine whether target genes which were identified via mRNA sequencing were also differentially expressed at the translational level, the focus was shifted to proteomics. Overnight cultures were established with NCC in the absence or presence of megakaryocytes. Next, both these groups were seeded with LSK cells and cultured for an additional two days after which OM contained within both NCC and NCC+MK were sorted using flow cytometry. Additionally, OM from fresh NCC were sorted as a control. OM from these three groups were labeled with TMTs and analyzed by mass spectrometry (LC-MS/MS). A total of 1548 proteins were identified of which 1359 proteins were quantified. The list of proteins which were upregulated and downregulated in OM contained within NCC+MK in comparison to OM contained within NCC is provided in Table 5.1 and 5.2 respectively. One of the top targets which was significantly upregulated in OM contained within NCC+MK was embigin. As can be seen in the volcano plots in Figure 5.2A embigin (highlighted black dot) was upregulated in OM contained within NCC+MK compared to both OM contained within cultured NCC, as well as fresh NCC (middle and right plot in Figure 5.2A). Also, there was no difference in the expression levels of embigin between OM contained within cultured NCC and fresh NCC (left plot). Thus, embigin, a protein which has previously been implicated in hematopoiesis (Silberstein, Goncalves et al. 2016), was upregulated due to crosstalk between OM, osteoblasts and megakaryocytes both at the transcriptional and translational level (Figure 5.1 and 5.2). None of the other targets which were more abundant or had a higher p-value than embigin had been previously implicated in hematopoiesis.

Table 5.1 List of proteins upregulated in NCC+MK in comparison to NCC.

Description	Abundance Ratio (log2)	Abundance Ratio -log10 P-Value
Solute carrier family 2, facilitated glucose transporter member 3	1.070	3.100
MCG130182, isoform CRA	1.190	3.015
Arginase-1	1.060	3.013
Protein S100-A4	1.010	3.010
Stefin-1	0.960	2.947
Protein FAM162A	1.480	2.772
Embigin	1.580	2.686
Ribosomal protein	1.120	2.538
Protein S100-A11	1.230	2.536
Alpha-enolase	0.870	2.513
Histone H1.1	1.130	2.342
Histone H1.3	0.990	2.249
Histone H1.4	0.880	2.239
Myosin regulatory light chain 12B	1.440	2.233
Myosin light polypeptide 6	1.100	2.228
Glyceraldehyde-3-phosphate dehydrogenase	0.880	2.165
Non-histone chromosomal protein HMG-17 (Fragment)	2.220	2.156
Protein S100-A9	0.960	2.068
Succinate dehydrogenase assembly factor 2, mitochondrial	1.210	1.990
Golgi-associated plant pathogenesis-related protein 1	0.970	1.972
Chromobox protein homolog 3	1.000	1.837
Myosin-9	0.920	1.807
Histone H1.5	1.580	1.629
High mobility group protein HMG-I/HMG-Y	2.210	1.620
Cytochrome b-245 heavy chain	1.380	1.591
Mast cell-expressed membrane protein 1	0.910	1.544

Description	Abundance Ratio (log2)	Abundance Ratio -log10 P-Value
Histone H4	0.880	1.543
High mobility group protein B2	1.200	1.476
Cytochrome c oxidase subunit 7A2, mitochondrial	0.840	1.473
Three-prime repair exonuclease 1	1.320	1.408
Bridging integrator 2	0.830	1.368
Lysophosphatidylcholine acyltransferase 2	0.930	1.318

Table 5.2 List of proteins downregulated in NCC+MK in comparison to NCC.

Description	Abundance Ratio (log2)	Abundance Ratio -log10 P-Value
Platelet glycoprotein 4	-1.760	3.865
Protein Ahnak2 (Fragment)	-1.080	3.142
Myelin protein P0	-0.880	3.045
Fatty acid-binding protein, adipocyte	-0.870	2.767
Switch-associated protein 70	-1.160	2.622
Peroxiredoxin-1	-0.990	2.319
Fatty acid-binding protein, epidermal	-0.940	2.220
Translin-associated factor X-interacting protein 1	-1.360	2.189
Gamma-enolase	-2.300	2.143
Low affinity immunoglobulin gamma Fc receptor III	-0.910	2.132
Synaptic vesicle membrane protein VAT-1 homolog	-1.000	2.039
Protein ATP1B4	-0.930	2.003
Heat shock 70 kDa protein 1B	-0.940	1.985
Thioredoxin domain-containing protein 12	-0.900	1.805
Serpin H1	-1.230	1.429
Macrosialin	-1.050	1.392

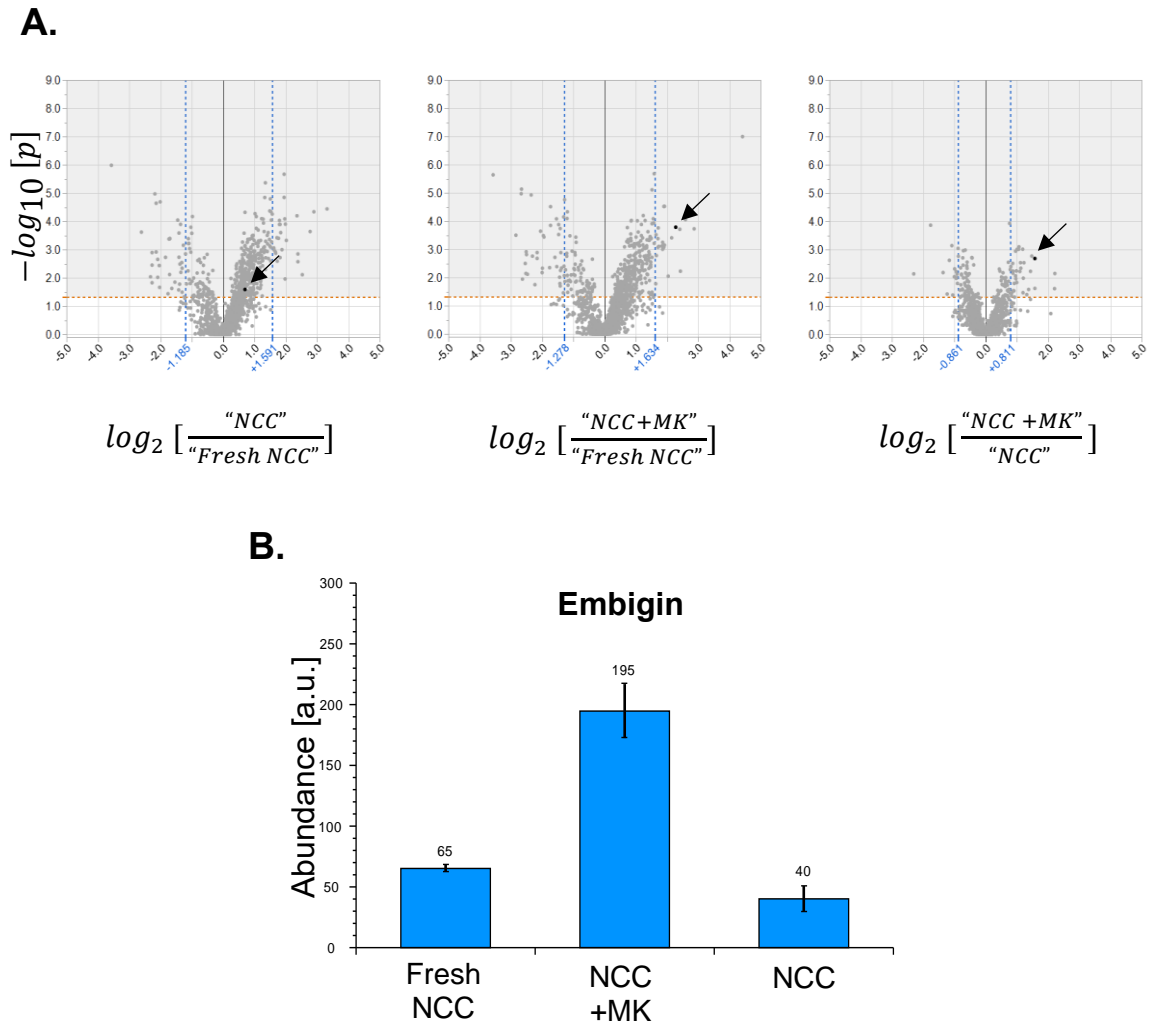


Figure 5.2 **Quantitative analysis of OM protein levels using LC-MS/MS.** NCC were co-cultured overnight in the absence (NCC) or presence (NCC+MK) of megakaryocytes. Each group was then seeded with LSK cells for 2 days followed by OM isolation through flow cytometry. OM from fresh NCC were sorted as a control. OM from each group were subjected to TMT based peptide labeling and LC-MS/MS. A total of 1548 proteins were identified, of which 1359 proteins were quantified. (A) Volcano plots comparing the protein expression of OM contained within NCC and fresh NCC (left), NCC+MK and fresh NCC (middle), and NCC+MK and NCC (right). The highlighted dot (black arrow) is the expression level of embigin in all three plots. The orange horizontal line is the p-value cut-off which was set at 0.05. (B) Average grouped abundance of embigin which was upregulated in OM contained within NCC+MK compared to the other two groups. Statistical accuracy was estimated using standard error.

5.4 Single cell CyTOF analysis identified CD166 and embigin as potential mediators through which OM maintain hematopoietic function

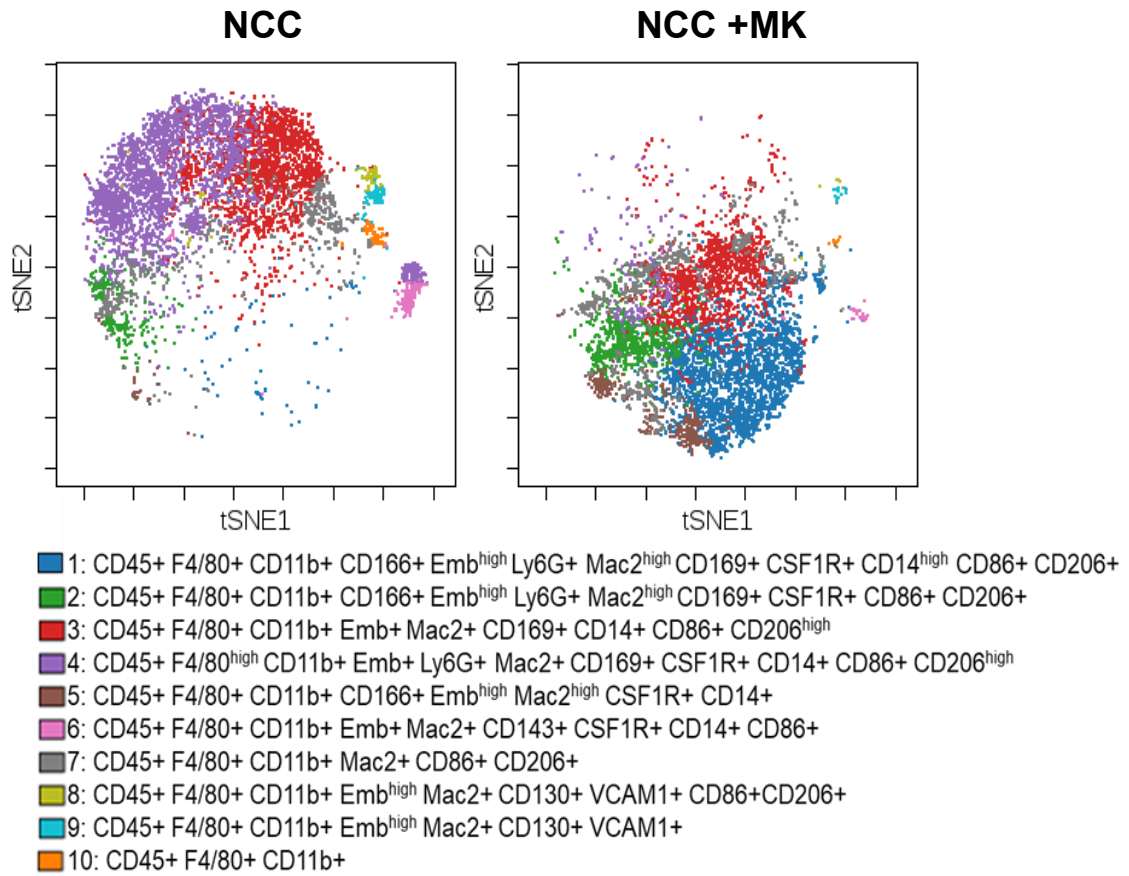
The LC-MS/MS data were unable to identify all the target genes that were detected through single cell-mRNA sequencing. Hence, single cell CyTOF was performed to validate the mRNA sequencing data. A panel of 17 surface and 13 intracellular antibodies was designed based on the sequencing data in Figure 5.1, as well as based on hypothetical molecular mediators through which OM might maintain hematopoietic function. The complete list of antibodies is provided in Table 2.2. Briefly, NCC were cultured for 2 days in the absence or presence of megakaryocytes; after which cells were stained and analyzed for CyTOF. It was hypothesized that 48 hrs of culture is long enough for protein expression on these cells but most likely not long enough for expression to wane and become undetectable by immunostaining. To maintain conditions similar to single cell mRNA sequencing, LSK cells were not included in culture. Also, CyTOF allows limited number of sample collection per day. Adding LSK cells in culture would vastly reduce the relative number of OM that could be collected and analyzed.

Both groups were first gated on CD45 and F4/80 to identify OM contained within NCC and NCC+MK. After this initial gating, OM from both groups were analyzed in a couple of different ways. ViSNE plots were generated to convert the high dimensional data into simple 2-D plots (Figure 5.3C). Also, a FlowSOM analysis was performed on these ViSNE plots to determine unbiased phenotypic heterogeneity between OM contained within both groups. As can be seen in Figure 5.3A, 8 metaclusters were observed within OM contained in NCC and 4 metaclusters were observed within OM contained in NCC+MK. 2 metaclusters (Metaclusters 2 and 3) overlapped between the two groups. Each of the metaclusters were characterized using the 17 surface antibodies. Interestingly, CD166 and embigin (designated as Emb in Figure 5.3A) which were upregulated in OM contained

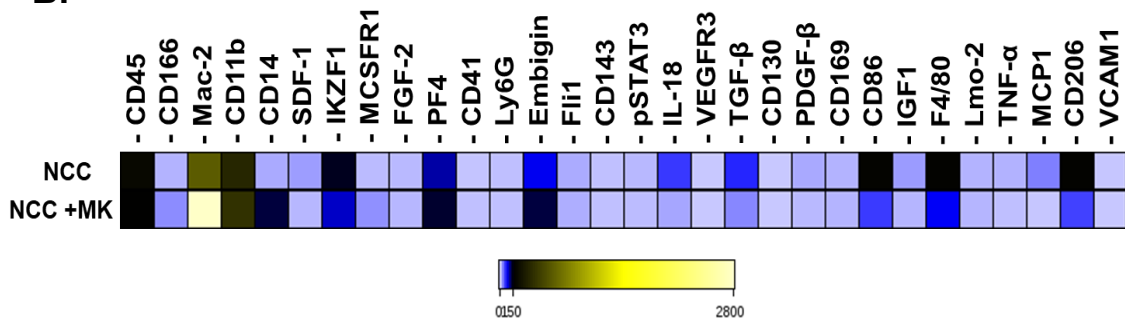
within NCC+MK (Figure 5.3C) were found within metacluster 1, 2 and 5. Of these three clusters, metacluster 1 was unique as it expressed the highest level of embigin and CD166 antigens and was absent in OM contained within NCC.

Heat maps and ViSNE plots were generated to analyze differential protein expression between the two groups (Figure 5.2B and C). Several surface proteins such as Mac-2 and CD14 were upregulated on OM within NCC+MK as compared to OM within NCC. CD166, an important functional marker of the hematopoietic niche (Chitteti, Cheng et al. 2010, Cheng, Chitteti et al. 2011, Chitteti, Bethel et al. 2013, Chitteti, Cheng et al. 2013, Chitteti, Kobayashi et al. 2014) was upregulated when OM were cultured with megakaryocytes. Interestingly, out of the five target genes identified in the single cell mRNA sequencing data (embigin, PF-4, Lmo-2, Fli-1 and Ikzf1), only embigin was upregulated on OM due to crosstalk between NCC and megakaryocytes. Lmo-2 and Fli-1 remain unchanged between the two groups; whereas PF-4 and Ikzf1 were downregulated in OM contained within NCC+MK (Figure 5.3B and C). Combined, the single cell genomics and proteomics data suggest that CD166 and embigin which are upregulated on OM due to crosstalk between NCC and megakaryocytes; might act as potential mediators through which OM maintain hematopoietic function. Also, both these groups were highest in expression in metacluster 1, indicating the possibility that the highest functionality of OM might be contained within this population.

A.



B.



C.

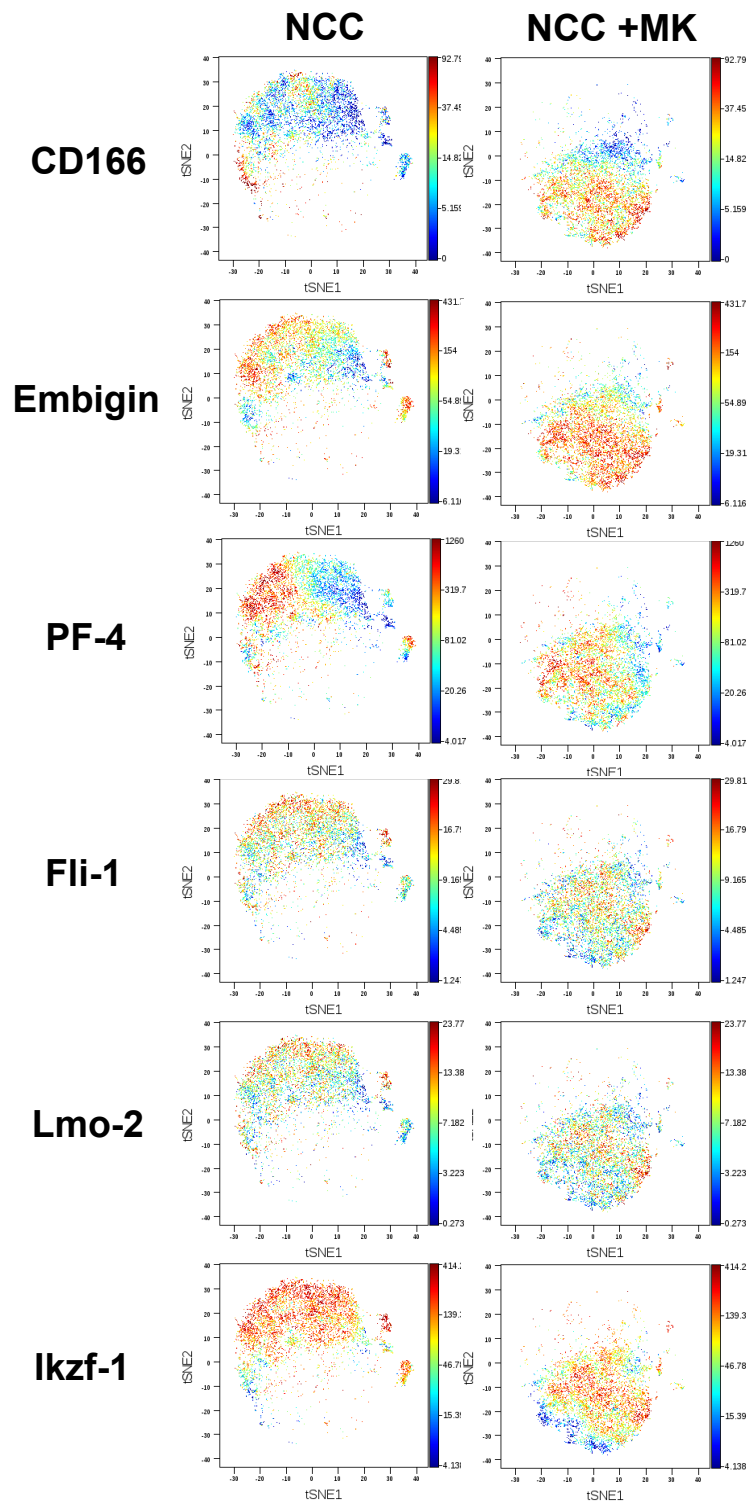


Figure 5.3 Multidimensional CyTOF analysis of OM contained within NCC cultured in the absence and presence of megakaryocytes. Single cell suspensions of NCC were cultured for 2 days in the absence or presence of megakaryocytes (MK) and then analyzed using a panel of 30 surface and intracellular antibodies. Data were gated on CD45+F4/80+ cells to indicate OM in NCC and NCC+MK. (A) Representation of the heterogeneity observed within subpopulations of OM from NCC and NCC+MK. Each subpopulation has been characterized depending on their expression of 17 surface markers. (B) Heat maps and (C) ViSNE plots indicating individual differences between OM obtained from NCC and NCC+MK. N=3.

5.5 Characterization of OM as potential osteolineage cells proximal to HSC

Recently, in a publication by Silberstein et. al., it was demonstrated that osteolineage cells proximal to HSPC (maximum of two cell diameters away) had increased mRNA expression of embigin, angiogenin and IL-18 compared to distal osteolineage cells (maximum of five cell diameters away) (Silberstein, Goncalves et al. 2016). Additionally, each of these three genes were shown to have an important role in maintaining hematopoiesis. These proximal osteolineage cells were defined as runx2+, osterix+, col1a+, osteopontin^{low} and osteocalcin^{low} when compared to distal osteolineage cells. A summary of the characterization of these proximal osteolineage cells is given in Figure 5.4A. Based on these studies, the next focus was to determine whether OM are similarly characterized as proximal osteolineage cells defined by Silberstein et. al and understand whether embigin, IL-18 and/or angiogenin were the molecular mediators through which OM maintained hematopoiesis.

To characterize OM, the mRNA gene expression profile of runx2, osterix, collagen 1a, osteopontin and osteocalcin was analyzed. As seen in Figure 5.4B, OM but not osteoblasts possessed an mRNA gene expression profile similar to proximal osteolineage cells (Silberstein, Goncalves et al. 2016). Flow cytometry and CyTOF analysis demonstrated that OM express high levels of VCAM-1 and SDF-1 further increasing the similarities between proximal osteolineage cells and OM (Figure 5.4 C and D). Since it was concluded that proximal osteolineage cells express higher levels of embigin, IL-18 and angiogenin mRNA, the mRNA levels of these genes between OM and osteoblasts was quantified. As seen in Figure 5.4E, OM also expressed higher mRNA levels of embigin, IL-18 and angiogenin compared to osteoblasts. Moreover, it was already demonstrated in Figure 5.3C that embigin protein expression is upregulated on OM due to crosstalk between OM, osteoblasts and megakaryocytes. IL-18 expression was present

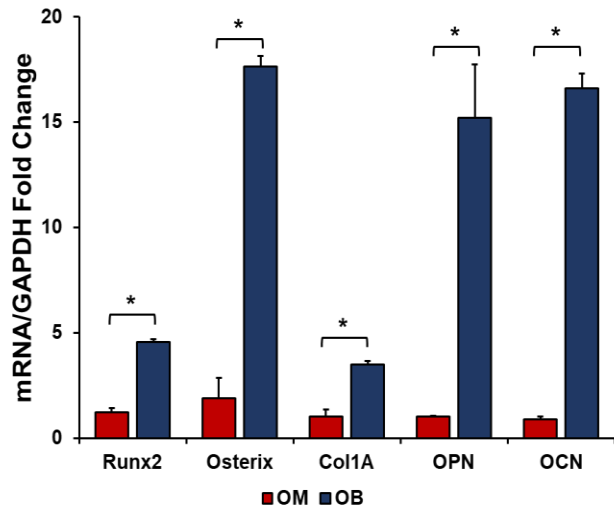
on OM, but downregulated (Figure 5.3B); whereas, angiogenin was not included in the CyTOF panel.

A.

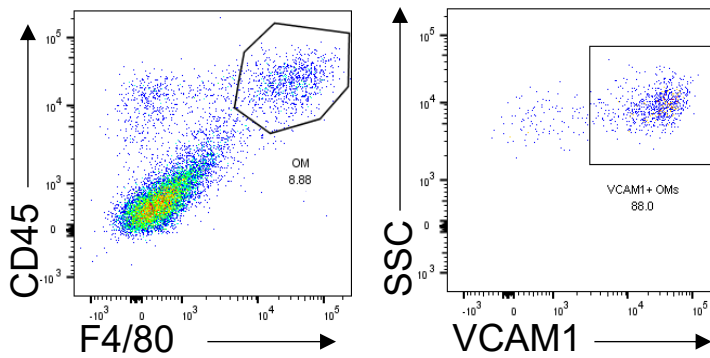
	POC	OM
Runx 2	+	+
Osterix	+	+
Col1a1	+	+
Osteopontin	Low	Low
Osteocalcin	Low	Low
VCAM-1	+	+
SDF1	+	+

Adapted from Silberstein,
Goncalves et al. 2016

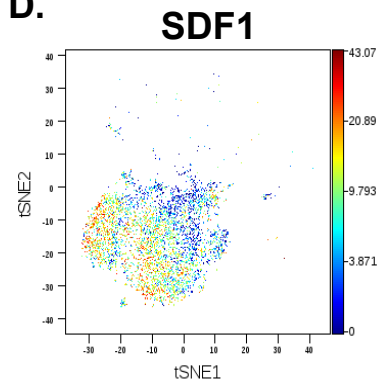
B.



C.



D.



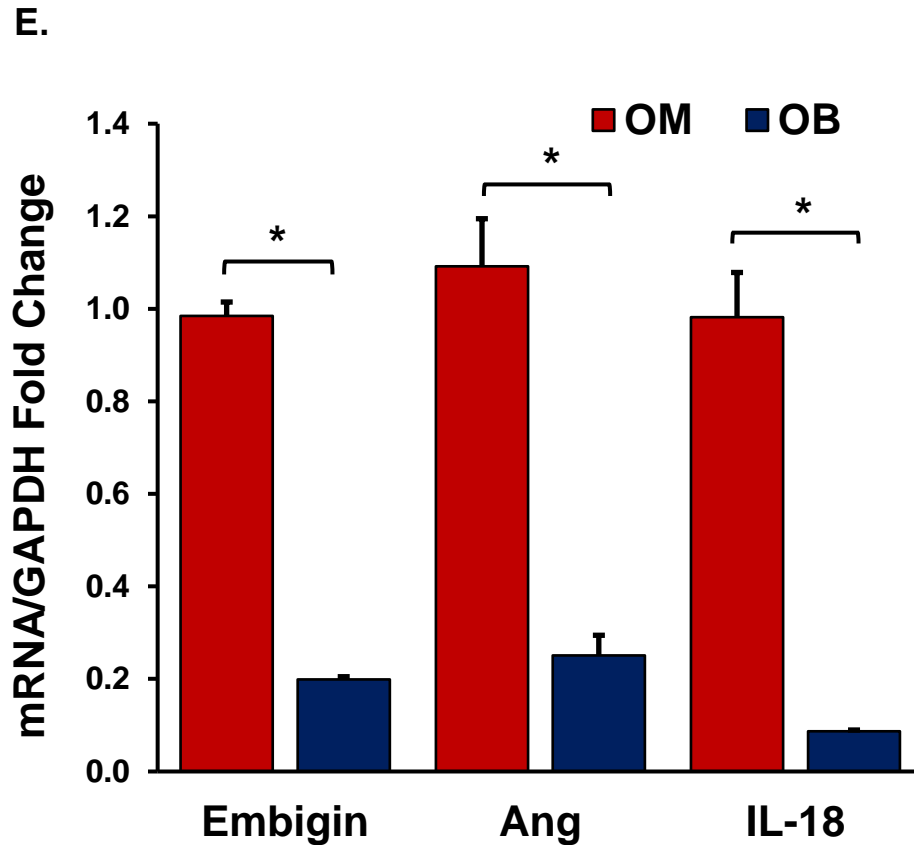


Figure 5.4 **Characterization of OM in relation to proximal osteolineage cells.** (A) Summary illustrating side by side comparison of proximal osteolineage cells (POC) and OM. (B) OM and osteoblasts (OB) were sorted from fresh NCC followed by qPCR quantitation of runx2, osterix, col1a, osteopontin, osteocalcin, N=3. (C) Flow cytometric analysis of VCAM-1 expression on OM (CD45+F4/80+) contained within NCC. N=3. (D) CyTOF analysis shown in Figure 3.5B. ViSNE plot for SDF-1 expression on NCC gated on CD45+F4/80+ OM. (E) qPCR quantitation of embigin, angiogenin and IL-18 on OM and OB, N=3.

5.6 Recombinant CD166 and embigin partially substitute OM mediated hematopoietic function

Colony forming assays were performed to determine whether recombinant CD166 and embigin could substitute for OM activity *in vitro*. Briefly, rCD166 and recombinant embigin (rEmb) were coated onto tissue culture plates. These coated plates were then used to culture osteoblasts (sorted from NCC and labeled as OB in Figure 5.5) in the absence or presence of megakaryocytes. BSA coated plates were used to set up cultures as one set of controls. OM were also cultured with osteoblasts in the absence or presence of megakaryocytes on non-coated tissue culture plates as a second set of controls. After one day of culture, LSK cells were seeded onto each of these groups. 7 days post LSK culture, a colony forming assay was set up to determine CFU fold change of cultured LSK progeny relative to 250 fresh LSK cells. No difference was observed in CFU fold change between OM+OB, rCD166+OB, rEmb+OB and rCD166+rEmb+OB (highlighted in the purple rectangle) indicating that rCD166 and rEmb could partially substitute for OM-mediated hematopoietic activity *in vitro* (Figure 5.5A). As expected, all four groups were significantly upregulated compared to osteoblasts cultured on BSA coated plates. In every experiment that was performed (N=3), the same non-significant trend was observed wherein rCD166+rEmb+OB was slightly upregulated compared to rCD166+OB and rEmb+OB suggesting that the combination of recombinant proteins might have an additive effect on hematopoiesis as compared to each individual protein alone. Of note, a further increase in the CFU fold change of these groups was expected when cultured in the presence of megakaryocytes. However, addition of megakaryocytes to these cultures did not further augment CFU fold change suggesting that the levels of endogenous factors added to the cultures may have exceeded the physiologic increase in those factors induced by megakaryocytes. Data depicting the breakdown of the CFU subtypes in these cultures are

shown in Figure 5.5 B, C and D. Overall, the data demonstrate that CD166 and embigin partially substitute for OM-mediated hematopoietic activity *in vitro*.

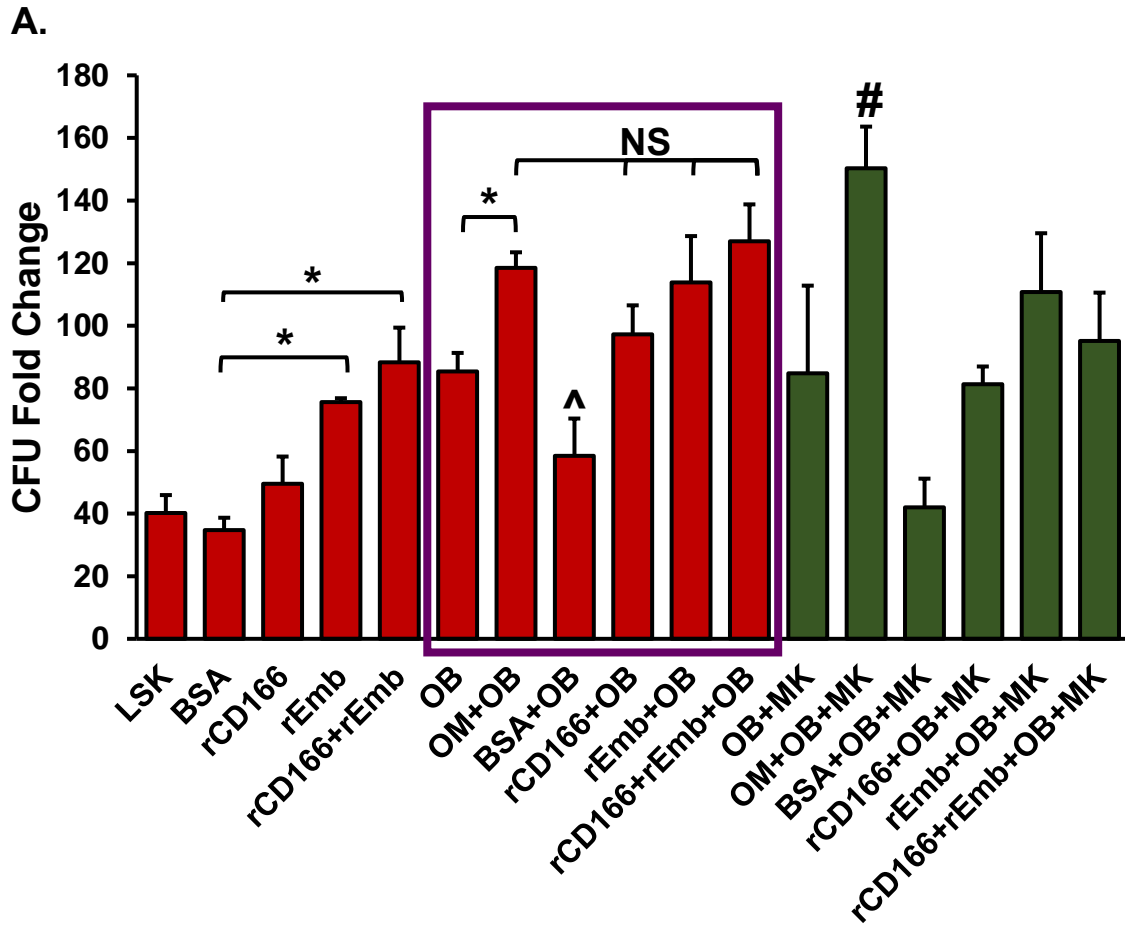
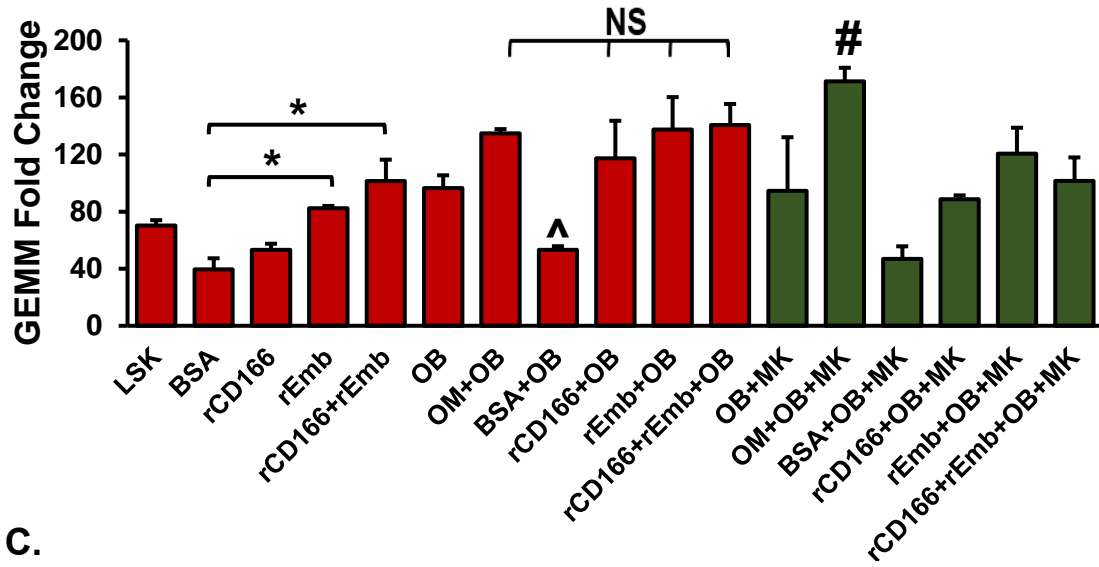
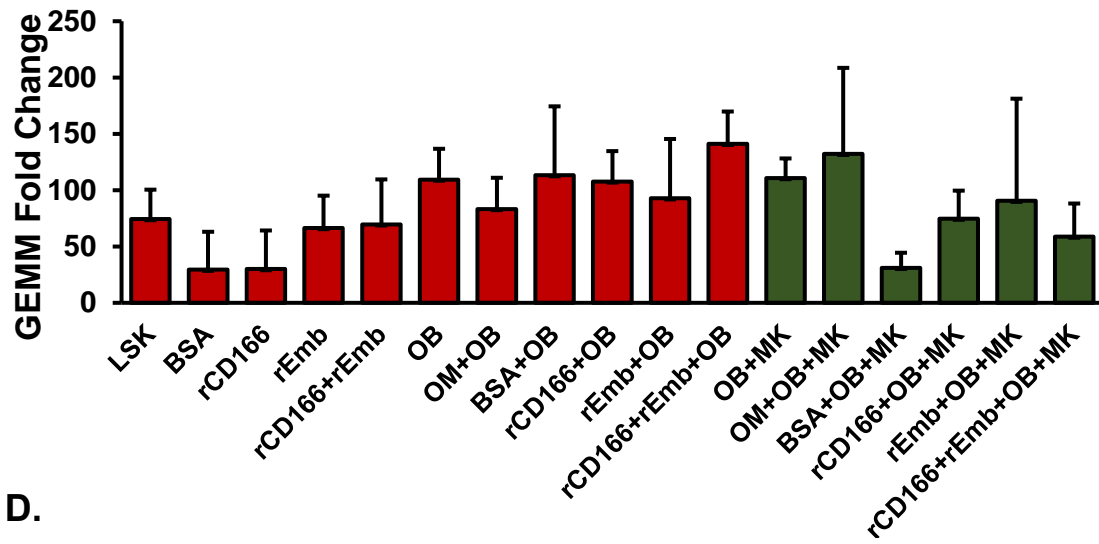


Figure 5.5 **CD166 and embigin are potential mediators through which OM maintain hematopoietic function.** Recombinant CD166 and embigin (as a substitute for OM) were coated on tissue culture plates. These plates were used to culture osteoblasts (OB) sorted from NCC in the absence (red bars) or presence (green bars) of megakaryocytes (MK). LSK cells were cultured for one week with each of these groups. CFU assays were set up to determine CFU fold change of cultured LSK progeny relative to 250 fresh LSK cells. Multilineage analysis was performed to identify the distribution of (B) GM, (C) GEMM and (D) BFU-E colonies. One of three independent experiments performed in triplicates. * $p < 0.05$, ^ $p < 0.05$ vs OM+OB, rCD166+OB, rEmb+OB and rCD166+rEmb+OB, # $p < 0.05$ vs OM+OB, BSA+OB+MK, rCD166+OB+MK, rEmb+OB+MK, rCD166+rEmb+OB+MK, One Way Anova.

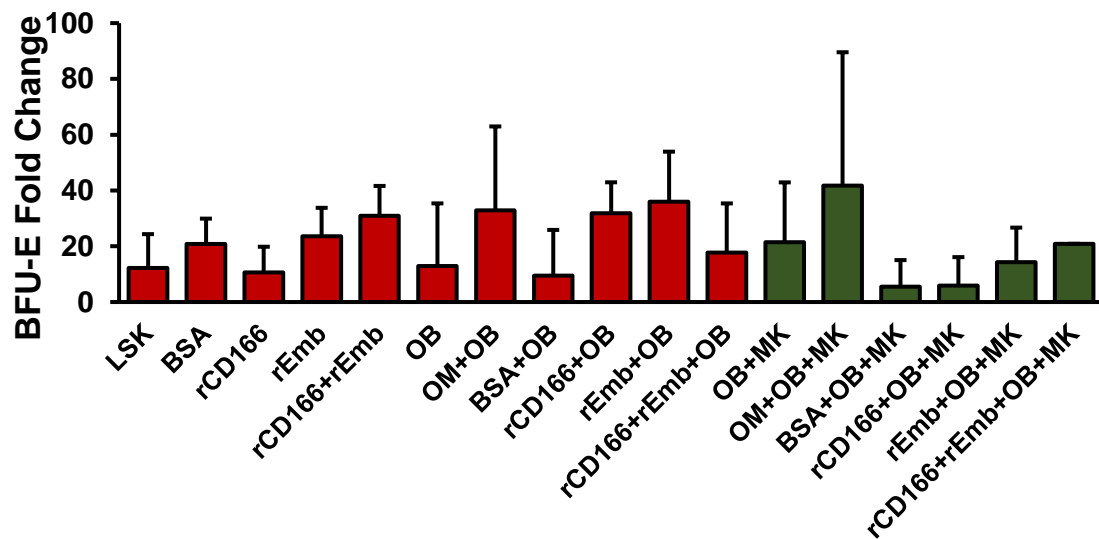
B.



C.



D.



5.7 CD166 as a molecular mediator through which OM maintain the hematopoietic function of osteoblasts

Since recombinant CD166 could partially substitute for OM activity *in vitro*, the next goal was to validate these results and determine whether the CD166+ fraction of OM was functionally more relevant than the CD166- fraction. To do this, OM processed from NCC were flow sorted into CD166+ and CD166- fractions. These fractions were individually cultured with osteoblasts (cultures labeled as CD166+OM +OB and CD166-OM +OB in Figure 5.6) also obtained from NCC. The cultures were maintained overnight and the next day were seeded with LSK cells. 7 days post LSK culture, a colony forming assay was set up to determine CFU fold change of cultured LSK progeny relative to 250 fresh LSK cells. The data demonstrated that the CFU fold change of CD166+OM +OB was statistically not significant compared to OM+OB (Figure 5.6). Interestingly, CD166-OM +OB had a significantly lower CFU fold change compared to the two groups mentioned above. This indicates that the CD166+ fraction of OM is functionally important to mediate hematopoiesis.

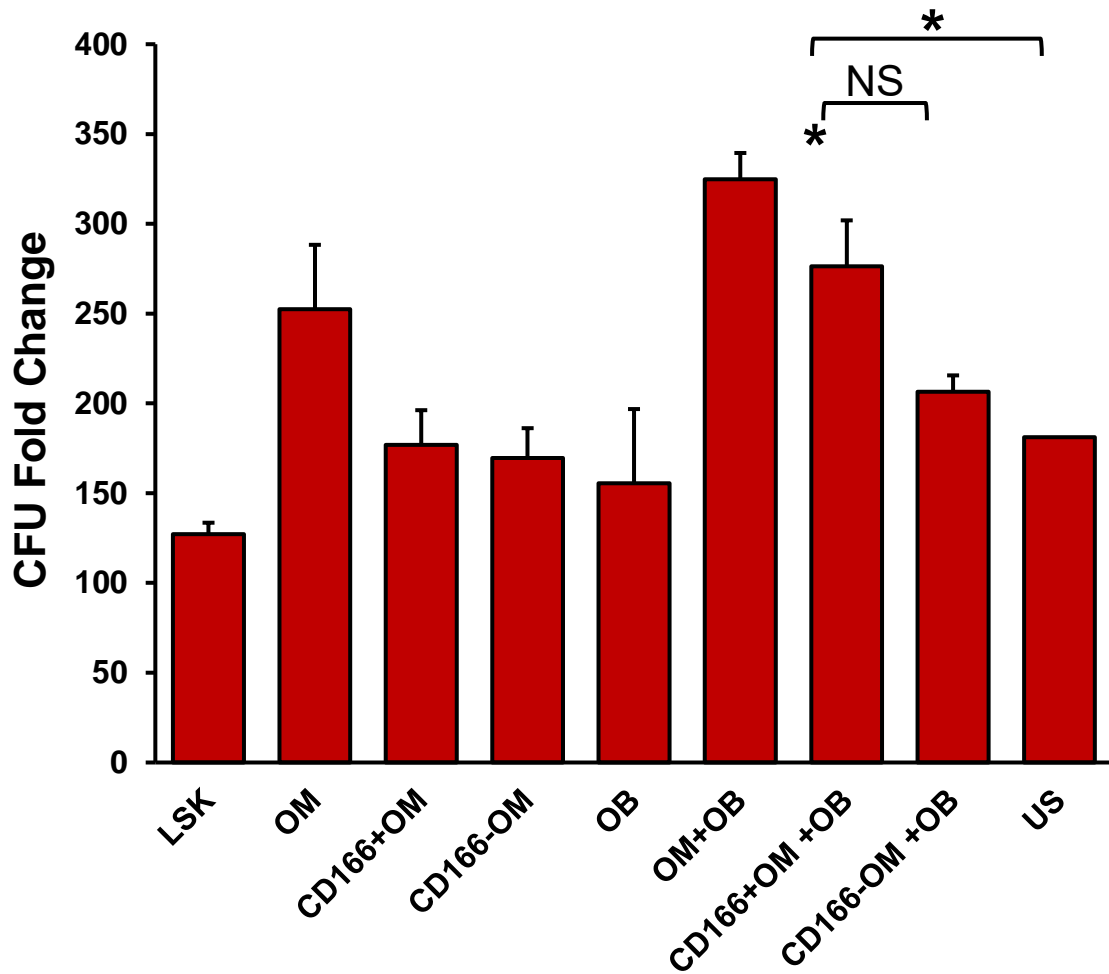
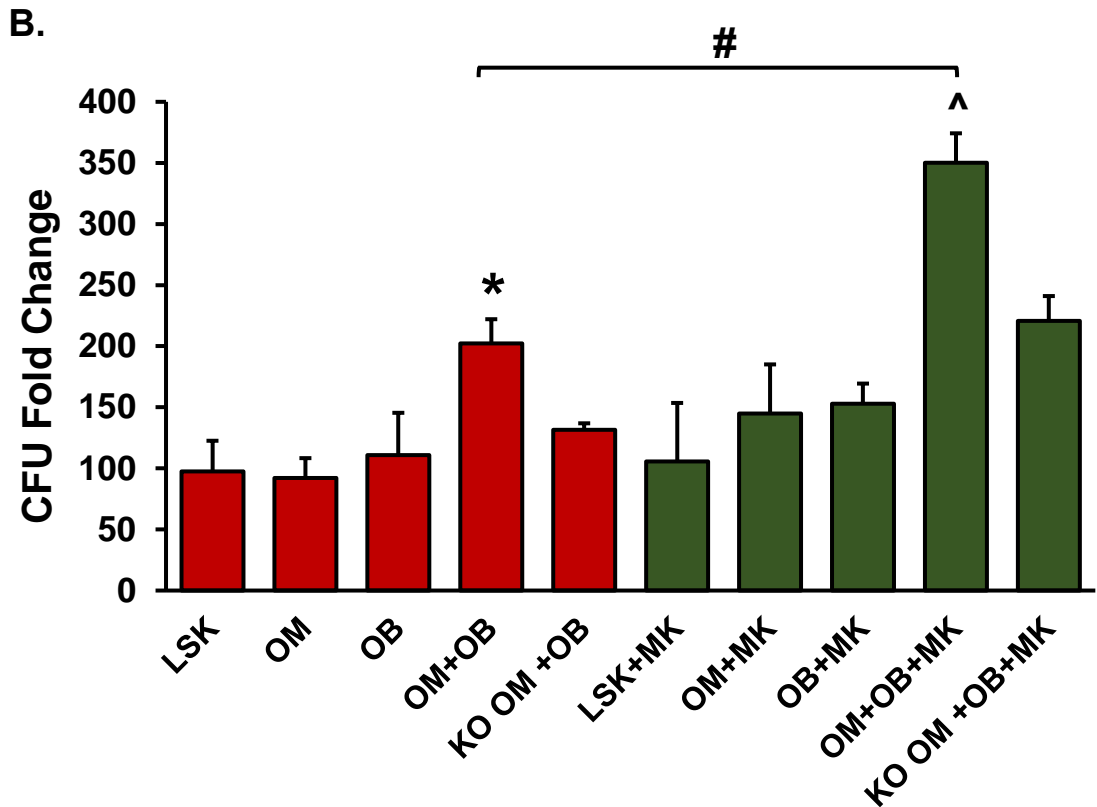
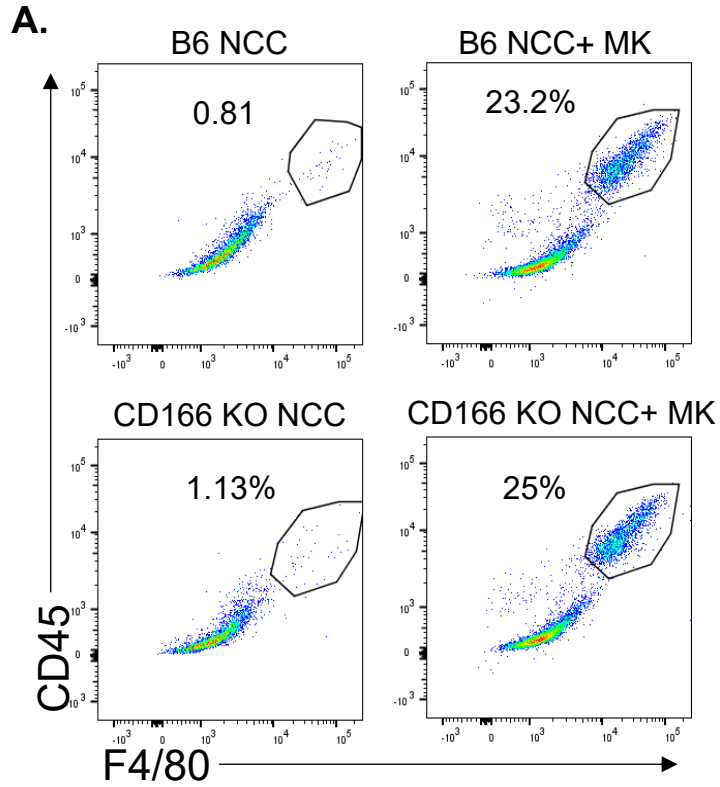


Figure 5.6 **The CD166+ fraction of OM mediates the hematopoietic enhancing activity of osteoblasts.** NCC were first fractionated into CD166+OM, CD166-OM and osteoblasts (OB). These CD166+ and CD166- OM were plated with OB and subsequently seeded with LSK for 7 days. CFU assays were set up to determine CFU fold change of cultured LSK progeny relative to 250 fresh LSKs. One of three independent experiments performed in triplicates, * $p < 0.05$ vs all controls besides CD166+OM +OB. One Way Anova.

Subsequently, CD166 knockout mice were utilized to better understand whether CD166 null OM support hematopoiesis. CD166 knockout OM (labeled as KO OM in Figure 5.7) or wild type OM (labeled as OM in Figure 5.7) were cultured with osteoblasts in the absence or presence of megakaryocytes. KO OM were collected from CD166 knockout NCC, whereas OM and osteoblasts were collected from wild type NCC. Megakaryocytes were obtained from fetal liver of wild type mice. Similar number of wild type and knockout OM were used to set up these cultures. 7 days post culture, flow cytometry was used to analyze cells for proliferation. As expected, wild type OM increased in numbers when cultured in the presence of osteoblasts and megakaryocytes (Figure 5.7A). Interestingly, CD166 KO OM also increased in numbers when cultured in the presence of osteoblasts and megakaryocytes indicating that presence of CD166 is not important for OM proliferation.

Next, colony forming assays were performed using CD166 knockout OM. Overnight cultures were set up using wild type or knockout OM along with wild type osteoblasts in the absence or presence of wild type megakaryocytes. 24 hrs later, LSK cells from wild type mice were added to all culture groups. 7 days post LSK culture, colony forming assays were set up to determine CFU fold change. As expected, an increased CFU fold change was observed when LSK cells were cultured with wild type OM and osteoblasts, which was further augmented with the addition of megakaryocytes (Figure 5.7B). However, CD166 knockout OM were unable to mediate the same hematopoiesis enhancing activity regardless of whether megakaryocytes were present in the co-culture or not. Data depicting the breakdown of the CFU subtypes in these cultures are shown in Figure 5.7 C, D and E. Overall, the data demonstrate that the absence of CD166 does not affect OM proliferation, but it does affect OM-mediated hematopoietic enhancing activity

suggesting that OM proliferation is disconnected from their ability to augment hematopoiesis.



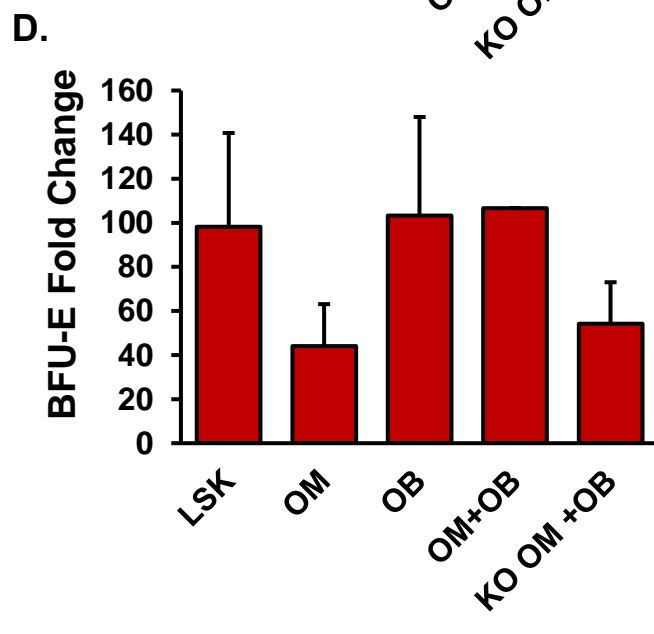
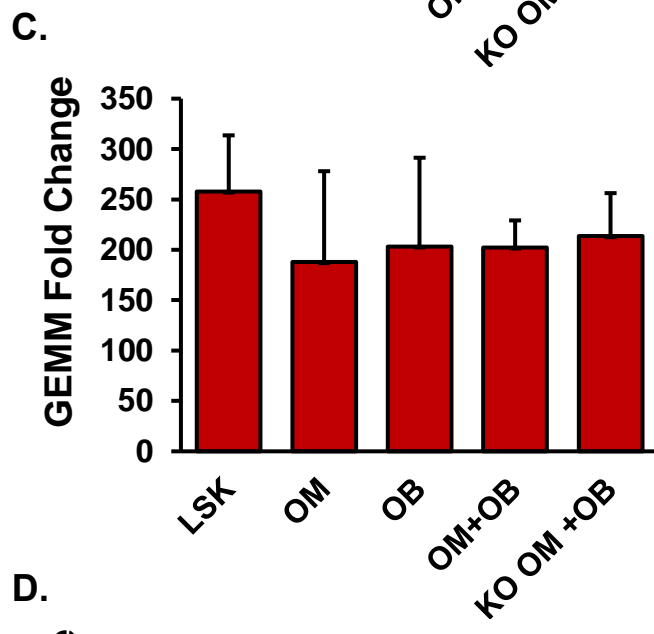
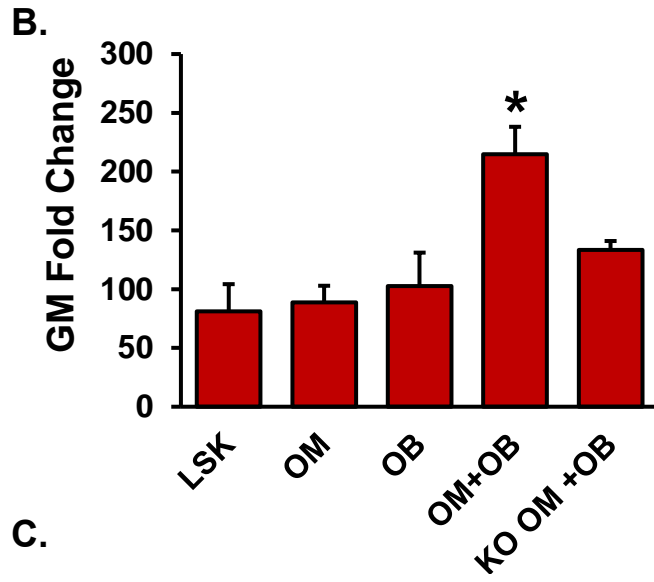


Figure 5.7 CD166 is one of the molecular mediators through which OM maintain hematopoietic function of osteoblasts. Co-cultures of NCC-derived osteoblasts (OB) mixed with either the original number of OM contained in freshly isolated NCC (OM+OB) or a complimentary number (equivalent to the original number of OM in NCC) of CD166 knockout OM (KO OM +OB) were established in the absence (red bars) or presence (green bars) of megakaryocytes (MK). (A) Flow cytometry at D7 of culture. (B) Overnight cultures were seeded with LSK cells and further cultured for one week with each of the groups mentioned above. CFU assays were set up to determine CFU fold change of cultured LSK progeny relative to 250 fresh LSKs. Multilineage analysis was performed to identify the distribution of (C) GM, (D) GEMM and (E) BFU-E colonies. One of three independent experiments performed in triplicates. * $p < 0.05$ vs controls without megakaryocytes, ^ $p < 0.05$ vs controls with megakaryocytes, # $p < 0.05$; One-way Anova.

5.8 Embigin as a molecular mediator through which OM maintain hematopoietic function of osteoblasts

To determine the importance of embigin expression on OM in mediating hematopoietic function, OM and osteoblasts were cultured for 7 days in the absence or presence of megakaryocytes. An embigin blocking antibody (1 µg per well) was added on day 0, day 3 and day 6 of culture. Cultures without the embigin blocking antibody were used as controls. On day 7, excess antibody was washed away, and the groups were seeded with LSK cells. Through this approach, embigin was temporarily blocked on OM, osteoblasts and megakaryocytes, but not on LSK cells which also express embigin on their surface. All groups were cultured with LSK cells for an additional 7 days, after which LSK progeny were plated in methylcellulose to perform colony forming assays. It was observed that blocking embigin in culture caused a decline in CFU fold activity when compared to controls (Figure 5.8). Furthermore, this decline in CFU fold change was observed irrespective of the absence or presence of megakaryocytes in culture. This indicates that blocking embigin on OM and osteoblasts causes a decline in hematopoietic activity.

Subsequently, the next study was to determine whether blocking embigin on OM is sufficient to cause the decline in hematopoietic activity. Due to the absence of embigin knockout mice, a shRNA mediated embigin knockdown was performed on OM obtained from NCC. Briefly, NCC were infected either with one of two shRNAs against embigin or with a virus containing an empty vector. One plate of NCC culture was left uninfected as a control. Post spinfection, megakaryocytes were added to the NCC cultures to promote increase in cell numbers. These cultures were maintained for 7 days, after which shRNA knocked down OM, empty vector OM, uninfected OM and uninfected osteoblasts were sorted via flow cytometry. The gating strategy is shown in Figure 5.9A and OM shown in the right most column were sorted out for CFU assays. shRNA knocked down OM

(GFP+Emb-) or empty vector OM (GFP+Emb+) or uninfected OM were cultured with osteoblasts for 1 day, after which all groups were seeded with LSK cells. Cultures were maintained for an additional 7 days, after which the progeny of LSK cells were plated onto methylcellulose to perform colony forming assays. No significant difference was observed in CFU fold change between the groups which contained LSK cells cultured with uninfected OM and osteoblasts (labeled as OM+OB in Figure 5.9B) and empty virus infected OM and osteoblasts (labeled as OM (EV) +OB in Figure 5.9B). However, a decline in CFU fold change was observed when OM knocked down for embigin were present in culture (labeled as OM (Emb KD1) +OB and OM (Emb KD2) +OB in Figure 5.9B) with osteoblast and LSK cells. These data indicate that loss of embigin expression on OM affects its hematopoietic enhancing activity. Data depicting the breakdown of the CFU subtypes in these cultures are shown in Figure 5.9 C, D and E. At present, it is not understood why the shRNA system is more consistent with previous findings than the anti-embigin antibody. Speculations suggest that the antibody used may not be fully neutralizing.

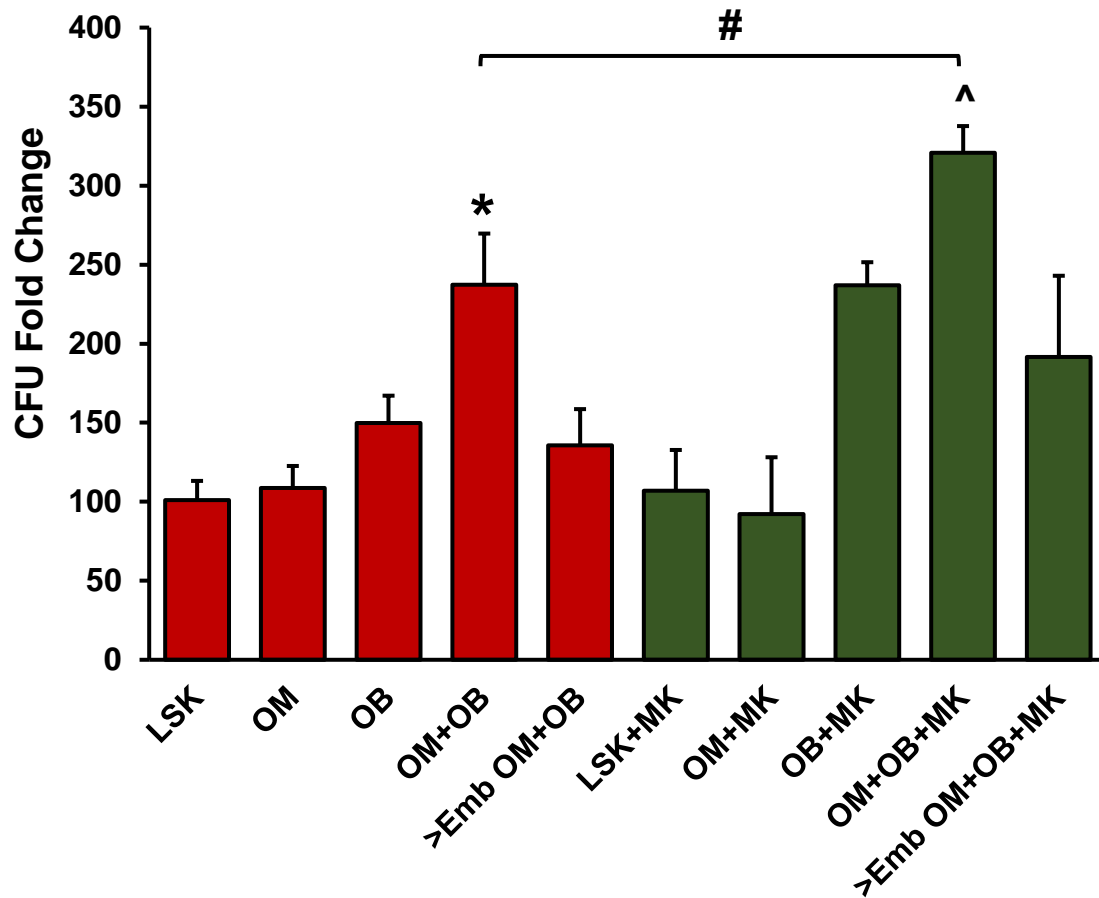
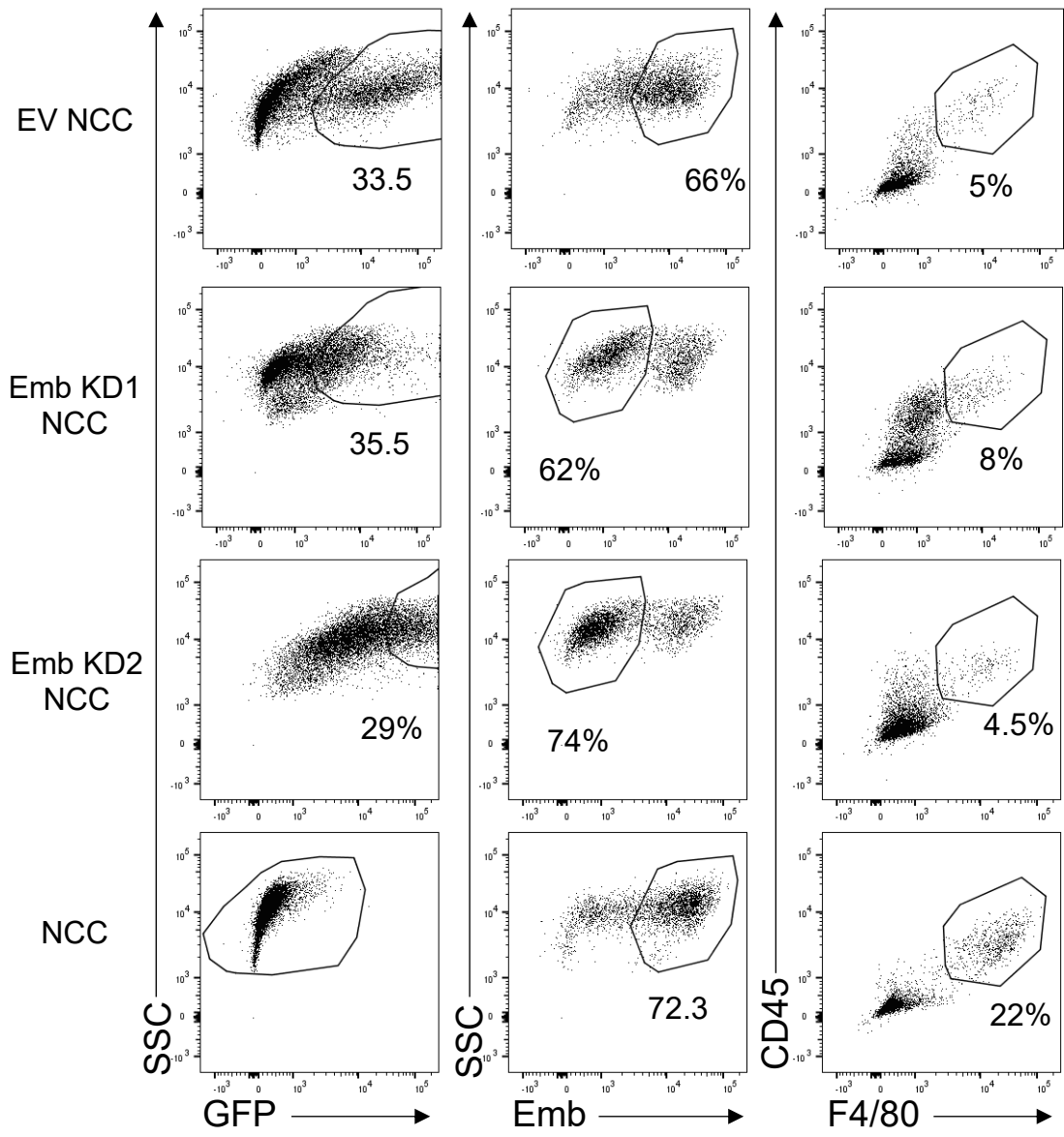


Figure 5.8 **Blocking embigin expression on NCC causes a decline in hematopoietic activity.** Osteoblasts (OB) were co-cultured with OM both of which are contained in freshly isolated NCC. Co-cultures were set up in the absence (red bars) or presence (green bars) of megakaryocytes (MK). An embigin blocking antibody was added to 3 wells containing OM+OB and 3 wells containing OM+OB+MK on D0, D3 and D6 of culture. On D7, excess antibody was washed away and LSK cells were cultured for 1 wk with each of these groups. CFU assays were set up to determine CFU fold change of cultured LSK progeny relative to 250 fresh LSKs. One of three independent experiments performed in triplicates. * $p < 0.05$ vs LSK, OM, OB, >Emb OM+OB; ^ $p < 0.05$ vs LSK+MK, OM+MK, OB+MK, >Emb OM+OB+MK, # $p < 0.05$; One-way Anova.

A.



B.

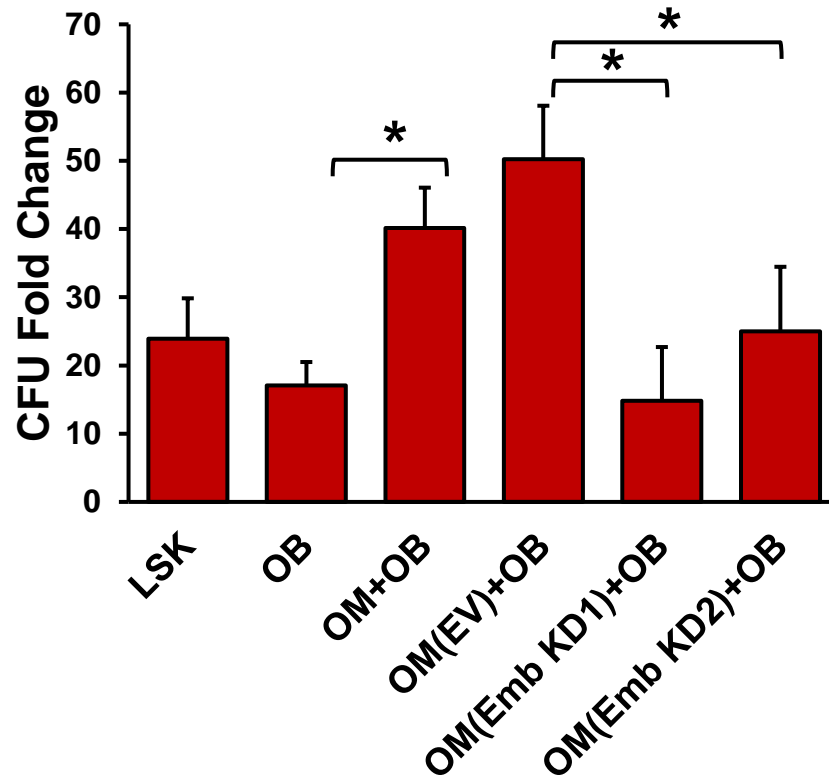
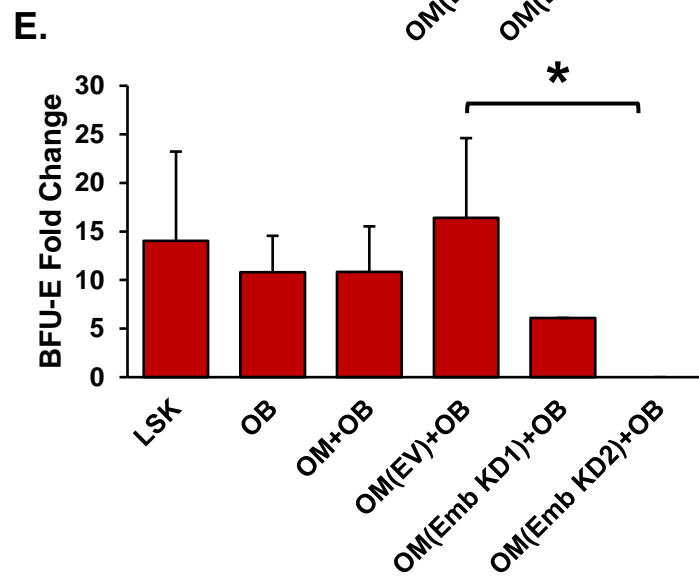
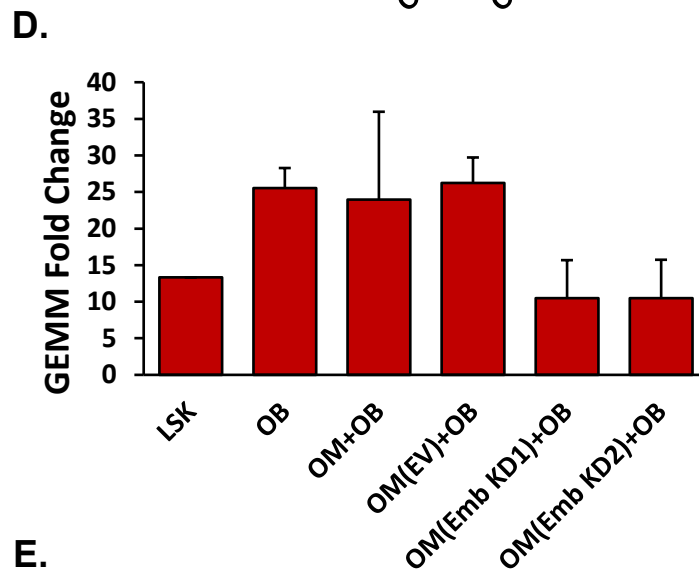
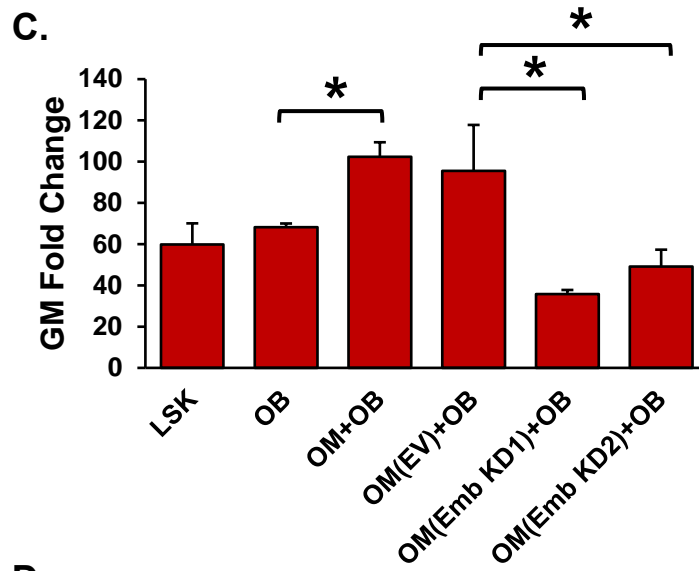


Figure 5.9 **Embigin is one of the molecular mediators through which OM maintain hematopoietic function of osteoblasts.** NCC were subjected to four spinfections over a span of two days to infect them with GFP+ virus containing shRNA against embigin or an empty vector. At the end of the fourth spinfection, megakaryocytes were cultured for 1 wk with each of these groups. On D7, OM which were GFP+Emb- (labeled as OM (Emb KD1/2)) and GFP+Emb+ (labeled as OM (EV)) were sorted out. (A) Gating strategy for the virus infected OM sort from left to right. Uninfected OM and osteoblasts (OB) were also sorted to set up controls. (B) Overnight co-cultures were set up with virus infected OM and uninfected OB. Uninfected OM+OB were cultured as a control. The next day, LSK cells were cultured for 1 wk with each of these groups. CFU assays were set up to determine CFU fold change of cultured LSK progeny relative to 250 fresh LSKs. Multilineage analysis was performed to identify the distribution of (C) GM, (D) GEMM and (E) BFU-E colonies. One of three independent experiments performed in triplicates. * $p < 0.05$; One-way Anova.



5.9 Discussion

Networking between HSC and cells of the hematopoietic niche is critical for the maintenance of stem cell renewal and function. Amongst the most characterized resident cells of the niche are osteoblasts. Their importance in the regulation of the hematopoietic niche has been well established (Calvi, Adams et al. 2003, Zhang, Niu et al. 2003, Chitteti, Cheng et al. 2010, Cheng, Chitteti et al. 2011, Cheng, Streicher et al. 2015, Alvarez, Xu et al. 2018). Moreover, not much is known about interactions between OM, osteoblasts and megakaryocyte and how together they regulate hematopoiesis. In fact, even though OM are a resident of the hematopoietic niche, more is known about their function in bone modeling (Chang, Raggatt et al. 2008, Alexander, Chang et al. 2011, Guihard, Danger et al. 2012, Wu, Raggatt et al. 2013, Cho, Soki et al. 2014, Raggatt, Wullschleger et al. 2014, Sinder, Pettit et al. 2015, Vi, Baht et al. 2015, Alexander, Raggatt et al. 2017, Batoon, Millard et al. 2017, Batoon, Millard et al. 2017, Kaur, Raggatt et al. 2017). than their role in hematopoiesis. However, in 2010, Winkler et. al. established that loss of OM caused a concurrent disruption of the endosteal niche and mobilization of HSPCs from the bone marrow to the peripheral blood (Winkler, Sims et al. 2010). Also, in the previous chapter, the importance of crosstalk between OM, osteoblasts and megakaryocytes to regulate hematopoietic function was demonstrated (Mohamad, Xu et al. 2017). In this chapter, the focus was to determine the molecular mediators which are triggered due to crosstalk between OM, osteoblasts and megakaryocytes and, ultimately how these molecular mediators support hematopoietic enhancing activity. Since much is known about interactions of osteoblasts and megakaryocytes within the hematopoietic niche, focus was shifted to the role of OM in these dynamics.

Single cell studies helped narrow down targets which could act as potential mediators through which OM functionally enhance hematopoiesis. Of interest, an upregulation in the

expression of embigin and CD166 on OM was observed when they interacted with osteoblasts and megakaryocytes (Figure 5.1, 2 and 3). Embigin, a molecule which has previously been implicated in hematopoiesis (Silberstein, Goncalves et al. 2016), was upregulated both at the single cell mRNA level, as well as the translational level. In fact, it was one of the top targets in the mass spectrometry data (Figure 5.2) in which the only targets above it were a glucose transporter member, arginase and some undefined proteins (Table 5.1). These targets could be potentially investigated in the future. On the other hand, CD166 which is a critical molecule for the hematopoietic niche (Chitteti, Cheng et al. 2010, Cheng, Chitteti et al. 2011, Chitteti, Bethel et al. 2013, Chitteti, Cheng et al. 2013, Chitteti, Kobayashi et al. 2014) was not upregulated on OM at the single cell mRNA level as a result of the crosstalk between OM, osteoblasts and megakaryocytes. However, the CyTOF data demonstrated an upregulation of CD166 (Figure 5.3C) at the single cell protein level indicating possible regulation at the translational level. The reason for this discrepancy between CyTOF and single cell mRNA sequencing is not known at this point. Also, CD166 was not a candidate protein in the mass spectrometry data. However, the culture conditions for both the proteomics experiments were different. Data for the mass spectrometry experiment was obtained from OM cultured with LSK cells unlike the single cell CyTOF analysis data which were collected from OM cultured without LSK. Since CD166-CD166 homophilic interactions are expected in the hematopoietic niche, there is a possibility that CD166 expressed by OM in the mass spectrometry experiment was bound to LSK cells and was lost in the cell processing methods. This limitation might be the reason CD166 was not identified in this experiment. Interestingly, unlike CD166 which was upregulated at the translational level, there were several targets such as PF-4, Lmo-2, Fli-1 and Irf1 which were upregulated at the mRNA level (Figure 5.1B) but remained unchanged at the protein level (Figure 5.3C). This points out one of the biggest shortcomings of single cell genomics, where genes which are regulated at the

transcriptional level may not necessarily behave the same way at the translational level. These shortcomings have already been pointed out in previous publications (Chitteti, Liu et al. 2011).

The next question was whether CD166 and embigin act as molecular mediators through which OM mediate hematopoietic function. Previous investigations have established that osteolineage cells proximal to HSC express embigin and are involved in maintenance of hematopoiesis (Silberstein, Goncalves et al. 2016). This was the first instance where embigin had been identified as a regulator of hematopoiesis. The studies in this chapter, have expanded on these previous data and have hypothesized that these proximal osteolineage cells mentioned by Silberstein et. al. might be OM. To give support to this hypothesis, several experiments were performed including qPCR, flow cytometry and CyTOF which identified similarities between the published proximal osteolineage cells and OM. Furthermore, *in vitro* progenitor assays establish the importance of embigin as a molecule which regulates OM-mediated hematopoietic function (Figure 5.8 and 5.9). However, due to lack of an embigin knockout model, knockdown studies were used to determine the effects of loss of embigin expression on OM. Even though knocked down OM were sorted out for the experiments, shRNA studies are generally unstable, and the use of embigin knockout OM would be preferred. Making an embigin knockout mouse model is currently underway, and future studies would include moving this project to an *in vivo* setting. Moreover, recombinant studies were performed which conclude that both embigin and CD166 are molecular mediators which can partially substitute for OM activity *in vitro* (Figure 5.5).

CD166 studies were more expansive due to prior laboratory investigations into its role in the hematopoietic niche and availability of CD166 KO mice (Chitteti, Cheng et al. 2010,

Chitteti, Cheng et al. 2010, Cheng, Chitteti et al. 2011, Chitteti, Bethel et al. 2013, Chitteti, Cheng et al. 2013, Chitteti, Kobayashi et al. 2014, Xu, Mohammad et al. 2016). Using CD166 knockout mice, it was demonstrated that CD166 knockout OM have reduced function and cannot maintain hematopoiesis *in vitro* (Figure 5.6, 5.7). CD166 expression on OM is upregulated due to the crosstalk between OM, osteoblasts and megakaryocytes and its absence affects hematopoietic activity which is at its maximum when LSK cells co-cultured with wild type OM, osteoblasts and megakaryocytes are transplanted (Figure 4.3). It was previously established that LSK cells co-cultured with CD166 knockout NCC demonstrate reduced engraftment potential (Chitteti, Kobayashi et al. 2014). The next step is to transplant LSK cells co-cultured with knockout OM, wild type osteoblasts and wild type megakaryocytes to validate these *in vitro* results *in vivo*. Transplant studies are currently underway and are very early to yield meaningful conclusions. Interestingly, through the CyTOF data it was observed that the same metacluster of OM (Metacluster 1) showed high expression of CD166 and embigin due to interactions between OM, osteoblasts and megakaryocytes (Figure 5.3A and C). This leads to another important unanswered question whether CD166 and embigin act through the same pathway or employ different pathways to maintain OM-mediated hematopoietic activity. Double knockout studies would be an important tool to answer this question in the future.

Overall, previous and current data corroborate the importance of crosstalk between OM, osteoblasts and megakaryocytes to maintain hematopoietic enhancing activity. As seen in Figure 5.10 (left to the axis), previous studies demonstrate that megakaryocytes suppress osteoblast differentiation; and immature osteoblasts which express high levels of CD166 best maintain HSC function (Chitteti, Cheng et al. 2010, Cheng, Chitteti et al. 2011, Chitteti, Cheng et al. 2013). HSC also express CD166 (transcriptional activation via STAT3 binding to promoter region) through which they possibly interact with osteoblasts

through CD166-CD166 homophilic interactions. CD166 expression on HSC is important for both homing and engraftment (Chitteti, Kobayashi et al. 2014). On the other hand, current studies (Figure 5.10, right to the axis) indicate that interaction with osteoblasts and megakaryocytes causes enhanced OM proliferation (Mohamad, Xu et al. 2017) and upregulation of CD166 and embigin expression on OM. Since STAT3 binds to the CD166 promoter causing its regulation in HSC, one could hypothesize that the same mechanism might be responsible for upregulating CD166 expression on OM. Both CD166 and embigin act as molecular mediators through which OM maintain hematopoietic function when they interact with osteoblasts and megakaryocytes.

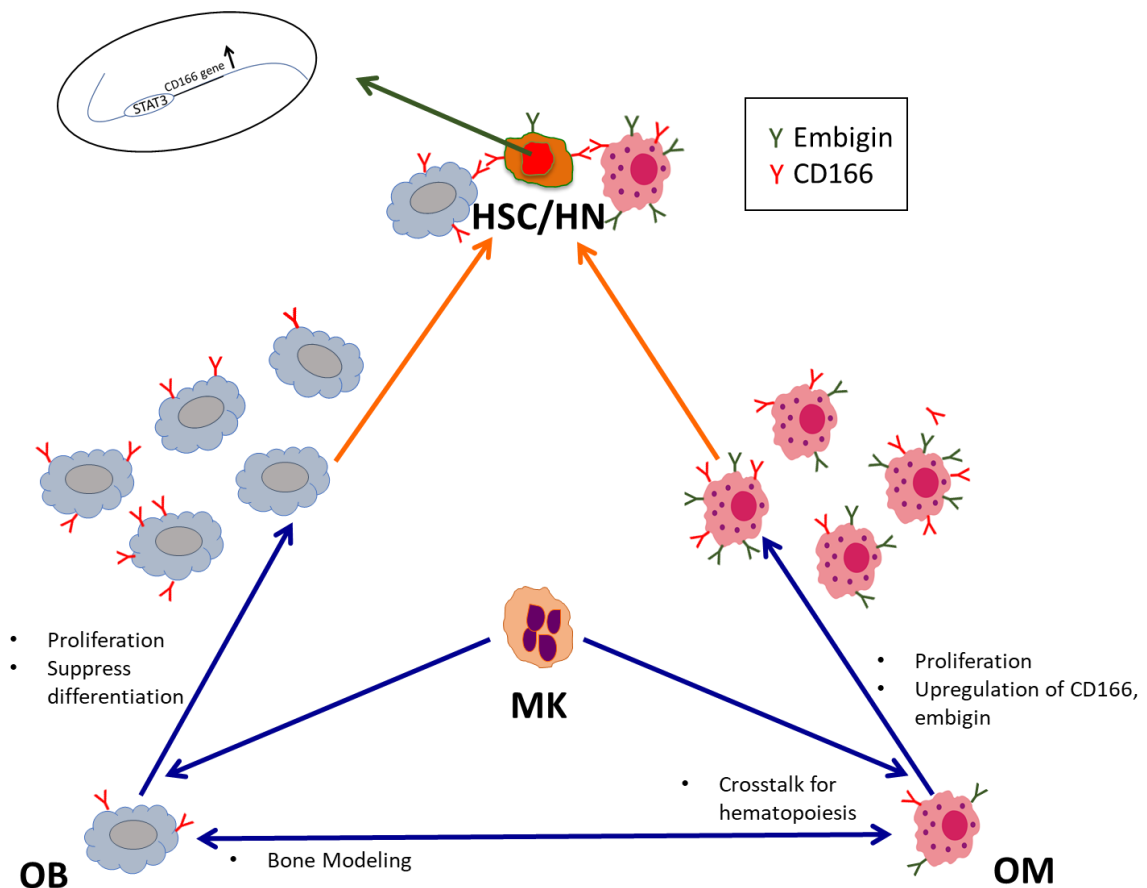


Figure 5.10 **Summary of previous and current studies.** Figure depicting the crosstalk between OM, osteoblasts and megakaryocytes in the hematopoietic niche.

CHAPTER SIX: Future Directions

6.1 The requirement of a phenotypic marker distinguishing adult OM from BM M ϕ

Currently, three *in vivo* macrophage depletion models have been reported: 1) *Mafia* transgenic mice through which a drug-induced *Fas* suicide gene can cause the apoptosis of a broad spectrum range of macrophages present in several tissues (Chang, Raggatt et al. 2008, Winkler, Sims et al. 2010); 2) Clodronate liposomes, which use the phagocytic capability of macrophages and osteoclasts to deplete them (van Rooijen and Hendriks 2010); and 3) CD169-diphtheria toxin receptor mouse which, via the activation of the diphtheria toxin depletes CD169+ cells including macrophages *in vivo* (Chow, Lucas et al. 2011). This CD169+ macrophage depletion model is currently the most commonly used model to understand the role of macrophages resident in the hematopoietic niche (Chow, Lucas et al. 2011, Chow, Huggins et al. 2013, Jacobsen, Forristal et al. 2014, Batoon, Millard et al. 2017). This model targets HSC niche resident BM M ϕ , OM and EIM. As discussed in chapter 3, CD169 is not a distinguishing marker between OM and BM M ϕ (Figure 3.3 and 3.6). In fact, a higher percentage of neonatal OM expressed CD169 than that detected amongst neonatal BM M ϕ ; and its expression on both cell types becomes similar with development. This makes it difficult to determine which subset of macrophages is responsible for maintaining the competence of the hematopoietic niche based on the CD169+ M ϕ depletion model as described by Chow et al, Chow and Lucas, and Kaur and Raggatt.

The lack of an OM specific depletion model is a setback for *in vivo* studies and something that needs to be discussed. My work in the laboratory was aimed to identify a distinguishing marker between OM and BM M ϕ which can potentially be used to make an

OM depletion mouse model. The results in this thesis successfully demonstrate phenotypic markers such as CD166, CD206 and CD110 which differentiate OM from BM M ϕ in neonates (Figure 3.3, 3.4 and 3.6). However, the expression of CD166 is limited to a subset of OM in adults and CD206 expression on OM is reduced with age (Figure 3.7). Hence, there is an urgent need to identify a phenotypic marker which distinguishes adult OM from BM M ϕ if genetic models are to be used in future investigations. Since CD110 expression has not been checked on adult OM, the search for a unique marker can begin by analyzing CD110 expression on OM in adults by flow cytometry. However, although CD110 might be a useful distinguishing surface marker between adult OM and BM M ϕ , this surface marker cannot be used for an OM depletion model due to its expression on megakaryocytes (Kacena, Gundberg et al. 2006, Bethel, Barnes et al. 2015). Other possible experiments could include single cell mRNA sequencing (10X genomics) which would help identify distinguishing markers between adult OM and BM M ϕ ; and mass spectrometry as performed in Figure 5.2. Once a novel marker is identified, it would help in the formation of an *in vivo* mouse model to specifically deplete OM similar to the CD169+ depletion model. This new model would be very useful in fully understanding the role of OM in the hematopoietic niche.

6.2 To identify the localization of OM, osteoblasts and megakaryocytes with respect to HSPCs in stressed and aged mice

The current work in 3D tissue cytometry is very encouraging. Paraffin embedded murine long bones were successfully stained and imaged for OM and megakaryocytes using a confocal microscope. Since the model is a Fgd5 mouse, HSC and vessels are GFP+ making it easy to identify them. Finally, the use of 2-photon imaging allows the user to visualize osteoblasts. Through concentrated efforts multiple fields were obtained wherein all four cell types were in close proximity to each other (Figure 4.6). However, a number of obstacles were encountered reaching this point. For example, it was difficult to attain several sections where the bone marrow was intact and attached to the bone. This was because the bone marrow easily sloughed off giving cracked sections. Also, the current sections are only 25 microns in depth which is not sufficient to fully understand the complexity of the hematopoietic niche. Finally, the bone is a highly auto fluorescent organ adding to these difficulties. To overcome these issues, and move this project to the next level, the following has been planned:

- The next step is to use whole bone rather than 25 micron sections. This will help image greater depths (minimum of 100 microns) of bone through confocal microscopy. Also, the use of whole bone will help overcome the issue of cracked sections. However, using whole bone would make staining more difficult. Hence, it would be simpler to make frozen sections instead of paraffinizing the bone. Frozen sections are known to be much easier to stain and image compared to paraffinized sections. Also, to reduce autofluorescence and make staining whole bone possible, a protocol which includes clearing the bone has been adapted. This is a protocol that was recently developed (Li, Germain et al. 2017) and attains excellent tissue transparency for most organs including bone.

- Once cleared, this new system will be used to quantitate the number of OM, osteoblasts, megakaryocytes and HSC in whole bone. The algorithm to quantitate cells in z-stacks was developed at Indiana University and has successfully been implemented in the kidney (Winfree, Khan et al. 2017). This quantitation will help understand the number of each cell type in unperturbed bone marrow. Moreover, this technology can be used to quantitate the number of each cell type in the epiphysis versus the diaphysis. Previous studies have demonstrated that most HSC reside within the growth plate of the bone (Ellis, Grassinger et al. 2011). Current studies can help corroborate this data and additionally understand the differences in the niche within the growth plate versus the rest of the bone.
- Finally, there is ample evidence indicating that the hematopoietic niche alters with age (Rossi, Bryder et al. 2005, Janzen, Forkert et al. 2006, Gekas and Graf 2013) and stress (Severe, Karabacak et al. 2019). For example, there are data demonstrating that megakaryocytes number increase with age (Rundberg Nilsson, Soneji et al. 2016). Similarly, flow cytometry data demonstrate that OM numbers decrease with age (Figure 6.1). This indicates the possibility of change in crosstalk between cells in aged bone marrow. Likewise, hematopoietic stress such as irradiation also changes the co-localization and crosstalk between different resident cells in the hematopoietic niche (Dominici, Rasini et al. 2009, Olson, Caselli et al. 2013). The ultimate goal is to understand and quantitate the differences in co-localization and number of OM, osteoblasts, megakaryocytes and HSC in hematopoietic stressed and aged bone marrow compared to unperturbed bone marrow. This is a novel and unique aspect of this research which might help understand the functional loss of HSC with age.

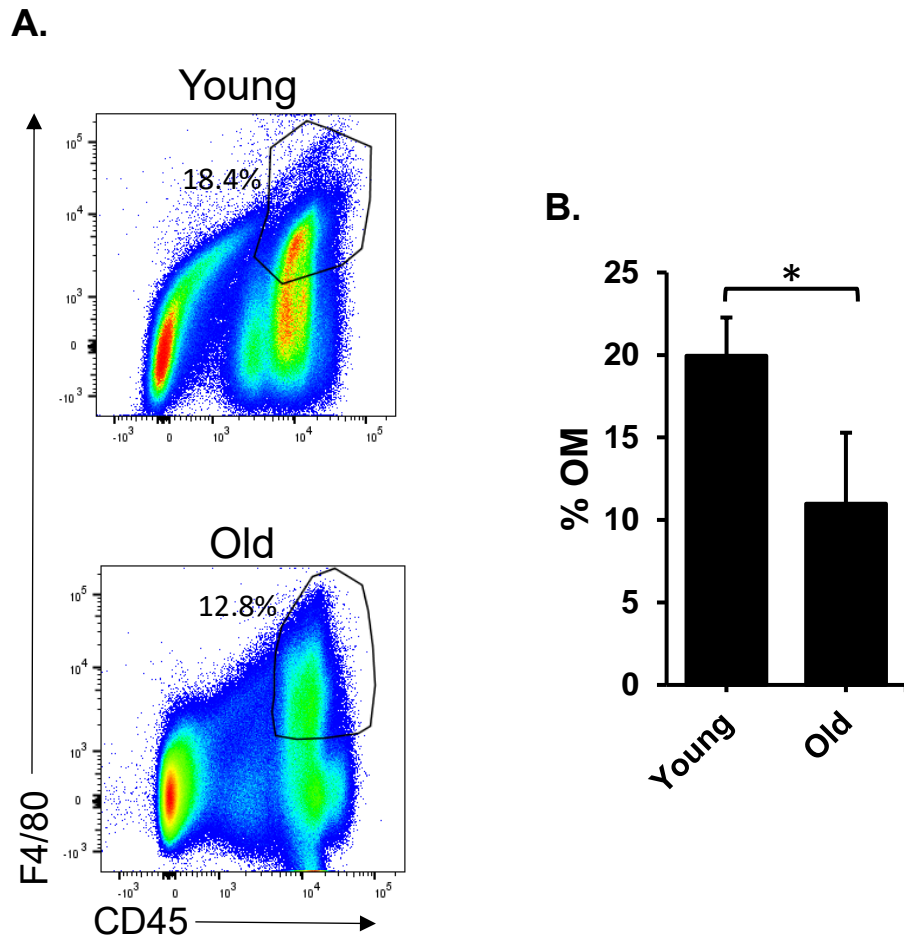


Figure 6.1 **Phenotypic characterization of young and old osteomacs.** (A) Representative flow cytometric data of freshly isolated digested bone from 8 wk young (top row) and 24 months old (bottom row) mice. (B) Combined average of percent young and old OM, $p < 0.001$, $N = 8$.

6.3 To determine the molecular mediators through which OM maintain hematopoietic activity *in vivo*

The work centered on CD166 and embigin as molecular mediators through which OM maintain hematopoietic function has mainly been focused on the use of *in vitro* experiments (Figure 5.5-5.9). However, the relevance of this work is based on translating the *in vitro* studies *in vivo*. For this, the next step would be to transplant LSK cells co-cultured with CD166 knockout OM, wild type osteoblasts and wild type megakaryocytes to validate these results *in vivo*. The transplant studies are currently underway and are very early to yield meaningful conclusions. Also, the embigin studies are based on a lentiviral knockdown system which is considered to be unstable. Ideally, for the embigin studies, it would be preferred to use an embigin knockout mouse to obtain embigin knockout OM for the co-cultures with osteoblasts, megakaryocytes and HSC which would culminate in progenitor and competitive transplantation assays. Since embigin knockout mice are currently unavailable, embigin flox/flox mice (Originally made by Dr. Jyrki Heino, Finland) will be obtained which can be used to make embigin global knockout mice or embigin conditional knockout mice.

The data using simultaneously a combination of recombinant CD166 and embigin proteins to substitute for OM functionality showed a trend towards non-significant increase in CFU fold change compared to individual recombinant protein data (Figure 5.5). These findings suggest that CD166 and embigin may work through the same pathway or mechanism. Following up on this observation, there is the possibility to potentially knockdown embigin using the lentivirus system in CD166 knockout OM. In this way, OM devoid of both CD166 and embigin expression could be isolated. This could help understand whether CD166 and embigin work separately or together to maintain OM-mediated hematopoietic enhancing activity.

It is unlikely that CD166 and embigin are the only two mediators through which OM mediate their hematopoiesis enhancing activity. Therefore, another avenue to explore would be to identify other molecular mediators (besides embigin and CD166) through which OM maintain hematopoiesis. Single cell mRNA sequencing data demonstrated the upregulation of over 200 genes in OM which were co-cultured with osteoblasts and megakaryocytes (Figure 5.1). Similarly, the mass spectrometry data identified 32 proteins which were upregulated on OM isolated from NCC+MK (Figure 5.2). These data could be used to test other mediators through which OM could potentially augment hematopoietic activity. One of the proteins from the mass spectrometry data that was upregulated on OM was arginase. Recent findings suggest that M2 M ϕ through the expression of arginase promote the self-renewal and expansion of HSC (Luo, Shao et al. 2018). Investigating arginase as a potential mediator of OM-mediated hematopoiesis is another avenue left unexplored.

REFERENCES

- Ahn, J.-Y., G. Park, J.-S. Shim, J.-W. Lee and I.-H. Oh (2010). "Intramarrow injection of β -catenin-activated, but not naïve mesenchymal stromal cells stimulates self-renewal of hematopoietic stem cells in bone marrow." **42**(2): 122.
- Aiuti, A., M. Tavian, A. Cipponi, F. Ficara, E. Zappone, J. Hoxie, B. Peault and C. Bordignon (1999). "Expression of CXCR4, the receptor for stromal cell-derived factor-1 on fetal and adult human lymphohematopoietic progenitors." **29**(6): 1823-1831.
- Aiuti, A., I. J. Webb, C. Bleul, T. Springer and J. C. Gutierrez-Ramos (1997). "The chemokine SDF-1 is a chemoattractant for human CD34+ hematopoietic progenitor cells and provides a new mechanism to explain the mobilization of CD34+ progenitors to peripheral blood." J Exp Med **185**(1): 111-120.
- Alexander, K. A., M. K. Chang, E. R. Maylin, T. Kohler, R. Muller, A. C. Wu, N. Van Rooijen, M. J. Sweet, D. A. Hume, L. J. Raggatt and A. R. Pettit (2011). "Osteal macrophages promote in vivo intramembranous bone healing in a mouse tibial injury model." J Bone Miner Res **26**(7): 1517-1532.
- Alexander, K. A., L. J. Raggatt, S. Millard, L. Batoon, A. Chiu-Ku Wu, M. K. Chang, D. A. Hume and A. R. Pettit (2017). "Resting and injury-induced inflamed periosteum contain multiple macrophage subsets that are located at sites of bone growth and regeneration." Immunol Cell Biol **95**(1): 7-16.
- Alvarez, M. B., L. Xu, P. J. Childress, K. A. Maupin, S. F. Mohamad, B. R. Chitteti, E. Himes, D. J. Olivos, 3rd, Y. H. Cheng, S. J. Conway, E. F. Srouf and M. A. Kacena (2018). "Megakaryocyte and Osteoblast Interactions Modulate Bone Mass and Hematopoiesis." Stem Cells Dev **27**(10): 671-682.

- Anjanappa, M., A. Cardoso, L. Cheng, S. Mohamad, A. Gunawan, S. Rice, Y. Dong, L. Li, G. E. Sandusky, E. F. Srouf and H. Nakshatri (2017). "Individualized Breast Cancer Characterization through Single-Cell Analysis of Tumor and Adjacent Normal Cells." Cancer Res **77**(10): 2759-2769.
- Arai, F., A. Hirao, M. Ohmura, H. Sato, S. Matsuoka, K. Takubo, K. Ito, G. Y. Koh and T. Suda (2004). "Tie2/Angiopoietin-1 Signaling Regulates Hematopoietic Stem Cell Quiescence in the Bone Marrow Niche." Cell **118**(2): 149-161.
- Avecilla, S. T., K. Hattori, B. Heissig, R. Tejada, F. Liao, K. Shido, D. K. Jin, S. Dias, F. Zhang, T. E. Hartman, N. R. Hackett, R. G. Crystal, L. Witte, D. J. Hicklin, P. Bohlen, D. Eaton, D. Lyden, F. De Sauvage and S. Rafii (2004). "Chemokine-mediated interaction of hematopoietic progenitors with the bone marrow vascular niche is required for thrombopoiesis." **10**(1): 64-71.
- Batoon, L., S. M. Millard, L. J. Raggatt and A. R. Pettit (2017). "Osteomacs and Bone Regeneration." Curr Osteoporos Rep **15**(4): 385-395.
- Batoon, L., S. M. Millard, M. E. Wullschleger, C. Preda, A. C. Wu, S. Kaur, H. W. Tseng, D. A. Hume, J. P. Levesque, L. J. Raggatt and A. R. Pettit (2017). "CD169(+) macrophages are critical for osteoblast maintenance and promote intramembranous and endochondral ossification during bone repair." Biomaterials.
- Bessis, M. (1958). "[Erythroblastic island, functional unity of bone marrow]." Rev Hematol **13**(1): 8-11.
- Bethel, M., C. L. Barnes, A. F. Taylor, Y. H. Cheng, B. R. Chitteti, M. C. Horowitz, A. Bruzzaniti, E. F. Srouf and M. A. Kacena (2015). "A novel role for thrombopoietin in regulating osteoclast development in humans and mice." J Cell Physiol **230**(9): 2142-2151.

- Bethel, M., B. R. Chitteti, E. F. Srouf and M. A. Kacena (2013). "The changing balance between osteoblastogenesis and adipogenesis in aging and its impact on hematopoiesis." Curr Osteoporos Rep **11**(2): 99-106.
- Bethel, M., E. F. Srouf and M. A. Kacena (2011). "Hematopoietic cell regulation of osteoblast proliferation and differentiation." Curr Osteoporos Rep **9**(2): 96-102.
- Boisset, J.-C. and C. Robin (2010). "Imaging the founder of adult hematopoiesis in the mouse embryo aorta." **9**(13): 2489-2490.
- Bowen, M. A., J. Bajorath, M. D'Egidio, G. S. Whitney, D. Palmer, J. Kobarg, G. C. Starling, A. W. Siadak and A. Aruffo (1997). "Characterization of mouse ALCAM (CD166): the CD6-binding domain is conserved in different homologs and mediates cross-species binding." Eur J Immunol **27**(6): 1469-1478.
- Bruder, S. P., N. S. Ricalton, R. E. Boynton, T. J. Connolly, N. Jaiswal, J. Zaia and F. P. Barry (1998). "Mesenchymal Stem Cell Surface Antigen SB-10 Corresponds to Activated Leukocyte Cell Adhesion Molecule and Is Involved in Osteogenic Differentiation." Journal of Bone and Mineral Research **13**(4): 655-663.
- Bruns, I., D. Lucas, S. Pinho, J. Ahmed, M. P. Lambert, Y. Kunisaki, C. Scheiermann, L. Schiff, M. Poncz, A. Bergman and P. S. Frenette (2014). "Megakaryocytes regulate hematopoietic stem cell quiescence through CXCL4 secretion." Nat Med **20**(11): 1315-1320.
- Calvi, L. M., G. B. Adams, K. W. Weibrecht, J. M. Weber, D. P. Olson, M. C. Knight, R. P. Martin, E. Schipani, P. Divieti, F. R. Bringhurst, L. A. Milner, H. M. Kronenberg and D. T. Scadden (2003). "Osteoblastic cells regulate the haematopoietic stem cell niche." Nature **425**(6960): 841-846.
- Calvi, L. M., O. Bromberg, Y. Rhee, J. M. Weber, J. N. P. Smith, M. J. Basil, B. J. Frisch and T. Bellido (2012). "Osteoblastic expansion induced by parathyroid hormone

- receptor signaling in murine osteocytes is not sufficient to increase hematopoietic stem cells." **119**(11): 2489-2499.
- Cannon, G. J. and J. A. Swanson (1992). "The macrophage capacity for phagocytosis." J Cell Sci **101 (Pt 4)**: 907-913.
- Catlin, S. N., L. Busque, R. E. Gale, P. Guttorp and J. L. Abkowitz (2011). "The replication rate of human hematopoietic stem cells in vivo." Blood **117**(17): 4460-4466.
- Chang, K. H., A. Sengupta, R. C. Nayak, A. Duran, S. J. Lee, R. G. Pratt, A. M. Wellendorf, S. E. Hill, M. Watkins, D. Gonzalez-Nieto, B. J. Aronow, D. T. Starczynowski, R. Civitelli, M. T. Diaz-Meco, J. Moscat and J. A. Cancelas (2014). "p62 is required for stem cell/progenitor retention through inhibition of IKK/NF-kappaB/Ccl4 signaling at the bone marrow macrophage-osteoblast niche." Cell Rep **9**(6): 2084-2097.
- Chang, M. K., L. J. Raggatt, K. A. Alexander, J. S. Kuliwaba, N. L. Fazzalari, K. Schroder, E. R. Maylin, V. M. Ripoll, D. A. Hume and A. R. Pettit (2008). "Osteal Tissue Macrophages Are Intercalated throughout Human and Mouse Bone Lining Tissues and Regulate Osteoblast Function In Vitro and In Vivo." The Journal of Immunology **181**(2): 1232-1244.
- Cheng, Y. H., B. R. Chitteti, D. A. Streicher, J. A. Morgan, S. Rodriguez-Rodriguez, N. Carlesso, E. F. Srour and M. A. Kacena (2011). "Impact of maturational status on the ability of osteoblasts to enhance the hematopoietic function of stem and progenitor cells." J Bone Miner Res **26**(5): 1111-1121.
- Cheng, Y. H., R. A. Hooker, K. Nguyen, R. Gerard-O'Riley, D. L. Waning, B. R. Chitteti, T. E. Meijome, H. L. Chua, A. P. Plett, C. M. Orschell, E. F. Srour, L. D. Mayo, F. M. Pavalko, A. Bruzzaniti and M. A. Kacena (2013). "Pyk2 regulates megakaryocyte-induced increases in osteoblast number and bone formation." J Bone Miner Res **28**(6): 1434-1445.

- Cheng, Y. H., D. A. Streicher, D. L. Waning, B. R. Chitteti, R. Gerard-O'Riley, M. C. Horowitz, J. P. Bidwell, F. M. Pavalko, E. F. Srour, L. D. Mayo and M. A. Kacena (2015). "Signaling pathways involved in megakaryocyte-mediated proliferation of osteoblast lineage cells." J Cell Physiol **230**(3): 578-586.
- Chitteti, B. R., M. Bethel, M. A. Kacena and E. F. Srour (2013). "CD166 and regulation of hematopoiesis." Curr Opin Hematol **20**(4): 273-280.
- Chitteti, B. R., Y. H. Cheng, M. A. Kacena and E. F. Srour (2013). "Hierarchical organization of osteoblasts reveals the significant role of CD166 in hematopoietic stem cell maintenance and function." Bone **54**(1): 58-67.
- Chitteti, B. R., Y. H. Cheng, B. Poteat, S. Rodriguez-Rodriguez, W. S. Goebel, N. Carlesso, M. A. Kacena and E. F. Srour (2010). "Impact of interactions of cellular components of the bone marrow microenvironment on hematopoietic stem and progenitor cell function." Blood **115**(16): 3239-3248.
- Chitteti, B. R., Y. H. Cheng, D. A. Streicher, S. Rodriguez-Rodriguez, N. Carlesso, E. F. Srour and M. A. Kacena (2010). "Osteoblast lineage cells expressing high levels of Runx2 enhance hematopoietic progenitor cell proliferation and function." J Cell Biochem **111**(2): 284-294.
- Chitteti, B. R., M. Kobayashi, Y. Cheng, H. Zhang, B. A. Poteat, H. E. Broxmeyer, L. M. Pelus, H. Hanenberg, A. Zollman, M. M. Kamocka, N. Carlesso, A. A. Cardoso, M. A. Kacena and E. F. Srour (2014). "CD166 regulates human and murine hematopoietic stem cells and the hematopoietic niche." Blood **124**(4): 519-529.
- Chitteti, B. R., Y. Liu and E. F. Srour (2011). "Genomic and Proteomic Analysis of the Impact of Mitotic Quiescence on the Engraftment of Human CD34+ Cells." **6**(3): e17498.
- Cho, S. W., F. N. Soki, A. J. Koh, M. R. Eber, P. Entezami, S. I. Park, N. Van Rooijen and L. K. McCauley (2014). "Osteal macrophages support physiologic skeletal

- remodeling and anabolic actions of parathyroid hormone in bone." **111**(4): 1545-1550.
- Choi, K., M. Kennedy, A. Kazarov, J. C. Papadimitriou and G. Keller (1998). "A common precursor for hematopoietic and endothelial cells." Development **125**(4): 725-732.
- Chow, A., M. Huggins, J. Ahmed, D. Hashimoto, D. Lucas, Y. Kunisaki, S. Pinho, M. Leboeuf, C. Noizat, N. van Rooijen, M. Tanaka, Z. J. Zhao, A. Bergman, M. Merad and P. S. Frenette (2013). "CD169(+) macrophages provide a niche promoting erythropoiesis under homeostasis and stress." Nat Med **19**(4): 429-436.
- Chow, A., D. Lucas, A. Hidalgo, S. Mendez-Ferrer, D. Hashimoto, C. Scheiermann, M. Battista, M. Leboeuf, C. Prophete, N. van Rooijen, M. Tanaka, M. Merad and P. S. Frenette (2011). "Bone marrow CD169+ macrophages promote the retention of hematopoietic stem and progenitor cells in the mesenchymal stem cell niche." J Exp Med **208**(2): 261-271.
- Christensen, J. L. and I. L. Weissman (2001). "Flk-2 is a marker in hematopoietic stem cell differentiation: A simple method to isolate long-term stem cells." **98**(25): 14541-14546.
- Ciovacco, W. A., Y. H. Cheng, M. C. Horowitz and M. A. Kacena (2010). "Immature and mature megakaryocytes enhance osteoblast proliferation and inhibit osteoclast formation." J Cell Biochem **109**(4): 774-781.
- Ciovacco, W. A., C. G. Goldberg, A. F. Taylor, J. M. Lemieux, M. C. Horowitz, H. J. Donahue and M. A. Kacena (2009). "The role of gap junctions in megakaryocyte-mediated osteoblast proliferation and differentiation." Bone **44**(1): 80-86.
- Coutu, D. L., K. D. Kokkalis, L. Kunz and T. Schroeder (2017). "Three-dimensional map of nonhematopoietic bone and bone-marrow cells and molecules." Nature biotechnology **35**(12): 1202-1210.

- Davies, L. C. and P. R. Taylor (2015). "Tissue-resident macrophages: then and now." Immunology **144**(4): 541-548.
- de Jong, J. P., P. J. Leenen, J. S. Voerman, A. J. van der Sluijs-Gelling and R. E. Ploemacher (1994). "A monoclonal antibody (ER-HR3) against murine macrophages. II. Biochemical and functional aspects of the ER-HR3 antigen." Cell Tissue Res **275**(3): 577-585.
- Degen, W. G., L. C. van Kempen, E. G. Gijzen, J. J. van Groningen, Y. van Kooyk, H. P. Bloemers and G. W. Swart (1998). "MEMD, a new cell adhesion molecule in metastasizing human melanoma cell lines, is identical to ALCAM (activated leukocyte cell adhesion molecule)." Am J Pathol **152**(3): 805-813.
- Dexter, T. M., T. D. Allen and L. G. Lajtha (1977). "Conditions controlling the proliferation of haemopoietic stem cells in vitro." **91**(3): 335-344.
- Dieterlen-Lievre, p. F. (1975). "On the origin of haemopoietic stem cells in the avian embryo: an experimental approach." Journal of Embryology and Experimental Morphology **33**(3): 607-619.
- Ding, L. and S. J. Morrison (2013). "Haematopoietic stem cells and early lymphoid progenitors occupy distinct bone marrow niches." **495**(7440): 231-235.
- Ding, L., T. L. Saunders, G. Enikolopov and S. J. Morrison (2012). "Endothelial and perivascular cells maintain haematopoietic stem cells." Nature **481**(7382): 457-462.
- Dominici, M., V. Rasini, R. Bussolari, X. Chen, T. J. Hofmann, C. Spano, D. Bernabei, E. Veronesi, F. Bertoni, P. Paolucci, P. Conte and E. M. Horwitz (2009). "Restoration and reversible expansion of the osteoblastic hematopoietic stem cell niche after marrow radioablation." Blood **114**(11): 2333-2343.
- Dutta, P., F. F. Hoyer, L. S. Grigoryeva, H. B. Sager, F. Leuschner, G. Courties, A. Borodovsky, T. Novobrantseva, V. M. Ruda, K. Fitzgerald, Y. Iwamoto, G.

- Wojtkiewicz, Y. Sun, N. Da Silva, P. Libby, D. G. Anderson, F. K. Swirski, R. Weissleder and M. Nahrendorf (2015). "Macrophages retain hematopoietic stem cells in the spleen via VCAM-1." J Exp Med **212**(4): 497-512.
- Ellis, S. L., J. Grassinger, A. Jones, J. Borg, T. Camenisch, D. Haylock, I. Bertocello and S. K. Nilsson (2011). "The relationship between bone, hemopoietic stem cells, and vasculature." Blood **118**(6): 1516-1524.
- Ema, M. and J. Rossant (2003). "Cell fate decisions in early blood vessel formation." Trends Cardiovasc Med **13**(6): 254-259.
- Fadini, G. P., F. Ferraro, F. Quaini, T. Asahara and P. Madeddu (2014). "Concise Review: Diabetes, the Bone Marrow Niche, and Impaired Vascular Regeneration." **3**(8): 949-957.
- Federman, N., J. Chan, J. O. Nagy, E. M. Landaw, K. McCabe, A. M. Wu, T. Triche, H. Kang, B. Liu, J. D. Marks and C. T. Denny (2012). "Enhanced Growth Inhibition of Osteosarcoma by Cytotoxic Polymerized Liposomal Nanoparticles Targeting the Alcam Cell Surface Receptor." **2012**: 1-11.
- Ferraro, F., S. Lympieri, S. Mendez-Ferrer, B. Saez, J. A. Spencer, B. Y. Yeap, E. Masselli, G. Graiani, L. Prezioso, E. L. Rizzini, M. Mangoni, V. Rizzoli, S. M. Sykes, C. P. Lin, P. S. Frenette, F. Quaini and D. T. Scadden (2011). "Diabetes Impairs Hematopoietic Stem Cell Mobilization by Altering Niche Function." Science Translational Medicine **3**(104): 104ra101-104ra101.
- Ferreiros-Vidal, I., T. Carroll, B. Taylor, A. Terry, Z. Liang, L. Bruno, G. Dharmalingam, S. Khadayate, B. S. Cobb, S. T. Smale, M. Spivakov, P. Srivastava, E. Petretto, A. G. Fisher and M. Merkenschlager (2013). "Genome-wide identification of Ikaros targets elucidates its contribution to mouse B-cell lineage specification and pre-B-cell differentiation." **121**(10): 1769-1782.

- Gekas, C. and T. Graf (2013). "CD41 expression marks myeloid-biased adult hematopoietic stem cells and increases with age." **121**(22): 4463-4472.
- Ghosh, J., S. F. Mohamad and E. F. Srour (2019). "Isolation and Identification of Murine Bone Marrow-Derived Macrophages and Osteomacs from Neonatal and Adult Mice." Methods Mol Biol **2002**: 181-193.
- Greenbaum, A., Y.-M. S. Hsu, R. B. Day, L. G. Schuettpelz, M. J. Christopher, J. N. Borgerding, T. Nagasawa and D. C. Link (2013). "CXCL12 in early mesenchymal progenitors is required for haematopoietic stem-cell maintenance." Nature **495**(7440): 227-230.
- Guihard, P., Y. Danger, B. Brounais, E. David, R. Brion, J. Delecrin, C. D. Richards, S. Chevalier, F. Rédini, D. Heymann, H. Gascan and F. Blanchard (2012). "Induction of Osteogenesis in Mesenchymal Stem Cells by Activated Monocytes/Macrophages Depends on Oncostatin M Signaling." **30**(4): 762-772.
- Haniffa, M., F. Ginhoux, X.-N. Wang, V. Bigley, M. Abel, I. Dimmick, S. Bullock, M. Grisotto, T. Booth, P. Taub, C. Hilkens, M. Merad and M. Collin (2009). "Differential rates of replacement of human dermal dendritic cells and macrophages during hematopoietic stem cell transplantation." The Journal of Experimental Medicine **206**(2): 371-385.
- Hashimoto, D., A. Chow, M. Greter, Y. Saenger, W.-H. Kwan, M. Leboeuf, F. Ginhoux, J. C. Ochando, Y. Kunisaki, N. Van Rooijen, C. Liu, T. Teshima, P. S. Heeger, E. R. Stanley, P. S. Frenette and M. Merad (2011). "Pretransplant CSF-1 therapy expands recipient macrophages and ameliorates GVHD after allogeneic hematopoietic cell transplantation." **208**(5): 1069-1082.
- Heazlewood, S. Y., R. J. Neaves, B. Williams, D. N. Haylock, T. E. Adams and S. K. Nilsson (2013). "Megakaryocytes co-localise with hemopoietic stem cells and release cytokines that up-regulate stem cell proliferation." **11**(2): 782-792.

- Heazlewood, S. Y., A. Oteiza, H. Cao and S. K. Nilsson (2014). "Analyzing hematopoietic stem cell homing, lodgment, and engraftment to better understand the bone marrow niche." Ann N Y Acad Sci **1310**: 119-128.
- Heissig, B., K. Hattori, S. Dias, M. Friedrich, B. Ferris, N. R. Hackett, R. G. Crystal, P. Besmer, D. Lyden, M. A. Moore, Z. Werb and S. Rafii (2002). "Recruitment of stem and progenitor cells from the bone marrow niche requires MMP-9 mediated release of kit-ligand." Cell **109**(5): 625-637.
- Hoggatt, J. and L. M. Pelus (2011). "Many mechanisms mediating mobilization: an alliterative review." Curr Opin Hematol **18**(4): 231-238.
- Hoggatt, J., P. Singh, T. A. Tate, B. K. Chou, S. R. Datari, S. Fukuda, L. Liu, P. V. Kharchenko, A. Schajnovitz, N. Baryawno, F. E. Mercier, J. Boyer, J. Gardner, D. M. Morrow, D. T. Scadden and L. M. Pelus (2018). "Rapid Mobilization Reveals a Highly Engraftable Hematopoietic Stem Cell." Cell **172**(1-2): 191-204.e110.
- Huang, H., H. Feng and D. Zhuge (2019). "M1 Macrophage Activated by Notch Signal Pathway Contributed to Ventilator-Induced Lung Injury in Chronic Obstructive Pulmonary Disease Model." J Surg Res **244**: 358-367.
- Huang, R. P., M. Ozawa, K. Kadomatsu and T. Muramatsu (1990). "Developmentally regulated expression of embigin, a member of the immunoglobulin superfamily found in embryonal carcinoma cells." Differentiation **45**(2): 76-83.
- Huang, R. P., M. Ozawa, K. Kadomatsu and T. Muramatsu (1993). "Embigin, a member of the immunoglobulin superfamily expressed in embryonic cells, enhances cell-substratum adhesion." Dev Biol **155**(2): 307-314.
- Hume, D. A. (2015). "The Many Alternative Faces of Macrophage Activation." **6**.
- Hur, J., J. I. Choi, H. Lee, P. Nham, T. W. Kim, C. W. Chae, J. Y. Yun, J. A. Kang, J. Kang, S. E. Lee, C. H. Yoon, K. Boo, S. Ham, T. Y. Roh, J. K. Jun, H. Lee, S. H. Baek and H. S. Kim (2016). "CD82/KAI1 Maintains the Dormancy of Long-Term

- Hematopoietic Stem Cells through Interaction with DARC-Expressing Macrophages." Cell Stem Cell **18**(4): 508-521.
- Jacobsen, R. N., C. E. Forristal, L. J. Raggatt, B. Nowlan, V. Barbier, S. Kaur, N. van Rooijen, I. G. Winkler, A. R. Pettit and J. P. Levesque (2014). "Mobilization with granulocyte colony-stimulating factor blocks medullar erythropoiesis by depleting F4/80(+)VCAM1(+)CD169(+)ER-HR3(+)Ly6G(+) erythroid island macrophages in the mouse." Exp Hematol **42**(7): 547-561.e544.
- Jacobsen, R. N., A. C. Perkins and J. P. Levesque (2015). "Macrophages and regulation of erythropoiesis." Curr Opin Hematol **22**(3): 212-219.
- Janzen, V., R. Forkert, H. E. Fleming, Y. Saito, M. T. Waring, D. M. Dombkowski, T. Cheng, R. A. Depinho, N. E. Sharpless and D. T. Scadden (2006). "Stem-cell ageing modified by the cyclin-dependent kinase inhibitor p16INK4a."
- Jiang, J., C. Y. Kao and E. T. Papoutsakis (2017). "How do megakaryocytic microparticles target and deliver cargo to alter the fate of hematopoietic stem cells?" J Control Release **247**: 1-18.
- Kacena, M. A., P. P. Eleniste, Y. H. Cheng, S. Huang, M. Shivanna, T. E. Meijome, L. D. Mayo and A. Bruzzaniti (2012). "Megakaryocytes Regulate Expression of Pyk2 Isoforms and Caspase-mediated Cleavage of Actin in Osteoblasts." **287**(21): 17257-17268.
- Kacena, M. A., C. M. Gundberg and M. C. Horowitz (2006). "A reciprocal regulatory interaction between megakaryocytes, bone cells, and hematopoietic stem cells." Bone **39**(5): 978-984.
- Kacena, M. A., C. M. Gundberg, T. Nelson and M. C. Horowitz (2005). "Loss of the transcription factor p45 NF-E2 results in a developmental arrest of megakaryocyte differentiation and the onset of a high bone mass phenotype." Bone **36**(2): 215-223.

- Kacena, M. A., R. A. Shivdasani, K. Wilson, Y. Xi, N. Troiano, A. Nazarian, C. M. Gundberg, M. L. Bouxsein, J. A. Lorenzo and M. C. Horowitz (2004). "Megakaryocyte-osteoblast interaction revealed in mice deficient in transcription factors GATA-1 and NF-E2." J Bone Miner Res **19**(4): 652-660.
- Katayama, Y., M. Battista, W.-M. Kao, A. Hidalgo, A. J. Peired, S. A. Thomas and P. S. Frenette (2006). "Signals from the Sympathetic Nervous System Regulate Hematopoietic Stem Cell Egress from Bone Marrow." Cell **124**(2): 407-421.
- Kaur, S., L. J. Raggatt, L. Batoon, D. A. Hume, J. P. Levesque and A. R. Pettit (2017). "Role of bone marrow macrophages in controlling homeostasis and repair in bone and bone marrow niches." Semin Cell Dev Biol **61**: 12-21.
- Kaur, S., L. J. Raggatt, S. M. Millard, A. C. Wu, L. Batoon, R. N. Jacobsen, I. G. Winkler, K. P. MacDonald, A. C. Perkins, D. A. Hume, J. P. Levesque and A. R. Pettit (2018). "Self-repopulating recipient bone marrow resident macrophages promote long-term hematopoietic stem cell engraftment." Blood **132**(7): 735-749.
- Kiel, M. J. and S. J. Morrison (2008). "Uncertainty in the niches that maintain haematopoietic stem cells." Nature Reviews Immunology **8**(4): 290-301.
- Kiel, M. J., Ö. H. Yilmaz, T. Iwashita, O. H. Yilmaz, C. Terhorst and S. J. Morrison (2005). "SLAM Family Receptors Distinguish Hematopoietic Stem and Progenitor Cells and Reveal Endothelial Niches for Stem Cells." **121**(7): 1109-1121.
- Kode, A., J. S. Manavalan, I. Mosialou, G. Bhagat, C. V. Rathinam, N. Luo, H. Khiabani, A. Lee, V. V. Murty, R. Friedman, A. Brum, D. Park, N. Galili, S. Mukherjee, J. Teruya-Feldstein, A. Raza, R. Rabadan, E. Berman and S. Kousteni (2014). "Leukaemogenesis induced by an activating β -catenin mutation in osteoblasts." **506**(7487): 240-244.
- Krause, D. S., K. Fulzele, A. Catic, C. C. Sun, D. Dombkowski, M. P. Hurley, S. Lezeau, E. Attar, J. Y. Wu, H. Y. Lin, P. Divieti-Pajevic, R. P. Hasserjian, E. Schipani, R. A.

- Van Etten and D. T. Scadden (2013). "Differential regulation of myeloid leukemias by the bone marrow microenvironment." **19**(11): 1513-1517.
- Krishnegowda, M. and V. Rajashekaraiyah (2015). "Platelet disorders: an overview." Blood Coagul Fibrinolysis **26**(5): 479-491.
- Kristiansen, G., C. Pilarsky, C. Wissmann, C. Stephan, L. Weissbach, V. Loy, S. Loening, M. Dietel and A. Rosenthal (2003). "ALCAM/CD166 is up-regulated in low-grade prostate cancer and progressively lost in high-grade lesions." Prostate **54**(1): 34-43.
- Kunisaki, Y., I. Bruns, C. Scheiermann, J. Ahmed, S. Pinho, D. Zhang, T. Mizoguchi, Q. Wei, D. Lucas, K. Ito, J. C. Mar, A. Bergman and P. S. Frenette (2013). "Arteriolar niches maintain haematopoietic stem cell quiescence." **502**(7473): 637-643.
- Lain, E., S. Carnejac, P. Escher, M. C. Wilson, T. Lomo, N. Gajendran and H. R. Brenner (2009). "A novel role for ephrins to promote sprouting of motor nerve terminals at the neuromuscular junction." J Biol Chem **284**(13): 8930-8939.
- Lancrin, C., P. Sroczynska, C. Stephenson, T. Allen, V. Kouskoff and G. Lacaud (2009). "The haemangioblast generates haematopoietic cells through a haemogenic endothelium stage." Nature **457**(7231): 892-895.
- Lapidot, T., A. Dar and O. Kollet (2005). "How do stem cells find their way home?" Blood **106**(6): 1901-1910.
- Latchney, S. E. and L. M. Calvi (2016). "The aging hematopoietic stem cell niche: Phenotypic and functional changes and mechanisms that contribute to hematopoietic aging."
- Layer, J. H., C. E. Alford, W. H. McDonald and U. P. Dave (2016). "LMO2 Oncoprotein Stability in T-Cell Leukemia Requires Direct LDB1 Binding." Mol Cell Biol **36**(3): 488-506.

- Lehmann, J. M., G. Riethmuller and J. P. Johnson (1989). "MUC18, a marker of tumor progression in human melanoma, shows sequence similarity to the neural cell adhesion molecules of the immunoglobulin superfamily." Proceedings of the National Academy of Sciences **86**(24): 9891-9895.
- Leimberg, M. J., E. Prus, A. M. Konijn and E. Fibach (2008). "Macrophages function as a ferritin iron source for cultured human erythroid precursors." Journal of Cellular Biochemistry **103**(4): 1211-1218.
- Leveen, P., M. Pekny, S. Gebre-Medhin, B. Swolin, E. Larsson and C. Betsholtz (1994). "Mice deficient for PDGF B show renal, cardiovascular, and hematological abnormalities." Genes Dev **8**(16): 1875-1887.
- Levesque, J. P., F. Liu, P. J. Simmons, T. Betsuyaku, R. M. Senior, C. Pham and D. C. Link (2004). "Characterization of hematopoietic progenitor mobilization in protease-deficient mice." Blood **104**(1): 65-72.
- Levesque, J. P., Y. Takamatsu, S. K. Nilsson, D. N. Haylock and P. J. Simmons (2001). "Vascular cell adhesion molecule-1 (CD106) is cleaved by neutrophil proteases in the bone marrow following hematopoietic progenitor cell mobilization by granulocyte colony-stimulating factor." Blood **98**(5): 1289-1297.
- Li, W., R. N. Germain and M. Y. Gerner (2017). "Multiplex, quantitative cellular analysis in large tissue volumes with clearing-enhanced 3D microscopy (Ce3D)." Proceedings of the National Academy of Sciences **114**(35): E7321-E7330.
- Lim, S.-E., V. Esain, W. Kwan, L. N. Theodore, M. Cortes, I. M. Frost, S. Y. Liu and T. E. North (2016). "HIF1 α -induced PDGFR β signaling promotes developmental HSC production via IL-6 activation."
- Lu, X. J., Q. Chen, Y. J. Rong, G. J. Yang, C. H. Li, N. Y. Xu, C. H. Yu, H. Y. Wang, S. Zhang, Y. H. Shi and J. Chen (2016). "LECT2 drives haematopoietic stem cell

expansion and mobilization via regulating the macrophages and osteolineage cells." Nat Commun **7**: 12719.

Ludin, A., T. Itkin, S. Gur-Cohen, A. Mildner, E. Shezen, K. Golan, O. Kollet, A. Kalinkovich, Z. Porat, G. D'Uva, A. Schajnovitz, E. Voronov, D. A. Brenner, R. N. Apte, S. Jung and T. Lapidot (2012). "Monocytes-macrophages that express alpha-smooth muscle actin preserve primitive hematopoietic cells in the bone marrow." Nat Immunol **13**(11): 1072-1082.

Luo, Y., L. Shao, J. Chang, W. Feng, Y. L. Liu, M. H. Cottler-Fox, P. D. Emanuel, M. Hauer-Jensen, I. D. Bernstein, L. Liu, X. Chen, J. Zhou, P. J. Murray and D. Zhou (2018). "M1 and M2 macrophages differentially regulate hematopoietic stem cell self-renewal and ex vivo expansion." Blood Adv **2**(8): 859-870.

Lymperi, S., N. Horwood, S. Marley, M. Y. Gordon, A. P. Cope and F. Dazzi (2007). "Strontium can increase some osteoblasts without increasing hematopoietic stem cells." **111**(3): 1173-1181.

Ma, Y., L. Visser, H. Roelofsen, M. De Vries, A. Diepstra, G. Van Imhoff, T. Van Der Wal, M. Luinge, G. Alvarez-Llamas, H. Vos, S. Poppema, R. Vonk and A. Van Den Berg (2008). "Proteomics analysis of Hodgkin lymphoma: identification of new players involved in the cross-talk between HRS cells and infiltrating lymphocytes." **111**(4): 2339-2346.

Malinge, S., C. Thiollier, T. M. Chlon, L. C. Dore, L. Diebold, O. Bluteau, V. Mabalalah, W. Vainchenker, P. Dessen, S. Winandy, T. Mercher and J. D. Crispino (2013). "Ikaros inhibits megakaryopoiesis through functional interaction with GATA-1 and NOTCH signaling." Blood **121**(13): 2440-2451.

Masedunskas, A., J. A. King, F. Tan, R. Cochran, T. Stevens, D. Sviridov and S. F. Ofori-Acquah (2006). "Activated leukocyte cell adhesion molecule is a component of the

- endothelial junction involved in transendothelial monocyte migration." **580**(11): 2637-2645.
- McCabe, A., Y. Zhang, V. Thai, M. Jones, M. B. Jordan and K. C. MacNamara (2015). "Macrophage-Lineage Cells Negatively Regulate the Hematopoietic Stem Cell Pool in Response to Interferon Gamma at Steady State and During Infection." Stem Cells **33**(7): 2294-2305.
- McGrath, K. E., J. M. Frame and J. Palis (2015). "Early hematopoiesis and macrophage development." Seminars in Immunology **27**(6): 379-387.
- Medvinsky, A. and E. Dzierzak (1996). "Definitive Hematopoiesis Is Autonomously Initiated by the AGM Region." **86**(6): 897-906.
- Medvinsky, A., S. Rybtsov and S. Taoudi (2011). "Embryonic origin of the adult hematopoietic system: advances and questions." Development **138**(6): 1017-1031.
- Meijome, T. E., J. T. Baughman, R. A. Hooker, Y. H. Cheng, W. A. Ciovacco, S. M. Balamohan, T. L. Srinivasan, B. R. Chitteti, P. P. Eleniste, M. C. Horowitz, E. F. Srour, A. Bruzzaniti, R. K. Fuchs and M. A. Kacena (2016). "C-Mpl Is Expressed on Osteoblasts and Osteoclasts and Is Important in Regulating Skeletal Homeostasis." J Cell Biochem **117**(4): 959-969.
- Mendez-Ferrer, S., D. Lucas, M. Battista and P. S. Frenette (2008). "Haematopoietic stem cell release is regulated by circadian oscillations." Nature **452**(7186): 442-447.
- Millard, S. M., A. R. Pettit, R. Ellis, J. K. Y. Chan, L. J. Raggatt, K. Khosrotehrani and N. M. Fisk (2015). "Intrauterine Bone Marrow Transplantation in Osteogenesis Imperfecta Mice Yields Donor Osteoclasts and Osteomacs but Not Osteoblasts." Stem Cell Reports **5**(5): 682-689.
- Mohamad, S. F., L. Xu, J. Ghosh, P. J. Childress, I. Abeysekera, E. R. Himes, H. Wu, M. B. Alvarez, K. M. Davis, A. Aguilar-Perez, J. M. Hong, A. Bruzzaniti, M. A. Kacena

- and E. F. Srouf (2017). "Osteomacs interact with megakaryocytes and osteoblasts to regulate murine hematopoietic stem cell function." Blood Adv **1**(26): 2520-2528.
- Mohle, R., F. Bautz, S. Rafii, M. A. Moore, W. Brugger and L. Kanz (1998). "The chemokine receptor CXCR-4 is expressed on CD34+ hematopoietic progenitors and leukemic cells and mediates transendothelial migration induced by stromal cell-derived factor-1." Blood **91**(12): 4523-4530.
- Mosley, A. L., L. Florens, Z. Wen and M. P. Washburn (2009). "A label free quantitative proteomic analysis of the *Saccharomyces cerevisiae* nucleus." J Proteomics **72**(1): 110-120.
- Mosley, A. L., M. E. Sardu, S. G. Pattenden, J. L. Workman, L. Florens and M. P. Washburn (2011). "Highly Reproducible Label Free Quantitative Proteomic Analysis of RNA Polymerase Complexes." **10**(2): M110.000687-M000110.
- Müller, A. M., A. Medvinsky, J. Strouboulis, F. Grosveld and E. Dzierzakt (1994). "Development of hematopoietic stem cell activity in the mouse embryo." **1**(4): 291-301.
- Nakamura-Ishizu, A., K. Takubo, M. Fujioka and T. Suda (2014). "Megakaryocytes are essential for HSC quiescence through the production of thrombopoietin." Biochemical and Biophysical Research Communications **454**(2): 353-357.
- Naveiras, O., V. Nardi, P. L. Wenzel, P. V. Hauschka, F. Fahey and G. Q. Daley (2009). "Bone-marrow adipocytes as negative regulators of the haematopoietic microenvironment." Nature **460**(7252): 259-263.
- Nilsson, S. K., H. M. Johnston and J. A. Coverdale (2001). "Spatial localization of transplanted hemopoietic stem cells: inferences for the localization of stem cell niches." Blood **97**(8): 2293-2299.
- Nombela-Arrieta, C., G. Pivarnik, B. Winkel, K. J. Canty, B. Harley, J. E. Mahoney, S.-Y. Park, J. Lu, A. Protopopov and L. E. Silberstein (2013). "Quantitative imaging of

- haematopoietic stem and progenitor cell localization and hypoxic status in the bone marrow microenvironment." Nature Cell Biology **15**(5): 533-543.
- Norozi, F., S. Shahrabi, S. Hajizamani and N. Saki (2016). "Regulatory role of Megakaryocytes on Hematopoietic Stem Cells Quiescence by CXCL4/PF4 in Bone Marrow Niche." Leuk Res **48**: 107-112.
- North, T. E., M. F. T. R. De Bruijn, T. Stacy, L. Talebian, E. Lind, C. Robin, M. Binder, E. Dzierzak and N. A. Speck (2002). "Runx1 Expression Marks Long-Term Repopulating Hematopoietic Stem Cells in the Midgestation Mouse Embryo." **16**(5): 661-672.
- Ohneda, O., K. Ohneda, F. Arai, J. Lee, T. Miyamoto, Y. Fukushima, D. Dowbenko, L. A. Lasky and T. Suda (2001). "ALCAM (CD166): its role in hematopoietic and endothelial development." Blood **98**(7): 2134-2142.
- Olson, T. S., A. Caselli, S. Otsuru, T. J. Hofmann, R. Williams, P. Paolucci, M. Dominici and E. M. Horwitz (2013). "Megakaryocytes promote murine osteoblastic HSC niche expansion and stem cell engraftment after radioablative conditioning." Blood **121**(26): 5238-5249.
- Orkin, S. H. and L. I. Zon (2008). "Hematopoiesis: An Evolving Paradigm for Stem Cell Biology." Cell **132**(4): 631-644.
- Palis, J., R. J. Chan, A. Koniski, R. Patel, M. Starr and M. C. Yoder (2001). "Spatial and temporal emergence of high proliferative potential hematopoietic precursors during murine embryogenesis." **98**(8): 4528-4533.
- Pang, W. W., E. A. Price, D. Sahoo, I. Beerman, W. J. Maloney, D. J. Rossi, S. L. Schrier and I. L. Weissman (2011). "Human bone marrow hematopoietic stem cells are increased in frequency and myeloid-biased with age." Proceedings of the National Academy of Sciences **108**(50): 20012-20017.

- Pettit, A. R., M. K. Chang, D. A. Hume and L. J. Raggatt (2008). "Osteal macrophages: a new twist on coupling during bone dynamics." Bone **43**(6): 976-982.
- Pimkin, M., A. V. Kossenkov, T. Mishra, C. S. Morrissey, W. Wu, C. A. Keller, G. A. Blobel, D. Lee, M. A. Beer, R. C. Hardison and M. J. Weiss (2014). "Divergent functions of hematopoietic transcription factors in lineage priming and differentiation during erythro-megakaryopoiesis." Genome Research **24**(12): 1932-1944.
- Porter, R. L., M. A. Georger, O. Bromberg, K. E. McGrath, B. J. Frisch, M. W. Becker and L. M. Calvi (2013). "Prostaglandin E2 Increases Hematopoietic Stem Cell Survival and Accelerates Hematopoietic Recovery After Radiation Injury." STEM CELLS **31**(2): 372-383.
- Pridans, C., M. L. Holmes, M. Polli, J. M. Wettenhall, A. Dakic, L. M. Corcoran, G. K. Smyth and S. L. Nutt (2008). "Identification of Pax5 target genes in early B cell differentiation." J Immunol **180**(3): 1719-1728.
- Pruijt, J. F. M., P. Verzaal, R. Van Os, E. J. F. M. De Kruijf, M. L. J. Van Schie, A. Mantovani, A. Vecchi, I. J. D. Lindley, R. Willemze, S. Starckx, G. Opendakker and W. E. Fibbe (2002). "Neutrophils are indispensable for hematopoietic stem cell mobilization induced by interleukin-8 in mice." **99**(9): 6228-6233.
- Qiao, J., L. Liu, Y. Xia, W. Ju, P. Zhao, Y. Jiang, M. Li, W. Li, L. Ding, Y. Wu, K. Qi, D. Li, X. Zhang, K. Xu and L. Zeng (2018). "Macrophages ameliorate bone marrow inflammatory injury and promote hematopoiesis in mice following hematopoietic stem cell transplantation." Exp Ther Med **16**(2): 567-572.
- Raggatt, L. J., M. E. Wullschleger, K. A. Alexander, A. C. Wu, S. M. Millard, S. Kaur, M. L. Maugham, L. S. Gregory, R. Steck and A. R. Pettit (2014). "Fracture healing via periosteal callus formation requires macrophages for both initiation and progression of early endochondral ossification." Am J Pathol **184**(12): 3192-3204.

- Ramos, P., C. Casu, S. Gardenghi, L. Breda, B. J. Crielgaard, E. Guy, M. F. Marongiu, R. Gupta, R. L. Levine, O. Abdel-Wahab, B. L. Ebert, N. Van Rooijen, S. Ghaffari, R. W. Grady, P. J. Giardina and S. Rivella (2013). "Macrophages support pathological erythropoiesis in polycythemia vera and β -thalassemia." **19**(4): 437-445.
- Rich, I. N., C. Vogt and S. Pentz (1988). "Erythropoietin gene expression in vitro and in vivo detected by in situ hybridization." Blood Cells **14**(2-3): 505-520.
- Rossi, D. J., D. Bryder, J. M. Zahn, H. Ahlenius, R. Sonu, A. J. Wagers and I. L. Weissman (2005). "Cell intrinsic alterations underlie hematopoietic stem cell aging." **102**(26): 9194-9199.
- Rundberg Nilsson, A., S. Soneji, S. Adolfsson, D. Bryder and C. J. Pronk (2016). "Human and Murine Hematopoietic Stem Cell Aging Is Associated with Functional Impairments and Intrinsic Megakaryocytic/Erythroid Bias." PLoS One **11**(7): e0158369.
- Sabzevari, H., J. Kantor, A. Jaigirdar, Y. Tagaya, M. Naramura, J. Hodge, J. Bernon and J. Schlom (2001). "Acquisition of CD80 (B7-1) by T cells." J Immunol **166**(4): 2505-2513.
- Schofield, R. (1978). "The relationship between the spleen colony-forming cell and the haemopoietic stem cell." Blood Cells **4**(1-2): 7-25.
- Schulz, C., E. G. Perdiguero, L. Chorro, H. Szabo-Rogers, N. Cagnard, K. Kierdorf, M. Prinz, B. Wu, S. E. W. Jacobsen, J. W. Pollard, J. Frampton, K. J. Liu and F. Geissmann (2012). "A Lineage of Myeloid Cells Independent of Myb and Hematopoietic Stem Cells." Science **336**(6077): 86-90.
- Severe, N., N. M. Karabacak, K. Gustafsson, N. Baryawno, G. Courties, Y. Kfoury, K. D. Kokkaliaris, C. Rhee, D. Lee, E. W. Scadden, J. E. Garcia-Robledo, T. Brouse, M. Nahrendorf, M. Toner and D. T. Scadden (2019). "Stress-Induced Changes in

Bone Marrow Stromal Cell Populations Revealed through Single-Cell Protein Expression Mapping." Cell Stem Cell.

Silberstein, L., K. A. Goncalves, P. V. Kharchenko, R. Turcotte, Y. Kfoury, F. Mercier, N. Baryawno, N. Severe, J. Bachand, J. A. Spencer, A. Papazian, D. Lee, B. R. Chitteti, E. F. Srour, J. Hoggatt, T. Tate, C. Lo Celso, N. Ono, S. Nutt, J. Heino, K. Sipila, T. Shioda, M. Osawa, C. P. Lin, G. F. Hu and D. T. Scadden (2016). "Proximity-Based Differential Single-Cell Analysis of the Niche to Identify Stem/Progenitor Cell Regulators." Cell Stem Cell **19**(4): 530-543.

Silver, L. and J. Palis (1997). "Initiation of murine embryonic erythropoiesis: a spatial analysis." Blood **89**(4): 1154-1164.

Sinder, B. P., A. R. Pettit and L. K. McCauley (2015). "Macrophages: Their Emerging Roles in Bone." J Bone Miner Res **30**(12): 2140-2149.

Sinder, B. P., L. Zweifler, A. J. Koh, M. N. Michalski, L. C. Hofbauer, J. I. Aguirre, H. Roca and L. K. McCauley (2017). "Bone Mass Is Compromised by the Chemotherapeutic Trabectedin in Association With Effects on Osteoblasts and Macrophage Efferocytosis." J Bone Miner Res **32**(10): 2116-2127.

Singh, P., J. Hoggatt, M. M. Kamocka, K. S. Mohammad, M. R. Saunders, H. Li, J. Speth, N. Carlesso, T. A. Guise and L. M. Pelus (2017). "Neuropeptide Y regulates a vascular gateway for hematopoietic stem and progenitor cells." Journal of Clinical Investigation **127**(12): 4527-4540.

Singh, P., P. Hu, J. Hoggatt, A. Moh and L. M. Pelus (2012). "Expansion of bone marrow neutrophils following G-CSF administration in mice results in osteolineage cell apoptosis and mobilization of hematopoietic stem and progenitor cells." Leukemia **26**(11): 2375-2383.

Smeets, M. F. M. A., A. C. Chan, S. Dagger, C. K. Bradley, A. Wei and D. J. Izon (2013). "Fli-1 Overexpression in Hematopoietic Progenitors Deregulates T Cell

- Development and Induces Pre-T Cell Lymphoblastic Leukaemia/Lymphoma." **8**(5): e62346.
- Smith-Kinnaman, W. R., M. J. Berna, G. O. Hunter, J. D. True, P. Hsu, G. I. Cabello, M. J. Fox, G. Varani and A. L. Mosley (2014). "The interactome of the atypical phosphatase Rtr1 in *Saccharomyces cerevisiae*." Mol Biosyst **10**(7): 1730-1741.
- Sonoda, Y. and K. Sasaki (2008). "Surface morphology of the central macrophages of erythroblastic islets in the spleen of aged and pregnant mice: an immunohistochemical light microscopic study." **71**(3): 155-161.
- Stier, S., Y. Ko, R. Forkert, C. Lutz, T. Neuhaus, E. Grünwald, T. Cheng, D. Dombkowski, L. M. Calvi, S. R. Rittling and D. T. Scadden (2005). "Osteopontin is a hematopoietic stem cell niche component that negatively regulates stem cell pool size." The Journal of Experimental Medicine **201**(11): 1781-1791.
- Sugiyama, T., H. Kohara, M. Noda and T. Nagasawa (2006). "Maintenance of the Hematopoietic Stem Cell Pool by CXCL12-CXCR4 Chemokine Signaling in Bone Marrow Stromal Cell Niches." Immunity **25**(6): 977-988.
- Taichman, R. S. and S. G. Emerson (1994). "Human osteoblasts support hematopoiesis through the production of granulocyte colony-stimulating factor." J Exp Med **179**(5): 1677-1682.
- Taichman, R. S., M. J. Reilly and S. G. Emerson (1996). "Human osteoblasts support human hematopoietic progenitor cells in vitro bone marrow cultures." Blood **87**(2): 518-524.
- Taichman, R. S., M. J. Reilly, R. S. Verma, K. Ehrenman and S. G. Emerson (2001). "Hepatocyte growth factor is secreted by osteoblasts and cooperatively permits the survival of haematopoietic progenitors." British Journal of Haematology **112**(2): 438-448.

- Till, J. E. and C. E. Mc (1961). "A direct measurement of the radiation sensitivity of normal mouse bone marrow cells." Radiat Res **14**: 213-222.
- Toda, S., K. Segawa and S. Nagata (2014). "MerTK-mediated engulfment of pyrenocytes by central macrophages in erythroblastic islands." **123**(25): 3963-3971.
- Tuljapurkar, S. R., T. R. McGuire, S. K. Brusnahan, J. D. Jackson, K. L. Garvin, M. A. Kessinger, J. T. Lane, B. J. O' Kane and J. G. Sharp (2011). "Changes in human bone marrow fat content associated with changes in hematopoietic stem cell numbers and cytokine levels with aging." **219**(5): 574-581.
- Turpen, J. B., C. M. Kelley, P. E. Mead and L. I. Zon (1997). "Bipotential Primitive-Definitive Hematopoietic Progenitors in the Vertebrate Embryo." **7**(3): 325-334.
- Uchida, N., Z. Yang, J. Combs, O. Pourquie, M. Nguyen, R. Ramanathan, J. Fu, A. Welply, S. Chen, G. Weddell, A. K. Sharma, K. R. Leiby, D. Karagogeos, B. Hill, L. Humeau, W. B. Stallcup, R. Hoffman, A. S. Tsukamoto, D. P. Gearing and B. Peault (1997). "The characterization, molecular cloning, and expression of a novel hematopoietic cell antigen from CD34+ human bone marrow cells." Blood **89**(8): 2706-2716.
- van Rooijen, N. and E. Hendrikx (2010). Liposomes for Specific Depletion of Macrophages from Organs and Tissues. Liposomes: Methods and Protocols, Volume 1: Pharmaceutical Nanocarriers. V. Weissig. Totowa, NJ, Humana Press: 189-203.
- Vas, V., C. Wandhoff, K. Dörr, A. Niebel and H. Geiger (2012). "Contribution of an Aged Microenvironment to Aging-Associated Myeloproliferative Disease." **7**(2): e31523.
- Vi, L., G. S. Baht, H. Whetstone, A. Ng, Q. Wei, R. Poon, S. Mylvaganam, M. Grynepas and B. A. Alman (2015). "Macrophages Promote Osteoblastic Differentiation In Vivo: Implications in Fracture Repair and Bone Homeostasis." **30**(6): 1090-1102.

- Visnjic, D., Z. Kalajzic, D. W. Rowe, V. Katavic, J. Lorenzo and H. L. Aguila (2004). "Hematopoiesis is severely altered in mice with an induced osteoblast deficiency." Blood **103**(9): 3258-3264.
- Walkley, C. R., G. H. Olsen, S. Dworkin, S. A. Fabb, J. Swann, Grant, S. V. Westmoreland, P. Chambon, D. T. Scadden and L. E. Purton (2007). "A Microenvironment-Induced Myeloproliferative Syndrome Caused by Retinoic Acid Receptor γ Deficiency." Cell **129**(6): 1097-1110.
- Walkley, C. R., J. M. Shea, N. A. Sims, L. E. Purton and S. H. Orkin (2007). "Rb Regulates Interactions between Hematopoietic Stem Cells and Their Bone Marrow Microenvironment." Cell **129**(6): 1081-1095.
- Wijeratne, A., J. Xiao, C. Reutter, K. W. Furness, R. Leon, M. Zia-Ebrahimi, R. N. Cavitt, J. M. Strelow, R. D. Van Horn, S. B. Peng, D. A. Barda, T. A. Engler and M. J. Chalmers (2018). "Chemical Proteomic Characterization of a Covalent KRASG12C Inhibitor." ACS Med Chem Lett **9**(6): 557-562.
- Wilson, M. C., M. Kraus, H. Marzban, J. R. Sarna, Y. Wang, R. Hawkes, A. P. Halestrap and P. W. Beesley (2013). "The neuroplastin adhesion molecules are accessory proteins that chaperone the monocarboxylate transporter MCT2 to the neuronal cell surface." PLoS One **8**(11): e78654.
- Winfrey, S., S. Khan, R. Micanovic, M. T. Eadon, K. J. Kelly, T. A. Sutton, C. L. Phillips, K. W. Dunn and T. M. El-Achkar (2017). "Quantitative Three-Dimensional Tissue Cytometry to Study Kidney Tissue and Resident Immune Cells." J Am Soc Nephrol **28**(7): 2108-2118.
- Winkler, I. G., A. R. Pettit, L. J. Raggatt, R. N. Jacobsen, C. E. Forristal, V. Barbier, B. Nowlan, A. Cisterne, L. J. Bendall, N. A. Sims and J. P. Lévesque (2012). "Hematopoietic stem cell mobilizing agents G-CSF, cyclophosphamide or

- AMD3100 have distinct mechanisms of action on bone marrow HSC niches and bone formation." **26**(7): 1594-1601.
- Winkler, I. G., N. A. Sims, A. R. Pettit, V. Barbier, B. Nowlan, F. Helwani, I. J. Poulton, N. van Rooijen, K. A. Alexander, L. J. Raggatt and J. P. Levesque (2010). "Bone marrow macrophages maintain hematopoietic stem cell (HSC) niches and their depletion mobilizes HSCs." Blood **116**(23): 4815-4828.
- Wright, J. H. (1910). "The histogenesis of the blood platelets." **21**(2): 263-278.
- Wu, A. C., L. J. Raggatt, K. A. Alexander and A. R. Pettit (2013). "Unraveling macrophage contributions to bone repair." Bonekey Rep **2**: 373.
- Xie, Y., T. Yin, W. Wiegraebe, X. C. He, D. Miller, D. Stark, K. Perko, R. Alexander, J. Schwartz, J. C. Grindley, J. Park, J. S. Haug, J. P. Wunderlich, H. Li, S. Zhang, T. Johnson, R. A. Feldman and L. Li (2009). "Detection of functional haematopoietic stem cell niche using real-time imaging." Nature **457**(7225): 97-101.
- Xu, L., K. S. Mohammad, H. Wu, C. Crean, B. Poteat, Y. Cheng, A. A. Cardoso, C. C. Marchal, H. Hanenberg, R. Abonour, M. A. Kacena, J. M. Chirgwin, A. Suvannasankha and E. F. Srour (2016). "Cell adhesion molecule CD166 drives malignant progression and osteolytic disease in multiple myeloma."
- Xu, Z., C.-C. Chang, M. Li, Q.-Y. Zhang, E.-R. M. Vasilescu, V. D'Agati, A. Floratos, G. Vlad and N. Suci-Foca (2018). "ILT3.Fc-CD166 Interaction Induces Inactivation of p70 S6 Kinase and Inhibits Tumor Cell Growth." The Journal of Immunology **200**(3): 1207-1219.
- Yamamoto, W. R., R. N. Bone, P. Sohn, F. Syed, C. A. Reissaus, A. L. Mosley, A. B. Wijeratne, J. D. True, X. Tong, T. Kono and C. Evans-Molina (2019). "Endoplasmic reticulum stress alters ryanodine receptor function in the murine pancreatic beta cell." J Biol Chem **294**(1): 168-181.

- Yamazaki, S., H. Ema, G. Karlsson, T. Yamaguchi, H. Miyoshi, S. Shioda, Makoto, S. Karlsson, A. Iwama and H. Nakauchi (2011). "Nonmyelinating Schwann Cells Maintain Hematopoietic Stem Cell Hibernation in the Bone Marrow Niche." **147**(5): 1146-1158.
- Yona, S., K.-W. Kim, Y. Wolf, A. Mildner, D. Varol, M. Breker, D. Strauss-Ayali, S. Viukov, M. Guillemins, A. Misharin, David, H. Perlman, B. Malissen, E. Zelzer and S. Jung (2013). "Fate Mapping Reveals Origins and Dynamics of Monocytes and Tissue Macrophages under Homeostasis." Immunity **38**(1): 79-91.
- Yoshihara, H., F. Arai, K. Hosokawa, T. Hagiwara, K. Takubo, Y. Nakamura, Y. Gomei, H. Iwasaki, S. Matsuoka, K. Miyamoto, H. Miyazaki, T. Takahashi and T. Suda (2007). "Thrombopoietin/MPL Signaling Regulates Hematopoietic Stem Cell Quiescence and Interaction with the Osteoblastic Niche." Cell Stem Cell **1**(6): 685-697.
- Yu, V. W. and D. T. Scadden (2016). "Hematopoietic Stem Cell and Its Bone Marrow Niche." Curr Top Dev Biol **118**: 21-44.
- Yu, V. W. C., B. Saez, C. Cook, S. Lotinun, A. Pardo-Saganta, Y.-H. Wang, S. Lympéri, F. Ferraro, M. H. G. P. Raaijmakers, J. Y. Wu, L. Zhou, J. Rajagopal, H. M. Kronenberg, R. Baron and D. T. Scadden (2015). "Specific bone cells produce DLL4 to generate thymus-seeding progenitors from bone marrow." **212**(5): 759-774.
- Zhang, G., C. Slaughter and E. H. Humphries (1995). "v-rel Induces ectopic expression of an adhesion molecule, DM-GRASP, during B-lymphoma development." **15**(3): 1806-1816.
- Zhang, J., J. Ghosh, S. F. Mohamad, C. Zhang, X. Huang, M. L. Capitano, A. M. Gunawan, S. Cooper, B. Guo, Q. Cai, H. E. Broxmeyer and E. F. Srouf (2019). "CD166

engagement augments mouse and human hematopoietic progenitor function via activation of stemness and cell cycle pathways." Stem Cells.

Zhang, J., C. Niu, L. Ye, H. Huang, X. He, W.-G. Tong, J. Ross, J. Haug, T. Johnson, J. Q. Feng, S. Harris, L. M. Wiedemann, Y. Mishina and L. Li (2003). "Identification of the haematopoietic stem cell niche and control of the niche size." Nature **425**(6960): 836-841.

Zhao, M., J. M. Perry, H. Marshall, A. Venkatraman, P. Qian, X. C. He, J. Ahamed and L. Li (2014). "Megakaryocytes maintain homeostatic quiescence and promote post-injury regeneration of hematopoietic stem cells." Nature Medicine **20**(11): 1321-1326.

Zhu, H., D. Traver, A. J. Davidson, A. Dibiase, C. Thisse, B. Thisse, S. Nimer and L. I. Zon (2005). "Regulation of the *lmo2* promoter during hematopoietic and vascular development in zebrafish." **281**(2): 256-269.

Zimmerman, A. W., B. Joosten, R. Torensma, J. R. Parnes, F. N. van Leeuwen and C. G. Figdor (2006). "Long-term engagement of CD6 and ALCAM is essential for T-cell proliferation induced by dendritic cells." Blood **107**(8): 3212-3220.

Zou, Y. R., A. H. Kottmann, M. Kuroda, I. Taniuchi and D. R. Littman (1998). "Function of the chemokine receptor CXCR4 in haematopoiesis and in cerebellar development." Nature **393**(6685): 595-599.

Curriculum Vitae

Safa F. Mohamad

Education

Indiana University (IUPUI), Indianapolis IN, 2014-2020

PhD in Microbiology and Immunology with a minor in Cancer Biology

- Thesis: The role of osteomacs in regulating stem cell function and the hematopoietic niche

Virginia Commonwealth University (VCU), Richmond VA, 2012-2014

M.S in Human and Molecular Genetics

- Thesis: The roles of transcription factors Krüppel Like factor1 (KLF1) and KLF2 in human globin gene regulation and fetal erythropoiesis

Ramnarain Ruia College (Part of University of Mumbai), Mumbai, India, 2011-2012

M.S in Biotechnology (1 year, with no degree)

R.D. National College (Part of University of Mumbai), Mumbai, India, 2008-2011

B.S in Biotechnology with a minor in Environmental Sciences

Certificate of Excellence- Honors in IVF

Research Experience

- March 2015- Present: Graduate student: Mentor, Dr. Edward F. Srouf on 'The role of osteomacs in regulating stem cell function and the hematopoietic niche'.
- January 2015- March 2015: Graduate student rotation: Dr. Reuben Kapur on 'LIM kinases: A potential therapeutic target for leukemias'.
- October 2014- December 2014: Graduate student rotation: Dr. Ronald Wek on 'ER stress mediated PERK activation'.
- August 2012- May 2014: Master's Graduate Research/ Employed Research Assistant in the Human and Molecular Genetics Department at Virginia

Commonwealth University: Mentor, Dr. Joyce Lloyd on 'The roles of transcription factors Krüppel Like factor1 (KLF1) and KLF2 in human globin gene regulation and fetal erythropoiesis'.

- May 2012- July 2012: Research Assistant in the Cytogenetics Department at National Institute of Immunohematology: Mentor, Dr. Babu Rao Vundinti on 'RFC gene polymorphism in mothers of Down syndrome'.

Teaching Experience

1. Trained one PhD rotation student and one high school student at Indiana University School of Medicine, 2018-2019.
2. Teaching Assistant for Microbiology and Immunology (J210), School of Nursing, IUPUI, Spring 2018.
3. Trained two M.S rotation students at Virginia Commonwealth University, 2013-2014

Skills and Techniques

- **Genomics:** Single cell capture through C1 STA assay, single cell qPCR through Biomark, single cell RNAseq
- **Proteomics:** CyTOF (Single cell mass cytometry) staining and antibody conjugation
- **Animal Training:** Mouse training
- **Cellular Biology:** Flow cytometry, colony forming assay, tissue culture, western blot, trypsinization, apoptosis and proliferation assays, MTS assay, nuclear fractionation, isolation of hematopoietic stem cells, osteomacs and osteoblasts from murine bone marrow and bone, isolation of CD34+ stem cells from human cord blood and differentiation into RBCs

- **Molecular Biology:** qRT-PCR, primer design, cloning, sh-RNA mediated knockdown, PCR, AGE, PAGE, restriction digestion, genotyping, RNA/DNA extraction, Agilent Bioanalyzer, cDNA synthesis
- **Virology:** Amplification, purification and transfection of lentivirus for in vitro work
- **Histology:** 3D imaging/ Tissue cytometry, immunofluorescent staining, giemsa staining, Confocal microscopy
- **Computer skills:** Microsoft word, Excel, PowerPoint, FlowJo, CytoBank, Singular, ImageJ, Prism, JMP
- **Languages:** English, Hindi, Marathi, Spanish

Oral Presentations

- Oral presentation on “Parameters contributing to the role of osteomacs in regulating stem cell function and the hematopoietic niche” at the **Midwest Blood Club symposium** (April 2019), Memphis, TN
- Oral presentation on “Calvariae-Resident Osteomacs That Are Phenotypically and Functionally Distinct from Marrow-Derived Macrophages Interact with Megakaryocytes to Regulate Hematopoietic Stem Cell Function” at the **58th American Society of Hematology Annual Meeting** and Exposition (December 2016) in San Diego, CA

Poster Presentations

- Poster presentation on “The role of osteomacs in regulating stem cell function and the hematopoietic niche” at the **48th International Society of Experimental Hematology Annual Meeting** (August 2019) in Brisbane, Australia
- Poster presentation on “Defining parameters attributing to the role of osteomacs in regulating stem cell function and the hematopoietic niche” at the **60th American**

Society of Hematology Annual Meeting and Exposition (December 2018) in San Diego, CA

- Poster presentation on “Osteomacs interact with megakaryocytes and osteoblasts to regulate murine hematopoietic stem cell function” at **IU Cancer Research Day** (May 2018), Indianapolis, IN
- Poster Presentation on “A novel CD45+F4/80+ population within calvariae-derived osteoblasts regulates the osteoblast-mediated hematopoiesis enhancing activity through interactions with megakaryocytes” at the **Midwest Blood Club symposium** (October 2015), French Lick, IN

Academic Experiences

- Attended biotechnology-based workshops and seminars organized by Thadomal Shahani Engineering College (Department of Biotechnology), Mumbai (October 2009)
- Attended a workshop on Current Instruments of Analysis and Research organized by Reliable Analytical Laboratories PVT LTD, Mumbai (October 2011)
- Attended the **3rd World Congress on Practical Infertility Management and Human Reproduction Conference** organized by Dr. Hrishikesh Pai, Mumbai (November 2008)
- Active participant in the annual Biotechnology Training program at **Haffkine Institute**, Mumbai (summer 2008)

Membership in Professional Societies

- **Association of Women in Science (AWIS)**, Indiana Chapter, June 2018-Present
- **American Society of Hematology (ASH)**, July 2018-Present
- **International Society of Experimental Hematology (ISEH)**. March 2019-Present

Awards and Honors

- IU School of Medicine **Graduate Student Travel Award**, Spring, 2019.
- **Travel fellowship** by the IUPUI graduate office, Spring 2019.
- **Abstract Achievement Award at the 60th ASH Annual Meeting** and Exposition (December 2018) in San Diego, CA
- **Travel grant** by the Graduate and Professional student government at IUPUI, Fall 2018
- Best presentation in the “**Research in Progress**” series by the department of Microbiology and Immunology, Indiana University School of Medicine, 2017-2018
- **Abstract Achievement Award at the 58th ASH Annual Meeting** and Exposition (December 2016) in San Diego, CA
- First place in the 2016 **Sigma Xi Graduate Biomedical Research Competition**
- **Meryllyn Hester Scholarship** for doctoral students in pediatric hematology, Indiana University School of Medicine, 2016-2017
- **Charles C. Clayton Award** for outstanding scholarly achievement at Virginia Commonwealth University, 2013-2014
- First Runner-Up in the **International Economic Convention** held at Kishinchand Chellaram College, Mumbai, 2009
- **Certificate of Excellence-Honors Award** for a project on IVF, 2008-2009
- Second Runner-Up in Poster Competition for **World Wetland Day** Organized by Enviro- Vigil, Thane, 2009
- Basico, Intermedio and Diploma Inicial level in Spanish from Instituto Hispania (Affiliated with F.I.D.E.S.C.U, Spain), 2009-2010

Leadership/Volunteer Experience

- Member of the **Student Diversity Advisory Board** at IUPUI, September 2017- May 2019
- IUPUI International Orientation (2017)
- Annual Departmental festival of Biotechnology- **“Chimera”** at Ramnarain Ruia College, Matunga, 2011
- Core Group Leader of the ‘Save Water, Save Earth’ Project organized by R.D. National College as part of the Environmental awareness program (2009-2010)
- Core committee member in the Annual Departmental festival of Biotechnology- **“HELIX”** at R.D. National College, Mumbai, 2009
- Volunteered to provide education to the needy students of The Spastics Society of India, Mumbai (2008)

Publications

1. Vinjamur DS, Wade KJ, **Mohamad SF**, Haar JL, Sawyer ST, Lloyd JA. Krüppel-like transcription factors KLF1 and KLF2 have unique and coordinate roles in regulating embryonic erythroid precursor maturation. *Haematologica*, Oct 2014 (PMID:25150253).
2. Vinjamur DS, Alhashem YN, **Mohamad SF**, Amin P, Williams DC Jr, Lloyd JA. Krüppel-Like Transcription Factor KLF1 Is Required for Optimal γ - and β -Globin Expression in Human Fetal Erythroblasts. *PLoS One*, Feb 2016 (PMID:226840243).
3. Anjanappa M, Cardoso AA, Cheng L, **Mohamad S**, Gunawan A, Rice S, Dong Y, Li L, Sandusky GE, Srour EF, Nakshatri H. Individualized breast cancer characterization through single cell analysis of tumor and adjacent-normal cells. *Cancer Research* May 2017 (PMID:28249895).

4. Kovilakath A, **Mohamad S**, Hermes F, Wang SZ, Ginder GD and Lloyd JA. In Vitro Erythroid Differentiation and Lentiviral Knockdown in Human CD34+ Cells from Umbilical Cord Blood. *Erythropoiesis: Methods and Protocols (Chapter 16)*, October 2017 (PMID:29076096).
5. **Mohamad SF**^{*}, Xu L^{*}, Ghosh J, Childress PJ, Himes ER, Wu H, Alvarez MB, Davis KM, Aguilar-Perez A, Bruzzaniti A, Kacena MA, Srour EF. Osteomacs interact with megakaryocytes to regulate hematopoietic stem cell function. *Blood Advances* (* First Co-author) December 2017 (PMID:29296903).
6. Alvarez MB, Xu L, Childress PJ, Maupin KA, **Mohamad SF**, Chitteti BR, Himes ER, Olivos III DJ, Cheng YH, Conway SJ, Srour EF, Kacena MA. Megakaryocyte and osteoblast interactions modulate bone mass and hematopoiesis. *Stem Cells and Development*, April 2018 (PMID:29631496).
7. Ghosh J, **Mohamad SF**, and Srour EF. Isolation and Identification of murine bone marrow-derived macrophages and osteomacs from neonatal and adult mice. *Springer Protocols*, December 2018 (PMID:30539348).
8. Zhang J, Ghosh J, **Mohamad SF**, Zhang C, Huang X, Capitano ML, Gunawan AM, Cooper S, Guo B, Cai Q, Broxmeyer HE, and Srour EF. CD166 engagement augments mouse and human hematopoietic progenitor function via activation of stemness and cell cycle pathways. *Stem Cells*, July 2019, (PMID:31260147).
9. Maupin KA, Himes ER, Plett AP, Chua HL, Singh P, Abeysekera I, Fisher A, Sampson C, Hong JM, Childress P, Alvarez M, Ghosh J, **Mohamad SF**, Srour EF, Bruzzaniti A, Pelus LM, Orschell CM, Kacena MA. Age-related decline in megakaryocyte induced enhancement of bone mass. *Bone*, July 2019, (PMID:31299382).

10. Kanagasabapathy D, Blosser R, Maupin KA, Hong JM, Alvarez M, Ghosh J, **Mohamad SF**, Aguilar-Perez A, Srour EF, Kacena MA, Bruzzaniti A. Megakaryocytes promote osteoclastogenesis in aging. *(Submitted)*.
11. Capitano ML, **Mohamad SF**, Cooper S, Guo B, Huang X, Gunawan A, Sampson C, Srour EF, Orschell C, Broxmeyer HE. Re-Evaluation of Age-Related Dysregulation of Hematopoiesis Based on Oxygen Sensitivity of Hematopoietic Stem and Progenitor Cells. *(Submitted)*.
12. **Mohamad SF**, Sheik D, Aguilar-Perez A, Childress P, Gunawan A, Abeysekara I, Ghosh J, Blosser R, Kacena MA, Srour EF, Bruzzaniti A. Neonatal calvarial osteomacs are different from age-matched bone marrow macrophages but can differentiate into functional osteoclasts. *(In preparation)*.
13. **Mohamad SF**, Ghosh J, Gunawan A, Kamocka MM, Blosser R, Zhang C, Dunn K, Mohammad KS, Kacena MA, Srour EF. Defining parameters attributing to the role of osteomacs in regulating stem cell function and the hematopoietic niche. *(In preparation)*.